

THE UNIVERSITY OF HULL

**THE OFF-LINE AND ON-LINE ANALYSIS OF LIQUID PROCESS  
STREAMS BY MASS SPECTROMETRY**

being a Thesis submitted for the Degree of

DOCTOR OF PHILOSOPHY

in the University of Hull

by

WARWICK BRIAN DUNN

B.Sc.

November, 1996.

## Acknowledgements

I would like to express my appreciation and thanks to many people and organisations.

Firstly I would like to thank my industrial and academic supervisors, Dr. John Green and Professor Alan Townshend, for their advice and guidance. I would also like to thank John Green for the various discussions while sharing an office and for his patience in his otherwise quiet office.

Thanks are also expressed for their financial assistance to BP Chemicals Hull Research and Technology Centre, The Analytical Chemistry Fund of The Royal Society of Chemistry and VG Gas Analysis Systems (Middlewich, Cheshire). Thanks are expressed to Victor Lough and Steve Reilly at VG Gas Analysis Systems for their support and frequent technical assistance.

Many thanks are given freely to a variety of people of which only a few are listed below; Malcolm Cooper, Kal Dhaliwal, Steve Lancaster and John Wilson at BP Chemicals for their friendship and advice and also to Neil Howarth and Simon Nelms for their friendship and encouragement.

Finally, but with the greatest appreciation I thank my parents for their infinite encouragement and support in what ever I choose to do in life and also I would like to thank Alison for her love, calm head and an excellent reason for being in Hull.

## Abstract

The work presented in this thesis describes the development and validation in the laboratory of four techniques employed for the off-line and on-line analysis of liquid chemical process streams by mass spectrometry, without previous chromatographic separation of sample components. The four techniques were total vaporisation analysis, headspace analysis, membrane introduction mass spectrometry and atmospheric pressure ionisation-mass spectrometry.

The technique of total vaporisation analysis completely vaporises liquid samples in a gas chromatograph heated injection inlet and analyses the vapour created with a mass spectrometer. Headspace analysis and membrane introduction mass spectrometry provide partial and selective transfer of compounds from the liquid sample phase to the gas phase and the subsequent analysis of the gas phase with a mass spectrometer. Headspace analysis has no third phase separating the liquid and gas phases whereas membrane introduction mass spectrometry places a membrane between the two phases. All three techniques were validated using an electron-impact quadrupole mass spectrometer and two model streams; acetone (analyte) in water and methyl iodide (analyte) in acetic acid.

As an alternative strategy atmospheric pressure ionisation-mass spectrometers ionise samples in ion sources operating at atmospheric pressure. The techniques of electrospray ionisation and atmospheric pressure chemical ionisation were investigated for the analysis of formic, acetic and propionic acids present in water and other carboxylic acids.

The techniques of total vaporisation analysis, headspace analysis and membrane introduction mass spectrometry provided low  $\mu\text{g ml}^{-1}$  or  $\mu\text{g l}^{-1}$  limits of detection for acetone and methyl iodide with relative standard deviation values for replicate analyses of  $100 \mu\text{g ml}^{-1}$  standards of less than 10 % in most cases. Off-line and on-line total vaporisation analysis and off-line headspace analysis provided accurate determination of acetone in similar process samples, whereas the matrix affected the accuracy of the determination when the techniques of on-line headspace analysis and membrane introduction mass spectrometry were employed. Electrospray ionisation could also detect formic, acetic and propionic acids in aqueous or carboxylic acid matrices at concentrations of and possibly less than  $100 \mu\text{g ml}^{-1}$ . Atmospheric pressure chemical ionisation could only detect carboxylic acids present in aqueous matrices at concentrations of  $100 \mu\text{g ml}^{-1}$  or greater.

## Presentation and Publications

### Presentations

1. The On-line Analysis of Liquid Process or Effluent Streams by Mass Spectrometry

*Poster presentation*, Royal Society of Chemistry Analytical Division Research and Development Topics meeting, University of Hertfordshire, 18.7.94.

2. The Off-line and On-line Analysis of Liquid Process Streams by Mass Spectrometry

*Oral presentation*, Royal Society of Chemistry Analytical Division meeting 'Spectroscopy in Process Analysis', BP Chemicals, Hull, 2.11.94.

3. The Application of Mass Spectrometry to the On-line Analysis of Industrial Liquid Streams

*Poster presentation*, Royal Society of Chemistry Analytical Division Research and Development Topics meeting and SAC '95 meeting, University of Hull, 10.7.95 and 14.7.95.

4. The On-line Analysis of Industrial Liquid Streams by Mass Spectrometry

*Poster presentation*, Royal Society of Chemistry Pre-doctoral Chemistry Symposium, University of Sheffield, 5.9.95.

5. The On-line Analysis of Liquid Process Streams using Mass Spectrometry

*Oral presentation* by J.D. Green (co-author W.B. Dunn), 22nd Annual Conference of the Federation of Analytical Chemistry and Spectroscopy Societies, Cincinnati, Ohio, USA, 16.10.95.

6. Novel Applications of Mass Spectrometry for the On-line Analysis of Liquid Process Streams

*Oral presentation*, Royal Society of Chemistry Analytical Division Research and Development Topics meeting, Nottingham Trent University, 22.7.96.

Publications

1. The Potential of On-line Headspace Analysis of Liquid Streams Using Direct Mass Spectrometry Detection

Townshend, A., Green, J.D., and Dunn, W.B., *Anal. Proc. Includ. Anal. Comm.*, 1995, **32**, 361.

2. Novel Techniques for the Off-line Analysis of Liquid Process Streams by Mass Spectrometry

Townshend, A., Green, J.D., and Dunn, W.B., *Analyst*, 1996, **121**, 1435.

# Contents

## **Chapter One            The Analysis of Chemical Industry Samples**

1.1 Introduction	1
1.1.1 Process Control in the Chemical Industry	2
1.1.2 Process Analysis	3
1.1.2.1 Off-line Analysis	5
1.1.2.2 At-line Analysis	6
1.1.2.3 On-line Analysis	7
1.1.3 The Implementation of On-line Process Analysis Technology	10
1.2 Off-line Mass Spectrometry	12
1.3 On-line Mass Spectrometry	17
1.4 Research Objectives	22
1.5 References	24

## **Chapter Two            Instrumentation**

2.1 Introduction	29
2.2 Electron Impact Ion Sources	32
2.3 Quadrupole Mass Analysers	35
2.4 Detectors	43
2.4.1 Faraday Cup	43
2.4.2 Electron Multipliers	44

2.5 Instrument Control	45
2.6 Instrument Used in this Research	46
2.7 Instrument Optimisation	48
2.7.1 Emission Current and Electron Energy	48
2.7.2 Channeltron Detection Voltage	50
2.8 References	52

## **Chapter Three          Total Vaporisation Analysis**

3.1 Introduction	53
3.1.1 Gas Chromatography Injection Strategies	53
3.1.1.1 Direct Injections	54
3.1.1.2 Split Injections	55
3.1.1.3 Splitless Injections	56
3.1.1.4 Programmed Temperature Vaporisation	57
3.1.1.5 On-column Injections	58
3.1.2 Mass Spectrometric Direct Analysis of Liquids	58
3.1.2.1 Off-line Analysis	59
3.1.2.2 On-line Analysis	61
3.2 Experimental	64
3.2.1 Reagents	64
3.2.2 Instrumentation and Procedures	64
3.2.2.1 Preliminary Studies	65
3.2.2.2 Off-line Total Vaporisation Analysis	67

3.2.2.3 On-line Total Vaporisation Analysis	69
3.3 Results and Discussion	71
3.3.1 Preliminary Investigations	71
3.3.2 Off-line Total Vaporisation Analysis	76
3.3.2.1 The mechanism of Vaporisation	76
3.2.2.2 The Effect of the Buffer Volume	79
3.2.2.3 The Effect of the Injection Temperature	82
3.2.2.4 The Effect of the Helium Flow Rate	83
3.2.2.5 The Effect of the Injection Volume	84
3.2.2.6 Calibration	85
3.3.3 On-line Total Vaporisation Analysis	91
3.3.3.1 Calibration	91
3.3.4 The Determination of Acetone in a Process Sample	94
3.3.4.1 The Effect of the Calibration Matrix	95
3.3.4.2 Calibration	99
3.3.4.3 Analysis of the Process Samples	101
3.4 Conclusions	105
3.5 References	106

## **Chapter Four          Static Headspace Analysis**

4.1 Introduction	109
4.1.1 Headspace Techniques	109
4.1.2 Static Headspace Analysis Techniques	110

4.2 Experimental	118
4.2.1 Reagents	118
4.2.2 Instrumentation and Procedures	119
4.3 Results and Discussion	120
4.3.1 The Effect of the Sampling Time of the Headspace	120
4.3.2 The Effect of Temperature	121
4.3.3 The Effect of the Phase Ratio	123
4.3.4 Determination of the Equilibration Times	126
4.3.5 Calibration	128
4.3.6 The Determination of Acetone in Two Process Samples	136
4.4 Conclusions	142
4.5 References	144

## **Chapter Five            Dynamic Headspace Analysis**

5.1 Introduction	146
5.2 Experimental	152
5.2.1 Reagents	152
5.2.2 Instrumentation and Procedures	153
5.3 Results and Discussion	159
5.3.1 The Effect of the Liquid Stream Flow Rate	159
5.3.2 The Effect of the Stream Temperature	160
5.3.3 Determination of the Rise and Fall Times	162
5.3.4 Calibration	167

5.3.5 Gas Purging of the Liquid Stream	172
5.3.5.1 The Effect of the Purging Gas Flow Rate	172
5.3.5.2 The Effect of the Liquid Stream Flow Rate	173
5.3.5.3 Determination of the Rise and Fall Times	174
5.3.5.4 Calibration	176
5.3.6 The Relative Headspace Concentration of the Matrix	178
5.3.7 The Determination of Acetone in a Process Sample	180
5.3.7.1 The Effect of the Calibration Matrix	180
5.3.7.2 Calibration	181
5.3.7.3 Analysis of the Process Sample	183
5.4 Conclusions	185
5.5 References	186

## **Chapter Six Membrane Introduction Mass Spectrometry**

6.1 Introduction	188
6.1.1 Membrane Types	189
6.1.1.1 Nonporous Membranes	190
6.1.1.2 Microporous Membranes	194
6.1.2 Applications of membrane introduction mass spectrometry	197
6.2 Experimental	204
6.2.1 Reagents	204
6.2.2 Instrumentation and Procedures	204
6.2.2.1 The Membrane Flow Cell	204

6.3 Results and Discussion	208
6.3.1 The Determination of Acetone Present in Water Streams	208
6.3.1.1 The Effect of the Stream Flow Rate	208
6.3.1.2 The Effect of the Stream Temperature	210
6.3.1.3 Determination of the Rise and Fall Times	212
6.3.1.4 Calibration	215
6.3.2 The Determination of Methyl Iodide Present in Acetic Acid Streams	218
6.3.2.1 The Effect of the Stream Flow Rate	218
6.3.2.2 The Effect of the Stream Temperature	220
6.3.2.3 Determination of the Rise and Fall Time	222
6.3.2.4 Calibration	223
6.3.3 The Relative Concentration of Water and Acetic Acid in the Acceptor Gas Phase	225
6.3.4 The Quantification of Acetone in a Process Sample	226
6.3.4.1 The Effect of the Concentration of Acetic Acid in the Sample Matrix	227
6.3.4.2 Calibration	229
6.3.4.3 Analysis of the Process Sample	231
6.4 Conclusions	233
6.5 References	235

<b>Preliminary Results</b>	<b>Atmospheric Pressure Ionisation</b>	
7.1 Introduction		240
7.1.1 Atmospheric Pressure Ion Sources		241
7.1.1.1 Atmospheric Pressure Chemical Ionisation		245
7.1.1.2 Electrospray Ionisation		249
7.1.1.3 Applications of Atmospheric Pressure Ionisation		
- Mass Spectrometry		254
7.2 Experimental		257
7.2.1 Reagents		257
7.2.2 Instrumentation and Procedures		260
7.3 Results and Discussion		
7.3.1 The Analysis of Samples Composed of a Water Matrix		260
7.3.2 The Analysis of Samples Composed of an Acetic Acid		
Matrix		272
7.4 Conclusions		275
7.5 References		277
<b>Chapter Eight</b>	<b>General Conclusions</b>	281
<b>Chapter Nine</b>	<b>Suggestions for Further Work</b>	285

# **Chapter One**

## **The Analysis of Chemical Industry**

### **Samples**

## 1.1 Introduction

When you can measure what you are speaking about, and express it in numbers, you know something about it; and when you cannot measure it, when you cannot express it in numbers, your knowledge is of meagre and unsatisfactory kind.

Lord Kelvin

Spoken first more than eighty years ago and discussed recently<sup>1</sup>, the quote above expresses the necessity of measurements to be able to understand many different processes and operations in everyday life. In the chemical industry the techniques employed to perform **process analysis** collect information concerned with the operation of chemical processes. The information collected during the performance of process research on laboratory scale or pilot plants, or later on the process plant, can be used to expand the volume of knowledge regarding process operations. Alternatively information collected during chemical production on a process plant can be employed in **process control** systems to ensure the plant is operating at, or within, limits specified in safety and environmental legislation while maintaining an appropriate level of productivity and product quality. Process control functions operate continuously during the manufacture of chemicals whereas process research is a periodic function. Therefore the majority of process analysis applications are used to enable processes to be controlled correctly.

### 1.1.1 Process Control in the Chemical Industry

In the chemical industry pilot and process plants can be viewed as a collection of vessels (reactors, separation units and storage tanks) linked by a network of pipes<sup>2</sup>. From one to over fifty vessels can be employed to react, separate and store process contents in any single manufacturing operation.

The processes operated in these plants are composed of many physical and dynamic variables<sup>3</sup>, temperature or chemical concentrations for example, which may or may not be interrelated. The assembly of dynamic variables in a chemical process do not allow a steady state of operation to be maintained in the process and a more probable occurrence is a change in one or several dynamic variables. Changes can proceed either spontaneously or because of the effect of an external influence and will affect the operation of the process either advantageously or unfavourably. To regulate one or several dynamic variables and therefore exercise control of the process is beneficial to the efficient operation of the process within determined limits. Process control and the systems required to perform the associated functions have the primary objective of maintaining a dynamic variable within a desired range<sup>2,3</sup>. The size of the plant and the required degree of control of the process determine the number of process control systems employed.

Process control has become a more frequently employed function in the last thirty years to ensure chemical processes are operated in the required way<sup>2</sup>. The process plant of the 1960s was relatively bulky with a large storage capacity which had the effect of averaging out fluctuations in the process. Also 'thinking time' was provided for plant

operators during the storage of process contents. As a result the processes operated on the plants were relatively easy to control and process control systems employed were less critical to the successful operation of the processes<sup>2</sup>.

Today resources available in the chemical industry are either not increasing or are only increasing slowly while productivity is still expected to be increased by improving the process plants economic efficiency<sup>4</sup>. This has resulted in the construction of less costly and smaller process plants in the 1990s which employ 'Just in Time' production principles and provide the product to the market more quickly<sup>2</sup>. 'Just in Time' production principles use a small volume or no storage capacity which limits the 'thinking time' available, removes the hazards associated with storing chemicals and reduces the costs of constructing the plant by eliminating the costs associated with building storage tanks. Also the flow of process contents through the plant are optimised by continuously using the contents, which are a substantial economic outlay. However, control of these processes is more difficult and critical. Therefore a larger number of process control systems are used and many are interlinked into a single control system.

### 1.1.2 Process Analysis<sup>1,2,4</sup>

Process analysis is employed to measure physical (for example, temperature and pressure) and chemical (qualitative and quantitative composition of process contents) dynamic variables. Process analytical chemistry (PAC)<sup>4,5</sup> discussed further in this chapter, describes the instrumentation and techniques employed for the measurement of chemical dynamic variables ranging from simple species like the proton to complex organic and inorganic compounds. The variety of techniques and instruments employed

and the current areas of research have been discussed recently<sup>6,7</sup>. Process analysis and PAC are employed for two functions<sup>1,4,5</sup>. As previously discussed they are employed to enable processes to be controlled and to assist in improving productivity and product quality while maintaining process operations at or within safety and environmental legislation. Alternatively process analysis can also be used for process research in the laboratory or on the pilot and process plants.

Process analysis employed on the laboratory scale or pilot plant is used to model and optimise process operations. The information collected can allow plant engineers and chemists to design a process plant which will provide economically efficient manufacture of chemicals at the rate of productivity required, and to choose the critical operating parameters to be monitored and regulated during chemical production.

Process analysis results can also be integrated into process control systems to ensure that productivity is maintained or improved while also sustaining the required quality specifications of the product. Product quality and the consistency of this quality has a major influence on the products price in the global market<sup>4</sup>. Producing product above or below the required specifications is uneconomical and is not favourable for high productivity. Product of too low quality requires recycling and product of too high quality requires extra time and energy to obtain the purity. Finally the highly automated nature of many process control systems provides consistent applications of functions required to conform with quality control and assurance programmes.

The safe operation of process plants with low emission volumes to the environment are required legally and by public demand. Process analysis can ensure that plants are operated within safety limits specified by legislation and automated process control procedures can remove plant personnel from potentially hazardous environments.

Furthermore with appropriate control of the process, emissions to the environmental matrices of air, water and land can be limited to or maintained below the legal requirements. Emissions can be either directly from the process plant or indirectly from the disposal of below specification products or waste chemicals. Finally the implementation of on-line instruments can provide monitoring of process environments for fugitive emissions that are hazardous to plant personnel and local communities.

A range of analysis strategies are currently employed in the chemical industry<sup>4,5</sup>, with classification based on the method of sampling, location and frequency of analyses and the instrument employed. Traditionally, analyses were performed in laboratories located away from the sampling point. Changes in the needs of the chemical industry to increase productivity and advances in technology are fuelling the migration of analyses from the laboratory onto or into the process.

#### 1.1.2.1 Off-line Analysis

The traditional approach for process analysis employs manual sampling and transport of the sample to a site-centralised laboratory located from tens to thousands of metres from several different plants on site. Samples are logged in, prioritised, prepared for analysis and analysed before the results are reported to the necessary personnel. The relatively long times required for sampling and analysis culminate in low analysis frequencies. A frequency greater than 2 analyses per day can provide results that can be used in process control systems employed on slowly operated plants. However lower analytical frequencies can not generally provide results rapidly enough for appropriate

use in a process control system. In these cases the results are used for post-mortem quality control and assurance<sup>8</sup> and can also be employed for process modelling and optimisation<sup>5</sup>.

The laboratory employs state-of-the-art instrumentation operated by highly trained scientists in most cases. The economy and efficiency of sharing expensive equipment and personnel with several process or pilot plants along with the availability of scientists for consultation, method development and maintenance are all economically and scientifically advantageous.

#### 1.1.2.2 At-line Analysis

The low analysis frequency obtainable for many off-line analyses is not normally compatible with required process control cycle times. The transfer of the analysis from the laboratory to a position in close proximity to the process allows analyses to be performed more quickly because of the shorter times required to transport samples from the process to the analytical instrument. Results produced at an adequate frequency for incorporation into process control systems are therefore achievable.

The analytical instrument used is employed normally for one application only and is easier to operate compared to laboratory instruments. The sampling, sample preparation and analysis steps are performed by plant personnel who are less highly trained than the scientists employed in the laboratory. All of the steps necessary for the production of analytical results must therefore be simple to perform. This ensures an accurate result is obtained by plant personnel which can be simply understood and incorporated into a process control system.

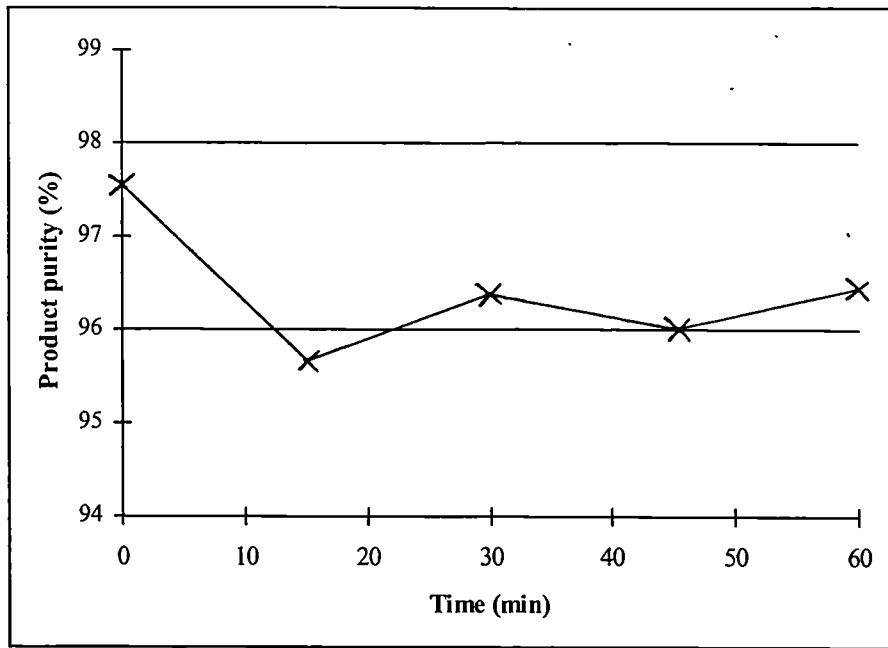
### 1.1.2.3 On-line Analysis

Automated sampling systems, instruments and data presentation are employed for on-line analyses. Automation and the close proximity of instrument and sampling point reduce the time required for a result to be produced by removing human intervention and the majority of time required for sample transportation and preparation. An analysis can be performed in the range of one second to 30 minutes. Real or near-real time information related to a process can therefore be provided to allow process control systems to operate with fast cycle times or to provide a large volume of information quickly during process modelling and optimisation. Dedicated to one application, instruments need to be tolerant and robust to operate successfully in the process environment.

Intermittent analyses employing periodic sample injections into an instrument can be used or alternatively continuous analyses employing the continuous flow of sample through an instrument can be used. 80-90% of all problems encountered in on-line analyses, however, are attributable to the sampling system which provides the sample to the instrument in an appropriate condition<sup>9</sup>. The application of non-invasive<sup>4</sup> and in-line<sup>10</sup> techniques eliminates the requirement for the sampling step and therefore removes the possible problems encountered. Non-invasive techniques use a flow cell placed in the process line to measure the changes in for example electromagnetic radiation passing through the sample, whereas in-line techniques employ probes placed in the sample stream to perform selective analyses.

The effect of the analysis frequency on product quality can be shown graphically in Figure 1.1, which shows the purity of product at the end of a process over a period of 60 minutes. A large time difference between analyses are observed with at-line strategies (Graph A) during which fluctuations in the process may not be detected. If a product of too low purity is being produced it will continue to be produced until the next analysis is performed, which may be from 15 minutes to six hours. This results in recycling of product and a drop in productivity. On-line strategies only have small time differences between analyses (Graph B) and the trends leading to production of too low purity or too high purity products are more likely to be detected. Therefore the trends can be reversed, before the product purity changes to a value outside the specified range, by the application of external influences (shown by an arrow in the graphs). Therefore the product is only produced within the specified range of purities. The application of on-line analysis will normally result in a more economically efficient process plant. The same conclusions can be observed when comparing off-line and on-line analysis frequencies.

Graph A



Graph B

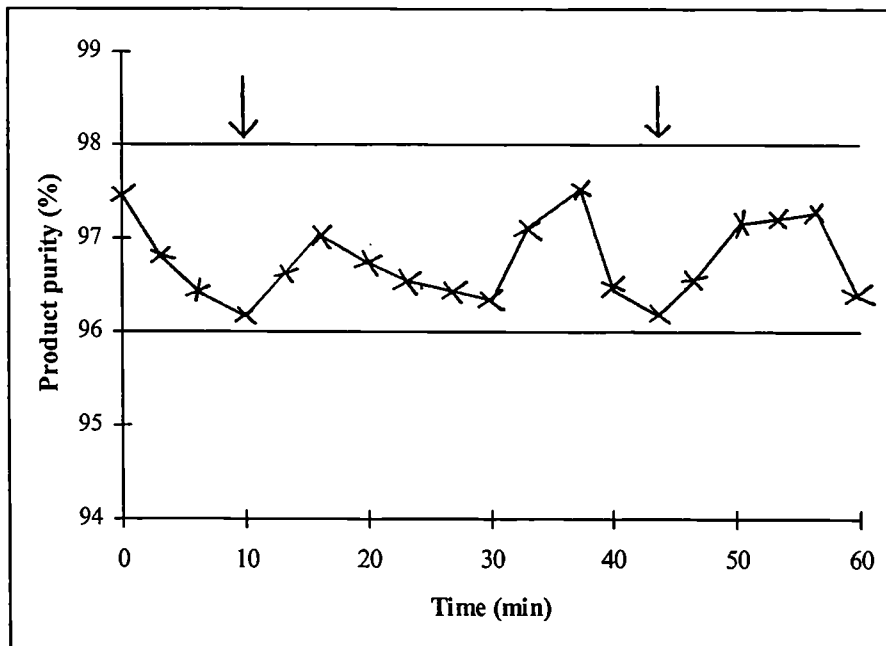


**Figure 1.1** The differences in analysis frequencies for at-line (A) and on-line (B) strategies

### 1.1.3 The Implementation of On-line Process Analysis Technology<sup>4,9</sup>

The implementation of instrumentation to be employed for on-line analyses is a complex operation composed of six distinct stages:

- 1) Establishment of the need for on-line analyses.
- 2) Collection of the required resources (financial and scientific personnel).
- 3) Selection of the appropriate technique to employ.
- 4) Selection of a reliable instrument to employ.
- 5) Validation of the instrument.
- 6) Maintenance.

Implementation of on-line analysis technology is normally a time consuming operation which is more time and economically intensive with respect to off-line technology implementation. This is because of the smaller volume of experience and knowledge currently available for the implementation of on-line analysis technology.

The requirement to use on-line analysis technology normally arises from the advantages it can provide to allow chemical companies to obtain a cutting edge in the market, as was discussed in section 1.1.1. However the resources to finance the purchase, validation and maintenance of an instrument need to be available and are normally greater than for the implementation of off-line instrumentation. Even when an instrument is purchased scientific personnel need to be available either from within the chemical company or from an external company to ensure validation and maintenance is performed correctly. Today multi-disciplinary working groups composed of analytical

chemists, engineers, plant operators and production managers are gathered together<sup>4,9</sup> to implement on-line analysis technology correctly for its most appropriate operation and also to ensure the technologies operate correctly with a minimum of problems.

The correct selection of an appropriate analytical technique is very important. For example, when analysis frequencies of two per minute are required chromatographic techniques which operate at a lower analysis frequency can not be used. However if a result every twenty minutes is adequate then gas or liquid chromatography should be selected if they can provide the required information because chromatographic techniques are relatively inexpensive and highly understood when compared with other currently used instrumentation for on-line analyses.

Reliable instrumentation was not always available in the early applications of on-line technology during the 1950s and 1960s. This resulted in a lack of confidence for the techniques employed and the results produced, and a relatively small number of applications with respect to laboratory analyses. The confidence of users to employ on-line analytical instrumentation needs to be achieved for on-line analysis to be successful. It has been remarked that a number of champions are required to push the cultural changes forward<sup>5</sup>. An increasing use of on-line instrumentation is being observed. A 12-13% annual growth in on-line instrumentation sales in the period 1992-1995 was predicted, of which the majority of growth was attributable to instruments employed for monitoring the workplace and environmental emissions<sup>9</sup>. Today instrument companies commercially supply specially designed process analysers which are employed with a high degree of reliability on a process plant for on-line analyses. Advances in technology (electronic circuitry, for example) and materials (for example, membranes) have enabled instruments to be designed robustly and to operate reliably.

Validation of an instrument, either purchased or used on loan for field evaluations, can be performed in the laboratory, on the plant or in both environments. Analytical parameters<sup>11</sup> investigated include sensitivity, calibration ranges, specificity, precision and accuracy. Reliability and ruggedness are other parameters which are important for instruments operating on the plant because of its harsher environment with respect to the laboratory.

Once the analytical instrument is validated and is collecting data for either process research or to be included in process control systems, calibration and maintenance is periodically required. The frequency of calibration, and maintenance of the instrument components, is dependant on the instrument and its ruggedness. Maintenance can be performed at a low frequency by either chemical company engineers or by instrument company engineers. Many instrument companies provide maintenance contracts because of the complexity of currently employed instruments.

## **1.2 Off-line Mass Spectrometry**

In the 100 years since mass spectrometry was introduced to the scientific world<sup>12</sup> many developments and improvements in the instruments employed have continuously enlarged the application field. Today a range of mass spectrometers combining a variety of different inlet systems, ion sources, mass analysers and detectors are available for the analysis of gaseous, liquid or solid samples.

The majority of off-line analyses have no time constraints and therefore time consuming sample preparation and analysis stages can be employed. This has resulted in the use of the complete range of mass spectrometer instrumentation available for the off-

line analysis of process samples. Table 1.1 displays the range of techniques currently available.

Technique	Comments
Gas chromatography-mass spectrometry (GC-MS) and liquid chromatography-mass spectrometry (LC-MS)	Most commonly applied techniques. These will be discussed in this section
Supercritical fluid chromatography mass spectrometry (SFC-MS) <sup>13,14</sup>	A less popular technique with respect to GC-MS and LC-MS, though the number of applications is increasing
Open access mass spectrometry <sup>15</sup>	New technique employed for the automated qualitative analysis of samples by non-mass spectrometrists. Can be developed for quantitative analyses
Heated probes <sup>16,17</sup>	Samples are placed on a probe and introduced through a vacuum lock into the mass spectrometer ion source
Field desorption (FD) <sup>16,18</sup>	Employs high electrical field strengths to ionise liquid samples coated on a filament by electron removal from sample molecules
Fast atom bombardment (FAB) <sup>19</sup> , secondary ion mass spectrometry (SIMS) <sup>16</sup> and matrix assisted laser desorption and ionisation (MALDI) <sup>20</sup>	Samples are dissolved in an appropriate matrix is bombarded with energetic beams of atoms (FAB), ions (SIMS) and electromagnetic radiation to obtain volatilisation and ionisation

**Table 1.1** The techniques currently available for the analysis of process liquid samples

The techniques listed, with the exception of employing mass spectrometers as gas and liquid chromatograph detectors, are generally limited to specific applications in certain sections of the chemical industry. The complex nature and expense of the majority of the instrumental techniques listed and in some cases the time consuming sample preparation and analysis stages has resulted in their limited use. However the combination of sample component separation in a gas or liquid chromatograph with a mass spectrometer providing selective and sensitive detection has become routinely applied in the laboratory for the analysis of gases, and volatile and involatile liquid analytes. Sample characterisation can be performed with mass range scanning or alternatively quantification of compounds can be performed with single ion monitoring (SIM).

Holmes and Morrell<sup>21</sup> first coupled a gas chromatograph and mass spectrometer in 1958, viewing the separate techniques as mutually compatible because of their use of gases or volatile liquids. The only limited operating parameter is the carrier gas flow rate entering the mass spectrometer, low flow rates are required to maintain vacuum pressures in the mass spectrometer. Today the majority of gas chromatographs employ capillary columns<sup>22</sup> and flow rates of 1-2 ml min<sup>-1</sup> which can be accommodated by the mass spectrometer. In these cases the capillary can be extended into the mass spectrometer ion source or the column effluent can be introduced through an open-split coupling<sup>23</sup>. Heating is required between the gas chromatograph and the mass spectrometer ion source to eliminate condensation, absorption of high boiling point compounds on active surfaces and the loss of chromatographic resolution.

Packed and wide bore columns employ higher gas flow rates in the range 5-50 ml min<sup>-1</sup>, which are too high to allow the introduction of the complete column effluent into

the mass spectrometer. One interface<sup>16</sup> involves splitting the column effluent flow so that a portion is transported to the mass spectrometer while the unused effluent flow is pumped away before it enters the mass spectrometer. A reduction in sensitivity, with respect to the use of capillary column gas chromatography, is observed with this interface because the total effluent flow is not analysed. To improve the sensitivity separators are employed to remove some or all of the carrier gas from the column effluent between the gas chromatograph and mass spectrometer. Membrane separators employ Teflon<sup>24</sup> or silicone rubber<sup>25</sup> membranes to provide preferential permeation of carrier gas or analyte through the membrane. Alternatively, jet separators<sup>26</sup>, first introduced by Ryhage<sup>27</sup>, use the differences in velocity of the carrier gas and organic compounds in an expanding supersonic jet to provide separation. The supersonic jet is created by passing the column effluent through a narrow orifice into a pumped region operating at low pressures<sup>27</sup>. Organic compounds of greater molecular mass than the carrier gas will obtain higher velocities, and 50-70% of these compounds are entrained into the mass spectrometer while the lower molecular mass carrier gas is pumped away.

A selection of books<sup>22,28,29</sup> and a review paper<sup>30</sup> have comprehensively discussed the technique of GC-MS including the associated challenges and applications. A recent review has listed the current companies manufacturing GC-MS instrumentation<sup>31</sup>.

Liquid chromatography-mass spectrometry is used as an alternative to GC-MS for analysing liquid samples of lower volatility than used in GC-MS. The coupling of the two analytical instruments has been demonstrated to be a difficult task and the problem of introducing a high pressure liquid flow to an instrument operated at vacuum pressures for the analysis of gaseous samples has no one perfect solution<sup>32</sup>. Several techniques are

currently available, and have been discussed<sup>32,33,34,35</sup>, to enable the coupling of a liquid chromatograph to a mass spectrometer. However, each technique applies constraints on the liquid chromatograph or mass spectrometer operating conditions.

Transport interfaces (moving belt, particle beam) remove the solvent and introduce the analyte to the mass spectrometer ion source, normally an electron impact ion source to provide structural information. Vaporisation of the column effluent and subsequent introduction of the vapour in to the mass spectrometer requires a fast vacuum pumping speed and a low effluent flow rate to maintain the instruments vacuum. This can be performed with the direct liquid introduction (DLI), thermospray and continuous flow-fast atom bombardment (CF-FAB) interfaces. To overcome the various problems concerned with maintaining the instrument vacuum pressures, the ion source and sample inlet system can be separated from the mass spectrometer components requiring operation at vacuum pressures. Here nebulisation can be performed into high pressure ion sources employing atmospheric pressure ionisation (API). Electrospray and atmospheric pressure chemical ionisation (APCI) can generate ions which are sampled into the mass analyser operating at vacuum pressures through an ion skimmer or a series of differentially pumped stages. These two techniques will be comprehensively discussed in the preliminary results shown in the section after chapter six.

### 1.3 On-line Mass Spectrometry

In the late 1940s and 1950s mass spectrometry was beginning to be applied for the on-line analysis of gaseous process streams in the chemical<sup>36,37</sup> and nuclear<sup>38</sup> industries. The development of gas chromatography<sup>39</sup> in the 1950s and its subsequent application<sup>40,41</sup> for the on-line analysis of gases and low boiling point liquids from the beginning of the 1960s posed a substantial obstacle to the application of mass spectrometry and the number of on-line applications employing process mass spectrometers decreased. Gas chromatographs were not only cheaper but also provided a greater reliability and ease of operation<sup>42</sup>. In comparison mass spectrometers were relatively expensive and large and were viewed as unreliable instruments that required skilled scientists to operate and maintain, and interpret the data.

The popularity and number of on-line applications of mass spectrometry has been growing since the early 1970s, even though the gas chromatograph was and still is very popular. The expected growth in market sales<sup>9</sup> of process mass spectrometers for the period 1991-1995 was 18%, caused by the changing needs of the chemical industry to increase productivity while complying with government and customer legislation. The improvements in instrument design and operation also aided the instruments resurgence<sup>43</sup>. Although still relatively expensive the currently available process mass spectrometers are smaller with respect to the mass spectrometers of thirty years ago because of the reductions in component sizes. Process mass spectrometers can provide reliable accurate operation with a minimum of periods of non-operation (downtime) in process environments, which are harsher than the laboratory environment. An improved instrument design, stable low cost electronics and more reliable vacuum systems have all

contributed to the highly improved reliability<sup>42</sup>. The incorporation of electronic hardware and computing power has also enabled the automation of the instrument and on-line processing and presentation of data for immediate feedback into the process control system with which it can be linked<sup>44</sup>. Presently, automated rapid multi-component and multi-point analyses of components in the concentration range ppb to 100% are achievable. The current specifications and limitations of process mass spectrometers are listed in Table 1.2<sup>45,46</sup>.

Large range of concentrations detectable (ppb to 100 %)
Rapid analysis times (< ten seconds for one analyte)
High accuracy and precision
Multi-component analyses (upto 16 analytes per sample)
Multi-point analyses (upto 64 different points of sampling)
Fully automated operation
Reliable operation in process environments
Expensive when compared to other on-line process analysers

**Table 1.2** The current specifications and limitations of process mass spectrometers

The majority of applications of process mass spectrometers have been for the analysis of gaseous streams and environments, as reviewed by Scrivens<sup>42</sup> and Nicholas<sup>45</sup>.

Applications in the iron and steel, semi-conductor, chemical and nuclear industries and for monitoring the atmosphere in real-time are discussed below.

The iron and steel industry employ process mass spectrometers to monitor blast furnace off-gases to optimise and control the production of metal alloys and ensure the correct product specifications are maintained<sup>47,48,49</sup>. Also on some production sites off-gases such as carbon monoxide and carbon dioxide are mixed and combusted to produce energy and reduce energy consumption from external sources. On-line monitoring of stations where gases are mixed can ensure that the gases are combined in the correct ratios to achieve the highest calorific value for combustion<sup>45</sup>. The production of low molecular weight organic compounds by bioorganisms during fermentation processes also requires on-line process analysis to monitor the progress of the fermentation process and detect the consumption and production of wanted and unwanted chemicals. Process mass spectrometers are employed to perform this task by monitoring the off-gases present in the fermentor headspace<sup>50,51,52</sup> and also by monitoring the liquid phase fermentation broth using membrane introduction mass spectrometry (MIMS)<sup>53,54,55</sup>.

Process mass spectrometers are employed for three different functions in the production of integrated circuits in the semi-conductor industry. The sub-atmospheric pressure gaseous environments employed during manufacture require impurities such as carbon dioxide and water to be present at low levels to maintain a minimal contamination of the circuit boards. Too high levels of contaminants in the gas phase will result in faulty circuit boards. The on-line monitoring of gases at parts per trillion concentrations during the manufacturing process is required for quality control. Atmospheric pressure ionisation mass spectrometry is employed for this function<sup>56,57</sup>. The vacuum environments surrounding the circuit boards are also monitored on-line for

the presence of contaminants by electron impact ionisation mass spectrometers<sup>58,59</sup>. Finally process mass spectrometers can be employed for analysing the plasma produced during some manufacturing processes and employing the results in a process control system<sup>60,61,62</sup>. The rapid analysis times required for all of these functions are provided by the mass spectrometer, also often called a residual gas analyser (RGA).

A limited number of applications in the chemical industry of on-line mass spectrometry can be found. The confidential and commercially sensitive nature of some of the processes monitored has probably resulted in the lack of open publication of the work. Cessna has used a process mass spectrometer for on-line analysis of organic and inorganic compounds present in fuel gas streams in a petrochemical plant<sup>63</sup>. LaPack et al. has employed MIMS for the analysis of influent and effluent gases and liquids in a wastewater treatment reactor and the subsequent control of the process<sup>64</sup>. MIMS has also been employed for the on-line monitoring of the liquid phase for nitrogen trichloride formation during wastewater treatment<sup>65</sup>. Scrivens<sup>43</sup> and Bartman<sup>66</sup> have both described the monitoring and subsequent process control of an ethylene oxide process plant with on-line mass spectrometric analysis of the gases involved in the process. Mass spectrometers were shown to provide the high accuracy required which other instruments could not provide. DesJardin et al. have recently described various applications of process mass spectrometers to provide a better understanding of pilot and process plant operations<sup>67</sup>. The application of heated inlets to provide vaporisation of a liquid for on-line monitoring of a rubber production<sup>68</sup> and a chemical process plant<sup>69</sup> have been recently reported. Finally the gaseous effluents flowing from a high temperature gas cooled reactor fuel particle preparation process in the nuclear industry has been monitored on-line by a mass spectrometer<sup>70</sup>.

Process mass spectrometers can also be employed for real-time monitoring of gaseous workplace environments and effluent stacks. Khan<sup>71</sup> and Erb<sup>72</sup> have used a multi-point sampling system with a mass spectrometer to analyse up to 64 different environments for releases or leaks of chemicals hazardous to personnel present in the environment. Detection of chemicals above a specified concentration results in alarms being raised and appropriate action being undertaken. Cycle times to analyse all 64 environments can be as small as two minutes. Erb<sup>72</sup> and Ketkar<sup>73</sup> have also performed real-time monitoring of actual and simulated stack emissions, respectively.

A variety of non-industrial applications of mass spectrometers involve real-time monitoring of the atmosphere. McLuckey et al. have employed glow discharges<sup>74</sup> for the sensitive detection of 2,4,6-trinitrotoluene at 1-2 ppt concentrations. Alternatively several authors have employed atmospheric pressure chemical ionisation-mass spectrometry (APCI-MS) for the detection of sulphur containing compounds<sup>75,76</sup> and chemical warfare agents<sup>77</sup> in the atmosphere. MIMS<sup>78</sup> can be employed to improve the sensitivity and tandem mass spectrometers<sup>77</sup> can be used to improve the selectivity. Molecular beam laser mass spectrometry has also been studied to provide real time detection of chemical agents<sup>79</sup>.

As can be observed in the short review above there are relatively few reported applications for the on-line mass spectrometric analysis of liquid streams or environments. The number of applications summarised above will be discussed further in Chapters three, five and six.

## 1.4 Research Objectives

Scrivens recently commented on the current remaining problem areas for process mass spectrometry<sup>43</sup>. One area presenting problems is sampling where improvements are needed in order to study liquid samples. The primary objective of the work presented in this thesis is to evaluate and validate appropriate techniques which enable the direct off-line and on-line analysis of liquids using a mass spectrometer.

Two strategies are available to provide the direct analysis of liquids by a mass spectrometer (Table 1.3).

Strategy	Partial or complete vaporisation of the liquid sample externally to the mass spectrometer and the subsequent introduction of the vapour created into a mass spectrometer	Application of previously developed interfaces employed to couple a liquid chromatograph and mass spectrometer
Technique / Interface employed	Headspace analysis (HSA), total vaporisation analysis (TVA), membrane introduction mass spectrometry (MIMS).	Moving belt (MB), particle beam direct liquid introduction (DLI), thermospray (TSP), electrospray (ESP), atmospheric pressure chemical ionisation (APCI)
Sample compatibility	Low boiling point analytes and / or matrices because of the requirement for selective or complete vaporisation	With the correct interface there is no significant limit on the analyte and matrix boiling points

**Table 1.3** Strategies that can be employed for the direct analysis of liquid samples by a mass spectrometer.

One strategy employs the partial or complete vaporisation of the liquid externally to the mass spectrometer with an appropriate interface used to fulfil this function. Process mass spectrometers currently employed for the analysis of gas phases are respected in the chemical industry and have a high level of reliability. These process mass spectrometers can be coupled with an interface described above to allow the rapid implementation of this strategy with no necessity to obtain the confidence of various chemical company personnel for an unvalidated process mass spectrometer. The second strategy employs the technology used for coupling a liquid chromatograph to a mass spectrometer discussed previously. The type of sample introduction and ionisation varies between the separate technologies.

The objectives of the research reported in this thesis are to study and validate, in the laboratory, a range of techniques that can be employed for the rapid and direct off-line and on-line analysis of liquid streams encountered in the section of the chemical industry manufacturing low molecular weight organic compounds. The techniques of headspace analysis, total vaporisation analysis, membrane introduction mass spectrometry and atmospheric pressure ionisation will be studied and validated.

Two liquid streams were employed during the work, chosen to be representative of a process and effluent stream respectively; methyl iodide (analyte) in acetic acid and acetone (analyte) in water. Process samples obtained from BP Chemicals in Hull were also analysed to ascertain the potential applicability of the techniques for the analysis of liquid streams.

## 1.5 References

- 1) Koch, M., *Proc. Cont. Qual.*, 1994, **6**, 3.
- 2) Ponton, J.W., *Chem. and Ind.*, 1993, **100**, 315.
- 3) Johnson, C.D., *Process Control Instrumentation and Technology*, Wiley, Chichester, 1982, Chapter one.
- 4) Callis, J.B., Illman, D.L., and Kowalski, B.R., *Anal. Chem.*, 1987, **59**, 624A.
- 5) McLennan, F., *Process Analytical Chemistry*, McLennan, F. and Kowalski, B., (Editors), Blackie Academic and Professional, London, 1995, Chapter one.
- 6) Beebe, K.R., Blaser, W.W., Bredeweg, R.A., Chauvel, J.P., Harner, R.S., LaPack, M., Leugers, A., Martin, D.P., Wright, L.G., and Deniz Yalvac, E., *Anal. Chem.*, 1993, **65**, 199R,
- 7) Blaser, W.W., Bredeweg, R.A., J.P., Harner, R.S., LaPack, M.A., Leugers, A., Martin, D.P., Pell, R.J., Workman Jr., J., and Wright, L.G., *Anal. Chem.*, 1995, **67**, 47R.
- 8) Riebe, M.T., and Eustace, D.J., *Anal. Chem.*, 1990, **62**, 65A.
- 9) Clevett, K.J., *Proc. Cont. Qual.*, 1994, **6**, 81.
- 10) Hirschfeld, T., Callis, J.B., and Kowalski, B.R., *Science*, 1984, **226**, 312.
- 11) Scrivens, J.H., *Vacuum*, 1982, **32**, 169.
- 12) Svec, H.J., *Int. J. Mass Spectrom. Ion Processes*, 1985, **66**, 3.
- 13) Sandra, P., *Supercritical Fluid Chromatography*, Smith, R.M., (Editor), Royal Society of Chemistry, Cambridge, 1987, Chapter five.
- 14) Pinkston, J.D., and Chester, T.L., *Anal. Chem.*, 1995, **67**, 650A.
- 15) Spreen, R.C., and Schaffter, L.M., *Anal. Chem.*, 1996, **68**, 414A.

- 16) Chapman, J.R., *Practical Organic Mass Spectrometry*, Wiley, Chichester, 2nd Edition, 1993.
- 17) Yergey, A.L., *Biomed. Mass Spectrom.*, 1979, **6**, 465.
- 18) Lattimer, R.P., and Schulten, H.R., *Anal. Chem.*, 1989, **61**, 1201A.
- 19) Caprioli, R.M., *Anal. Chem.*, 1990, **62**, 477A.
- 20) Hillenkamp, F., Karas, M., Beavis, R.C., and Chait, B.T., *Anal. Chem.*, 1991, **63**, 1193A.
- 21) Holmes, J.C., and Morrell, F.A., *Appl. Spectrosc.*, 1957, **11**, 86.
- 22) Masucci, J.A., and Caldwell, G.W., *Modern Practice of Gas Chromatography*, Grob, R.L., (Editor), Wiley, Chichester, 3rd Edition, 1995, Chapter six.
- 23) Henneberg, D, Henrichs, U., and Schomburg, G., *J. Chromatogr.*, 1975, **112**, 343.
- 24) Lipsky, S.R., Horvath, C.G., and McMurray, W.J., *Anal. Chem.*, 1966, **38**, 1585.
- 25) Black, D.R., Flath, R.A., and Teranishi, R., *J. Chromatogr. Sci.*, 1969, **7**, 284.
- 26) Novotny, M., *Chromatographia*, 1969, **2**, 350.
- 27) Ryhage, R., *Anal. Chem.*, 1964, **36**, 759.
- 28) McFadden, W., *Techniques of Combined Gas Chromatography/Mass Spectrometry: Applications in Organic Analysis*, Wiley, London, 1973.
- 29) Evershed, R.P., *Gas Chromatography : A Practical Approach*, Baugh, P.J., (Editor), Oxford University Press, Oxford, 1993, Chapter eleven.
- 30) Hinshaw, J.V., *LC-GC Int.*, 1995, **8**, 22.
- 31) Wach, F., *Anal. Chem.*, 1994, **66**, 927A.
- 32) Niessen, W.M.A., and Greef, J.V.D., *Liquid Chromatography-Mass Spectrometry : Principles and Applications*, Marcel Dekker Inc., New York, 1992.



- 33) Tomer, K.B., *HPLC Detection : Newer Methods*, Patonay, G., (Editor), VCH Publishers, New York, 1992, Chapter eight.
- 34) Covey, T.R., Lee, E.D., Bruins, A.P., and Henion, J.D., *Anal. Chem.*, 1986, **58**, 1451A.
- 35) Garcia J.F., and Barceló, J., *J. High Resolution Chromatogr.*, 1993, **16**, 633.
- 36) Robinson, C.F., *Chem. Eng.*, 1951, **58**, 136.
- 37) Walker, J.K., Gifford, A.P., and Nelson, R.H., *Ind. Eng. Chem.*, 1954, **46**, 1400.
- 38) Nier, A.O., Abbott, T.A., Pickard, J.K., Leland, W.T., Taylor, T.I., Stevens, C.M., Dukey, D.L., and Goertzel, G., *Anal. Chem.*, 1948, **20**, 188.
- 39) James A.T., and Martin, A.J.P., *Analyst.*, 1952, **77**, 915.
- 40) Escher, E.E., *Chem. Eng.*, 1959, **66**, 113.
- 41) Petrocelli, J.A., Puzniak, T.J., and Clark, R.O., *Anal. Chem.*, 1964, **36**, 1008.
- 42) Scrivens, J.H., *Trans. Inst and Measurement Control*, 1985, **7**, 2.
- 43) Scrivens, J.H., *Reviews on Analytical Chemistry - Euroanalysis VIII*, Littlejohn, D., and Burns, T.D., (Editors), Royal Society of Chemistry, Cambridge, 1994, p 145.
- 44) Damoth, D.C., and Montgomery, K.L., *Chem. Eng. Progr.*, 1972, **68**, 51.
- 45) Nicholas, P., *Spectroscopy*, 1991, **6**, 36.
- 46) Walsh, M.R., and LaPack, M.A., *ISA Trans.*, 1995, **34**, 67.
- 47) Schuy, K.D., and Reinhuld, B., *Meas. and Cont.*, 1971, **4**, T84.
- 48) Smith, A., and Pettifor, M.J., *Vacuum*, 1982, **32**, 175.
- 49) Nicholas, P., *Met. Mater.*, 1990, **57**, 165.

- 50) Berecz, I., Bohátka, S., Diós, Z., Gál, I., Gál, J., Kiss, L., Kovacs, R.M., Langer, G., Molnár, J., Paál, A., Sepsy, K., Szakó, I., and Székely, G., *Vacuum*, 1987, **37**, 85.
- 51) Coppella, S.J., and Dhurjati, P., *Biotechnol. Bioeng.*, 1987, **29**, 679.
- 52) Dadd, A.T., *Am. Biotechnol. Lab.*, 1990, **8**, 35.
- 53) Heinzle, E., Kramer, H., and Dunn, I.J., *Biotechnol. Bioeng.*, 1985, **27**, 238.
- 54) Srinivasan, N., Kasthurikrishnan, N., Cooks, R.G., Krishnan, M.S., and Tsao, G.T., *Anal. Chim. Acta*, 1995, **316**, 269.
- 55) Hayward, M.J., Kotiaho, T., Lister, A.K., Cooks, R.G., Austin, G.D., Narayan, R., and Tsao, G.T., *Anal. Chem.*, 1990, **62**, 1798.
- 56) Mitsui, Y., Kambara, H., Kojima, M., Tomita, H., Katoh, K., and Satoh, K., *Anal. Chem.*, 1983, **55**, 477.
- 57) Fisons Instruments Application Note G.A.S. 008.
- 58) Koprio, J., Mural, P., Rettinghaus, G., and Strasser, G., *Vacuum*, 1990, **41**, 2106.
- 59) Buckley, M.E., *Vacuum*, 1993, **44**, 665.
- 60) Koprio, J.A., Peter, G., and Fischer, H., *Vacuum*, 1988, **38**, 783.
- 61) Fischer, H., Grob, M., Peter, G., and Koprio, J.A., *J. Vac. Sci. Technol. A*, 1988, **6**, 2103.
- 62) Choudhury, A., *Metallurgical Plant and Tech.*, 1988, **5**, 44.
- 63) Cessna, G.D., *Adv. Instrum. Control*, 1990, **45**, 383.
- 64) LaPack, M.A., Tou, J.C., and Enke, C.G., *Anal. Chem.*, 1991, **63**, 1631.
- 65) Savickas, P.J., LaPack, M.A., and Tou, J.C., *Anal. Chem.*, 1989, **61**, 2332.
- 66) Bartman, C.D., *Am. Lab.*, 1985, **17**, 57.
- 67) DesJardin, M.A., Doherty, S.J., Gilbert, J.R., LaPack, M.A., and Shao, J., *Proc.*

- Cont. Qual.*, 1995, **6**, 219.
- 68) Tou, J.C., and Reddy, D., *Anal. Chim. Acta*, 1990, **229**, 9.
- 69) Didden, C., and Duisings, J., *Proc. Cont. Qual.*, 1992, **3**, 263.
- 70) Lee, D.A., Constanzo, D.A., Stinton, D.P., Carpenter, J.A., Rainey, W.T., Canada, D.C., and Carter, J.A., *Nuclear Technol.*, 1977, **34**, 89.
- 71) Khan, K., *INTECH*, 1993, **40**, 40.
- 72) Erb, J., Ortiz, E., and Woodside, G., *Chem. Eng. Progr.*, 1990, **86**, 40.
- 73) Ketkar, S.N., Dulak, J.G., Fite, W.L., Buchner, J.D., and Dheandhanoo, S., *Anal. Chem.*, 1989, **61**, 260.
- 74) McLuckey, S.A., Glish, G.L., Asano, K.G., and Grant, B.C., *Anal. Chem.*, 1988, **60**, 2220.
- 75) Berresheim, H., Tanner, D.J., and Eisele, F.L., *Anal. Chem.*, 1993, **65**, 84.
- 76) Eisele, F.L., and Berresheim, H., *Anal. Chem.*, 1992, **64**, 283.
- 77) Ketkar, S.N., Penn, S.M., and Fite, W.L., *Anal. Chem.*, 1991, **63**, 457.
- 78) Cisper, M.E., Gill, G.C., Townsend, L.E., and Hemberger, P.H., *Anal. Chem.*, 1995, **67**, 1413.
- 79) Syage, J.A., *Anal. Chem.*, 1990, **62**, 505A.

## **Chapter Two**

### **Instrumentation**

## 2.1 Introduction

While experimenting in the first decade of the 20th century, J.J. Thompson separated positively charged rays in his laboratory<sup>1</sup>. The technique of mass spectrometry was born and in the following 90 years many pioneers, including Dempster, Aston and Nier, have contributed to the development of the mass spectrometer<sup>2,3</sup>. This has resulted in the current state of maturity of the technique. Today a wide range of gaseous, liquid and solid samples can be analysed to acquire qualitative information concerned with the molecular weight and structure of compounds, or alternatively, samples can be analysed to obtain quantitative data relating to the presence of atomic or molecular species.

The construction of a mass spectrometer can be divided into five components (Figure 2.1), each with a separate function<sup>2,4</sup>. Mass spectrometers operate by creating gaseous ions in the ion source and subsequently separating ions of different mass to charge ( $m/e$ ) ratios in the mass analyser, before the separated ions are detected electrically. A wide variety of different approaches have been used to accomplish the function of each component and a few examples are listed in Table 2.1 for four of the components.

Mass discrimination in the mass analyser is achieved by the application of an external field, in which ions of dissimilar mass and charge are forced to follow different spatial trajectories and therefore ions are separated. With a controlled alteration of the applied field ions of increasing mass to charge ratios can be separated and detected in series to generate a mass spectrum of  $m/e$  versus ion intensity.

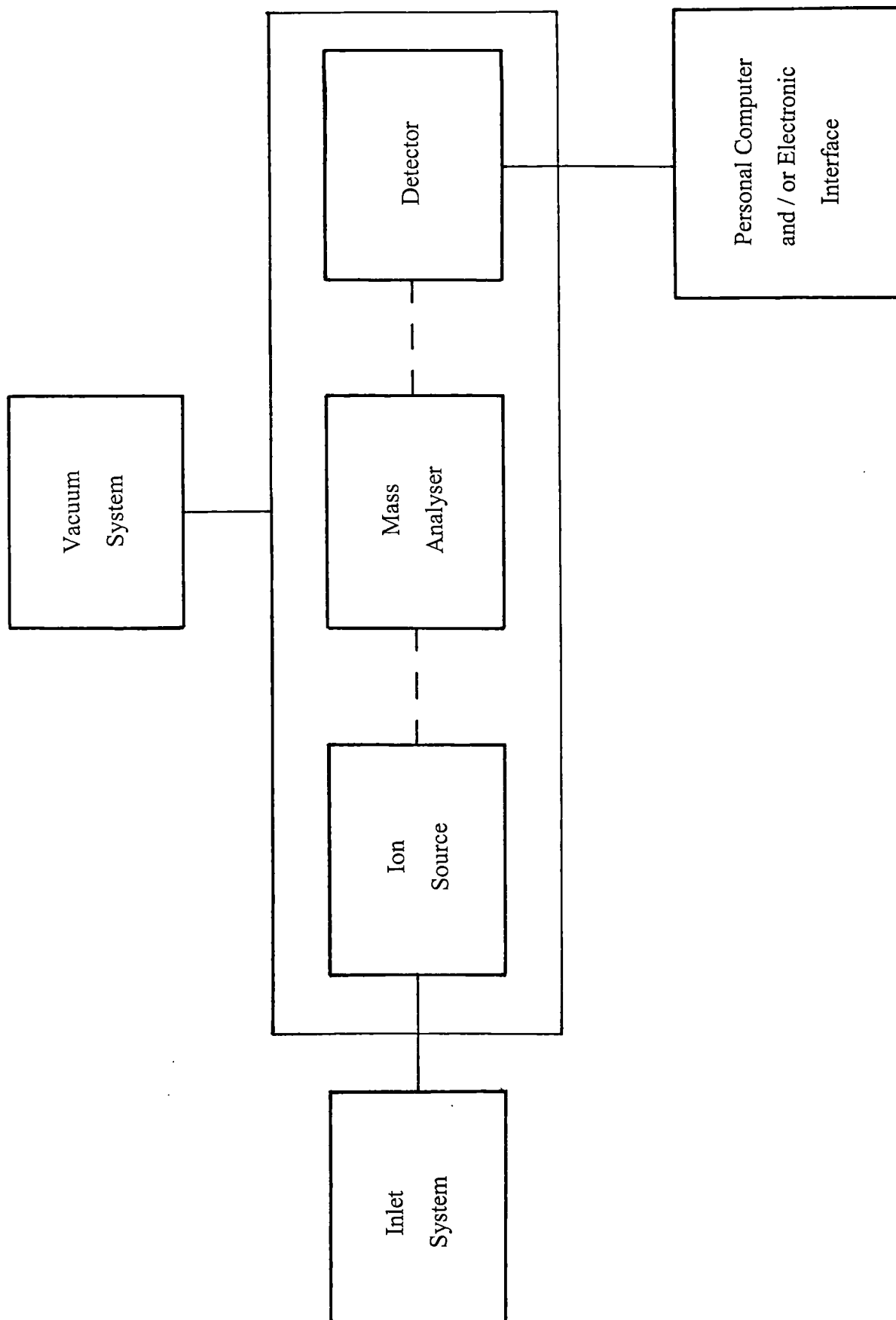


Figure 2.1 The construction of mass spectrometers

Component	Examples
Inlet system	capillary inlet, chromatographic interfaces, heated probe
Ion source	electron impact, chemical ionisation, fast atom bombardment, matrix assisted laser desorption and ionisation, electrospray
Mass analyser	quadrupole, ion trap, magnetic sector, time of flight, Fourier transform ion cyclotron resonance
Detector	photographic plate, Faraday cup, electron multiplier

**Table 2.1** Examples of mass spectrometer components

Most small molecular weight (MW) detected species discussed in this thesis contain only one charge and therefore  $m/e$  values are normally simplified to mass values with units of Daltons (Da). Vacuum pressures ( $< 10^{-5}$  torr) are maintained in the mass analyzer and detector regions, and normally in the ion source region also. The reduced pressures are employed to decrease the probability of unwanted ion - molecule collisions.

In this chapter the mass spectrometer employed in Chapters three, four, five and six is discussed. Electron impact ion sources, quadrupole mass analysers, Faraday cup and electron multiplier detectors and instrument control will all be reviewed. The ion source

and electron multiplier operating parameters will also be investigated and optimised with respect to the instruments sensitivity.

## **2.2 Electron Impact Ion Sources**<sup>2,4,5,6</sup>

Although it was one of the first forms of ionisation employed over 70 years ago, the electron impact ion source is still highly popular. Dempster<sup>2</sup> first used electrons to ionise gaseous molecules and Nier<sup>3</sup> further developed the ion source. The relative ease of operation and control of the electron beam intensity, lack of contamination problems because of the high source temperatures (100 - 200°C) maintained by the hot filaments and a relatively high sensitivity all contribute to this popularity<sup>2,7</sup>.

The ion source is constructed to perform three functions; electron formation, ion formation by electron bombardment of gaseous molecules and instantaneous extraction of the ions formed into the mass analyzer. An enclosed ion source is shown in Figure 2.2. The majority of electron impact ion sources contain two filaments (one is operational and the second is available for immediate use), so as to allow for the failure of one filament without the need for its immediate replacement<sup>7</sup>. The ionisation region has a volume of 1 cm<sup>3</sup> and is maintained at a pressure of 10<sup>-3</sup> to 10<sup>-5</sup> torr to reduce unwanted ion - molecule collisions that will take place at higher pressures.

Electrons are created by electrically heating<sup>5</sup> a metal filament to temperatures of 1000 - 2000°C with a current of 3-4 A. Tungsten, rhenium, lanthanum hexaboride and thorium coated iridium have all been employed as filament materials because of their low work function which allows relatively easy electron release from the metal<sup>7</sup>. The emission current of electrons released from a filament is maintained at a constant value by

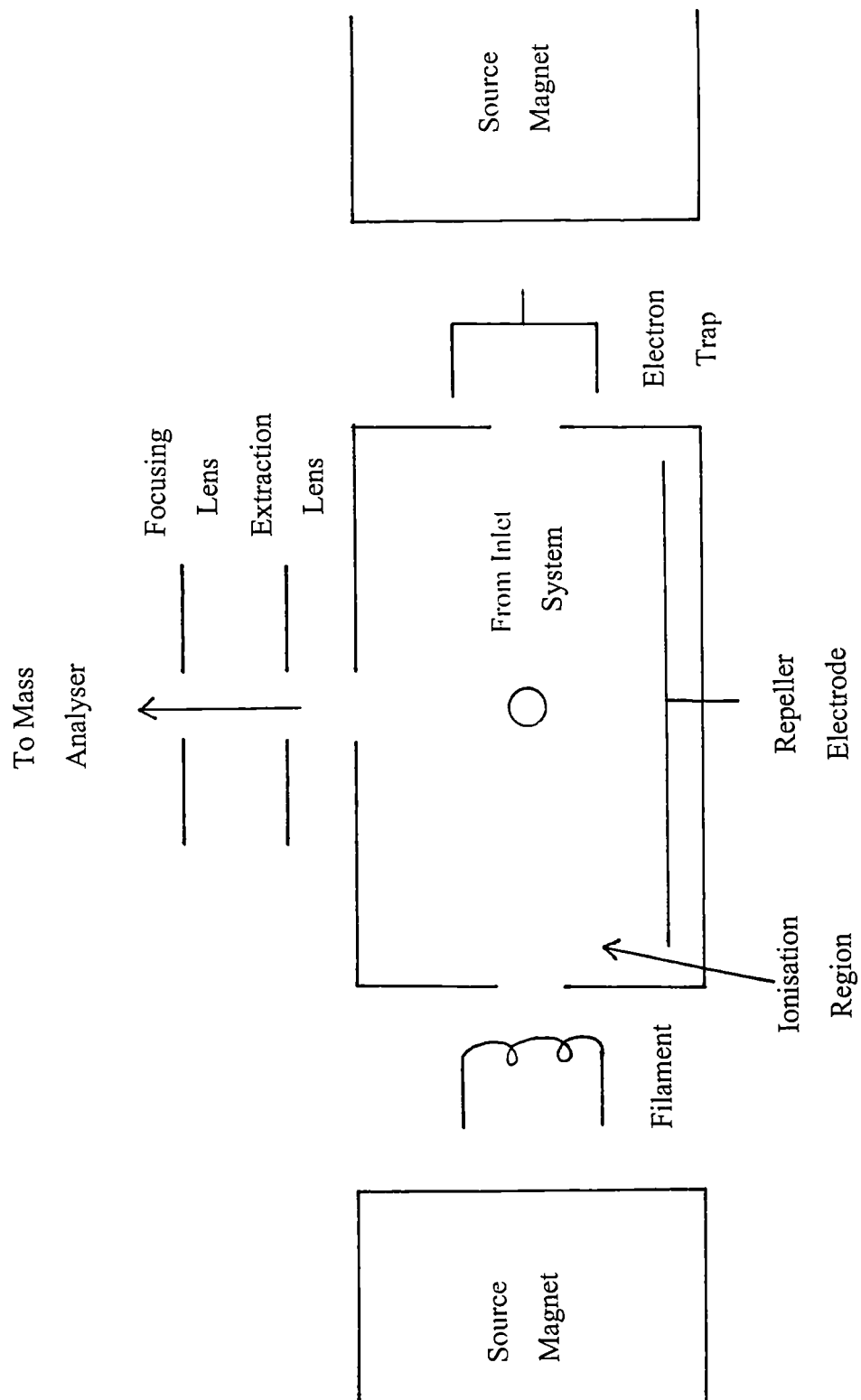


**Figure 2.2** The enclosed ion source  
(only one filament shown)

monitoring the electron current striking the trap plate and employing the measurement in a feedback control loop<sup>2</sup>.

Once released from the filament electrons are accelerated through the ionisation region by a potential difference (-10 to -100V) operated between the filament and the ionisation region walls (ground potential)<sup>7</sup>. The velocity and energy (5 - 100 eV) of electrons is dependant on the potential difference employed. Electron energies of 50 - 100 eV are generally used as they allow a maximum sensitivity to be achieved and also reduce the effect on the fragmentation patterns of molecules when the electron energy is altered<sup>5,6</sup>. To increase the probability of an electron - molecule interaction a few hundred Gauss magnetic field can be applied parallel to the electron beam to confine the electron to a narrow helical path and increase the effective path length of the electron in the ionisation region<sup>5</sup>.

Gaseous samples enter the ionisation region perpendicular to the flow of electrons. The most probable reaction in the ionisation region is the collision of a bombarding electron and gas molecule to create a positive charged radical cation ( $M^{\cdot+}$ ), known as the molecular ion<sup>2,5</sup>:



Approximately 1 in 100 molecules entering the ion source is ionised to create a positive ion; this depends upon the ionisation cross section of the molecule and the electron energy<sup>2</sup>. The ionisation potentials of most compounds are lower than 20 eV and therefore the high energy electrons used not only result in ion formation but they also impart internal energy to ionised molecules<sup>5</sup>. The excess energy is reduced by dissociation (or

fragmentation) of the molecular ion to produce lower mass fragment ions and neutral molecules<sup>5</sup>. The fragmentation pathway and intensity of the fragment ions created is dependant on the electron energy and the structure of the molecular ion. The electron energy and the structure of molecular ions affect the fragmentation mechanism.

After formation, ions are instantaneously extracted, accelerated and focused into the mass analyzer by a potential difference applied between a repeller plate and a series of extraction and focusing lenses.

Open ion sources operate at a uniform pressure of  $10^{-5}$  torr. Enclosed (gas tight) sources however operate at pressures of  $10^{-5}$  torr in the region of the hot filament and  $10^{-3}$  torr in the ionisation region<sup>7</sup>. A gas tight ionisation region, maintained with small electron entry and ion exit slits, increases the sample residence time in the source and therefore increases the probability of interactions between electrons and gas molecules. The higher pressure also reduces background signals whereas the hot filaments are still operated at a pressure suitable for a relatively long operational lifetime. Although the conductance (volume of gas per unit of time passing through the ion source) of the enclosed ion source is reduced because of the gas tightness of the ionisation region, the fast pumping speeds maintain a residence time of molecules in the ion source of less than 0.5 s. This residence time is sufficient to monitor rapid changes in the concentration of an analyte<sup>5</sup>.

### **2.3 Quadrupole Mass Analysers**<sup>7,8,9</sup>

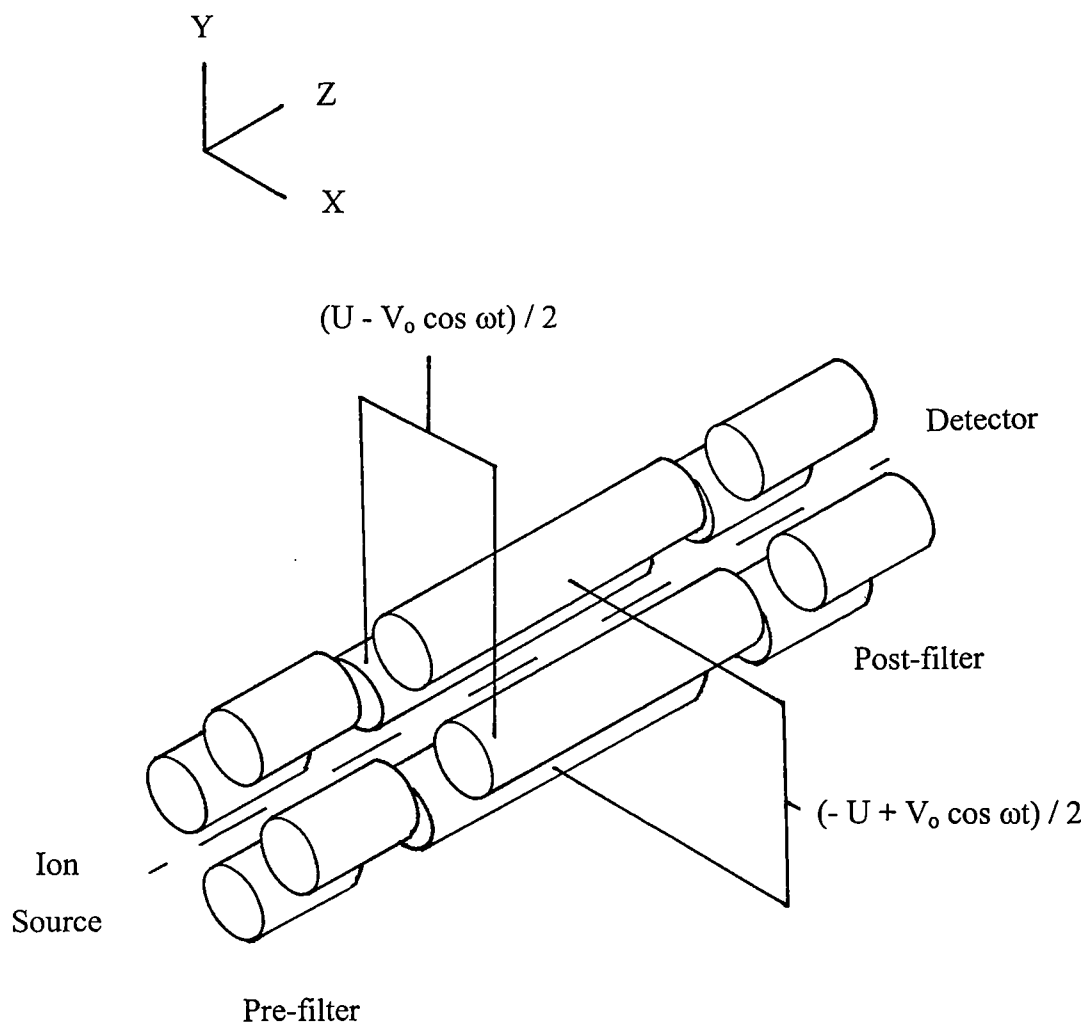
Also known as a mass filter because of its function to filter ions of different mass and charge before detection, the quadrupole mass analyser employs a combination of direct

current and periodically alternating electric fields to achieve mass discrimination. The quadrupole mass analyser was first developed and patented in the early 1950s by Wolfgang Paul at the University of Bonn. Three decades of use for the highly popular commercial quadrupole mass analyzers resulted in Paul receiving the 1989 Nobel Prize for Physics for his work in connection with quadrupole mass analyzers and ion traps<sup>10</sup>. The popularity is exhibited by the estimated 75% share of the world market for quadrupole mass analyzers and ion traps, equivalent to \$750 million sales in 1994<sup>11</sup>. A high popularity has been achieved because of its compactness, relative cheapness, simple operation and the ease of coupling the mass analyzer with a wide range of ion sources and inlet systems<sup>2</sup>. The wide range of ion sources with which the mass analyser can be interfaced is a result of exact ion focusing and high ion velocities not being required in contrast to alternative mass analysers.

The quadrupole mass analyzer (Figure 2.3) is constructed of four parallel electrical conducting electrodes positioned around the z axis with a symmetrical and circular cross section. The electrodes have a diameter of 6 mm. The circle inscribing the cross section and touching all four electrodes is described by a radius of  $r_0$ . Opposite electrodes are electrically connected and each pair of electrodes are biased with either positive or negative direct current potentials.

A three dimensional electric field [ $\phi(x,y,z)$ ] created within the volume enclosed by the four electrodes and composed of direct current (dc) and radio frequency (rf) components, can be described by the potential variation<sup>7,8</sup>:

$$\phi(x, y, z) = \phi_0(x^2 - y^2) / 2r_0^2 \quad (2.2)$$



— — Central Axis and Direction of Transmitted Ions

**Figure 2.3** The quadrupole mass analyser

An ion injected in to the electric field with a small accelerating voltage of 10 - 20 V will travel through the field or collide with an electrode depending on the periodic variation with time of the potential  $\phi_0$ . To create a potential composed of periodic fluctuations ( $\phi_0$ ) a voltage composed of a dc component (U) and an alternating rf component ( $V \cos \omega t$ ), with a frequency  $\omega$ , is employed<sup>7,8</sup>:

$$\phi_0 = U + V \cos \omega t \quad (2.3)$$

The periodic fluctuations of the voltage deflect ions travelling through the mass analyzer along an oscillating path with movements towards and away from the central z axis in the xz and yx planes. The oscillations over time (t) of an ion of mass m and charge e in the x, y and z axis are created by the electric field and can be expressed by the following differential equations<sup>8,9</sup>:

$$m(d^2x / dt^2) + 2e(U + V \cos \omega t)x / r_0^2 = 0 \quad (2.4)$$

$$m(d^2y / dt^2) - 2e(U + V \cos \omega t)x / r_0^2 = 0 \quad (2.5)$$

$$m(d^2z / dt^2) = 0 \quad (2.6)$$

Equation 2.6 shows that ions travel at a constant axial velocity equivalent to the entrance velocity along the z axis.

By substitution of the dimensionless parameters<sup>7</sup>:

$$a = 8eU / m\omega^2 r_0^2 \quad (2.7)$$

$$q = 4eV / m\omega^2 r_0^2 \quad (2.8)$$

$$\varepsilon = \omega t / 2 \quad (2.9)$$

equations 2.4 - 2.6 can be transposed to yield the standard Mathieu equation, which can be used to calculate the restoring forces towards the z axis of an ion at position (x, y).

$$d^2u / d\varepsilon^2 + (a - 2q \cos (2\varepsilon) u ) = 0 \quad (2.10)$$

where u is a directional vector which represents the position of an ion in either the x or y axis.

Solving equation 2.10 yields two solutions<sup>9</sup>; stable and unstable oscillations. Stable trajectories occur when ions travel along the z axis with oscillation amplitudes in the xz and yz planes less than  $r_0$ . These ions oscillate within the boundary of the electrodes and reach the detector. Alternatively when the oscillation amplitudes increase exponentially to values greater than  $r_0$  unstable trajectories result and ions collide with the electrodes and are lost. Ions with a smaller m/e ratio with respect to the ions transmitted are lost by collisions in the xz plane whereas ions of greater m/e ratios are lost by collisions in the yz plane.

The conditions used to create stable trajectories can be represented on a Mathieu diagram<sup>7,8,9</sup> with zones of stable combinations, observed when regions of stability in the xz and yz planes overlap. Four zones of stable combinations can be used though only one zone has currently been applied (Figure 2.4).

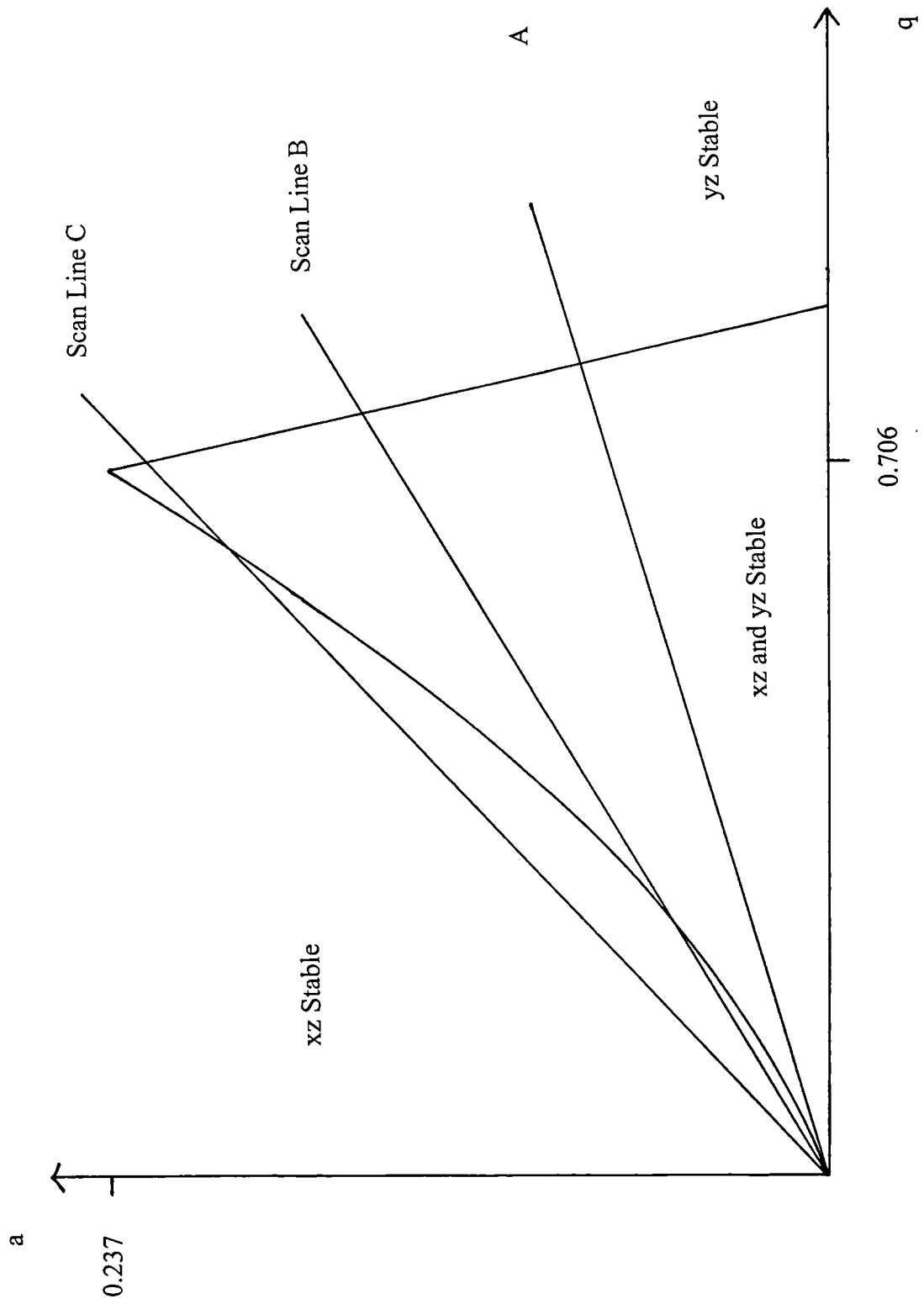


**Figure 2.4** A Mathieu stability diagram

Mass scanning is achieved by increasing the magnitude of the dc and rf components (i.e. increasing the values of  $a$  and  $q$ ) simultaneously while keeping their ratio and the frequency of the rf applied potential ( $\omega$ ) constant<sup>7,8</sup>. The function of mass scanning is represented on a Mathieu diagram as a scan line (Figure 2.4; lines A, B and C), which intersect the zone of stable combinations at two points representative of the  $m/e$  range limits of ions transmitted to the detector<sup>8</sup>. The slope of the scan line ( $a/q$ ) affects the resolution achieved as can be seen in Figure 2.4 and Table 2.2<sup>11</sup>.

Scan line	$a / q$	Masses transmitted to the detector (Da)
A	0.22	124 - 253
B	0.30	132 - 140
C	0.34	136

**Table 2.2** The effect of the scan line gradient on the resolution

Large  $a$  and  $q$  ratios and therefore larger scan line gradients create a higher mass resolution. Unit mass resolution is normally employed with quadrupole mass analysers to obtain adequate sensitivity.

The resolution, and sensitivity, is not only dependant on the gradient of the scan line but is also dependant on the ion velocity, direction of ion movement and position of the ion as it enters the electric field<sup>7,8</sup>. These dependencies result in the loss of ions with the selected  $m/e$  ratios and a lower sensitivity is observed. Misaligned electrodes and fringing fields can also result in the loss of sensitivity<sup>8</sup>, though electrodes pre-aligned in ceramic disks before installation into the mass spectrometer have greatly reduced the

probability of misaligned electrodes. Non-perfect electric fields (fringing fields) can also be created by contamination of the electrodes with non - conducting compounds. These imperfections distort the symmetry of the electric field and result in reduced sensitivities and mass resolution. The introduction of rf-only pre and post filters focus ions before and after the mass analyser, respectively, improve the mass resolution and sensitivity<sup>12</sup>.

Three different modes of operation can be employed with the quadrupole mass analyser. Mass scanning and measuring the transmitted ion current provides a mass spectrum of the ions present in the ion source. Calibration of the mass scale is easily achieved because mass and the applied rf component are related linearly<sup>7</sup>. Equal peak widths are obtained with scan lines which approach the apex of the zone of stable combinations. As an alternative to mass scanning the values for  $a$  and  $q$  can be maintained at a constant value so that ions of one  $m/e$  value is continuously transmitted to the detector. This mode of operation is called single ion monitoring (SIM) and is often employed for quantification<sup>2</sup>. Finally a voltage composed of a small rf component only will allow the transmission of all the ions created in the ion source through the mass analyser to the detector. In this mode the mass analyzer can be used to monitor the total pressure in the ion source<sup>7</sup>.

## 2.4 Detectors

Although photographic plates were once used for ion detection, the time required to qualitatively process the plates and the imprecision of quantified results means electrical detection with Faraday cup or electron multiplier detectors are almost exclusively employed today.

### 2.4.1 Faraday Cup Detectors<sup>2,4,7</sup>

A detector of low sensitivity, with minimum detectable ion currents of  $10^{-14}$  A ( $10^4$  ions per second), the Faraday cup is constructed of a small electrode placed in a closed box to eliminate loss of created secondary electrons before they strike the electrode. The transmitted ion beam from the mass analyser passes through a focusing slit and strikes the electrode where it is neutralised by a flow of electrons from ground. The potential drop across a high ohmage resistor when a flow of electrons pass through is measured and is proportional to the incoming ion current. The current measured is transformed to a voltage, which is dependant on the number of ions and number of charges per ion but is independent of the chemical nature and kinetic energy of the ion beam. The voltage is amplified with a high impedance amplifier.

The high ohmage resistor employed requires a delay between measurements of the potential drop to allow the signal to return to a baseline value. The Faraday cup is therefore a relatively slow detector and the delay time is dependant on the ion current measured. However, higher ion currents can be measured with respect to the electron multiplier.

#### 2.4.2 Electron Multiplier Detectors<sup>2,7</sup>

Detection of ions with an electron multiplier is based on the amplification of the incoming ion current. Detection of ion currents of  $10^{-18}$  A (6 ions per second) can be achieved by amplification in the gain range of  $10^4$  to  $10^8$ .

Discrete dynode electron multipliers are constructed of 12 - 20 dynodes, composed of a 2% beryllium / copper alloy, connected electrically in series by a resistive network. A copper / beryllium alloy is used as it has good electron emission properties. Ions are accelerated by a voltage applied to the entrance of the detector and the first dynode (conversion dynode) and these ions collide with the conversion dynode which will release a number of electrons for each ion impact. The released electrons are then accelerated to the second dynode where impacting electrons release a number of electrons for each electron-dynode impact. The continued mechanism of electron multiplication at each dynode results in an amplified current with respect to the incoming ion current. The application of a Faraday plate with an electrometer allows smaller measurement times as fast as 50 ns to be achieved. These times are quicker than are possible with the Faraday cup which employs a high ohmage resistor. The current produced is subsequently amplified and converted to a voltage which is suitable for measurement and storage.

The channeltron (continuous dynode electron multiplier) uses a lead coated glass tube as a continuous but single dynode. The tube is located in a magnetic field and a 3000 V potential is applied along its length to create a uniform electric field. The resistance (80 - 100 M $\Omega$ ) of the lead coated glass creates an electrical potential gradient down the tube in which electrons move in a cycloidal path. Electron multiplication, after ion acceleration

at the entrance of the detector and ion-dynode collisions, is performed by a large number of electron-wall collisions. Several electrons are released for each electron-dynode impact. The electron current is again measured, amplified and transformed into a voltage. Curved channeltrons are used to prevent the formation of unwanted electrical pulses from positive ions created within the detector. These electrical pulses reduce the sensitivity by decreasing the signal to noise ratio. Unlike the discrete dynode electron multiplier the channeltron is tolerant to ambient air exposure and therefore loss of vacuum pressures during operation is not a significant problem for the detector.

The gain obtainable from an electron multiplier and therefore the sensitivity is dependant on the voltage applied to the entrance of the detector, the angle of ion incidence and the nature of the dynode material. The sensitivity decreases over periods of time unless the applied voltage is increased. The decrease in the sensitivity occurs over time periods of months and years.

## **2.5 Instrument Control**<sup>7,13</sup>

Commercial instruments today use complex operations and are supplied to allow both automatic control (by computer and electronic hardware) and technician control. The majority of mechanical and electrical operations are controlled automatically while some controls that need to be altered at regular intervals can be controlled by the technician, with easy access to the mass spectrometer operations achieved via a computer keyboard or electronic interface unit. This is different to the early commercial instruments where the majority of operating functions were controlled by a technician. The result today is the transformation of a once difficult-to-operate instrument into a routinely and easy-to-

use instrument that can be operated by less experienced operators than was required forty years ago.

The advantages of automatic control and a lower interaction between instrument and technician are many. Firstly a complex-to-use instrument has been simplified to the point where analyses can be fully automated with no instrument-technician interaction. This releases the technician for other duties. Secondly the large volume of data produced by mass spectrometers, especially when applied as a chromatograph detector, can not be fully processed on - line by technicians. Therefore digital recording of the data and either on - line or off - line data processing can be performed by computer. Also routine data processing including normalisation of mass spectra, data presentation, regression analysis of calibration data and matching analyte and library spectra can all be performed automatically by an interfaced computer resulting again in the release of the technician for other duties.

## **2.6 Instrument Used In This Research**<sup>14</sup>

A VG Gas Analysis Systems (Middlewich, Cheshire, UK) SX200 mass spectrometer was employed during the research performed in Chapters three - six. A gaseous sample flow ( $> 20 \text{ ml min}^{-1}$  at 1000 torr) continuously flowed through a 1.5 metre long silica capillary inlet with the assistance of a rotary pump from atmospheric pressure to a glass frit positioned at the entrance of the ion source. The glass frit acted as a molecular leak through which a small portion of the gas flow passes in to the ion source while a large portion is pumped away by a rotary pump. The inlet was heated to a maximum temperature of  $170^{\circ}\text{C}$  to eliminate condensation or adsorption of gaseous compounds on silica surfaces. Ions were created in an enclosed ion source constructed with two tungsten

filaments. A quadrupole mass analyzer (length = 125 mm, electrode diameter = 6.3 mm, mass range = 0 - 200 atomic mass units) was employed with pre and post filters to focus ions entering and leaving the mass analyzer. Ions were detected with either a Faraday cup or channeltron. The measured ion current was automatically converted to the partial pressure of the analyte in the ion source. The maximum measurable partial pressures were  $9.99 \times 10^{-8}$  bar (Faraday cup) and  $9.99 \times 10^{-10}$  bar (channeltron). The vacuum pressure of  $0.3 - 2.0 \times 10^{-6}$  bar was maintained with a  $240 \text{ L s}^{-1}$  turbo molecular pump backed up with two two-stage rotary pumps. One pump was also connected to the ion source end of the capillary inlet to pump gaseous samples from atmospheric pressures through the pressure reducing capillary to the ion source. A glass frit placed between the capillary inlet and ion source acted as a second pressure reducing stage.

Spectralab software and an electronic interface unit were used for automatic and operator control of instrument functions. Mass scanning or single ion monitoring was employed. Although most of the instruments operations were automated several operations could be controlled manually. These were emission current, electron energy, applied voltage to the channeltron entrance (detection voltage) and de-gas (heating of the ion source to remove condensed materials). Other operations available in the single ion monitoring mode were peak top finding, cycle time (time used to produce one displayed measurement) and accuracy code (number of pressure measurements per cycle). Sixteen measurements per cycle (accuracy code two) was employed with peak top finding and a cycle time in the range 0.1 to 5 seconds.

The masses employed for single ion monitoring were 43 and 58 Da (acetone) and 142 Da (methyl iodide). The peaks of highest sensitivity (base peaks) for acetone and methyl iodide were observed at masses 43 and 142 Da, respectively.

## 2.7 Instrument Optimisation

### 2.7.1 Emission Current and Electron Energy

The emission current and electron energy employed in the ion source were both investigated for acetone and methyl iodide using the static headspace technique described in Chapter four. Acetone standards in water [2.0 % (v/v)] and methyl iodide standards in acetic acid [5.0 % (v/v)] were used with ion detection provided by a Faraday cup. The experimental conditions employed were; temperature (22°C), phase ratio (9.0) and equilibration time (60 minutes). The response was measured as the mean of six replicate analyses.

The results shown in Figures 2.5 and 2.6 all show a maximum response in the range investigated, which corresponds to the highest sensitivity. The optimum values employed in future work are shown in Table 2.3. The emission current controls the rate of electron release from the filament and therefore the number of electron - molecule interactions and ionisation. The optimum emission currents represent the highest number of ionisation reactions achievable. The optimum value, with respect to sensitivity, of 60 eV provides the smallest degree of fragmentation for the molecular ion of methyl iodide at  $m/e$  142 while maintaining a high degree of ionisation. However the same electron energy results in a relatively high degree of fragmentation of the acetone molecular ion and a base peak (peak of maximum intensity in the mass spectrum) for acetone at  $m/e$  43, which corresponds to a relatively stable ion  $\text{CH}_3\text{CO}^+$ .

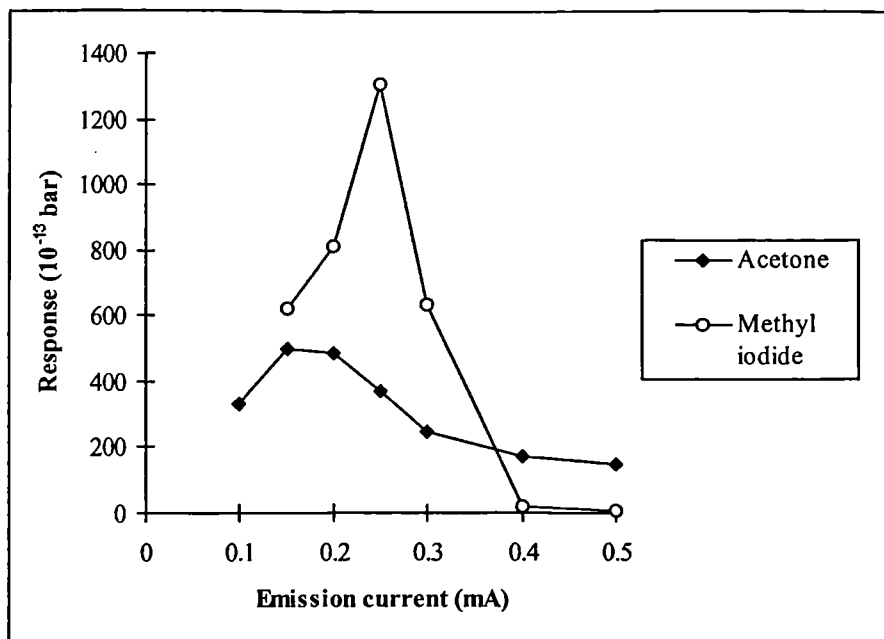


**Figure 2.5** The effect of the emission current on response for acetone and methyl iodide

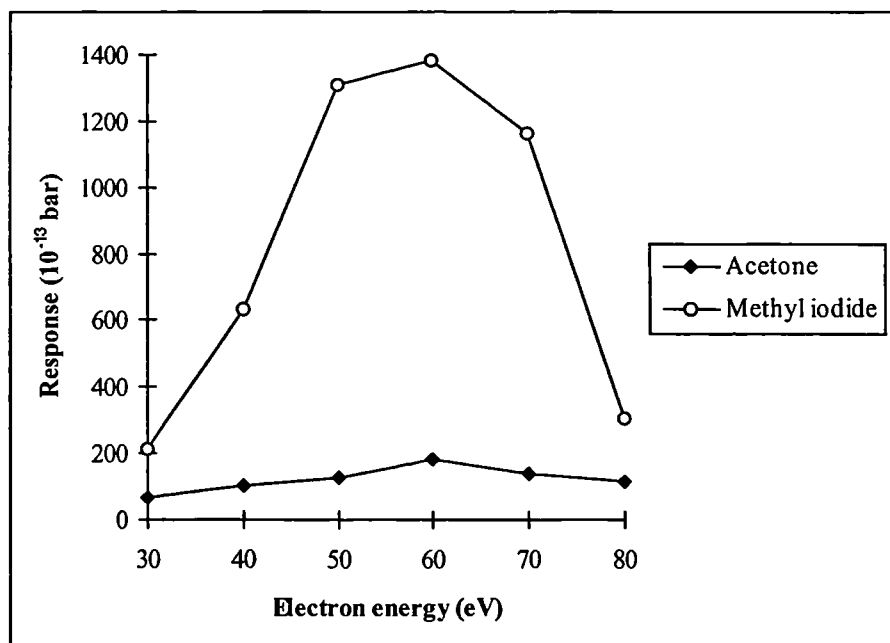


**Figure 2.6** The effect of the electron energy on the response for acetone and methyl iodide

Analyte	Emission current (mA)	Electron energy (eV)
Acetone	0.15	60
Methyl iodide	0.25	60

**Table 2.3** Optimised emission current and electron energy values

### 2.7.2 Channeltron Detection Voltage

The effect of the voltage applied to the mouth of the channeltron (detection voltage) was studied in the range -1000 to -3000 V using the static headspace technique (Chapter four) and a  $500 \mu\text{g ml}^{-1}$  (v/v) acetone standard in water. The experimental conditions employed were the same as in section 2.7.1 and the response was measured as the mean of six replicate analyses.

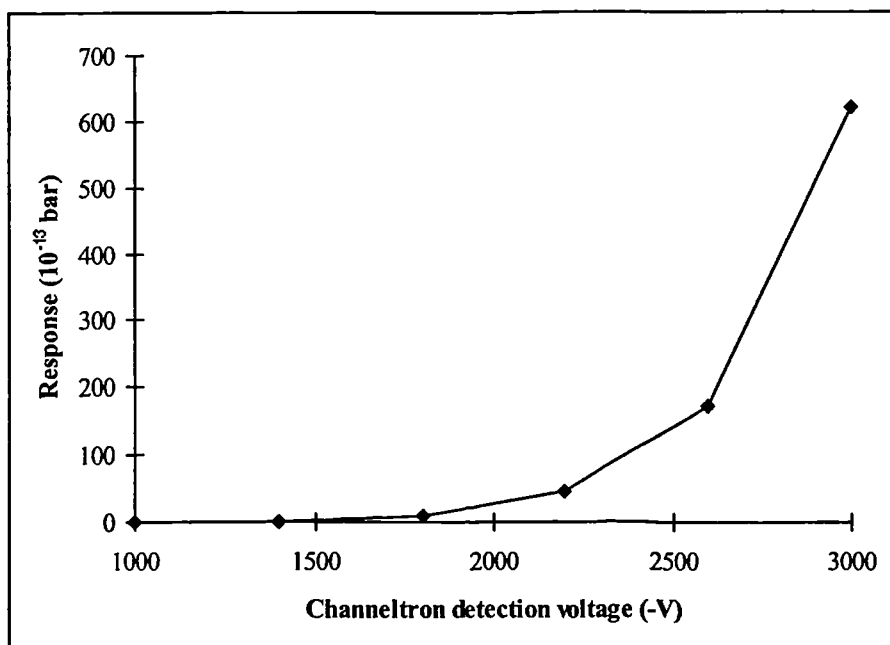


**Figure 2.7** The effect of the channeltron detection voltage on the response

The response increases exponentially as the detection voltage is increased (Figure 2.7). A greater sensitivity is therefore achieved as the detection voltage is increased. This is observed because of the greater acceleration of ions as they approach the conversion dynode and the resulting higher ion velocities which impart more energy to the conversion dynodes. This results in a higher number of electrons being released from the conversion dynode. Although the greatest sensitivity was achieved at a detection voltage of -3000 V the detector lifetime would be significantly shortened, with respect to smaller voltages, because of the greater collisional damage caused by more energetic ions on the conversion dynode. Therefore a detection voltage of -1800 V was used in further work as a compromise value between sensitivity and detector lifetime.

## 2.8 References

- 1) Svec, H.J., *Int. J. Mass Spectrom and Ion Processes*, 1985, **66**, 3.
- 2) Chapman, J.R., *Practical Organic Mass Spectrometry*, Wiley, Chichester, 2nd Edition, 1993, Chapter 1.
- 3) Nier, A.O., and Hanson, E.E., *Phys. Rev.*, 1936, **50**, 722.
- 4) McFadden, W., *Techniques of Combined Gas Chromatography / Mass Spectrometry: Applications in Organic Analysis*, Wiley, London, 1973, Chapters 2, 4 and 7.
- 5) Busch, K.L., *Spectroscopy*, 1995, **10**, 39.
- 6) Milberg, R.M., and Cook Jr, J.C., *J. Chromatographic. Sci.*, 1979, **17**, 17.
- 7) Batey, J.H., *Vacuum*, 1987, **37**, 659.
- 8) Dawson, P.H., *Quadrupole Mass Spectrometry and its Applications*, Elsevier, Amsterdam, 1976, Chapters 1 - 6.
- 9) Lawson, G., and Todd, J.F.J., *Chem. Brit.*, 1972, **8**, 373.
- 10) Paul, W., *Nobel Lectures - Physics 1981 to 1990*, World Scientific, London, 1993, 601.
- 11) Finnigan, R.E., *Anal. Chem.*, 1994, **66**, 969A.
- 12) Brubaker, W.M., *Adv Mass Spectrom.*, 1968, **4**, 293.
- 13) Chapman, J.R., and Ryan, P.A., *Trends Anal. Chem.*, 1988, **7**, 244.
- 14) VG Gas Analysis Systems, SX models operation manual, 1991.

## **Chapter Three**

### **Total Vaporisation Analysis**

### **3.1 Introduction**

A diverse range of analytical techniques enable liquid samples obtained from industrial, environmental or biological sources to be qualitatively and quantitatively analysed for organic species. Many of the techniques allow the direct analysis of liquid samples to be performed, with or without a sample pre-treatment stage external to the analytical instrument. However, liquid samples composed of many different compounds may not provide the required sensitivity or selectivity when a direct analysis strategy is employed. These samples can be successfully analysed indirectly using gas, liquid or supercritical fluid chromatography to separate compounds present in the sample prior to their detection. Gas chromatography (GC) is employed for the indirect analysis of volatile and semi-volatile liquid phase samples as well as gases and vapours.

#### **3.1.1 Gas Chromatography Injection Strategies**<sup>1, 2, 3, 4, 5</sup>

Gas chromatography (GC) and electron impact ion source mass spectrometry (EI-MS) require vaporisation of liquid phase samples before compound separation (GC) or direct analysis (EI-MS) of the compounds present can be performed. Gas chromatographs employ an inlet to vaporise the liquid sample, mix the vapour created with an appropriate carrier gas and transport the mixture to the chromatographic column entrance<sup>1</sup>. An ideal inlet delivers a representative vapour sample to the column in which the compounds present are chemically unchanged and in the correct proportions as observed in the liquid phase<sup>6</sup>. A gas chromatograph inlet has been employed in the work discussed in this

chapter for the total vaporisation of liquid samples prior to the analysis of the vapour created by an electron impact ion source mass spectrometer.

Injection techniques employed in a variety of gas chromatograph inlets can be classified according to the flow path and thermal profile experienced by the sample<sup>6</sup>. Poole and Poole<sup>1</sup>, Grob<sup>4</sup>, Hinshaw<sup>5</sup> and Hinshaw Jr.<sup>6</sup> have all comprehensively discussed the application, advantages and limitations of the inlets employed. A range of injection strategies currently employed with gas chromatograph inlets will be discussed in this section.

### 3.1.1.1 Direct Injections<sup>1</sup>

All gas chromatograph inlets are constructed with a small volume (approximately 1 ml) hollow glass liner heated by a metal block and continuously purged with a flow of carrier gas, which is preheated by the metal block to prevent condensation of the sample vapour when mixed with the carrier gas<sup>1</sup>. Glass liners are used to reduce the number of catalytic surfaces available for compound decomposition when the liquid or vapour sample is exposed to the hot inlet surfaces. In the absence of glass liners the inlet surface would be composed of catalytically active hot metal and compound decomposition would be more probable<sup>1</sup>. The glass liner is connected at one end to the chromatographic column and is sealed with a silicone rubber septum at the opposite end. Liquid phase samples (0.5 - 10 µl) are quantitatively introduced rapidly into the inlet with a calibrated glass syringe.

Inlets employed for direct injections provide flash vaporisation of the liquid sample with heat supplied from the glass liner. Glass liners have a sufficient thermal mass<sup>1</sup> and

is therefore a good source of heat whereas preheated carrier gas is a poor source of heat. The vapour formed is mixed with a carrier gas and transferred to the column. Direct injections are normally applied with packed columns. However, capillary columns can be used to improve the resolution and sensitivity of the analysis. Column inlet adapters are required to couple the capillary column and inlet and also to focus the broad band of vapours approaching the capillary column<sup>5</sup>.

Other injection strategies can be employed to improve the sensitivity, eliminate the decomposition of thermally labile compounds and eliminate the discrimination of compounds with a wide range of boiling points sometimes observed with this inlet.

#### 3.1.1.2 Split Injections<sup>1,2,3,4,6</sup>

Capillary GC columns have small sample capacities<sup>1</sup> and so require the injection of small liquid phase sample volumes (0.001-0.5  $\mu\text{l}$ ) to ensure there is no loss in the column efficiency caused by sample overloading. Split injections<sup>7</sup> can be used to provide the small volumes of vapour required by the column while injecting larger and more reproducible liquid phase sample volumes (> 0.5  $\mu\text{l}$ ). Injection and vaporisation proceeds as is observed for direct injections however the mixture of vapour is divided between two streams as it approaches the column<sup>1</sup>. A minority of the flow enters the column whereas the majority exits the inlet through a split vent of lower gas flow resistance than the column. Split ratios [flow(vent) : flow(column)] can range from 10 : 1 to 1000 : 1 and are controlled by a needle valve or flow controller present in the split vent line. The split ratio is only an approximate indication of flows, which change during vaporisation because of the sudden increase in the inlet pressure and gas viscosities<sup>1</sup>. As most of the

flow is vented away from the column, high carrier gas flow rates can be used. Therefore narrow initial bands of vapour are observed at the column entrance because of rapid transfer of vapours to the column.

Discrimination can be defined as the selective loss of compounds during injection of the sample either in the syringe needle or in the inlet<sup>1</sup>. Split injections require complete vaporisation and homogeneous mixing of the vapours with the carrier gas before the mixture approaches the column entrance to reduce the probability of discrimination<sup>1</sup>. High inlet temperatures are used to ensure vaporisation is completed and no discrimination of high boiling point compounds is observed in the syringe needle or inlet.

#### 3.1.1.3 Splitless Injections<sup>1,2,3,4,5,6</sup>

An increase in the sensitivity and reduction in the volume of solvent entering the column which results in the reduction of the effect of solvent peak tailing can be obtained with splitless injections<sup>1</sup>. Injections are performed into a split vent inlet with a closed vent. Splitless injections, also called split/splitless injections, vaporise and transport the majority of the sample to the column as is observed with direct injections. After a sufficient time, however, the split vent is opened to remove the remaining solvent vapour present in the inlet. First used by Grob and Grob<sup>8</sup> the injection strategy introduces the solute onto the column while transporting a large volume of the solvent away from the column.

Low carrier gas flow rates are used to eliminate overloading of the column that can be observed because the majority of the sample vapour enters the column. Long sampling times result and broad bands of vapour enter the column. To refocus the vapour and

improve the chromatographic resolution and sensitivity, cold trapping<sup>9</sup>, retention gaps<sup>10</sup> or solvent effects<sup>1</sup> can be used. Discrimination of high boiling point compounds can be observed if the split vent is opened before vaporisation is completed and would result in purging of the high boiling point compounds from the inlet with the solvent.

#### 3.1.1.4 Programmed Temperature Vaporisation (PTV)<sup>1,6,11</sup>

Employed to allow venting of the solvent after large sample volume injections (< 200 µl) PTV uses a relatively small volume inlet constructed with a split vent and packed glass liner<sup>1,6</sup>. The glass liner has a high thermal mass to provide rapid changes in the inlet temperature on heating<sup>1</sup>. Sample introduction is performed at an inlet temperature lower than the solvent boiling point. After withdrawal of the syringe to eliminate discrimination from the needle the inlet temperature is increased with the split vent open to vaporise and discharge the solvent from the inlet. The vent is then closed and the inlet temperature is elevated rapidly to vaporise the solutes present and transport the vapours created to the column.

The inlet acts to increase the sensitivity by eliminating the solvent before the solutes are vaporised. Compounds with boiling points similar to the solvent however are purged with the solvent through the split vent. The cost and complexity of the inlet, which requires automatic control and timing, has limited the number of applications of this injection strategy.

### 3.1.1.5 On-column Injections<sup>1,4,5,6</sup>

Discrimination and decomposition of thermally labile compounds in heated inlets can be a serious problem with the injection strategies described above. To overcome these problems the liquid samples can bypass the inlet and be injected directly into the chromatographic column which has been moved up into the inlet, or into a retention gap placed between the inlet and column to prevent contamination and solvent overloading of the column<sup>1</sup>. A needle guide accurately aligns the needle and column or retention gap before the injection.

The column or retention gap may be heated (hot on-column)<sup>12</sup>, or to reduce the possibility of discrimination from the needle in a hot region the inlet and column may be cool (cold on-column)<sup>13</sup>.

Vaporisation processes are complicated and difficult to observe in the confined regions of the inlets described. Each step of the process has been comprehensively discussed by Grob<sup>4</sup> to describe the various problems that can be encountered with, for example, discrimination. Some quantitative estimates of heat consumption during vaporisation<sup>14</sup> and some visual observations of the vaporisation process<sup>15</sup> have been reported by the same author.

### 3.1.2 Mass Spectrometric Direct Analysis of Liquids

Many liquid phase samples can not be directly analysed with the analytical techniques currently available and therefore indirect chromatographic analyses are used to provide

an adequate sensitivity and selectivity. Mass spectrometry can also provide a high sensitivity and significant level of selectivity for many multi-component samples without the requirement of a time consuming stage of separation before detection. The electron impact ion source instrument is the most commonly applied mass spectrometer today and requires vaporisation of the liquid sample to provide a gaseous sample compatible with the electron impact ion source. The variety of strategies employed for vaporisation of liquid phase samples prior to mass spectrometry detection is reviewed in this section.

#### 3.1.2.1 Off-line Analysis

A significant problem of mass spectrometry is the requirement to interface the high pressure of the laboratory with the vacuum pressure of the electron impact ion source. Early applications employed an expansion chamber (EC) operating at an intermediate pressure to provide a pressure reduction stage and couple these two regions. Vapour present in the EC can pass through a pressure reduction interface (molecular leak, glass frit or sample valve) into the ion source for analysis. The combination of low pressures and high temperatures in the EC can provide the complete vaporisation of liquid samples introduced into the chamber. Methods of sample introduction into the EC have varied between groups of mass spectrometer users.

Early techniques employed in the petroleum industry during the 1940s and 1950s by O'Neal and Wier<sup>16</sup>, Purdy and Harris<sup>17</sup>, Friedel et al.<sup>18</sup> and Rowe<sup>19</sup> used a sintered glass frit covered with mercury<sup>17,18</sup> or gallium<sup>16,19</sup> to seal the expansion chamber from the laboratory environment and pressure. Liquid samples were quantitatively introduced into

the EC with self filling micropipets<sup>16,17,18</sup> of volume 1  $\mu$ l. Gaseous samples were introduced after vaporisation at atmospheric pressure with a flat ended needle<sup>19</sup>. In 1951 O'Neal and Wier<sup>16</sup> increased the boiling point range of hydrocarbons that could be analysed up to C<sub>40</sub> with this method by employing a higher temperature EC and a mass spectrometer modified to increase the mass range from 200 to 600 Da. Dunn and Hooper<sup>20</sup> sealed the EC with a silicone rubber septum similar to those employed today with gas chromatograph inlets, and used a calibrated syringe to inject liquid samples into the EC. Alternatively Patillo and Howard<sup>21</sup> inserted a metal rod with a drill hole containing a sample into the EC through a Teflon plug seal to introduce a liquid into the EC. Finally a three valve inlet system designed by Mumbach<sup>22</sup> has been used to trap quantitative volumes of liquid sample in a T-piece before the sample is flash vaporised into the EC with the aid of heat.

Other mass spectrometer users have designed home-made interfaces to insert cups or capillaries filled with the sample into the EC. Caldecourt<sup>23</sup> employed a Teflon cup containing a liquid sample, inserted through a inlet port sealed with a Teflon plug to introduce liquid samples. The Teflon cups were introduced with a sample loader and after insertion the sample loader resealed the inlet port with another Teflon plug. Alternatively Peterson<sup>24</sup> and Padrta and Donohue<sup>25</sup> placed liquid samples in sealed or unsealed capillaries. The capillaries were introduced into the EC through a heated glass inlet<sup>24</sup> or vacuum lock<sup>25</sup> before the capillaries were broken to release the liquid sample. Many repetitive analyses could be performed before the EC required dismantling to remove the broken capillaries.

The methods discussed above were initially described and used in the period 1940-1970. However the number of reported applications during the three subsequent decades

is very small and another strategy has become employed as the standard method. Heated probes, first described by Kearns<sup>26</sup> and Gohlke<sup>27</sup>, insert a probe containing the liquid sample through a vacuum lock into the ion source<sup>28</sup>. The lower pressures present in the ion source, with respect to the evacuation chamber, and the availability of heat from the probe can vaporise liquids, even liquids of low volatility which could not be analysed by the other strategies described. With the placement of the sample within a few mm of the ionising electron beam representative mass spectra of thermally unstable compounds can be determined. The collection of these mass spectra is assisted by *rapid* heating in the ion source which favours vaporisation of the sample instead of decomposition<sup>29</sup>. A range of samples have been analysed using heated probes introduced into an electron impact<sup>30</sup> and chemical ionisation ion source<sup>31</sup>.

To collect spectra of compounds present in multi-component samples Grigsby et al.<sup>32</sup> and Franzen, Kuper and Riepe<sup>33</sup> have used heated probes to subject samples to micromolecular distillations in the ion source. A constant temperature ramp was employed by Grigsby and his co-authors while Franzen et al. used a constant total ion current to control the heating process. With this approach sample compounds can be vaporised into the gas phase at different times to provide mass spectra of pure compounds. The strategy has been employed to provide clean spectra of a contaminated compound or compounds present in mixtures containing a few components only.

#### 3.1.2.2 On-line Analysis

Only three applications have been reported in the literature concerned with on-line total vaporisation of samples prior to mass spectrometry detection. However, the secrecy

of many industrial processes may have inhibited the publication of other applications. All three groups used a liquid sampling valve of different design to introduce a liquid sample from a flowing stream into a heated vaporisation region.

Tou and Reddy<sup>34</sup> at Dow Chemicals in the USA have used a 1-2  $\mu\text{l}$  volume Bendix liquid injection valve. The injection valve is constructed around a piston containing a sample groove which moves between a liquid stream and vaporisation region and transports liquid samples through a seal into a heated flow of helium gas for flash vaporisation. The vapour created is transported through a series of dilution chambers into the mass spectrometer to provide a symmetrical peak profile and reduce the analysis time observed when dilution of samples is performed. The performance of the system was evaluated in the laboratory by studying the hydrolysis rate of methyl acetate in an open reactor.

Didden and Duisings<sup>35</sup> employed a similar liquid injection valve for the continuous on-line process monitoring of ethane, propane, ethylene and propylene present in the reactor feed of a synthetic rubber process plant. An injection volume of 20  $\mu\text{l}$  required a minimum cycle time of two minutes. The system was validated over an eighty day period with good precision and satisfactory accuracy when compared with process gas chromatographs, the analytical tool normally used. No re-calibration of the mass spectrometer was required during the validation period.

Brodbelt, Willis and Chowdhury<sup>36</sup> have studied the potential of an inverse sampling valve which operates in a similar manner to the two sampling valves described above by transferring a liquid sample, present in a sample groove etched in a piston, to the vaporisation region. A rapid response ( $< 100$  ms) was achieved with a peak width of 5-15

s for an undetermined sample volume. Analytical precision was measured by the relative standard deviation to be 2-4 %.

The secrecy expressed in these papers has not allowed a true validation of the sampling valves to be described and all three groups of authors do not discuss the limits of detection that can be achieved. All the work presented appears to analyse compounds present at percent level concentrations.

In this chapter an interface employed to transfer a sample from a liquid stream to a heated region for vaporisation and to transport the vapour created to a mass spectrometer for quantitative analysis is investigated. A gas chromatograph inlet was chosen to provide vaporisation of liquid samples, though different methods of introducing samples were employed to provide off-line and on-line analyses.

The reduction in the pressure of the gaseous sample required to maintain the vacuum pressures in the mass spectrometer is performed by a molecular leak present between the capillary inlet and ion source. This pressure reduction component of the mass spectrometer allows only a small proportion of the sample flowing through the capillary inlet to enter the ion source while the majority of the flow is pumped away to waste. No pressure reduction is required in the total vaporisation inlet and therefore a gas chromatographic inlet employed for direct injections was used because of its simplicity, robustness and ease of operation. The interface was investigated and validated for off-line and on-line applications in the laboratory using two model samples; methyl iodide (analyte) in acetic acid and acetone (analyte) in water.

## **3.2 Experimental**

### **3.2.1 Reagents**

Standard solutions were prepared in either 2.0 ml glass vials (Chromacol Ltd., Welwyn Garden City, Hertfordshire, UK) sealed with aluminium caps containing silicone rubber septa (off-line total vaporisation analysis) or 100 ml volumetric flasks (on-line total vaporisation analysis). AR Grade acetone and ethanol (Fisons Scientific Equipment, Loughborough, Leicestershire, UK) and methyl iodide (Aldrich, Gillingham, Dorset, UK) were employed with doubly deionised water (Elgastat, 18 M $\Omega$  cm<sup>-1</sup>) and acetic acid (99.9 % purity, BP Chemicals, Hull, East Yorkshire, UK).

Solutions were prepared on a volume to volume (v/v) basis. Standard solutions of concentration 1000  $\mu\text{g ml}^{-1}$  or greater were prepared by dissolving acetone in water and methyl iodide in acetic acid. Serial dilution was employed to prepare standard solutions of concentrations less than 1000  $\mu\text{g ml}^{-1}$ . The preparation of acetone solutions containing ethanol as an internal standard was performed by dissolving acetone and ethanol in water.

### **3.2.2 Instrumentation and Procedures**

A VG Gas Analysis Systems SX200 mass spectrometer (Middlewich, Cheshire, UK) was employed during the work described in this chapter. The instrument description and optimised operating parameters used are discussed in Chapter two. Acetone, ethanol and

methyl iodide were monitored at masses 43, 46 and 142 Da, respectively, except in section 3.3.4 when mass 58 Da was used to monitor acetone.

#### 3.2.2.1 Preliminary Studies

The manifold employed to perform preliminary studies on the vaporisation and analysis of liquid samples is shown in Figure 3.1. A tapered glass liner (length = 80 mm, i.d. = 3.0 mm, o.d. = 6.0 mm) placed in a gas chromatograph (Chrompack model 437, London, UK) heated injection inlet were employed to vaporise liquid samples. The mass spectrometer capillary inlet, used to transport vapours to the ion source, was positioned tightly in the restriction present in the glass liner and the bottom of the heated injection inlet was sealed with a graphite ferrule and Swagelok screw fitting, through which the capillary inlet was placed. The glass liner was heated by a metal block and the temperature of the metal block was controlled by the gas chromatograph instrument controls. A helium flow entering the manifold at the top section of the glass liner continuously purged the contents of the glass liner into the capillary inlet. A glass wool plug of depth 10 mm was placed at the bottom of the glass liner to ensure no dust or particulate matter entered the capillary inlet and caused a blockage.

Liquid samples were injected into the heated inlet with a 10  $\mu$ l glass syringe calibrated in 0.2  $\mu$ l increments. The syringe needle (length = 5 cm) was pushed completely through the rubber septum (Chrompack Chromsep Red), acting as a seal from the atmosphere, into the heated inlet before the contents of the syringe were expelled.

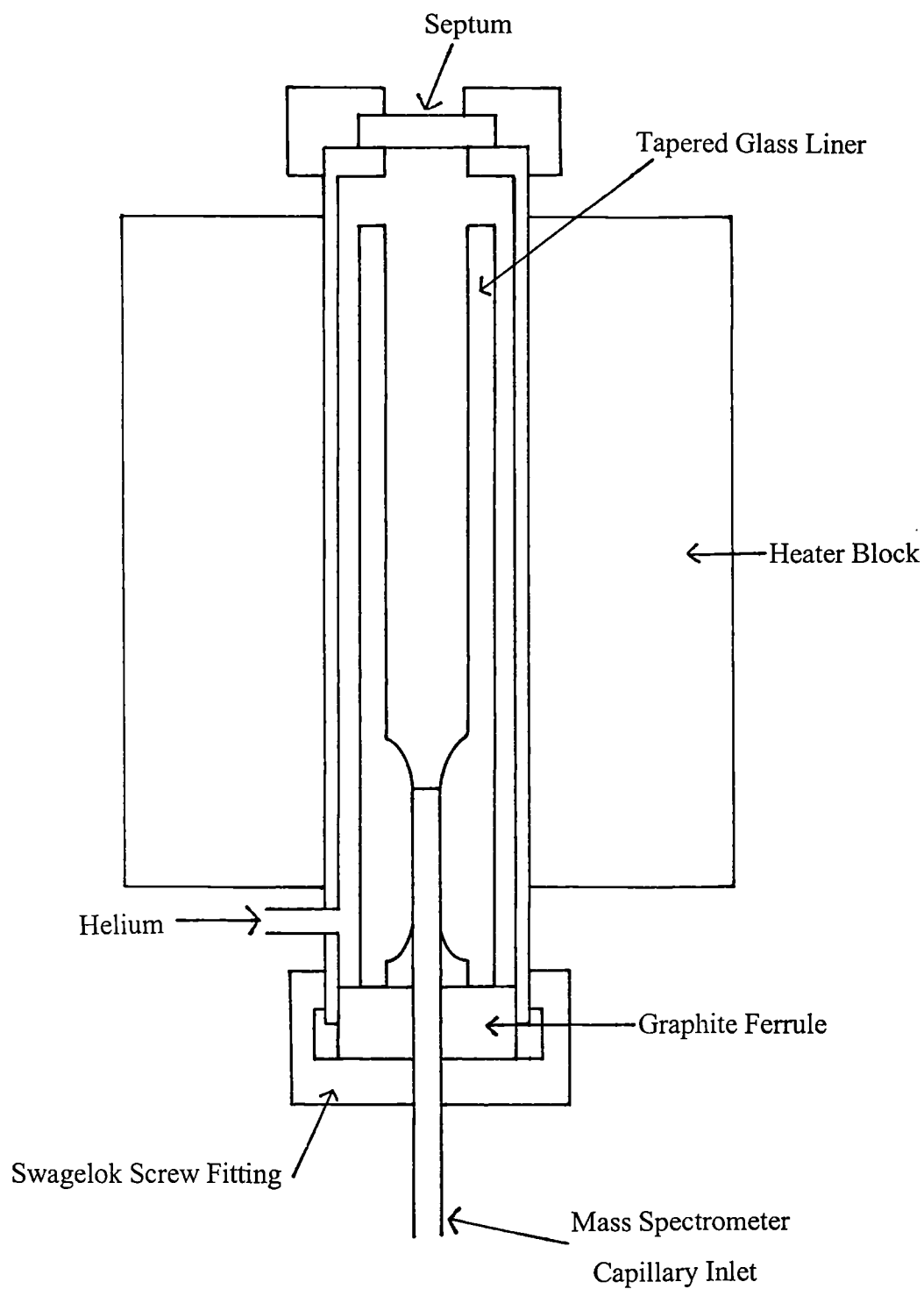


**Figure 3.1** The total vaporisation manifold employed during preliminary investigations  
(not to scale)

The investigation of the inlet temperature, helium flow back pressure and injection volume was performed twice using the manifold described above. In one investigation acetone standards containing no internal standard was used whereas in a second investigation the acetone standards did contain an internal standard.

#### 3.2.2.2 Off-line Total Vaporisation Analysis

The total vaporisation manifold used (Figure 3.2) consisted of a gas chromatograph (Chrompack model 437, London, UK) containing two heated inlets (A and B) connected by a 4.6 mm i.d. glass chromatography column containing no stationary phase. The length of the three columns used to provide buffer volumes of 12.1, 18.9 and 25.1 ml where 100, 150 and 200 cm, respectively. The construction of the heated inlets was described in section 3.2.2.1. Heated inlets A and B contained a straight glass liner and inverted tapered glass liner, respectively, each of length 80 mm, o.d. 6.0 mm and a maximum i.d. of 3.0 mm. The end of the mass spectrometer capillary inlet was placed firmly in the restriction of the inverted tapered glass liner present in heated inlet B to ensure that all of the vapour created was swept by a helium flow travelling from the top section of inlet A through the glass column and inlet B into the capillary inlet. The gas chromatograph oven was maintained at 20°C greater than the inlet temperature to eliminate condensation onto the glass column walls. Liquid samples were injected in to heated inlet A as was described in section 3.2.2.1.

The effect of inlet temperature, helium flow rate, buffer volume and injection volume were all investigated. The buffer volume will be discussed in section 3.3.2. Calibration data were collected for acetone and methyl iodide and the concentration of acetone in a process sample was quantified.

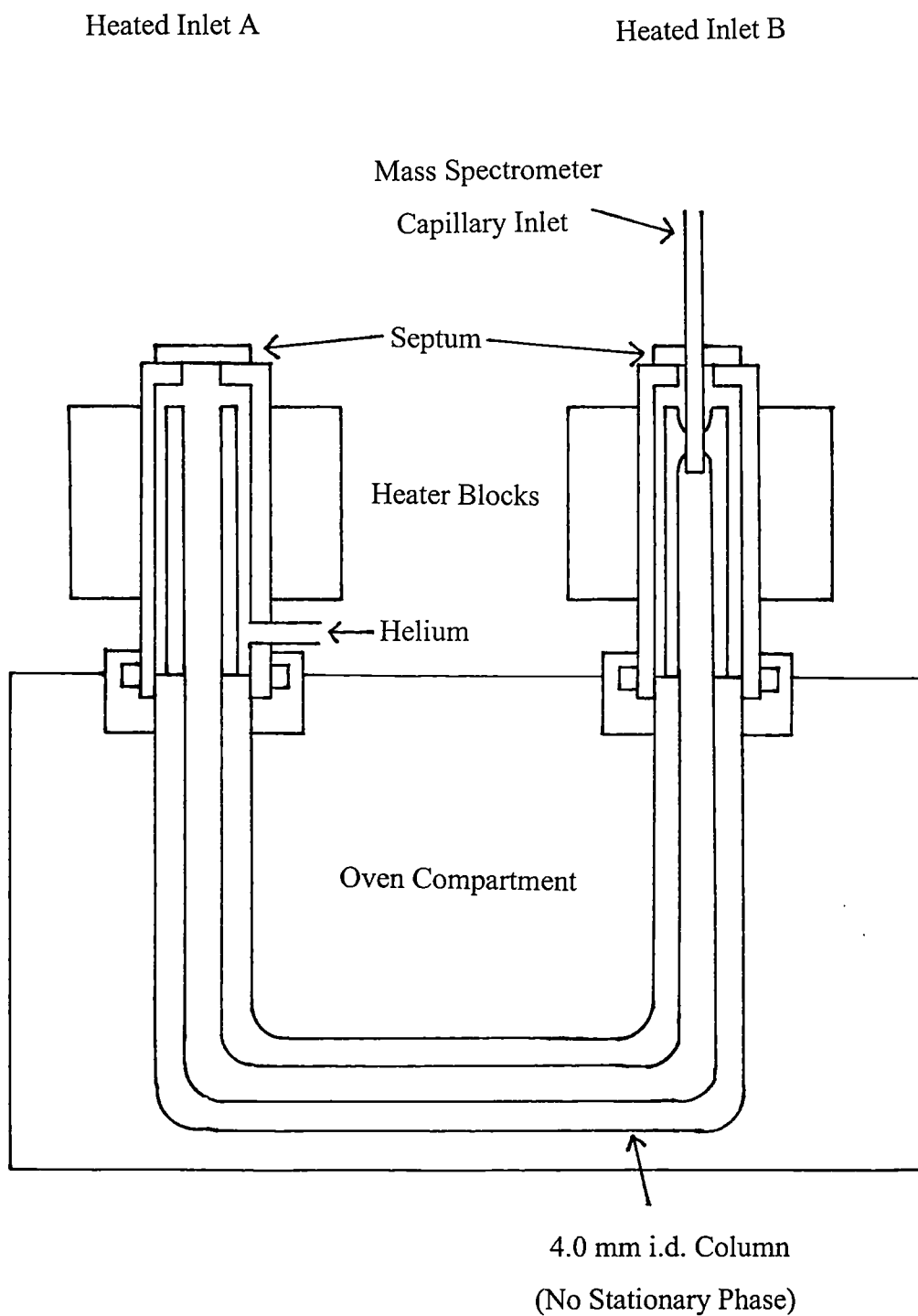


**Figure 3.2** The total vaporisation manifold employed for the off-line analysis of liquids  
(not to scale)

### 3.2.2.3 On-line Total Vaporisation Analysis

A similar manifold was employed for on-line total vaporisation analysis as was described in section 3.2.2.2, however a different strategy was used for the introduction of the liquid samples into the manifold. The total vaporisation manifold used is shown in Figure 3.3.

A Vici AG Valco internal volume sample valve with manual actuation (Thames Chromatography, Maidenhead, Berkshire, UK) was used to introduce 0.5  $\mu\text{l}$  liquid aliquots through a metal capillary (length = 8.0 mm, o.d. = 2.0 mm, i.d. = 1.0 mm), placed in empty heated inlet A, and into the front section of the glass column. No glass liner was placed in heated inlet A and vaporisation proceeded in the front section of the glass column. A liquid chromatography pump (Kontron Instruments, Watford, Hertfordshire, UK) continuously circulated a liquid stream through the sample valve which elevated the temperature of the liquid to 45 - 60°C because of heat transfer to the sample valve from heated inlet A. A flow of helium gas continuously passed through the sample valve into the glass column and was employed to purge liquid aliquots from the sample valve through the metal capillary into the glass column. Sample vaporisation and the passage of vapour created to the mass spectrometer for analysis was performed as discussed in section 3.2.2.2.

Calibration data were collected for acetone and methyl iodide using the manifold described above and the optimised operating conditions employed for off-line total vaporisation analysis. The concentration of acetone present in a process sample was also determined.

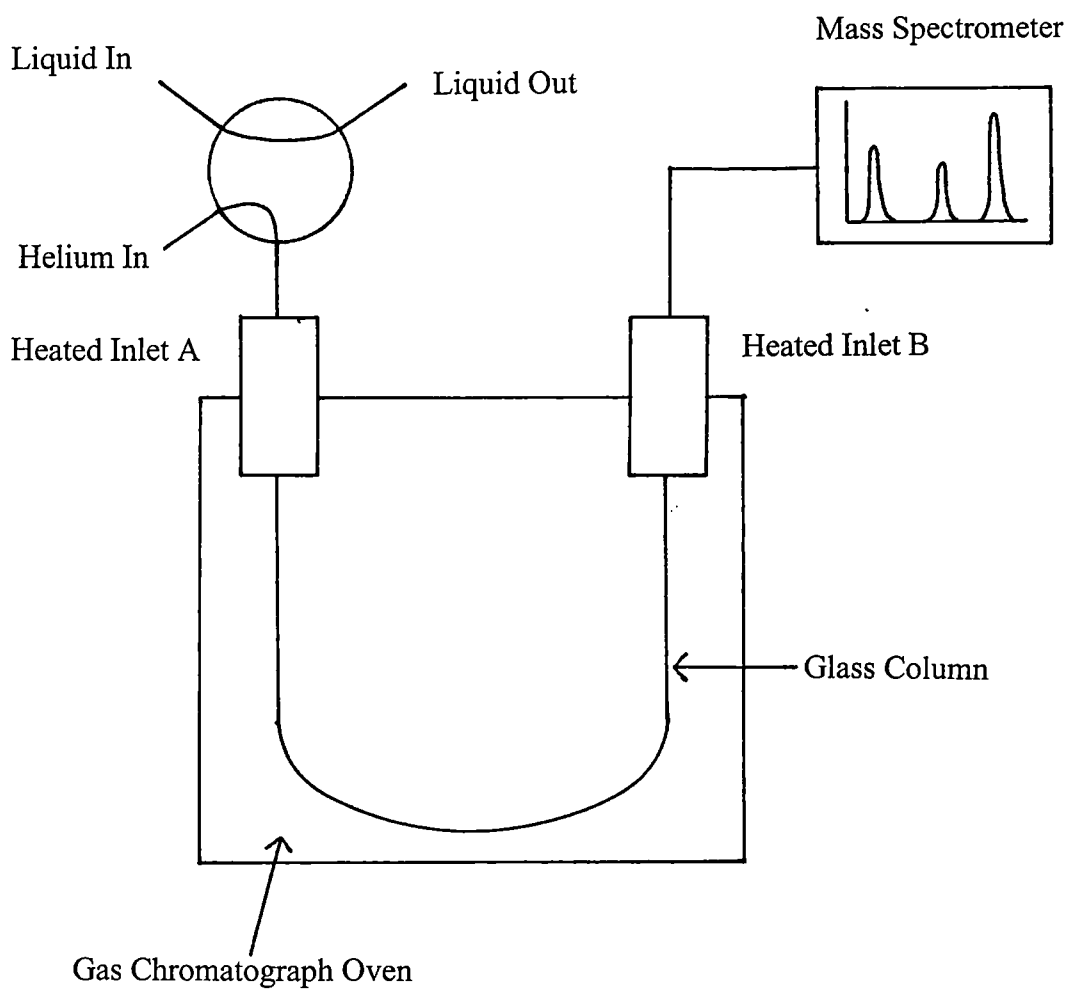


**Figure 3.3** The total vaporisation manifold employed for the on-line analysis of liquids  
(not to scale)

### 3.3 Results and Discussion

#### 3.3.1 Preliminary Investigations

Employing the total vaporisation manifold described in section 3.2.2.1 the injection temperature (heated injection inlet temperature), helium flow back pressure and injection volume (liquid sample volume) were all investigated. An aqueous solution containing  $1000 \mu\text{g ml}^{-1}$  acetone (analyte) and  $10000 \mu\text{g ml}^{-1}$  ethanol (internal standard) was used. The experimental conditions employed are shown in Table 3.1.

Variable investigated	Inlet temperature (°C)	Helium flow back pressure (kPa)	Injection volume ( $\mu\text{l}$ )
Inlet temperature	110 - 250	200	1.0
Helium flow back pressure	150	0 - 250	1.0
Injection volume	150	200	0.5 - 5.0

**Table 3.1** The experimental conditions employed during the preliminary investigations

Two sets of results were collected. The first set measured the *response* (mean peak height measured for six replicate injections) for acetone and the second set measured the *relative response* (mean ratio [equation 3.1]) measured for six replicate injections) for acetone and ethanol. The internal standard was used to compensate for experimental variations encountered.

$$\text{Ratio} = \text{peak height (acetone)} / \text{peak height (ethanol)} \quad (3.1)$$

Tables 3.2 - 3.4 show the results produced during the investigation.

Injection temperature (°C)	Response (Acetone monitored) ( $10^{-13}$ bar)	RSD (n=6) (%)	Relative response (Acetone and internal standard monitored)	RSD (n=6) (%)
110	748	15.2	0.91	4.1
150	1252	9.3	0.88	5.2
200	5120	48.9	0.74	11.4
250	6589	40.2	0.86	7.0

**Table 3.2** The effect of the injection temperature on the response and analysis precision

Injection volume ( $\mu$ l)	Response (Acetone monitored) ( $10^{-13}$ bar)	RSD (n=6) (%)	Relative response (Acetone and internal standard monitored)	RSD (n=6) (%)
0.5	335	19.8	0.79	2.2
1.0	1253	15.5	0.78	3.4
2.0	3106	12.6	0.72	5.8
5.0	7772	38.4	0.95	4.6

**Table 3.3** The effect of the injection volume on the response and analysis precision

Helium flow back pressure (kPa)	Response (Acetone monitored ( $10^{-13}$ bar))	RSD (n=6) (%)	Relative response (Acetone and internal standard monitored)	RSD (n=6) (%)
0	2349	21.3	0.94	10.0
50	3738	55.9	0.83	9.8
100	2518	52.9	0.81	8.7
150	1908	29.8	0.74	5.4
200	1296	6.4	0.85	8.1
250	1264	23.8	1.10	6.2

**Table 3.4** The effect of the helium flow back pressure on the response and analysis precision

Analyses of adequate precision (relative standard deviation [RSD (n=10)] < 10 %) are not obtained without the application of an internal standard to compensate for variations in the total vaporisation manifold operating conditions, vaporisation mechanism and vapour transport to the mass spectrometer ion source. Relative standard deviations ranged from 6.4 - 55.9 % when no internal standard was employed whereas an adequate precision [RSD (n=6) = 2.2 - 11.4 %] was obtained when an internal standard was used. The results exhibit optimum operating conditions with respect to the techniques sensitivity for the three experimental variables investigated.

A linear relationship between response and injection volume was expected. The observed exponential increase in the response as the injection volume is increased can be accounted for by the increase in pressure at the ion source entrance as the injection volume increases, which is described in the next paragraph. The higher pressures

observed provided a greater transfer rate of vaporised samples through the glass frit molecular leak in to the ion source.

The ion source pressure was observed to rapidly increase from a value less than  $1 \times 10^{-9}$  bar to  $1.5 - 2.0 \times 10^{-9}$  bar after the injection of a liquid sample into the heated inlet was performed. The pressure decreased to its original value after a period of time (< one minute) and the magnitude of the pressure change was dependant on the experimental conditions employed. For example, high injection temperatures provide a rapid vaporisation process and a relatively large increase in the ion source pressure.

The rapid pressure increase measured in the ion source is created by the increase in the volume as the sample passes from the liquid to vapour phase during vaporisation. The volumes of vapour created when water and acetic acid samples are vaporised at the gas chromatograph conditions employed in this section are shown in Table 3.5.

Volume of liquid ( $\mu$ l)	Volume of vapour produced ( $\mu$ l)	
	Water	Acetic acid
0.5	1920	600
1.0	3840	1210
2.0	7700	1840
5.0	19190	6040

**Table 3.5** The volume of vapour created when liquid samples are vaporised using the experimental conditions employed in this investigation

The volume of the glass liner (0.6 ml) is not large enough to allow the volume of vapour created to be contained within the glass liner during vaporisation. Instead the

expanding volume of the sample as it passes from the liquid to gas phase purges vapour forwards through the capillary inlet to the ion source and backwards along the helium gas transfer line. The result of this process was an observed increase in the ion source pressure and decrease in the helium flow back pressure. The reduction in the back pressure represents a drop in the flow rate of helium entering the glass liner caused by the vapour formed purging the helium backwards along the gas transfer line and not allowing the helium to flow through the glass liner.

The increase in the volume of the sample during vaporisation therefore does not provide an adequate reproducible flow of sample vapour to the mass spectrometer ion source when this manifold is employed. The application of an internal standard does, however, compensate for the changes observed. The mass spectrometer capillary inlet is designed to continuously transport a gas at a constant flow rate to the ion source. The total vaporisation manifold employed periodically pulses a high flow rate of vapour to the ion source during vaporisation. The continued application of the manifold would continuously increase and decrease the operating pressure which may be detrimental to the operation and lifetime of the ion source, even with the enclosed ion source employed which uses an ionisation region and filament which are separated and operated at different pressures.

### 3.3.2 Off-line Total Vaporisation Analysis

The problem of rapid pressure increases observed in the mass spectrometer ion source when the region of liquid vaporisation is interfaced directly with the mass spectrometer was observed and described in the previous section. The use of internal standards is not easily achieved when performing on-line total vaporisation analysis. Therefore to eliminate the problems of rapid pressure increases and increase the analysis precision, without the requirement to employ an internal standard, a gas chromatography glass column was used to enclose a buffer volume between the region of vaporisation and the mass spectrometer. The buffer volume was designed to provide a larger vaporisation region volume than was employed in the previous section and eliminate the rapid flow of vapour formed to the mass spectrometer ion source. The response in this section was measured as the mean change in the peak height measured of six replicate injections and an electron multiplier detector was employed unless otherwise described.

#### 3.3.2.1 The Mechanism of Vaporisation

The expulsion of a liquid from a syringe needle into a heated region creates a series of droplets which can obtain heat from a warm flow of gas or from the glass liner walls. The transfer of heat to the liquid droplets enables vaporisation of the liquid surface of the droplet and a reduction in the diameter of the droplets, which proceeds until vaporisation is complete and only vapour is present. During the vaporisation period droplets may also divide into a larger number of smaller droplets because of the formation of vapour in the

droplet, which causes expansion of the liquid and the subsequent explosive splitting of the droplet.

Figure 3.4 shows the peak profiles measured when acetone standards prepared in water were injected into the vaporisation manifold described in section 3.2.2.2. The same experimental conditions were employed as for calibration of the technique (section 3.3.2.6). Injections were performed at time 0 and 60 s for injection volumes of 5.0 and 0.5  $\mu\text{l}$ , respectively. The peak profile for methyl iodide prepared in acetic acid using the same experimental conditions and an injection volume of 5.0  $\mu\text{l}$  is shown in Figure 3.5. The peak profiles display the variation in the rate of release of the analyte during vaporisation.

The peak profile for acetone standards when an injection volume of 5.0  $\mu\text{l}$  was employed shows a slow uniform release of acetone (A) followed by a rapid increase (B) in the release of acetone, before the release again slows to zero as vaporisation is completed and the manifold is purged of the vapour formed (C). The slow uniform release of acetone displayed on the peak profile as a shoulder represents a non-optimum droplet diameter for the greatest release of acetone from the liquid phase. Instead in this stage the droplet diameter decreases and a relatively lower rate of release is observed before the optimum droplet diameter is approached and the faster rate of release of acetone is observed. Vaporisation is completed in 90 s.

The peak profiles for acetone (injection volume = 0.5  $\mu\text{l}$ ) and methyl iodide (injection volume = 5.0  $\mu\text{l}$ ) show a faster vaporisation process with no shoulder observed. The liquid droplet diameters therefore are at a near optimum value as they enter the vaporisation region and no reduction in the droplet diameter is required. The liquid

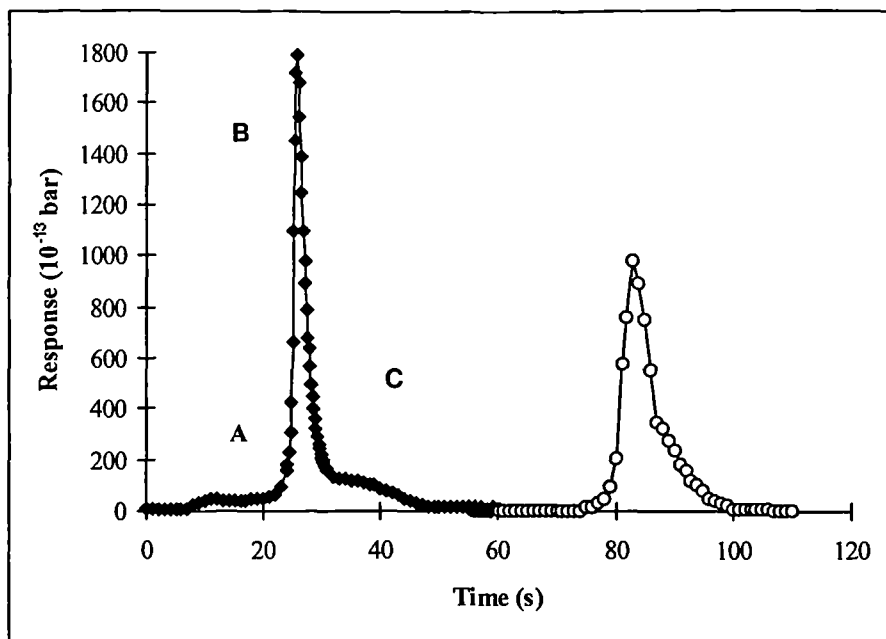


**Figure 3.4** Peak profiles for acetone using 0.5 (o) and 5.0 (◆) μl injection volumes

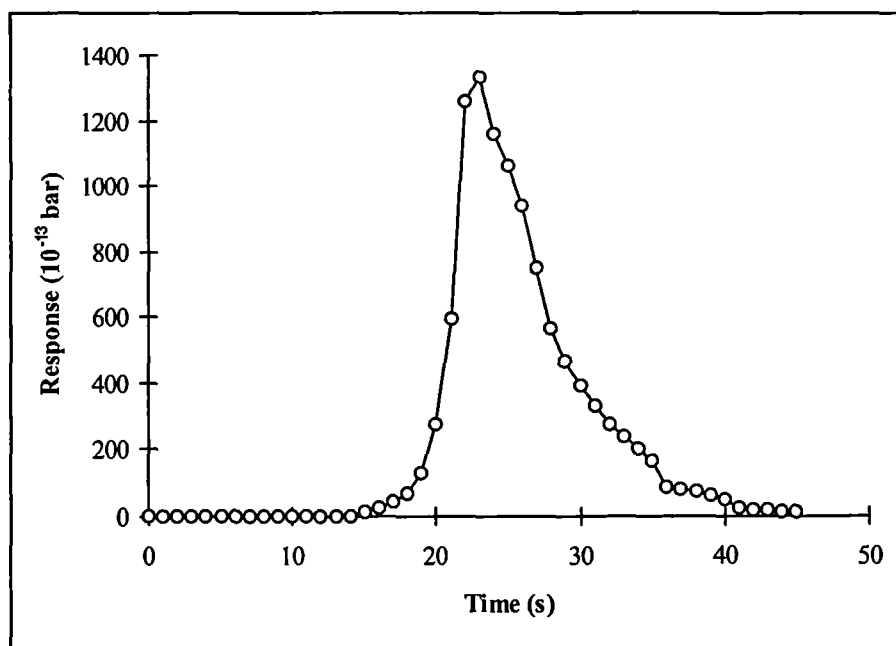


**Figure 3.5** Peak profile for methyl iodide using an injection volume of 5.0 μl

matrix and injection volume, which influences the mechanism of liquid expulsion from the syringe needle, therefore affect the process of vaporisation.

The variation in the droplet diameters of water and acetic acid expelled from a syringe needle can be observed visually at room temperature and atmospheric pressure. The diameters of water droplets expelled from a syringe are large with respect to the diameter of droplets created by the expulsion of acetic acid. The droplet diameters for acetic acid are small enough to be termed an aerosol. These differences in the diameters of the droplets can be explained by the larger surface tension<sup>37</sup> of water at 20°C ( $73.1 \times 10^{-3} \text{ N m}^{-1}$ ) with respect to acetic acid ( $27.8 \times 10^{-3} \text{ N m}^{-1}$ ). The larger surface tension of water does not allow the formation of relatively small diameter droplets for injection volumes of 5  $\mu\text{l}$  when water is expelled from a syringe. This explains the differences in the peak profiles for the two matrices studied. Although the droplet diameter does not exclusively affect the vaporisation mechanism of liquids by this technique, it clearly has an influence.

The time required for vaporisation to be completed, independent of the sample matrix and injection volume, is long and shows that the reservoir of heat available in the vaporisation region is either not large enough or not transported efficiently enough to allow very rapid vaporisation in periods of less than 2 s. The vaporisation process is however shorter when smaller injection volumes are employed.

### 3.3.2.2 The Effect of the Buffer Volume

The glass column placed between heated inlets A and B was employed to eliminate rapid pressure increases in the mass spectrometer ion source and therefore buffer the

mass spectrometer from the region of vaporisation. For this reason the volume enclosed by the glass column was called the buffer volume.

The relationship between the response and buffer volume was investigated using blank solutions, 1000  $\mu\text{g ml}^{-1}$  acetone standards and 100  $\mu\text{g ml}^{-1}$  methyl iodide standards. An injection temperature of 200°C, helium gas flow rate of 77  $\text{ml min}^{-1}$  and an injection volume of 5  $\mu\text{l}$  were used. The results are shown in Figure 3.6 for the acetone and methyl iodide standards.

The response decreases as the buffer volume is increased for acetone standards which is caused by an increase in the gas phase dilution of the vaporised liquid with helium as it passes through progressively larger buffer volumes. The change in gas phase dilution for vaporised methyl iodide standards is smaller and is shown by the relatively constant response as the buffer volume is increased. The influence of the buffer volume on the response is therefore dependant on the sample matrix and analyte. The slower rate of vaporisation for water matrices, described in section 3.3.2.1, allow the vaporised sample to mix well with increasingly larger volumes of helium gas as the buffer volume increases. Complete vaporisation of acetic acid matrices is faster and therefore dilution with helium is relatively uniform and independent of the buffer volume.

Although the above description may be correct presently it is not clearly understood why the response decreases as the buffer volume increases for acetone standards whereas the response remains constant as the buffer volume is increased for methyl iodide standards.

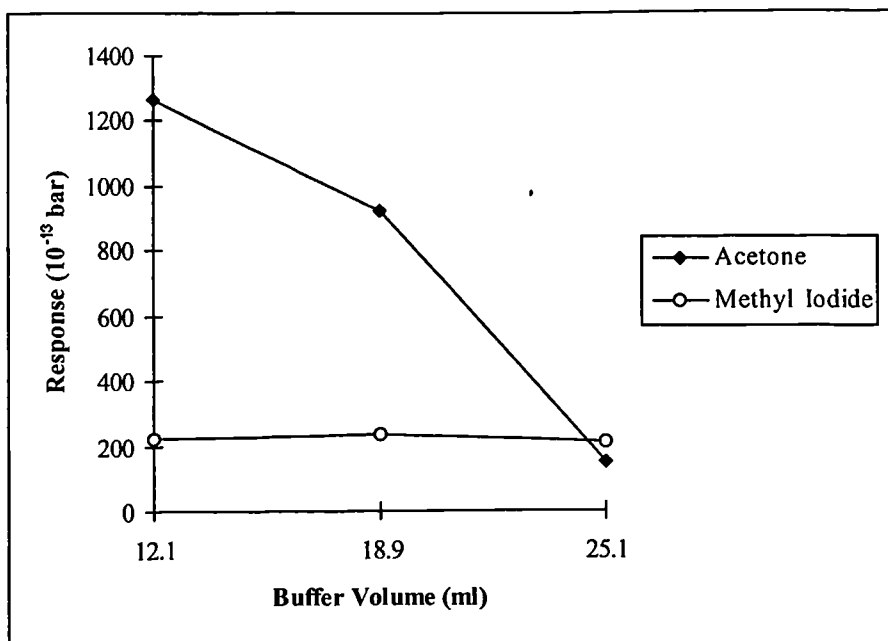


**Figure 3.6** The effect of the buffer volume

The injection of blank solutions produces a small measured response and therefore the application of 5  $\mu$ l injection volumes creates a pressure increase in the mass spectrometer ion source even though a buffer volume is used. The peak maximum for blank and standard solutions occur at the same time after injection. Therefore the time when the highest rate of analyte release is measured by the mass spectrometer is equivalent to the time when the pressure in the ion source reaches a maximum.

In further studies a buffer volume of 12.1 ml will be used to provide a sensitive response for both analytes.

### 3.3.2.3 The Effect of Injection Temperature

The relationship between the injection temperature and response was investigated using  $1000 \mu\text{g ml}^{-1}$  acetone and methyl iodide standards. A buffer volume of 12.1 ml, helium flow rate of  $77 \text{ ml min}^{-1}$  and injection volume of  $5 \mu\text{l}$  were employed.

The response increases as the injection temperature increases for both analyte standards (Figure 3.7). This shows a larger amount of heat is available for vaporisation of liquid samples and a greater rate of vaporisation is achieved as the temperature is increased.

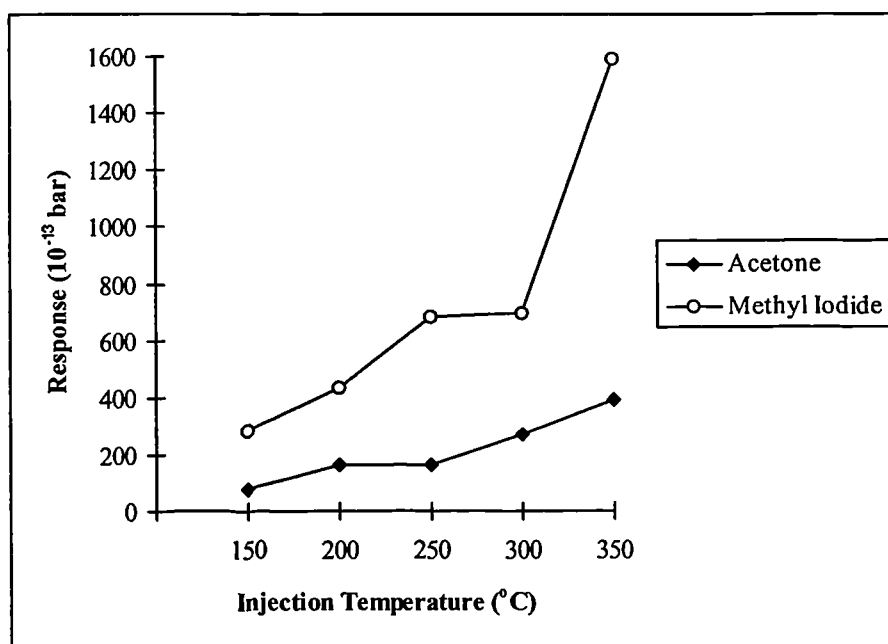


**Figure 3.7** The effect of the injection temperature

### 3.3.2.4 The Effect of the Helium Flow Rate

The response was measured over a range of helium flow rates with  $1000 \mu\text{g ml}^{-1}$  acetone and methyl iodide standards. A buffer volume of 12.1 ml, injection temperature of  $200^{\circ}\text{C}$  and an injection volume of  $5 \mu\text{l}$  was employed. An optimum flow rate with respect to sensitivity was observed at a flow rate of  $56 \text{ ml min}^{-1}$  for acetone standards and  $34 \text{ ml min}^{-1}$  for methyl iodide standards (Figure 3.8). At flow rates lower than the optimum values the transport time of the vapour created to the mass spectrometer is longer and allows a greater rate of gas phase sample dilution with the helium. At flow rates higher than the optimum values the decrease in the response may be caused by incomplete vaporisation or the greater dispersion of the liquid droplets formed during injection by the faster velocity of the helium flow.

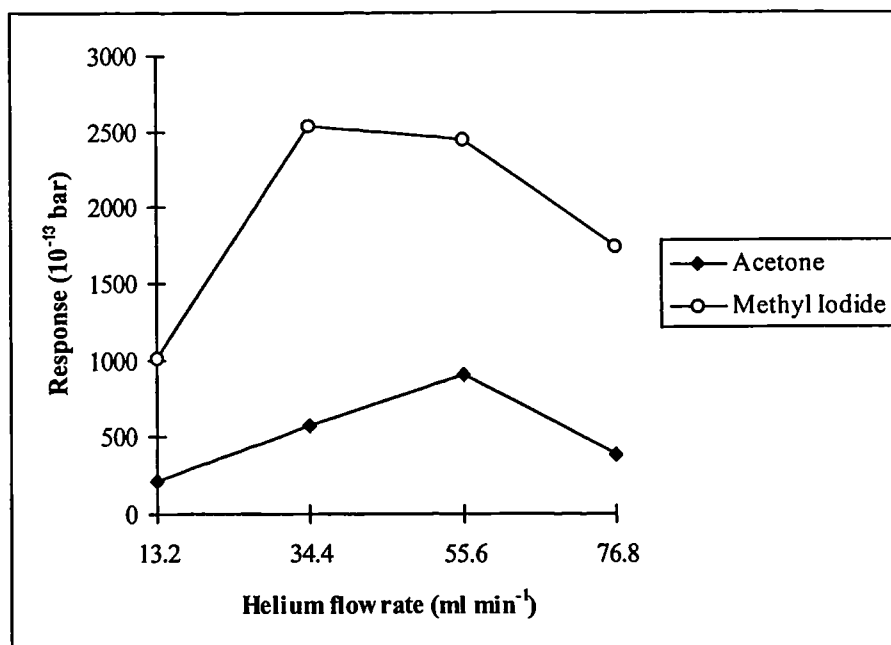


**Figure 3.8** The effect of the helium flow rate

### 3.3.2.5 The Effect of the Injection Volume

The influence of the injection volume was investigated using a 12.1 ml buffer volume, injection temperature of 200°C and helium flow rate of 56 ml min<sup>-1</sup>. 1000 µg ml<sup>-1</sup> acetone and methyl iodide standards were also used. Figure 3.9 shows the increase in response as the injection volume is increased.

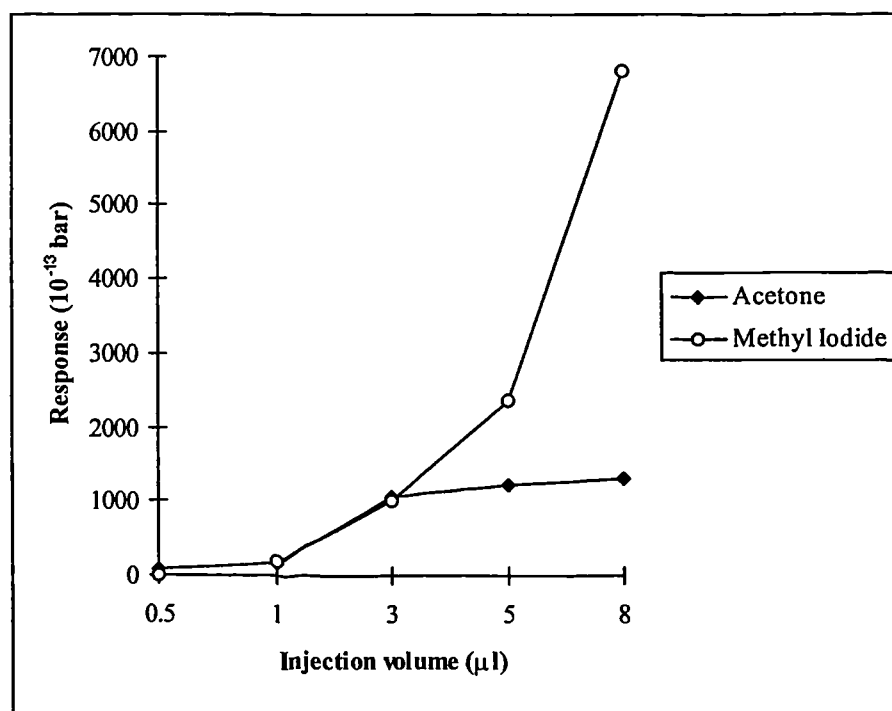


**Figure 3.9** The effect of the injection volume

The increase in the response is exponential in the range studied for methyl iodide standards. However the increase appears to be exponential in the range 0.5 - 3.0 µl for acetone standards and the response increases at a significantly lower rate as the injection volume is increased above 3 µl. The increase in response observed for both analytes is

caused by the larger mass of analyte present in the liquid sample as the injection volume increases, and by the faster rate of release of analyte from the liquid phase. A linear relationship between response and injection volume would be observed if the rate of analyte release was constant over the range of injection volumes investigated. The lower rate of increase in the response measured for acetone standards when injection volumes greater than 3  $\mu\text{l}$  are employed exhibits a decrease in the rate of release of acetone from the liquid droplets caused by a combination of the sample matrix and injection volume.

The responses measured for an injection volume of 1.0  $\mu\text{l}$  in this section are approximately four times smaller than the responses measured during the preliminary studies (Section 3.3.1) for the same injection volume. This exhibits the degree of sample vapour dilution with helium gas that is present when a buffer volume is employed. The high blank solution responses measured during the preliminary studies however may not allow lower limits of detection to be achieved with the manifold employed during the preliminary studies.

#### 3.3.2.6 Calibration

Calibration data were collected for acetone and methyl iodide using a buffer volume of 12.1 ml, injection temperature of 350°C and helium flow rate of 56 ml  $\text{min}^{-1}$  and an electron multiplier. A larger response can be obtained with a flow rate of 34 ml  $\text{min}^{-1}$  with methyl iodide standards but the time required for the manifold to be purged of vaporised liquid is significantly longer at the lower flow rate. A flow rate of 56 ml  $\text{min}^{-1}$  was therefore employed which contributed to a 7 % decrease in the response. Injection volumes of 0.5 and 5.0  $\mu\text{l}$  were used to provide a comparative investigation of the limits

of detection when the injection volume is increased for acetone and methyl iodide standards. An internal standard (5000  $\mu\text{g ml}^{-1}$  ethanol) was applied to provide quantification of acetone standards analysed when an injection volume of 5.0  $\mu\text{l}$  was used, to provide an adequate precision. The application of an internal standard with methyl iodide standards and acetone standards injected as a smaller volume did not improve the precision.

The relative response was measured, when an internal standard was used, as the mean ratio (equation 3.2) of the peak heights of acetone and ethanol for ten replicate injections:

$$\text{Ratio} = \text{peak height (acetone)} / \text{peak height (ethanol)} \quad (3.2)$$

The response employed when no internal standard was used was measured as the mean peak height for acetone or methyl iodide for ten replicate injections. Calibration graphs of response (ratio or peak height [ $10^{-13}$  bar]) vs. analyte concentration ( $\mu\text{g ml}^{-1}$ ) were plotted and the linear calibration ranges, equations of the calibration line and correlation coefficients were calculated using the method of least squares<sup>38</sup>. The parameters x and y in the equations of the calibration lines represent the analyte concentration and response, respectively.

The limits of detection (LOD) were calculated<sup>39</sup> using the response (y) providing a signal equivalent to the blank signal ( $y_B$ ), represented as the intercept value in the calculated equation of the calibration line, plus three standard deviations of the responses measured when analysing the blank solution ( $3\sigma$ ):

$$y = y_B + 3\sigma \quad (3.3)$$

The analyte concentration representing the calculated response ( $y$ ) using the equation of the calibration line was employed as the limit of detection ( $3\sigma$ ).

For example, if the equation of the calibration line was  $y = 0.25x + 0.12$  and the standard deviation of the responses measured for the blank solution was 0.05, the calculated value of  $y$  would be 0.27 [ $0.12 + 3(0.05)$ ] and the limit of detection would be 0.6 units.

Tables 3.6 and 3.7 show the calibration data collected for acetone when injection volumes of 0.5 and 5.0  $\mu\text{l}$ , respectively, were used.

[Acetone] ( $\mu\text{g ml}^{-1}$ )	Response ( $10^{-13}$ bar)	RSD (n=10) (%)
0	22.9	6.2
10	31.2	6.7
50	43.3	2.5
100	65.2	3.0
1000	348	2.9
10000	3192	4.2

$$y = 0.32x + 28.6$$

$$r = 0.9999 \text{ (n=6)}$$

$$\text{Limit of detection} = 13.5 \mu\text{g ml}^{-1}$$

**Table 3.6** Calibration data for acetone when an injection volume of 0.5  $\mu\text{l}$  was used

[Acetone] ( $\mu\text{g ml}^{-1}$ )	Relative Response ( $10^{-13}$ bar)	RSD (n=10) (%)
0	0.96	3.0
10	1.08	4.3
50	1.23	2.8
100	1.33	2.0
500	3.67	5.5
1000	5.83	3.2
5000	24.2	16.9

$$y = 0.005x + 1.06$$

$$r = 0.9998 \text{ (n=7)}$$

$$\text{Limit of detection} = 19 \mu\text{g ml}^{-1}$$

**Table 3.7** Calibration data for acetone when an injection volume of 5.0  $\mu\text{l}$  was used

The detection limit is lower when a smaller injection volume is employed and exhibits the effect of the slower rate of release of acetone from the liquid phase when an injection volume of 5  $\mu\text{l}$  is employed. Both detection limits are similar, however, and are in the low  $\mu\text{g ml}^{-1}$  range. Linear calibration ranges extending over 3 or 4 decades of concentration were achieved with good linearity [ $r > 0.9997$ ,  $n=6$  (0.5  $\mu\text{l}$ ),  $n=7$  (5.0  $\mu\text{l}$ )] and an adequate precision [RSD (n=10) < 7 %] with or without the use of an internal standard. An adequate precision is defined as a RSD value measured for replicate analyses of less than 10 %. The large relative standard deviation calculated for the analysis of a 5000  $\mu\text{g ml}^{-1}$  acetone standard was caused by the inability of the electron multiplier to rapidly switch between the responses of the two masses monitored at 43

(acetone) and 46 (ethanol) Da, which were of a significantly different magnitude. Achievable analysis frequencies were calculated for 0.5 and 5.0  $\mu\text{l}$  injection volumes, respectively, as 40 and 80  $\text{h}^{-1}$ .

The calibration data collected for methyl iodide is shown in Tables 3.8 and 3.9 for injection volumes of 0.5 and 5.0  $\mu\text{l}$ , respectively.

[Methyl iodide] ( $\mu\text{g ml}^{-1}$ )	Response ( $10^{-13}$ bar)	RSD (n=10) (%)
0	8.92	8.5
10	11.3	6.0
100	24.4	6.0
200	37.2	7.0
500	81.9	2.4
5000	564	3.4
10000	1144	3.5

$$y = 0.11x + 13.2$$

$$r = 0.9998 \text{ (n=7)}$$

$$\text{Limit of detection} = 20.6 \mu\text{g ml}^{-1}$$

**Table 3.8** Calibration data for methyl iodide when an injection volume of 0.5  $\mu\text{l}$  was used

[Methyl iodide] ( $\mu\text{g ml}^{-1}$ )	Response ( $10^{-13}$ bar)	RSD (n=10) (%)
0	4.04	12.8
1	5.08	9.4
10	20.5	5.6
50	72.1	6.3
100	156	3.8
500	711	5.7
1000	1556	6.3
5000	8395	3.8

$$y = 01.68x - 34.2$$

$$r = 0.9998 \text{ (n=8)}$$

$$\text{Limit of detection} = 0.9 \mu\text{g ml}^{-1}$$

**Table 3.9** Calibration data for methyl iodide when an injection volume of 5.0  $\mu\text{l}$  was used

The detection limits of 20.6  $\mu\text{g ml}^{-1}$  and 0.9  $\mu\text{g ml}^{-1}$  for injection volumes of 0.5 and 5.0  $\mu\text{l}$ , respectively, show the opposite trend to that observed for acetone standards. An increase in the injection volume results in the detection limit becoming smaller for methyl iodide standards. This exhibits an increase in the rate of release of methyl iodide when the injection volume is increased. A reduction in the rate of release is observed for acetone standards when the injection volume is increased. Linear calibration ranges [ $r = 0.9998$ ,  $n=7$  (0.5  $\mu\text{l}$ ),  $n=8$  (5.0  $\mu\text{l}$ )] covering 3 or 4 decades of concentration were

observed. The analysis precision [RSD (n=10) < 10 %] was adequate and an analysis frequency of 60 - 80 h<sup>-1</sup> were achieved for both injection volumes investigated.

### 3.3.3 On-line Total Vaporisation Analysis

The application of the off-line total vaporisation manifold in the previous section has shown potential for the analysis of liquid streams. In this section the use of a different strategy for sample introduction into the total vaporisation manifold is employed to provide a method to automate the sampling and analysis stages, which is required for on-line process analysis. The sampling strategy employs an internal volume sampling valve with manual actuation, though pneumatic actuation can be implemented for the complete automation that would be required for on-line process applications of the technique.

The vaporisation mechanism and sample volumes employed in this section are similar to those used in section 3.3.2 for off-line total vaporisation analysis. Therefore the same optimised manifold conditions were employed as in the previous section.

#### 3.3.3.1 Calibration

Calibration data were collected for acetone and methyl iodide using the manifold described in section 3.2.2.3. and a sampling valve with an internal volume of 0.5 µl. The vaporisation region at the front section of the glass column was maintained at 350°C by the gas chromatograph oven and heated inlet B was maintained at 370°C. Heated inlet A was heated to 200°C to ensure the sampling valve placed in close proximity to the inlet

was not heated to temperatures greater than 200°C, the manufacturer's recommended maximum operating temperature. A buffer volume of 12.1 ml was employed though unlike in the previous section all of the vaporisation region is contained in the glass column and therefore a smaller buffer volume connects the region of vaporisation and the mass spectrometer. A higher flow rate of 95 ml min<sup>-1</sup>, with respect to the flow rate used in the off-line manifold, was employed to ensure that rapid expulsion of the liquid sample through the capillary is obtained.

The response was measured as the mean peak height of the analyte for ten replicate injections. Calibration graphs of response (10<sup>-13</sup> bar) vs. analyte concentration (µg ml<sup>-1</sup>) were plotted and the equations of the calibration lines, correlation coefficients and limits of detection (3σ) were calculated using the method of least squares<sup>38,39</sup>. The calculation of these parameters was described in section 3.3.2.6.

Limits of detection calculated using all of the calibration points did not represent a LOD which was achievable with the manifold used. The higher concentration standards distorted the gradients and intercept values calculated to use in the equations of the calibration line and the calibration line did not represent the correct relationship between analyte concentration and response at low analyte concentrations. To overcome this problem the five calibration points representing the five lowest concentration standards analysed were used to calculate a more accurate value for the limit of detection.

Tables 3.10 and 3.11 show the calibration data collected for acetone and methyl iodide, respectively.

[Acetone] ( $\mu\text{g ml}^{-1}$ )	Response ( $10^{-13}$ bar)	RSD (n=10) (%)
0	22.9	4.8
10	20.4	4.5
50	28.6	10.6
100	45.0	3.7
500	137	6.3
1000	292	5.3
5000	1496	4.4
10000	2745	1.3
15000	4500	3.0

$$y = 0.29x + 3.48$$

$$r = 0.9989 \text{ (n=9)}$$

Limit of detection =  $11.2 \mu\text{g ml}^{-1}$

**Table 3.10** Calibration data for acetone

[Methyl iodide] ( $\mu\text{g ml}^{-1}$ )	Response ( $10^{-13}$ bar)	RSD (n=10) (%)
0	3.07	10.2
5	5.23	13.3
10	5.57	5.0
50	11.2	6.2
100	20.2	2.7
500	79.7	1.7
1000	132	3.0
5000	796	2.0
10000	1696	1.4
15000	2595	3.3
20000	3460	2.8

$$y = 0.17x - 11.3$$

$$r = 0.9998 \text{ (n=11)}$$

$$\text{Limit of detection} = 5.4 \mu\text{g ml}^{-1}$$

**Table 3.11** Calibration data for methyl iodide

Limits of detection of 11 and  $5 \mu\text{g ml}^{-1}$  were achieved with the manifold for acetone and methyl iodide, respectively, which are similar to those achieved using the off-line total vaporisation manifold and injection volumes of  $0.5 \mu\text{l}$ . However, larger calibration ranges extending over four decades of concentration were achieved for the on-line technique with good linearity [ $r = 0.9989$ ,  $n=9$  (acetone),  $n=11$  (methyl iodide)] and the precision at concentrations greater than  $100 \mu\text{g ml}^{-1}$  is similar [RSD ( $n=10$ )  $< 7\%$ ] to those observed for the off-line technique.

### 3.3.4 The Determination of Acetone in a Process Sample

To investigate the accuracy that can be achieved with the off-line and on-line total vaporisation manifolds, process samples obtained from BP Chemicals in Hull were analysed to quantify the concentration of acetone present in the samples. The approximate composition of two process samples (one and two) are shown in Table 3.12. The exact concentration of acetone in the samples was determined by gas chromatography at BP Chemicals, the technique normally employed for the analysis of a wide variety of process samples.

Compound	Process sample one composition (% v/v)	Process sample two composition (% v/v)
Formic acid	7	7
Acetic acid	30	30
Propionic acid	5	5
Acetone	9.4	8.4
Water	14	14
Methyl acetate	4	4
Ethyl and propyl acetate	3	3
Butanone	2.5	2.5
2-pentanone and 3-hexanone	3.5	3.5
Pentane	11	1
Benzene	4	4

**Table 3.12** The composition of process samples one and two

#### 3.3.4.1 The Effect of the Calibration Matrix

The influence of the sample matrix on the vaporisation mechanism and response measured has been observed and described for the off-line technique in section 3.3.2.1 when the two different matrices of water and acetic acid were analysed. In cases where the sample matrix does effect the response measured there is a requirement for the sample matrix and calibration matrix to influence the response in an identical manner.

The relationship between the response and concentration of acetic acid present in the standard solution was investigated using aqueous 10.0 % (v/v) acetone solutions

containing 0, 10, 30 or 50 % acetic acid. The experimental conditions employed are shown in Table 3.13.

Analysis Type	Off-line	On-line
Buffer volume (ml)	12.1	12.1
Inlet A temperature (°C)	350	200
Inlet B temperature (°C)	370	370
Oven temperature (°C)	350	370
Helium flow rate (ml min <sup>-1</sup> )	51	95
Injection volume (μl)	0.5	0.5

**Table 3.13** Experimental conditions employed for the quantification of acetone in section 3.3.4

Acetic acid contributes significantly to the response measured at mass 43 Da and therefore the response at mass 58 Da was monitored to quantify acetone. The response at mass 58 Da contains no contribution from acetic acid. Eight components in the process samples analysed in section 3.3.4.3 also contribute to the response at mass 43 Da and therefore this mass could not be used to provide an accurate determination of acetone when process samples one and two were analysed.

The response increases as the acetic acid concentration increases when the off-line total vaporisation manifold is employed but remains constant when the on-line technique is used (Figure 3.10).

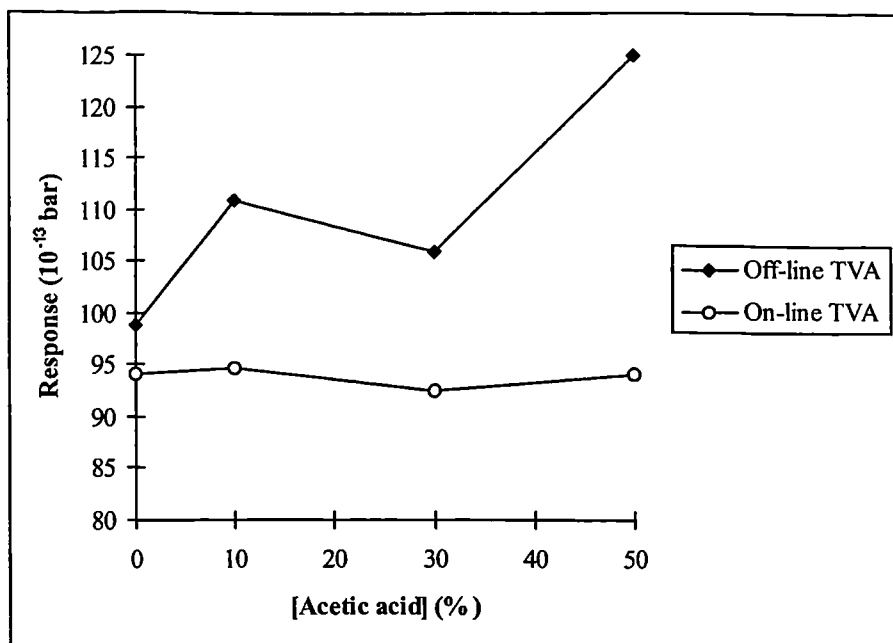


**Figure 3.10** The effect of the acetic acid concentration present in the calibration matrix on the response

The calibration matrix employed can affect the vaporisation mechanism and response measured, though only for the off-line technique. The absence of any effect when the on-line total vaporisation analysis technique is used can be explained by the two differences in the manifolds employed for the off-line and on-line techniques. These two differences are the method of introducing the liquid into the vaporisation region and the flow rate of helium used. The higher flow rate and rough ended capillary end used in the on-line total vaporisation manifold can nebulise the liquid leaving the capillary more efficiently to

produce a range of droplets with smaller diameters than can be achieved when a syringe needle is employed for sample introduction. This allows a faster vaporisation process to proceed and the effect of the acetic acid is not observed. Also the liquid stream is heated to temperatures of 45 - 60°C when continuously circulated through the sample valve operating at temperatures above 100°C. The liquid aliquot ejected from the metal capillary inlet is therefore heated and partial vaporisation of the liquid in the sample valve will produce bubbles of vapour in the liquid which when ejected from the end of the capillary will aid explosive nebulisation of the liquid. For off-line total vaporisation analysis when relatively efficient nebulisation and fast vaporisation is not present the sample matrix is influential. In these cases the increase in the concentration of acetic acid produces an increase in the rate of release of acetone from the liquid droplets. This was observed when the different matrices of water and acetic acid were investigated in section 3.3.2.1.

The process samples contain a high proportion (89 %) of organic components (ionic, polar and non-polar). A calibration matrix of 85 % acetic acid and 15 % water was employed for the collection of calibration data to mimic the sample matrix and provide a chemically similar matrix which can be prepared quickly and easily. The concentration of water, which reduces the rate of acetone release is therefore equal to that observed in the process samples.

The concentration of acetone in the process samples is higher than can be measured using an electron multiplier as the ion detector. Therefore to avoid the requirement for sample dilution, which can be time consuming and technically complex when applied with the on-line total vaporisation manifold, a Faraday cup was employed to quantify acetone present in the standard solutions and process samples.

### 3.3.4.2 Calibration

Calibration data was collected using the experimental conditions listed in Table 3.13 and the off-line and the on-line total vaporisation manifolds described in sections 3.2.2.2 and 3.2.2.3, respectively. Calibration graphs of response ( $10^{-13}$  bar) vs. analyte concentration (%) were plotted. The method of least squares<sup>38,39</sup> was employed to calculate the equations of the calibration line, correlation coefficients and limits of detection ( $3\sigma$ ). The calculations performed were discussed in section 3.3.2.6.

The calibration data collected can be seen in Tables 3.14 and 3.15.

[Acetone] (%)	Response ( $10^{-13}$ bar)	RSD (n=10) (%)
0	0.0	104
0.1	0.85	15.8
0.5	3.35	4.7
1	6.82	3.2
5	34.9	3.3
10	69.1	4.3
20	144	2.3
30	215	2.6
40	293	3.7

$$y = 7.28x - 1.00$$

$$r = 0.9999 \text{ (n=9)}$$

$$\text{Limit of detection} = 0.06 \%$$

**Table 3.14** Calibration data for acetone using the off-line total vaporisation analysis technique

[Acetone] (%)	Response (10 <sup>-13</sup> bar)	RSD (n=10) (%)
0	0.37	24.9
0.1	1.24	12.2
1	8.98	4.4
5	56.4	2.0
10	108	3.1
15	172	2.1
30	305	1.1

$$y = 10.3x + 3.05$$

$$r = 0.9980 \text{ (n=7)}$$

Limit of detection = 0.03 %

**Table 3.15** Calibration data for acetone using the on-line total vaporisation analysis technique

A calibration range covering three decades of concentration was achieved with good precision throughout the measured range [RSD (n=6) < 5 % when standards of concentration greater than 0.1 % were analysed]. The limits of detection of 0.06 and 0.03 % for the off-line and on-line techniques, respectively, are not as low as can be achieved with the more sensitive electron multiplier detector. However the combination of the electron multiplier and Faraday cup detectors allows acetone to be measured in the range 10 to 300000 µg ml<sup>-1</sup> (five decades of concentration).

### 3.3.4.3 Analysis of the Process Samples

Although mass 58 Da is monitored to measure the presence of acetone and eliminate the interferences caused by eight components present in the process samples at mass 43 Da, two components (2-pentanone and 3-hexanone) also contribute to the response at mass 58 Da. To overcome this problem the method discussed below will be used<sup>40</sup>. This method employs three simultaneous equations representing the contribution of acetone, 2-pentanone and 3-hexanone to the peak height responses measured at the compounds molecular peaks at masses 58, 86 and 100 Da.

The mean peak height for each compound at mass 58 Da and the two parent ion masses for 2-pentanone (86 Da) and 3-hexanone (100 Da) was calculated using aqueous solutions containing 3 % acetone, 3 % 2-pentanone or 3% 3-hexanone. The experimental conditions used are listed in Table 3.13. Ten replicate injections were performed at each mass separately because of the slow speed of the Faraday cup detector which allows only one mass to be monitored using the total vaporisation manifolds described. The mean peak heights, dependant on the ion source operating parameters and fragmentation mechanisms of the compounds, are shown in Table 3.16.

Compound	Peak height at mass 58 Da ( $10^{-13}$ bar)	Peak height at mass 86 Da ( $10^{-13}$ bar)	Peak height at mass 100 Da ( $10^{-13}$ bar)
Acetone	21.4	0.0	0.0
2-pentanone	10.9	16.4	0.0
3-hexanone	47.7	0.0	7.74

**Table 3.16** The mean peak heights measured for acetone, 2-pentanone and 3-hexanone

Three simultaneous equations can be written representing the peak heights measured at the three masses:

$$R^{58} = PH^{58}_{(\text{acetone})} + PH^{58}_{(\text{2-pentanone})} + PH^{58}_{(\text{3-hexanone})} \quad (3.4)$$

$$R^{86} = PH^{86}_{(\text{2-pentanone})} \quad (3.5)$$

$$R^{100} = PH^{100}_{(\text{3-hexanone})} \quad (3.6)$$

$R^A$  is the response measured at mass A Da

$PH^A_0$  is the contributing peak height at mass A Da for the compound indicated in the bracket.

Using the peak heights listed in Table 3.16 the relationship for 2-pentanone and 3-hexanone at masses 58 and 86 Da and masses 58 and 100 Da, respectively, can be calculated:

$$16.4 \text{ PH}^{58}_{(2\text{-pentanone})} = 10.9 \text{ PH}^{86}_{(2\text{-pentanone})} \quad (3.7)$$

and therefore:

$$\text{PH}^{58}_{(2\text{-pentanone})} = 0.67 \text{ PH}^{86}_{(2\text{-pentanone})} \quad (3.8)$$

also for 3-hexanone:

$$7.74 \text{ PH}^{58}_{(3\text{-hexanone})} = 47.7 \text{ PH}^{100}_{(3\text{-hexanone})} \quad (3.9)$$

and therefore:

$$\text{PH}^{58}_{(3\text{-hexanone})} = 6.17 \text{ PH}^{100}_{(3\text{-hexanone})} \quad (3.10)$$

Substituting equations 3.8 and 3.10 into equation 3.4 yields:

$$\text{R}^{58} = \text{PH}^{58}_{(\text{acetone})} + 0.67\text{PH}^{86} + 6.17\text{PH}^{100} \quad (3.11)$$

By monitoring the peak heights at masses 86 and 100 Da and the response at mass 58 Da ( $\text{R}^{58}$ ),  $\text{PH}^{58}_{(\text{acetone})}$  can be calculated. With the use of calibration data collected in section 3.3.4.2 the concentration of acetone in the process samples can be calculated.

Two process samples were analysed using the off-line (process sample one) and on-line (process sample two) total vaporisation manifolds previously described and the

experimental conditions listed in Table 3.13. The measured response at mass 58 Da and peak heights at masses 86 and 100 Da (Table 3.17) were used to calculate  $PH^{58}_{(\text{acetone})}$  and the acetone concentration in the process samples from the calibration data collected. Table 3.18 shows the concentration of acetone in the process samples calculated by using gas chromatography at BP Chemicals in Hull and the off-line and on-line total vaporisation analysis techniques.

Process sample	Response measured at mass 58 Da ( $10^{-13}$ bar)	Peak heights measured at mass 86 Da ( $10^{-13}$ bar)	Peak heights measured at mass 100 Da ( $10^{-13}$ bar)
one	77.7	9.55	0.54
two	108	14.4	2.87

**Table 3.17** The responses measured for two process samples using the off-line and on-line total vaporisation analysis techniques

Process sample	Acetone concentration determined by gas chromatography (%)	Acetone concentration determined by total vaporisation analysis (%)
one	$9.4 \pm 0.2$	$9.5 \pm 0.7$
two	$8.4 \pm 0.2$	$8.5 \pm 0.8$

**Table 3.18** Calculated concentrations of two process samples using the gas chromatography and total vaporisation analysis techniques

As can be seen the calibration matrix of 85 % acetic acid and 15 % water simulates the sample matrix sufficiently and the manifold and mass spectrometer employed provide an accurate result when compared with the routine technique used at BP Chemicals for the analysis of process samples. The application of total vaporisation analysis for the off-

line and on-line analysis of liquid process or effluent streams to provide accurate results is therefore possible.

### **3.4 Conclusions**

Total vaporisation analysis techniques provide the precise analysis of liquid samples at concentrations ranging from less than  $1 \mu\text{g ml}^{-1}$  to 40 % when electron multiplier and Faraday cup detectors are employed. This wide range of concentrations allows a variety of analytes at different concentrations to be determined. The application of the technique to complex process samples has been investigated and has shown that accurate results can be achieved when compared to the routine analytical technique employed, gas chromatography. However, an analysis time of approximately one minute was obtained with the total vaporisation analysis technique which is significantly shorter than can be obtained with gas chromatography (analysis time  $> 10$  minutes). Therefore a larger sample throughput can be maintained with the off-line strategy and results presented in near-real time can be achieved with the on-line technique.

Several experimental variables affect the vaporisation mechanism and the response measured. These are analyte, sample matrix, temperature of the vaporisation region, helium flow rate and injection volume. A buffer volume is also required to separate the region of vaporisation and mass spectrometer to provide precise results without the requirement to use an internal standard. Without the buffer volume a high pressure flow of vapour enters the mass spectrometer ion source during vaporisation which does not allow reproducible results to be measured.

### 3.5 References

- 1) Poole, C.F., and Poole, S.K., *Chromatography Today*, Elsevier, Oxford, 1991, Chapter 3.
- 2) Klee, M.S., in *Modern Practice of Gas Chromatography*, Grob, R.L. (Editor), Wiley, Chichester, 1995, Chapter eight.
- 3) Tipler, A., in *Gas Chromatography : A Practical Approach*, Baugh, P.J. (Editor), Oxford University Press, 1993, Chapter two.
- 4) Grob, K., *Anal. Chem.*, 1994, **66**, 1009A.
- 5) Hinshaw, J.V., *J. Chromatographic Sci.*, 1988, **26**, 142.
- 6) Hinshaw Jr, J.V., *J. Chromatographic Sci.*, 1987, **25**, 49.
- 7) Grob Jr., K., Neukom, H.P., and Hilling, P., *J. High Res. Chromatogr.*, 1981, **4**, 203.
- 8) Grob, K., and Grob, G., *J. Chromatographic Sci.*, 1969, **7**, 584.
- 9) Termonia, M., Munari, F., and Sandra, P., *J. High Res. Chromatogr. Chromatogr. Comm.*, 1987, **10**, 263.
- 10) Grob Jr, K., *J. Chromatogr.*, 1982, **237**, 15.
- 11) Vogt, W., Jacob, K., Ohnesonge, A.B., and Obwexer, H.W., *J. Chromatogr.*, 1980, **199**, 191.
- 12) Cramers, C.A., and Kessel, M.V., *J. Gas Chromatogr.*, 1968, **6**, 577.
- 13) Grob Jr, K., and Laubli, T., *J. Chromatogr.*, 1986, **357**, 345.
- 14) Grob, K., *J. High Res. Chromatogr.*, 1992, **15**, 190.
- 15) Grob, K., and Martin, M.D., *J. High. Res. Chromatogr.*, 1992, **15**, 335.
- 16) O'Neal, M.J., and Wier Jr, T.P., *Anal. Chem.*, 1951, **23**, 830.

- 17) Purdy, K.M., and Harris, R.J., *Anal. Chem.*, 1950, **22**, 1337.
- 18) Friedel, R.A., Sharkey Jr., A.G., and Humbert, C.R., *Anal. Chem.*, 1949, **21**, 1572.
- 19) Rowe, E.H., *Rev. Sci. Instrum.*, 1957, **28**, 1094.
- 20) Dunn, W.G., and Hooper, J.B., *Anal. Chem.*, 1973, **49**, 216.
- 21) Pattillo, A.D., and Young, H.A., *Anal. Chem.*, 1963, **35**, 1768.
- 22) Mumbach, N.R., *Anal. Chem.*, 1961, **33**, 318.
- 23) Caldecourt, V.J., *Anal. Chem.*, 1955, **27**, 1670.
- 24) Peterson, L., *Anal. Chem.*, 1962, **34**, 1850.
- 25) Padrta, F.G., and Donohue, J.J., *Anal. Chem.*, 1970, **42**, 950.
- 26) Kearns, G.L., *Anal. Chem.*, 1964, **36**, 1402.
- 27) Gohlke, R.S., *Chem. and Ind.*, 1963, 946.
- 28) Chapman, J.R., *Practical Organic Mass Spectrometry*, Wiley, Chichester, 2nd Edition, 1993, p 43.
- 29) Daves Jr., G.D., *Accounts Chem. Res.*, 1979, **4**, 359.
- 30) Dell, A., Williams, D.H., Morris, H.R., Smith, G.A., Feeney, J., and Roberts, G.C.K., *J. Amer. Chem. Soc.*, 1975, **97**, 2497.
- 31) Baldwin, M.A., and McLafferty, F.W., *Org. Mass Spectrom.*, 1973, **7**, 1353.
- 32) Grigsby, R.D., Hansen, K.O., Mannering, D.G., Fox, W.G., and Cole, R.H., *Anal. Chem.*, 1971, **43**, 1135.
- 33) Franzen, J., Kuper, H., and Riepe, W., *Anal. Chem.*, 1974, **46**, 1863.
- 34) Tou, J.C., and Reddy, D., *Anal. Chim. Acta*, 1990, **229**, 9.
- 35) Didden, C., and Duisings, J., *Proc. Cont. Qual.*, 1992, **3**, 263.
- 36) Brodbelt, J.S., Willis, R.S., and Chowdhury, A.K., *Anal. Chem.*, 1992, **64**, 827.

- 37) Lide, D.R. (Editor-in-chief), *Handbook of Chemistry and Physics*, CRC Press, Boston, 72nd Edition, 1991, p 6-118.
- 38) Miller, J.C., and Miller, J.N., *Statistics for Analytical Chemistry*, Ellis Horwood, Chichester, 2nd Edition, 1992, p 109.
- 39) Miller, J.C., and Miller, J.N., *Statistics for Analytical Chemistry*, Ellis Horwood, Chichester, 2nd Edition, 1992, p 115.
- 40) Skoog, D.A., *Principles of Instrumental Analysis*, Saunders College Publishing, London, 3rd Edition, 1985, p 560.

## **Chapter Four**

### **Static Headspace Analysis**

## **4.1 Introduction**

### **4.1.1 Headspace Techniques**

The direct investigation with analytical instrumentation of many samples composed of dirty or complex matrices is impractical because the matrix may have detrimental effects on the analytical result or instrument. In these cases the partial or complete extraction of the compounds of interest from the sample matrix into a separate, clean and inert matrix may eliminate these problems.

Headspace techniques<sup>1-4</sup> facilitate the extraction of volatile and semi - volatile compounds from a liquid or solid phase to a clean inert gas phase (the headspace). Extraction of the compounds of interest is based on the distribution of the compounds present between the condensed and headspace phases. When the two procedures of extraction and subsequent analysis of the headspace are performed the procedure is called headspace analysis (HSA). Qualitative and quantitative information regarding the composition of the condensed phase can be obtained with two alternative approaches; static headspace analysis (SHSA) and dynamic headspace analysis (DHSA). SHSA will be described and employed for off-line analyses in the research presented in this chapter. Alternatively DHSA can be employed for on-line monitoring of liquid streams and will be discussed and employed in Chapter five.

Headspace analysis was introduced in the early 1960s<sup>5,6</sup> to be applied with gas chromatographs for the analysis of samples which were difficult to handle by conventional liquid injection techniques into gas chromatographs. Problems that may be

solved<sup>2,3</sup> include the elimination of high boiling point solutes which create late eluting peaks or contamination of the injection inlet or column. Alternatively when matrix components obscure analytes which are present at trace levels, the interfering matrix components may be removed partially or completely from the final matrix to be analysed and allow the analysis to be more informative. Today headspace techniques are still almost exclusively applied with gas chromatography because of the good resolution and sensitivity<sup>2</sup> achievable for multi-component analysis. Higher sensitivities are achievable by the enrichment of the analyte concentration in the headspace with respect to the sample phase, either directly (SHSA) or indirectly (DHSA).

The transfer of a compound from the liquid to headspace phases is dependant on the compound's volatility, the matrix in which it is present and the temperature and pressure. The techniques are generally used only for the determination of low boiling point compounds because involatile compounds present at low concentrations in the sample do not provide a significant concentration (or vapour pressure) in the headspace for analysis. The term 'GC nose' is sometimes employed<sup>2</sup> which shows the similarity between the techniques described in this chapter and the operation of a human or animal nose.

#### 4.1.2 Static Headspace Analysis Techniques

Experimentally the simplest to perform, static headspace analysis<sup>1,2,3</sup> involves the use of a stationary headspace of constant volume throughout the extraction procedure. Performed in a closed system, sample and headspace phases are contained in glass vials sealed with metal caps containing a septum. The vial is thermostated and the analytes and other compounds present in the condensed phase partition between the two phases

present until equilibration is established and the concentration of the analytes in both phases remains constant. The concentrations, however, are not normally the same for both phases. An aliquot of the headspace is then transferred to an instrument for analysis. The procedures described above can be performed manually with headspace transference performed with a gas tight syringe<sup>2,3</sup>, or automatically with a headspace instrument employing electropneumatic sampling<sup>1,7,8</sup>.

The closed system allows a mass balance to be created for a compound of interest (a) at equilibrium in a sealed vial<sup>9</sup>:

$$C_a^0 V^S = C_a^S V^S + C_a^V V^V \quad (4.1)$$

$C_a^0$  = concentration of compound a in the original sample.

$C_a^S, C_a^V$  = concentration of compound a in the sample and headspace phases, respectively, at equilibrium.

$V^S, V^V$  = volume of the sample and headspace phases, respectively.

Rearrangement of equation 4.1 yields the concentration of compound a in the headspace at equilibrium:

$$C_a^V = C_a^0 / [K + \beta] \quad (4.2)$$

$K$  = partition coefficient

$\beta$  = phase ratio

The partition coefficient describes the ratio of concentrations of compound a in the condensed and headspace phases:

$$K = C_a^s / C_a^v \quad (4.3)$$

With values<sup>1,10</sup> ranging from less than 1 to greater than 10 000, the partition coefficient is dependent on the temperature and sample matrix<sup>4</sup>. The dependence on temperature requires the vials to be thermostated to provide reproducible results. For sensitive analyses in the  $\mu\text{g l}^{-1}$  range elevated temperatures are normally required, which provide a larger concentration of the analyte in the headspace. K is also concentration dependent, but for the calibration ranges investigated for trace analyses K is normally uniform<sup>1</sup>. Values of the partition coefficient can be determined by a variety of methods<sup>11</sup> including the temperature, standard additions, continuous extraction, phase ratio variation, multiple headspace extractions and vapour phase calibration methods.

The phase ratio (of the vial) describes the ratio of the volumes of the headspace and sample phases<sup>12</sup>:

$$\beta = V^v / V^s \quad (4.4)$$

It has been reported that the phase ratio influences  $C_a^v$  when the partition coefficient is small ( $K < 100$ ); when K was larger than 250 no influence was observed for the analyte and matrix investigated<sup>12</sup>. When the phase ratio is influential small headspace volumes (small phase ratios) provide larger concentrations of compound a in the headspace.

In the majority of analyses at low pressures (< 2 atmospheres) the response for a compound in the headspace (headspace response,  $R_a$ ) is directly related to the partial pressure of the component a ( $P_a$ ) in the headspace above a sample phase. The partial pressure for this closed system can be represented as<sup>2,13</sup>:

$$P_a = \chi_a \gamma_a P_a^\circ \quad (4.5)$$

$\chi_a$  = mole fraction of compound a present in the liquid sample

$\gamma_a$  = activity coefficient of compound a in the liquid phase

$P_a^\circ$  = vapour pressure of pure compound a at the analysis temperature and pressure employed

The activity coefficient of compound a quantifies the strength of interactions between the compound and the sample matrix, and is temperature dependant. In a system where  $\chi_a$  and  $P_a^\circ$  are constant three different situations can be observed<sup>2</sup>:

Ideal solution	$P_a = \gamma_a = 1$	(4.6)
----------------	----------------------	-------

Ideal dilute solution	$P_a = \gamma_a = \text{constant value}$	(4.7)
-----------------------	--	-------

Real solution	$P_a = \gamma_a = f(\chi_a)$	(4.8)
---------------	------------------------------	-------

Ideal solutions obey Raoult's law<sup>14</sup> (4.9) and calibration is possible in the range 0 - 100% assuming the detector response is also linear for the complete range of concentrations:

$$P_a = \chi_a \quad (4.9)$$

Most solutions exhibit ideality only when compound a is present to form a dilute solution and these ideal dilute solutions obey Henry's law<sup>14</sup>:

$$P_a = \chi_a k_a \quad (4.10)$$

$k_a$  = proportionality constant (dimensions of pressure)

At higher concentrations when the solution does not exhibit ideality the partial vapour pressure shows positive ( $\gamma_i > 1$ ) or negative ( $\gamma_i < 1$ ) deviations from Raoult's law<sup>2</sup>. A linear dependence of the partial pressure on the sample phase concentration of compound a is therefore observed for a limited concentration range. Linear calibration is possible at low compound a concentrations when Henry's law is obeyed. For these reasons headspace analysis is normally used to analyse compounds present at trace concentrations in the sample. Real solutions do not obey Raoult's or Henry's laws and linear calibration is not possible because the activity coefficient of the analyte is dependent on the liquid phase concentration of the analyte.

The partial pressure of compound a in the headspace ( $P_a$ ) for a uniform sample phase concentration can be increased by a variety of methods. Elevation of the temperature or reduction of the headspace pressure will increase the value of the saturated vapour pressure of pure compound a ( $P_a^0$ )<sup>15</sup>. Alternatively the value of the activity coefficient can be increased by the addition of electrolytes or non - electrolytes to the sample, which

decrease compound interactions with the matrix and therefore its solubility<sup>2,3,16</sup>. Salting out effects are employed when salts are added to decrease the component solubility in water matrices. The salt employed and its concentration will influence the degree of change in the headspace concentration<sup>2</sup>. Water can also be added to organic matrices to obtain the same effect<sup>2</sup>.

Other methods employed to increase the component concentration in the headspace include varying the pH of the liquid sample to decrease the solubility of the analyte in the matrix<sup>16</sup>. This technique can be used to provide a higher concentration in the sample phase of an undissociated form of a compound which at other pH values may be present in the dissociated and undissociated forms. The presence of the dissociated form will result in a lower sensitivity because ionically charged molecules can not be easily transported from the liquid phase to the headspace. Alternatively the derivatisation of the compounds of interest to less soluble compounds will result in a higher concentration of the derivative in the headspace with respect to the analyte<sup>17</sup>.

Calibration techniques employed for static headspace analysis are dependent on the sample matrix<sup>2,9</sup>. Table 4.1 describes the variety of sample matrices encountered and the calibration techniques employed.

Sample matrix	Calibration technique
Matrix composition known and can be reproduced or simulated	a) Determination of K and calibration of the analytical instrument with gas standards b) Liquid phase external standards c) Internal standards d) Standard additions
Matrix composition unknown but is available in pure form	a) Determination of K and calibration of the analytical instrument with gas standards b) Liquid phase external standards c) Internal standards d) Standard additions
Matrix composition unknown and is not available or matrix varies between consecutive samples	a) Standard additions b) Full evaporative technique c) Multiple headspace extractions

**Table 4.1** The calibration techniques employed with static headspace analysis

All of the calibration techniques are standard analytical methods except for the full evaporative technique (FET) and multiple headspace extractions (MHE) technique. FET and MHE both provide matrix independent analyses and are therefore employed for the analysis of samples whose matrix composition is unknown or periodically changes.

The full evaporative technique<sup>18</sup> involves the equilibration at elevated temperatures of mg amounts of sample in a sealed vial. The analyte is completely or nearly completely transferred to the headspace and therefore gas standards can be employed for calibration

of the analytical instrument. The FET is simple and robust because of the complete transfer of compounds to the headspace, less time consuming than MHE and has a relative sensitivity comparable with other static headspace techniques. Schubert<sup>19</sup> has applied the technique to the analysis of volatile organic compounds (VOCs) in pharmaceutical products.

Multiple headspace extractions<sup>20</sup> involve the stepwise gas extractions from sealed vials, and re-equilibration of the analyte between the two phases present in the vial between each extraction step. The technique was first developed by McAuliffe<sup>21</sup>, and mathematical models can be used to provide component quantification in the sample phase. A review of the MHE technique by Grob describes the mathematical basis of the technique and its application<sup>22</sup>. The technique is time consuming because of the multiple equilibration and extraction stages. Generally three gas extractions are performed for quantitative analyses.

The various applications of the static and dynamic headspace techniques for the analysis of environmental, food, biological and industrial samples have been reviewed by McNally and Grob<sup>23, 24</sup>.

In this chapter static headspace analysis will be combined with direct analysis of the headspace by mass spectrometry to enable liquid samples to be analysed.

## 4.2 Experimental

### 4.2.1 Reagents

Standard solutions were prepared on a volume to volume (v/v) basis with AR grade acetone (Fisons Scientific Equipment, Loughborough, Leicestershire, UK) and methyl iodide (Aldrich, Gillingham, Dorset, UK). Doubly deionised water (Elgastat, 18 M $\Omega$  cm<sup>-1</sup>) and acetic acid (99.9 % purity; BP Chemicals, Hull, East Yorkshire, UK) were used as solvents.

All solutions were prepared daily in 2.0 ml glass vials (Chromacol Ltd, Welwyn Garden City, Hertfordshire, UK) ensuring a negligible headspace volume was present to prevent analyte loss from the liquid phase. Vials were sealed with aluminium caps which contained a silicone rubber septum whose inner surface was coated with PTFE to eliminate adsorption which has been reported for silicone rubber septa<sup>25,26</sup>. Stock and standard solutions of concentration 5000  $\mu\text{g ml}^{-1}$  or greater were prepared by dissolving analyte in solvent in a sealed vial. Standard solutions of lower concentration were prepared by serial dilution of a stock solution.

Aliquots of known volume were transferred to sealed 2.0 ml glass vials for equilibration of the analyte between the two phases present before the headspace was analysed.

#### 4.2.2 Instrumentation and Procedures

A VG Gas Analysis Systems SX200 mass spectrometer (Middlewich, Cheshire, UK) was employed during the work described in this chapter. The optimised operating parameters were used as discussed in Chapter two. SIM at masses 43 (acetone) and 142 (methyl iodide) Da, respectively, was employed for all investigations discussed.

The sampling interface employed to allow the mass spectrometer to pump headspace vapours to the ion source consisted of a bevelled needle (i.d. = 0.5 mm, o.d. = 1.0 mm, length = 30 mm) attached to the capillary inlet with a length of PTFE tubing (i.d. = 1.2 mm, o.d. = 2.4 mm, length = 20 mm; Polypenco Ltd, Welwyn Garden City, Hertfordshire, UK). The needle was used to eliminate blockage of the capillary inlet. Dust or liquid entering the sampling interface collected in the needle which when blocked could be more easily removed and cleaned than would be possible for the capillary inlet

Aliquots of the headspace present in the sealed vials were sampled directly into the mass spectrometer by rapid insertion of the sampling interface needle into the headspace. The needle tip was inserted to a depth of 60 - 80 % (the vial septum was assigned 0 % depth and the liquid surface was assigned a depth of 100 %). The needle was removed when the maximum response had been recorded.

A Multi - blok heater (LabLine Instruments, Melrose Park, Illinois, USA) was used to thermostat samples at temperatures higher than 25°C. Vials were placed in hollow cartridges present in a heated metal block and water was placed in the cartridge to the

vial top to ensure a uniform temperature throughout the vial. This reduced the probability of condensation of the headspace on cool glass surfaces.

A range of experimental variables (time needle was inserted in the headspace, sample temperature, phase ratio and equilibration times) were investigated for both analytes and optimised to obtain a high sensitivity and precision, with a relatively short analysis time. Calibration data was also collected for acetone and methyl iodide at sample temperatures of 25 and 71°C. Six replicate analyses were performed for the optimisation experiments and collection of calibration data and the mean peak height measured was used as the response.

### **4.3 Results and Discussion**

#### **4.3.1 The Effect of the Sampling Time of the Headspace**

The effect on the response of the time the sampling needle is inserted into the headspace present in the vial (sampling time) was investigated using 2.0 % aqueous acetone standards and a Faraday cup for ion detection. The experimental variables employed were; temperature (23°C), phase ratio (9.0) and equilibration time (60 minutes).

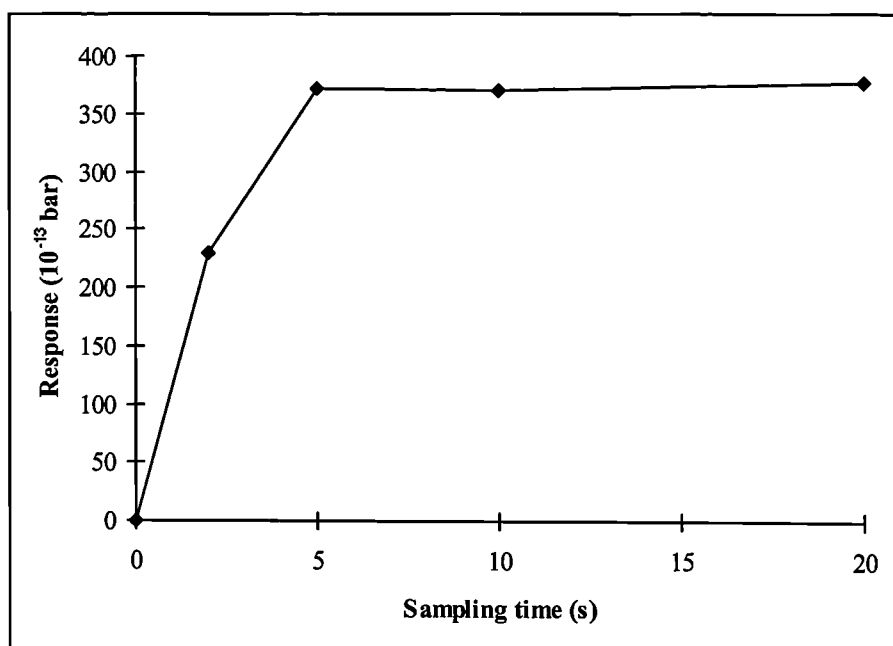


**Figure 4.1** The effect of the sampling time for acetone

The results displayed in Figure 4.1 show that the response measured is uniform for sampling times in the range 5 - 20 seconds. Therefore the rate of transport of acetone to the mass spectrometer ion source is constant after the needle has been inserted in the headspace for a period greater than five seconds. A sampling time of 20 seconds will be employed in the future work described in this chapter.

#### 4.3.2 The Effect of Temperature

The response was measured with an electron multiplier over a range of temperatures (27 - 81°C) with 100  $\mu\text{g ml}^{-1}$  acetone standards and 50  $\mu\text{g ml}^{-1}$  methyl iodide standards. A phase ratio of 9.0 was used for both standards and times of 45 and 60 minutes was

employed to provide complete equilibration for the acetone and methyl iodide standards, respectively.

Figure 4.2 shows the increase in response as the temperature is increased. The results for both analytes show an increase in the concentration (or partial pressure) of the analyte in the headspace when the temperature is increased as has previously been discussed<sup>4</sup>. Complete analyte extraction from the liquid phase is achieved when the response becomes constant and therefore complete extraction is not achievable at the temperatures employed. It can be expected that lower detection limits will be achievable at 70°C with respect to 25°C.

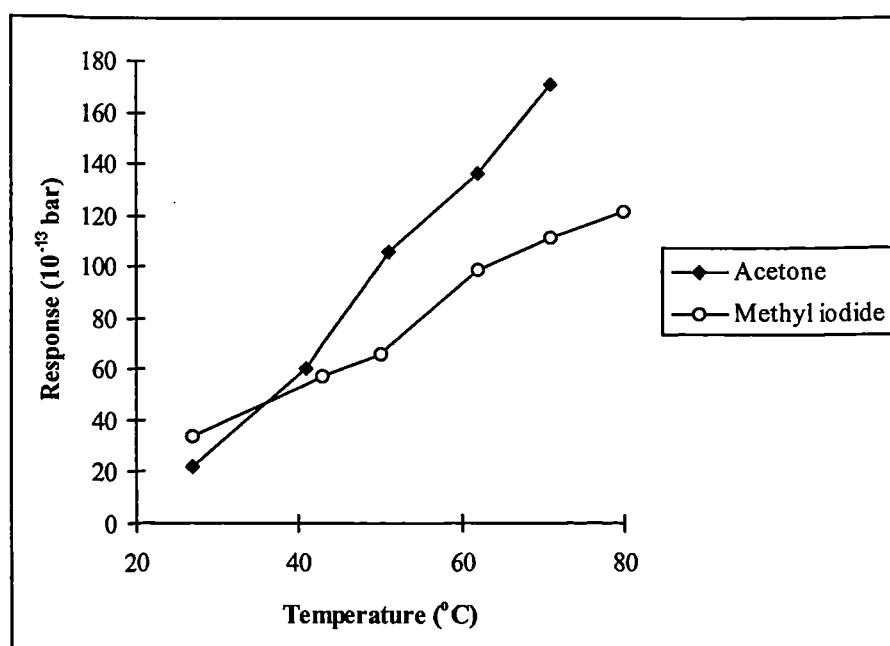


Figure 4.2 The effect of sample temperature

The analysis of samples at temperatures greater than those employed in this work caused blockage of the sampling interface needle with liquid, which was present on the under surface of the vial septum. A temperature of 71°C was employed in further studies to eliminate this problem.

#### 4.3.3 The Effect of the Phase Ratio

As was discussed in the introduction to this chapter the phase ratio can affect the response measured by the analytical instrument. The relationship between the phase ratio and response for acetone was investigated at sample temperatures of 24 and 71°C using, respectively, 20000 and 100  $\mu\text{g ml}^{-1}$  standards. The Faraday cup and electron multiplier detectors were employed for investigations at temperatures of 24°C and 71°C, respectively. The relationship between the phase ratio and response measured was also investigated using 20000 and 50  $\mu\text{g ml}^{-1}$  methyl iodide standards at 24 and 71°C, respectively. The Faraday cup and electron multiplier detectors were employed for investigations at temperatures of 24°C and 71°C, respectively. All the samples were left overnight (16 hours) to ensure complete equilibration was achieved.

Figures 4.3 and 4.4 show the results obtained for acetone and methyl iodide standards. The error bars (99%) included show that although the response appears to vary as the phase ratio is increased for acetone (24 and 71°C) and methyl iodide (24°C) standards the errors associated with the responses measured may indicate that the response remains constant over the range of phase ratios studied.

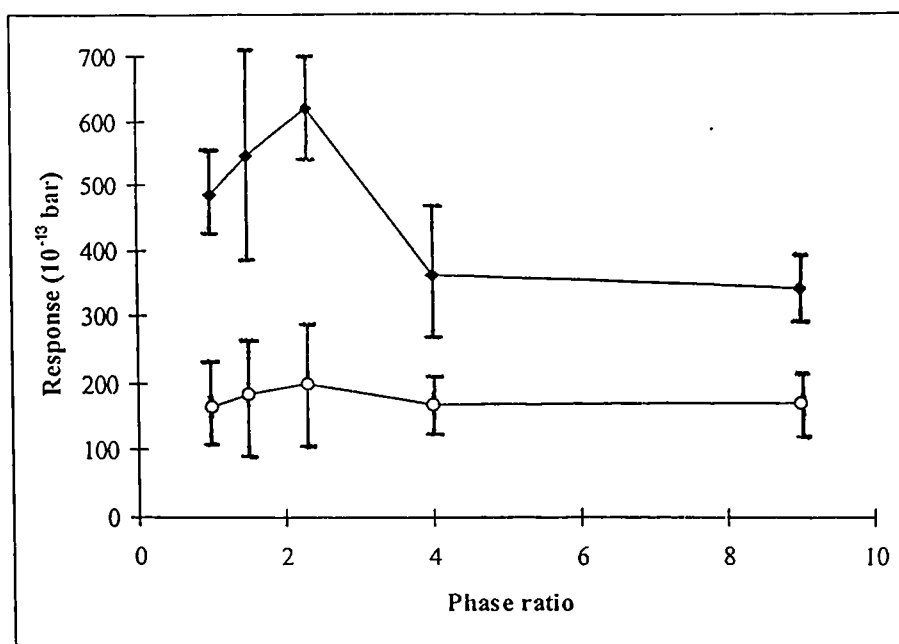


Figure 4.3 The effect of the phase ratio for acetone at 24 (◆) and 71 (○) °C

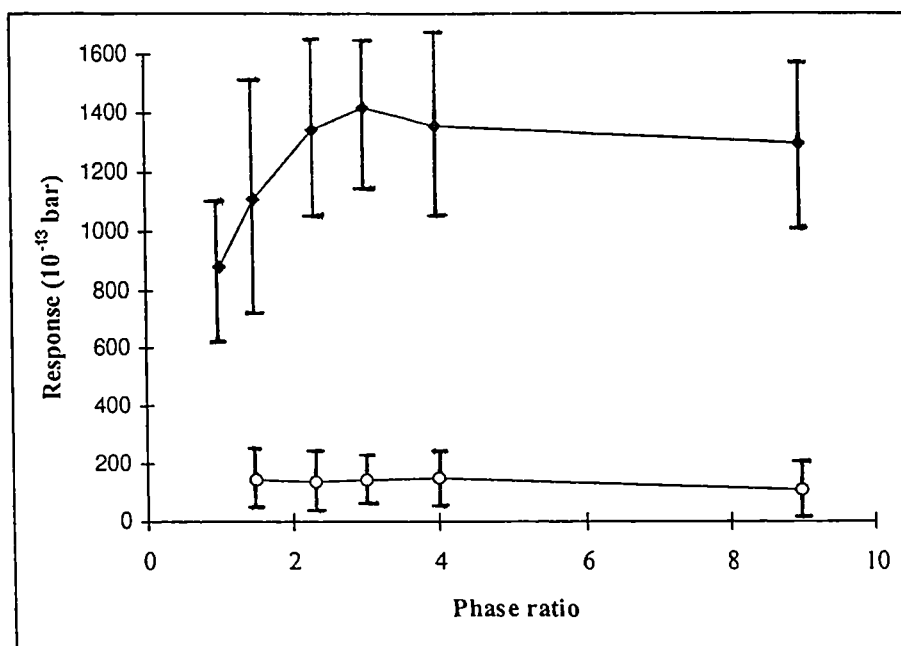


Figure 4.4 The effect of the phase ratio for methyl iodide at 24 (◆) and 71 (○) °C

The effect of the sampling procedure on the relationship between the phase ratio and response at a sample temperature of 20°C for single component liquid phases of acetone and methyl iodide was investigated. The headspace contained in the vial was composed of a uniform analyte concentration for the range of phase ratios studied. The response measured should therefore be a constant value for the range of phase ratios studied. The samples were left overnight to ensure complete equilibration. A similar relationship was not measured (Table 4.2) as was observed for the standard solutions composed of two compounds investigated.

Phase Ratio	Acetone response (10 <sup>-13</sup> bar)	Methyl iodide response (10 <sup>-13</sup> bar)
1.0	11365	11506
1.5	11132	11806
2.3	11383	12973
4.0	11635	11924
9.0	10818	12471

**Table 4.2** The effect of the phase ratio for one component samples

The sampling procedure employed therefore does not influence the rate of introduction of an aliquot of the headspace to the mass spectrometer. The response measured by the mass spectrometer for two component solutions is therefore not dependent on the phase ratio.

#### 4.3.4 Determination of the Equilibration Times

Equilibration profiles present visually the change in response as the time between the sample introduction into the vial and analysis time of the headspace is increased. A constant headspace response is observed when equilibration of the analyte between the liquid and headspace phases is complete. The time required for this to be achieved is called the equilibration time. Maximum sensitivity is obtained when equilibration is complete.

The equilibration profiles were determined at sample temperatures of 24 and 71°C for both analytes with the analysis of separate standards at specific times after sample introduction into the vial for equilibration. Phase ratios of 2.3 (acetone) and 9.0 (methyl iodide) were used. Faraday cup and electron multiplier detectors were employed, respectively, at sample temperatures of 24 and 71°C.

The equilibration profiles at sample temperatures of 24 and 71°C for acetone present in water (Figure 4.5) and methyl iodide present in acetic acid (Figure 4.6) exhibit the equilibration times shown in Table 4.3.

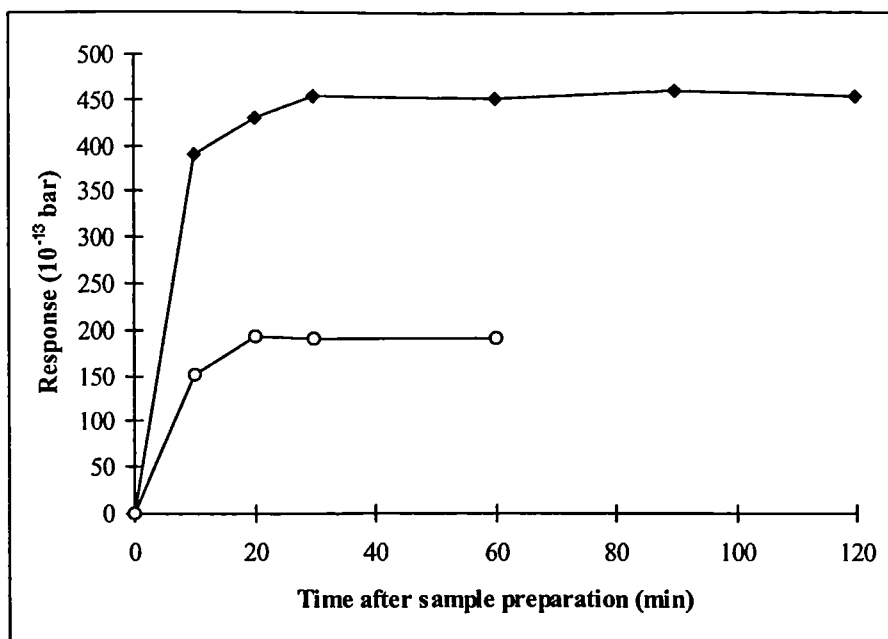


**Figure 4.5** Equilibration profiles for acetone at 24 (◆) and 71 (○) °C

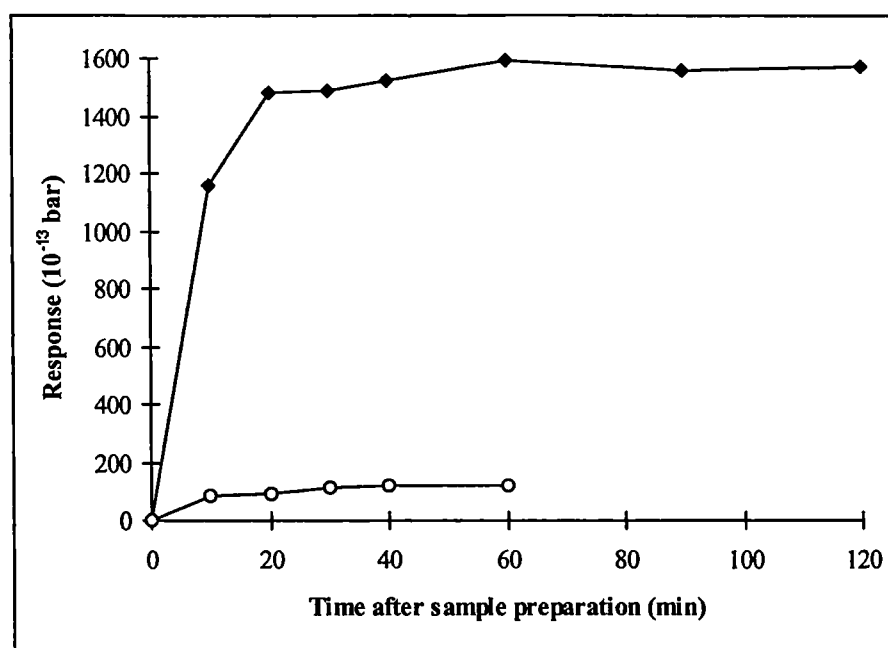


**Figure 4.6** Equilibration profiles for methyl iodide at 24 (◆) and 71 (○) °C

Analyte	Temperature (°C)	Equilibration time (min)
Acetone	24	30
	71	20
Methyl iodide	24	60
	71	40

**Table 4.3** Equilibration times for acetone and methyl iodide

The application of elevated sample temperatures are beneficial as they assist in the faster rate of analyte transfer to the headspace which results in the shorter equilibration times observed. The sample matrix viscosity<sup>27</sup> ( $1.02 \times 10^{-3} \text{ kg m}^{-1} \text{ s}^{-1}$  for water at 20°C and  $1.16 \times 10^{-3} \text{ kg m}^{-1} \text{ s}^{-1}$  for acetic acid at 25°C) also effects the equilibration time. The mobility of the analyte in the liquid phase influences the rate of transfer of the analyte to the headspace. The higher viscosity of acetic acid will reduce the mobility of methyl iodide to a greater extent than the lower viscosity of water will affect the mobility of acetone. Elevation of the sample temperature will reduce the viscosity of water and acetic acid while also increasing the internal energy of the analyte molecules to allow the easier transfer of analytes from the liquid phase to the headspace. Therefore analyte transfer to the headspace is greater at the higher temperatures for the same matrix, and results in the lower equilibration times observed at 71°C.

#### 4.3.5 Calibration

Calibration data were collected for acetone at a sample temperature of 21 - 24°C (Faraday cup and electron multiplier detectors) and at 71°C (electron multiplier detector).

The experimental parameters used are shown in Table 4.4. The response was measured as the mean peak height for ten replicate analyses.

Analyte	Acetone	Methyl iodide
Phase ratio	2.3	9.0
Equilibration time 21-24°C	30	60
(min) 71°C	20	40

**Table 4.4** Experimental conditions applied for calibration

Calibration graphs of response ( $10^{-13}$  bar) vs. analyte concentration ( $\mu\text{g ml}^{-1}$ ) were plotted for all the sets of calibration data collected. Linear calibration ranges, equations of the calibration lines, correlation coefficients, and limits of detection ( $3\sigma$ ) were calculated using the method of least squares<sup>28</sup>. The methods of calculating these parameters was described in Chapter three (section 3.3.2.6) and will not be discussed here.

The large calibration ranges observed for the majority of calibration data sets did not allow a single accurate calibration line to be calculated for the complete calibration range. Errors in the response measured for standards of high concentration resulted in inaccurate calculated gradient and intercept values for the equation of the calibration line. The calibration line therefore did not represent the relationship between analyte concentration and the response measured for standards of low concentration. Accurate limits of detection were calculated using the method of least squares<sup>27</sup> for three or four calibration points representing the smallest concentration standards analysed. All the

limits of detection are quoted with the number of calibration points used for its calculation.

Tables 4.5 and 4.6 show the calibration data for acetone at a sample temperature of 22 and 21°C using the Faraday cup and electron multiplier detectors respectively. Table 4.7 shows the calibration data for acetone at a sample temperature of 71°C using the electron multiplier detector.

[Acetone] ( $\mu\text{g ml}^{-1}$ )	Response ( $10^{-13}$ bar)	RSD (n=10) (%)
0	0.10	73.2
100	1.87	8.3
500	13.9	4.1
1000	23.8	4.3
5000	107	3.6
10000	222	2.9
20000	535	1.6
50000	1416	3.9
100000	2611	2.6
150000	4055	3.6

$$y = 0.03x - 8.33$$

$$r = 0.9996 \text{ (n = 10)}$$

$$\text{Limit of detection} = 14 \mu\text{g ml}^{-1} \text{ (n = 4)}$$

$$\text{Temperature} = 22^\circ\text{C}$$

**Table 4.5** Calibration data for acetone at 22°C using the Faraday cup detector

[Acetone] ( $\mu\text{g ml}^{-1}$ )	Response ( $10^{-13}$ bar)	RSD (n=10) (%)
0	0.22	3.1
1	0.32	13.3
10	0.48	8.1
100	3.94	6.3
1000	5.15	2.9
10000	990	3.3
20000	2096	4.0
40000	5035	2.3
70000	8888	3.0

$$y = 0.127x - 101.5$$

$$r = 0.9987 \text{ (n = 9)}$$

$$\text{Limit of detection} = 5.6 \mu\text{g ml}^{-1} \text{ (n = 4)}$$

$$\text{Temperature} = 21^\circ\text{C}$$

**Table 4.6** Calibration data for acetone at 21°C using the electron multiplier detector

[Acetone] ( $\mu\text{g ml}^{-1}$ )	Response ( $10^{-13}$ bar)	RSD (n=10) (%)
0	0.0	4.4
0.5	0.91	12.7
1	1.78	9.8
10	6.43	4.4
50	94.6	4.1
100	196	1.7
500	1366	2.7

$$y = 2.75x - 21.8$$

$$r = 0.9983 \text{ (n = 7)}$$

$$\text{Limit of detection} = 2.4 \mu\text{g ml}^{-1} \text{ (n = 4)}$$

$$\text{Temperature} = 71^\circ\text{C}$$

**Table 4.7** Calibration data for acetone at 71°C

A small response or no response was observed when the blank standard was analysed at both temperatures showing that the sampling procedure has no significant effect on the measurement performed by the mass spectrometer. The calibration range achievable using the Faraday cup detector exhibits the concentration range of analyte that obeys Henry's law at 22°C (0 - 15 %), assuming the detector response for acetone is linear up to concentrations greater than 15 %. At a sample temperature of 71°C a linear calibration range covering two decades of concentration was observed. This is in contrast to the calibration range observed at 21°C covering four decades of concentration. Therefore standards containing more than 500  $\mu\text{g ml}^{-1}$  acetone may exhibit non-ideality at 71°C. However, the most probable cause of the smaller calibration range is the increased concentration of water in the headspace at 71°C. Large transfers of analyte and matrix in to the headspace occur at elevated temperatures and subsequently the concentration of water present in the electron impact ion source used is also increased. High concentrations of water in the ion source can effect ionisation mechanisms and the rate of ion formation. Adequate precision is defined as RSD values less than 10 %. The precision of replicate analyses [RSD (n=6) = 1.6 - 13.3 %] was adequate except at the lowest concentration standards analysed.

The decrease in the limits of detection ( $6 \mu\text{g ml}^{-1}$  at  $21^\circ\text{C}$  and  $3 \mu\text{g ml}^{-1}$  at  $71^\circ\text{C}$ ) and increase in the calibration sensitivity ( $0.13 \text{ bar ml } \mu\text{g}^{-1}$  at  $21^\circ\text{C}$  and  $2.8 \text{ bar ml } \mu\text{g}^{-1}$  at  $71^\circ\text{C}$ ) both show the benefit of detecting lower concentrations of acetone in the liquid phase by the analysis of the headspace at temperatures greater than  $21^\circ\text{C}$ .

The calibration data for methyl iodide at sample temperatures of  $24$  and  $71^\circ\text{C}$  are shown in Tables 4.8 and 4.9 respectively.

[Methyl iodide] ( $\mu\text{g ml}^{-1}$ )	Response ( $10^{-13} \text{ bar}$ )	RSD (n=10) (%)
0	11.9	38.3
1	12.5	9.7
10	17.2	4.7
100	58.5	4.5
1000	366	4.3
10000	3966	4.6
20000	7915	3.8

$$y = 0.40x + 6.39$$

$$r = 0.9999 \text{ (n=7)}$$

$$\text{Limit of detection} = 0.9 \mu\text{g ml}^{-1} \text{ (n = 4)}$$

$$\text{Temperature} = 24^\circ\text{C}$$

**Table 4.8** Calibration data for methyl iodide at  $24^\circ\text{C}$

[Methyl iodide] ( $\mu\text{g ml}^{-1}$ )	Response ( $10^{-13}$ bar)	RSD (n=10) (%)
0	5.43	14.3
10	19.5	5.6
50	88.3	3.9
100	181	5.3
500	862	4.3
1000	1352	11.0
5000	6633	5.7

$$y = 1.32x + 52.0$$

$$r = 0.9996 \text{ (n = 7)}$$

$$\text{Limit of detection} = 1.3 \mu\text{g ml}^{-1} \text{ (n = 4)}$$

$$\text{Temperature} = 71^\circ\text{C}$$

**Table 4.9** Calibration data for methyl iodide at  $71^\circ\text{C}$

Higher limits of detection ( $0.9 \mu\text{g ml}^{-1}$  [ $24^\circ\text{C}$ ],  $1.3 \mu\text{g ml}^{-1}$  [ $71^\circ\text{C}$ ]) and higher calibration sensitivities ( $0.40 \text{ bar ml } \mu\text{g}^{-1}$  [ $24^\circ\text{C}$ ],  $1.32 \text{ bar ml } \mu\text{g}^{-1}$  [ $71^\circ\text{C}$ ]) are achieved at the elevated sample temperature of  $71^\circ\text{C}$ . The relative increase in the calibration sensitivity is lower for methyl iodide with respect to acetone and therefore elevation of the sample temperature to  $71^\circ\text{C}$  is a more efficient technique to increase the headspace concentration of acetone present in a water matrix than to increase the headspace concentration of methyl iodide present in an acetic acid matrix. This may be caused by a lower mass spectrometer sensitivity for methyl iodide with respect to acetone. A more

probable explanation is a larger partition coefficient for methyl iodide between the liquid phase and headspace with respect to acetone.

The linear calibration range extends over one extra decade of concentration than was observed for acetone at a sample temperature of 71°C. The boiling point of acetic acid is 120°C and therefore higher than water. The relative concentration of acetic acid in the headspace is lower with respect to water at the same temperature, and the interference of the matrix in the analysis of the headspace is not being observed until a higher concentration of methyl iodide is present in the headspace. A response was measured at mass 142 Da at both temperatures for a blank standard. The origin of the response is most likely caused by impurities present in the acetic acid and not by the sampling procedure effecting the pressure measurement performed by the mass spectrometer.

All the limits of detection are quoted as concentrations in the liquid phase. The corresponding analyte concentrations in the headspace measured by the mass spectrometer are lower and are present in the low  $\mu\text{g l}^{-1}$  range. For example, the partition coefficient for acetone<sup>1</sup> present in a water matrix at 25°C is 551. The relative concentration of acetone in the headspace when the liquid concentration of acetone is equivalent to the detection limit of  $2 \mu\text{g ml}^{-1}$  is therefore  $4 \mu\text{g l}^{-1}$ .

The equilibration times allow the analysis of 1 - 2 samples per hour if each sample was equilibrated and analysed consecutively. However the batch equilibration of many samples and their subsequent analysis would allow a frequency of analysis of  $30 \text{ h}^{-1}$ . If the batch equilibration method is used static headspace analysis is quicker than many other analytical techniques which require either sample pre-treatment or chromatographic separation of sample components for complex or dirty samples.

#### 4.3.6 The Determination of Acetone in Two Process Samples

The concentrations of acetone in two industrial process samples (one and three) obtained from BP Chemicals (Hull) were determined to assess the accuracy of the static headspace technique applied in this chapter. The composition of process samples one and three is shown in Table 4.10.

Compound	Process sample one composition (% v/v)	Process sample three composition (% v/v)
Formic acid	7	1
Acetic acid	30	1
Propionic acid	5	1
Acetone	9.4	24.5
Water	14	1
Methyl acetate	4	9
Ethyl and propyl acetate	3	8
Butanone	2.5	7
2-pentanone and 3-hexanone	3.5	8
Pentane	11	27
Benzene	4	11

**Table 4.10** Approximate composition of process samples one and three

The composition of the matrix can change between consecutive samples and therefore the partition coefficient will not be a constant value for all the samples analysed. The application of liquid phase external standards would not provide the accurate

quantification and therefore the standard additions method was employed for the quantification of acetone. The accuracy of the standard additions method is not affected by changes in the sample composition.

1700  $\mu\text{l}$  samples were spiked with 0, 50, 100, 150 and 200  $\mu\text{l}$  of acetone and 9  $\mu\text{l}$  of each sample and spiked sample was diluted in 1800  $\mu\text{l}$  of a diluent (70 % acetic acid : 30 % water). 200  $\mu\text{l}$  aliquots were transferred to sealed 2.0 ml vials and equilibrated for two hours. The headspace of all the equilibrated samples and spiked samples was analysed for process sample one and the results were used to determine the acetone concentration in the sample<sup>29</sup>. The method of standard additions can also be employed with the analysis of the sample and only one standard addition solution to quantify the presence of acetone. This method is quicker with respect to analysing and preparing several standard additions solutions and will be employed here for the quantification of acetone in process sample three. The headspace of the sample and 50  $\mu\text{l}$  spiked sample was analysed<sup>30</sup>. Six replicate analyses were performed for each sample and spiked sample.

Mass 58 Da was monitored during the analysis of solutions because all the components present in the sample, with the exception of water, contribute to the response measured at mass 43 Da which was previously used for the quantification of acetone. As shown in Chapter three (section 3.3.4) acetone, pentanone and hexanone contribute to the response at mass 58 Da. However at the diluted concentrations employed in this section it was experimentally determined that no response was measured for 2-pentanone and 3-hexanone in the process samples at mass 58 Da. Therefore the partial pressure of all the compounds present in the diluted process samples, except acetone, is not high enough to be detected by the mass spectrometer at mass 58 Da. Therefore mass 58 Da can be

employed for the quantification of acetone without any interference from other compounds present in the sample.

The responses recorded by the mass spectrometer are not accurate because of the sample preparation stage<sup>30</sup>. Relatively large volumes of acetone were added to the sample during the standard additions stage. Therefore the volume of each standard prepared is not uniform and the acetone present in the original process samples are increasingly diluted as larger volume standard additions are performed. For example, the standard addition of 200 µl results in acetone in the process sample being present in 1900 µl of the liquid phase whereas the acetone in the process sample with no acetone added is present in 1700 µl of the liquid phase. The problem of dilution can be solved by calculating corrected responses for each standard addition which takes into account the effect of different degrees of dilution<sup>30</sup>:

$$\text{Corrected response} = \frac{[(\text{Volume of sample} + \text{volume of standard addition}) / (\text{volume of sample})]}{\text{x measured response}} \quad (4.11)$$

Therefore

$$\text{Corrected response} = \frac{[(1700 + \text{volume of standard addition}) / 1700]}{\text{x measured response}} \quad (4.12)$$

For example, when 200  $\mu\text{l}$  of acetone was added to a process sample the corrected response is  $([1900 / 1700] \times \text{measured response})$ .

The results for process samples one and two are shown in Table 4.11.

Volume of acetone added ( $\mu\text{l}$ )	Process sample one corrected response ( $10^{-13}$ bar)	Process sample three corrected response ( $10^{-13}$ bar)
0	30.8	228
50	41.9	263
100	50.2	-
150	64.1	-
200	70.7	-

**Table 4.11** Results for the analysis of process samples one and three

The standard additions plot for process sample one is shown in Figure 4.7.

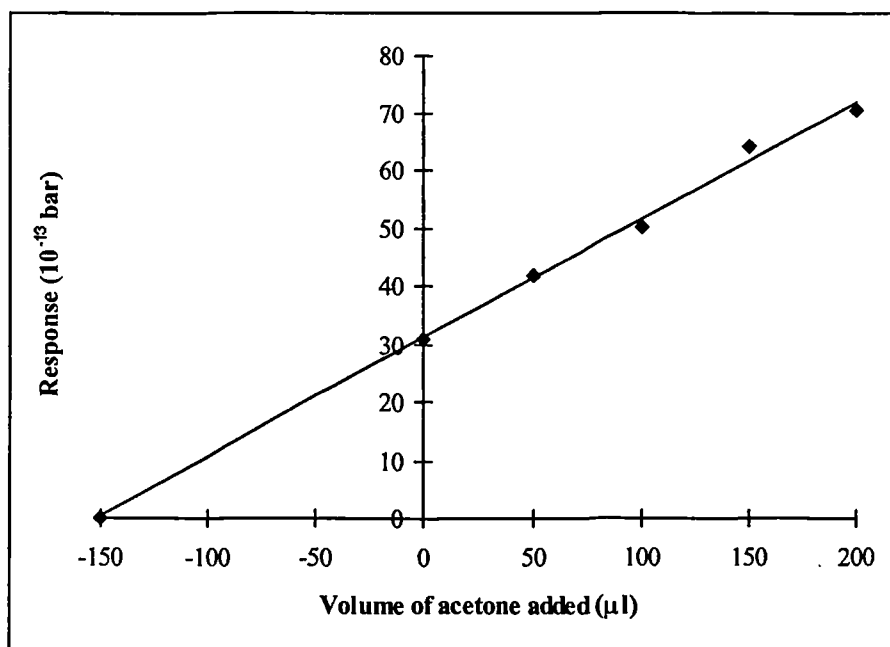


**Figure 4.7** The standard additions graph for process sample one

The equation of the standard additions line is  $y = 0.204x + 31.14$ . The intercept value of the standard additions line and x axis can be calculated as follows<sup>29</sup>:

$$\text{Intercept} = \text{gradient} / \text{intercept at y axis} \quad (4.13)$$

Therefore 153  $\mu\text{l}$  of acetone was present in the original process sample of volume 1700  $\mu\text{l}$ . The concentration of acetone in process sample one is therefore 8.9 %.

The calculation for the quantification of acetone in process sample three is shown below<sup>30</sup>:

The response representing 50  $\mu\text{l}$  of acetone:

$$= 263 - 228 \times 10^{-13} \text{ bar} \quad (4.14)$$

$$= 35 \times 10^{-13} \text{ bar} \quad (4.15)$$

Therefore the volume of acetone providing a measured response of  $228 \times 10^{-13}$  bar:

$$= (228 / 35) \times 50 \mu\text{l} \quad (4.16)$$

$$= 325.7 \mu\text{l in } 1700 \mu\text{l of sample} \quad (4.17)$$

The concentration of acetone present in process sample three is therefore:

$$= (325.7 / 1700) \times 100 \quad (4.18)$$

$$= 19.2 \% \text{ (v/v)} \quad (4.19)$$

Process sample	GC analysis (%)	SHSA-MS (%)
one	9.4 ± 0.2	8.9 ± 1.0
three	24.2 ± 0.4	19.2 ± 1.1

**Table 4.12** Calculated concentrations of acetone present in process samples one and three

The results (Table 4.12) show that the static headspace technique employed can be used for the analysis of complex process samples with direct mass spectrometric detection. However accurate quantification was only achieved for process sample one using the standard additions method. The inaccuracy observed for the analysis of process sample three is most likely the result of employing only one standard addition. A linear relationship has been shown to exist between concentration and response at the acetone concentration present in the diluted sample and therefore this does not affect the accuracy.

The dilution of the process samples described in this section would also enable the multiple headspace extractions technique to be used with mass spectrometer detection, without the requirement to employ gas chromatographic separation of the headspace components prior to detection. The FET may not be used because the majority or all of the liquid phase compounds will be transferred to the headspace and therefore without

separation the response measured at mass 58 Da will be composed of the measured values for acetone, 2-pentanone and 3-hexanone present in the sample.

#### **4.4 Conclusions**

The application of static headspace techniques for the off-line analysis of liquid process streams has shown that  $\mu\text{g ml}^{-1}$  -  $\mu\text{g l}^{-1}$  detection limits are achievable, and analyses with acceptable precision can be performed. The experimental conditions (temperature and phase ratio) and the sample matrix control the partitioning of the analyte between the liquid and headspace phases.

The variation in the composition of two process samples analysed required the use of the standard additions method for quantification. The analysis provided an accurate result for one process sample, however an inaccurate result was obtained for a different process sample. Therefore further investigations would need to be performed before the technique of SHSA and standard additions quantification could be used on a routine basis.

Relatively long analysis times are required for the static headspace technique. Direct gas chromatographic analysis, where the liquid sample is introduced directly into the chromatograph, is a quicker technique to currently employ for consecutive analyses. However batch equilibrations and subsequent SHSA-MS analyses would provide a greater sample throughput. Each SHSA is performed in two minutes and therefore an analysis frequency of  $30 \text{ h}^{-1}$  can be achieved. 2-3 analyses per hour are currently achieved

with gas chromatographic analyses. A wide range of samples at BP Chemicals are analysed directly by gas chromatography.

#### 4.5 References

- 1) Ioffe, B.V., and Vitenburg, A.G., *Head-Space Analysis and Related Methods in Gas Chromatography*, Wiley, Chichester, 1984.
- 2) Hachenburg, H., and Schmidt, A.P., *Gas Chromatographic Headspace Analysis*, Heyden, London, 1977.
- 3) Poole, C.F., and Poole, S.K., *Chromatography Today*, Elsevier, Oxford, 1991, p 818.
- 4) Seto, Y., *J. Chromatogr. A.*, 1994, **674**, 25.
- 5) Buttery, R.G., and Teranishi, R., *Anal. Chem.*, 1961, **33**, 1439.
- 6) Bassette, R., Ozeris, S., and Whitnah, C.H., *Anal. Chem.*, 1962, **34**, 1540.
- 7) Hewlett Packard 7694 Headspace sampler brochure, 1993.
- 8) Perkin-Elmer HS 40 Automatic headspace sampler brochure, 1991.
- 9) Green, J.D., *Encyclopedia of Analytical Science*, Townshend, A. (Editor-in-chief), Academic Press, London, 1995, p 5401.
- 10) Rohrschneider, L., *Anal. Chem.*, 1973, **45**, 1241.
- 11) Namiesnik, J., Gõrecki, T., Biziuk, M., and Torres, L., *Anal. Chim. Acta*, 1990, **237**, 1.
- 12) Ettre, L.S., and Kolb, B., *Chromatographia*, 1991, **32**, 5.
- 13) Kettrup, A., *Trends Anal. Chem.*, 1982, **1**, 142.
- 14) Atkins, P.W., *Physical Chemistry*, Oxford Univ. Press, Oxford, 1990, p 161.
- 15) Alberty, R.A., *Physical Chemistry*, Wiley, Chichester, 1987, p 188.
- 16) Friant S.L., and Suffet, I.H., *Anal. Chem.*, 1979, **51**, 2167.

- 17) Efer, J., Müller, S., Engewald, W., Knobloch, Th., and Levsen, K.,  
*Chromatographia*, 1993, **37**, 361.
- 18) Markelov, M., and Guzowski Jr., J.P., *Anal. Chim. Acta*, 1993, **276**, 235.
- 19) Schubert, J., *Anal. Chem.*, 1996, **68**, 1317.
- 20) Kolb, B., *Chromatographia*, 1982, **15**, 587.
- 21) McAullife, C., *ChemTech*, 1971, 46.
- 22) Kolb, B., and Ettre, L.S., *Chromatographia*, 1991, **32**, 505.
- 23) McNally, M.E., and Grob, R.L., *Am. Lab.*, 1985, **17**, 20.
- 24) McNally, M.E., and Grob, R.L., *Am. Lab.*, 1985, **17**, 106.
- 25) Gilliver, P.J., and Nursten, H.E., *Chem. and Ind.*, 1972, 541.
- 26) Davis, P.L., *J. Chromatogr. Sci.*, 1970, **8**, 423.
- 27) Lide, D.R. (Editor-in-chief), *Handbook of Chemistry and Physics*, CRC Press,  
Boston, 72nd Edition, 1991, section 6.
- 28) Miller, J.C., and Miller, J.N., *Statistics for Analytical Chemistry*, Ellis Horwood,  
Chichester, 2nd Edition, 1992, pp 105 and 109.
- 29) Miller, J.C., and Miller, J.N., *Statistics for Analytical Chemistry*, Ellis Horwood,  
Chichester, 2nd Edition, 1992, p 117.
- 30) Skoog, D.A., West, D.M., and Holler, F.J., *Fundamentals of Analytical Chemistry*,  
Saunders College, London, 5th Edition, 1988, p 516.

## **Chapter Five**

### **Dynamic Headspace Analysis**

## 5.1 Introduction<sup>1,2,3</sup>

The sensitivity<sup>1</sup> ( $\alpha$ ) of the static headspace techniques described in Chapter four when compared to the direct injection of a liquid sample into the gas chromatograph can be calculated by applying equation 5.1:

$$\alpha = v_g / [v_l (K + \beta)] \quad (5.1)$$

$v_g$  = volume of headspace introduced into the gas chromatograph

$v_l$  = volume of liquid introduced into the gas chromatograph with direct  
liquid injection

$K$  = partition coefficient

$\beta$  = phase ratio

When the value for  $\alpha$  is greater than one the SHSA technique provides a higher sensitivity than direct injection of the liquid phase into a gas chromatograph will provide. Assuming 1000  $\mu\text{l}$  of the headspace and 1  $\mu\text{l}$  of liquid are analysed equation (5.1) can be written as:

$$\alpha = 10^3 / K + \beta \quad (5.2)$$

In this example a higher sensitivity for the static headspace analysis technique will be provided when  $K < 10^3 - \beta$ .  $\beta$  is small (1 - 10) with respect to a value of 1000 and therefore can be removed from the equation.

In many examples  $K$  is greater than  $10^3$  and therefore an improvement in the sensitivity is not possible when the static headspace technique is used. Dynamic headspace techniques are employed in these examples to provide a greater sensitivity with respect to the direct introduction of a liquid into a gas chromatograph. The techniques are also used to provide a higher sensitivity when the static headspace techniques do not provide an adequate detection limit because of very low analyte concentrations in the sample.

Dynamic headspace analysis (DHSA)<sup>1,2,3</sup> employs continuous removal of the headspace with a flow of inert gas. The removal of the headspace allows a greater transfer of analyte from the liquid sample to be achieved because of the larger sample / headspace surface area provided during the extraction procedure<sup>2</sup>. The surface area is larger than those used during static headspace techniques. The larger surface area creates a greater probability of analyte approaching the sample / headspace interface and passing into the headspace. The adsorption of headspace components in a trap before an analysis is performed also acts as an extra step to achieve analyte enrichment<sup>3</sup>. Dynamic headspace techniques can be applied with stationary sample phases (periodic samples) or with a flowing liquid (continuous system)<sup>3</sup>.

The flow of an inert gas used in DHSA can be passed over the sample. Alternatively the gas can be passed through the sample in the form of small bubbles to strip components more efficiently from the sample phase. Purge and trap (P & T) techniques pass the gas through the sample once and the compounds in the headspace are collected on an adsorbent or cryogenic trap. Closed Loop Stripping Analysis (CLSA) continuously recycles the gas in a closed system between the sample and trap. This provides an

improved sensitivity by the trapping of compounds during the recycling of the gas that were not trapped during their first passage through the trap.

For the techniques of P & T and CLSA the rate of analyte stripping from the liquid phase ( $dW_a / dt$ ) can be expressed as<sup>4</sup>:

$$dW_a / dt = -W_a [F / (V_L K + V_G)] \quad (5.3)$$

$W_a$  = instantaneous total mass of compound a in the liquid phase sample.

$t$  = time of gas extraction step.

$F$  = volume flow rate of stripping gas.

$V_G$  = volume of gaseous phase.

$V_L$  = volume of liquid phase.

$K$  = partition coefficient for compound a.

Equation 5.3 can be solved<sup>4</sup> for the initial conditions  $t = 0$  and  $W_a = W_a^0$ :

$$W_a / W_a^0 = \exp [-F t / (V_G + K V_L)] \quad (5.4)$$

$W_a^0$  = mass of compound a present in the sample before the gas stripping stage.

Therefore the time required to strip 95 % of the analyte mass from the sample ( $t_{0.05}$ ) can be represented as<sup>4</sup>:

$$t_{0.05} = 3(V_G + K V_L) \quad (5.5)$$

The application of these equations assume that the analyte can be stripped completely from the sample,  $K$  is concentration independent, the liquid phase is relatively non-volatile and no breakthrough of absorbed compounds in the trap occurs<sup>2</sup>

The purge and trap technique was first reported in 1967<sup>6</sup> and was further developed in 1974<sup>7</sup>. The manifold employed is shown in Figure 5.1. Gas is introduced to the liquid phase through a glass frit or tubing and subsequently passes through an adsorptive or cryogenic trap. Compounds are thermally released from the trap, after a period of gas purging, and introduced to the instrument for analysis as a narrow plug of vapour. A variety of vessels have been used in this technique<sup>8,9,10</sup>. To reduce sample foaming specially designed vessels<sup>3,8</sup>, anti-foaming agents<sup>11,12</sup> or heat dispersion of the foam<sup>12</sup> can be used to eliminate blockage of transfer lines or trap with matrix components. Fully automated instruments are available<sup>13</sup>.

Applied as a more sensitive alternative to P & T, CLSA<sup>5,14</sup> can determine purgeable volatiles at  $\text{ng l}^{-1}$  concentrations.  $\text{C}_{24}$  compounds present at concentrations of 1 in  $10^{13}$  (w/w) have been detected<sup>5</sup>. Figure 5.2 shows the manifold used. Although charcoal traps and the solvent desorption of adsorbed compounds was commonly applied when CLSA was first developed, adsorptive or cryogenic traps are now generally used. Problems of contamination caused by low purity gases and trapping media can be observed and result in sensitivity reductions because of the higher background response. These problems can be solved by using ultra-pure gases and correctly treating the trapping media<sup>15</sup>.

Adsorptive trapping media used<sup>3,16</sup> include a variety of polymeric or carbon sorbents which include charcoal, Tenax, Chromosorb and liquid coated materials. Rapid heating

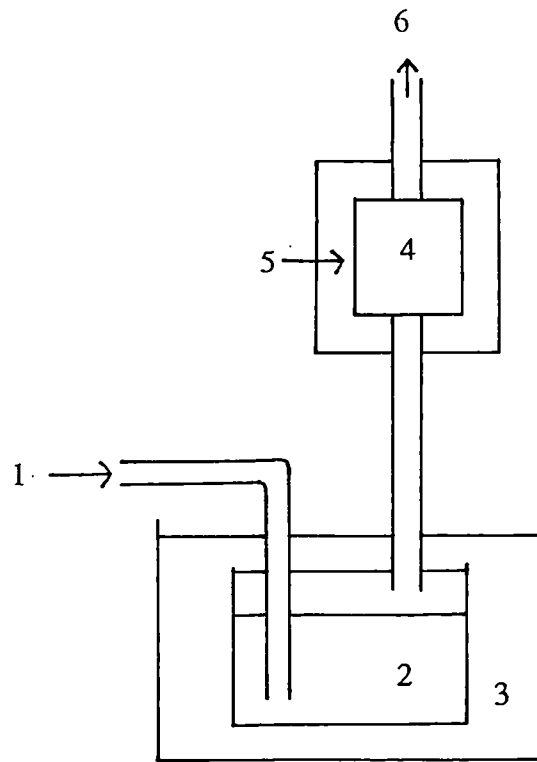


**Figure 5.1** The purge and trap manifold. (1 purging gas; 2 sample; 3 water bath; 4 trap; 5 oven; 6 to gas chromatograph)

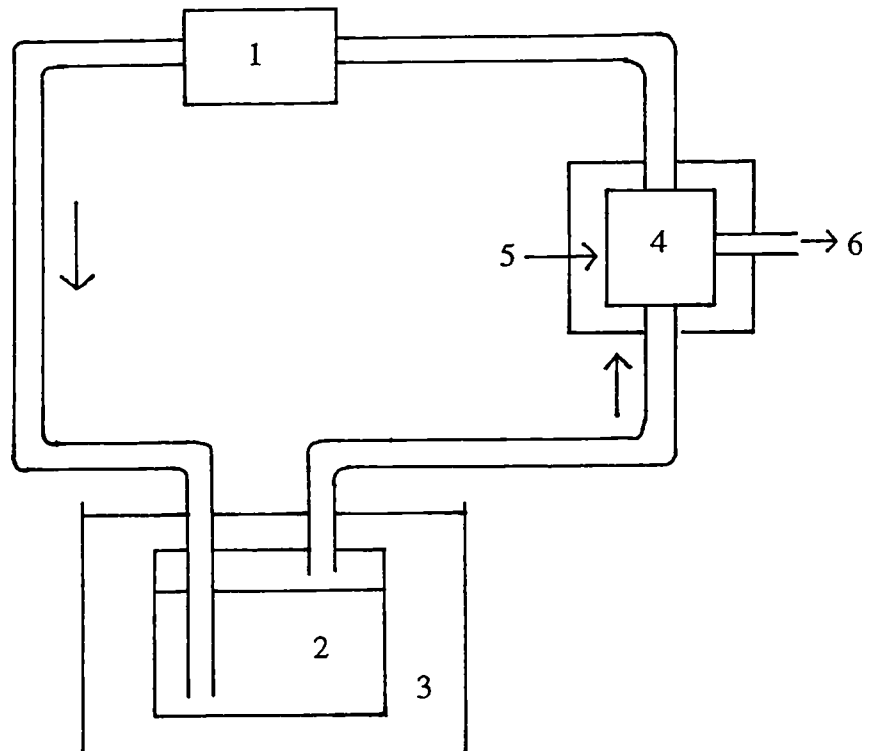


**Figure 5.2** The closed loop stripping analysis manifold. (1 pump; 2 sample; 3 water bath; 4 trap; 5 oven; 6 to gas chromatograph)

releases the adsorbed species for analysis. For thermally labile or polar compounds rapid heating of the materials described above will produce, respectively, compound decomposition or slow elution from the trap. In these cases a silica capillary cooled to liquid nitrogen temperatures (approximately  $-80^{\circ}\text{C}$ ) is used to collect the compounds of interest<sup>3,17</sup>. Less energetic thermal conditions are used to elute the trapped compounds. Water removal with an efficient condenser<sup>17,18</sup> or Nafion tubing<sup>18</sup> prior to component trapping is required to eliminate ice formation in the capillary and its possible blockage. Cryogenic trapping can be performed outside the gas chromatograph<sup>17</sup> or a length of the gas chromatographic capillary column present in the gas chromatographic oven can be maintained at low temperatures<sup>19</sup>.

A number of applications of the dynamic headspace technique, without the presence of component trapping, have been employed in industrial and non - industrial applications for the on-line analysis of liquid streams. Soleta<sup>20</sup> has transferred a laboratory based dynamic headspace - gas chromatography method to the process plant for on-line analysis applications. Schieck and Brown<sup>21</sup> have evaluated four different dynamic headspace - gas chromatography systems for the on-line analysis of industrial liquid streams, and Lesage and Brown<sup>22</sup> have applied a DHSA - GC technique to assess the effectiveness of surfactants in the dissolution of organic solvents in water. A differently designed constant volume headspace flow cell to that used by Lesage and Brown was also employed in this chapter. Finally Kozlowski et al. have employed continuously flowing thin layers of the liquid sample to optimise the transfer of analytes from the liquid phase to the headspace<sup>23</sup>.

As a more sensitive alternative to the techniques described above, spray extraction methods create an aerosol from a liquid flow to provide a more efficient transfer of analyte from the liquid to headspace phases. Matz and Kesners<sup>24</sup> and Baykut and Voigt<sup>25</sup> have applied the technique with GC - MS. St - Germain et al.<sup>26</sup> have coupled a spray extraction interface directly to an ion trap mass spectrometer.

The application of dynamic headspace analysis techniques is investigated in this chapter for the on - line monitoring of liquid streams. A variety of experimental variables are studied and optimised and calibration data is collected for acetone present in a water matrix and methyl iodide present in an acetic acid matrix.

## **5.2 Experimental**

### **5.2.1 Reagents**

AR grade acetone (Fisons Scientific Equipment, Loughborough, Leicestershire, UK) and methyl iodide (Aldrich, Gillingham, Dorset, UK) were dissolved in doubly deionised water (Elgastat,  $18 \text{ M}\Omega \text{ cm}^{-1}$ ) and acetic acid (99.9 % purity; BP Chemicals, Hull, East Yorkshire, UK), respectively, to prepare standard solutions. All the concentrations quoted are on a volume to volume (v/v) basis.

Standard solutions were prepared in 500 ml glass bottles or 250 or 100 ml volumetric flasks. Aliquots were transferred to 100 or 50 ml volumetric flasks for analysis. To

assure no analyte was lost from the liquid phase a negligible headspace volume was present in all the storage vessels.

### 5.2.2 Instrumentation and Procedures

A VG Gas Analysis Systems SX200 mass spectrometer (Middlewich, Cheshire, UK) was employed during the work described in this chapter. The optimised operating parameters were used as discussed in Chapter two.

The sampling interface employed to allow the mass spectrometer to pump headspace vapours to the ion source was described in Chapter four (section 4.2.2).

Flowing liquid streams were simulated using a manifold shown in Figure 5.3. A liquid chromatography pump (Kontron Instruments, Watford, Hertfordshire, UK) delivered the liquid through an all glass flow cell to waste. PTFE tubing was used throughout the manifold (i.d. = 2.4 mm, o.d. = 3.2 mm; Fisons Scientific Equipment, Loughborough, Leicestershire, UK). The headspace present in the flow cell was continuously pumped through the sampling interface into the mass spectrometer. The headspace phase was not sealed from the atmosphere otherwise a vacuum is created in the flow cell with a sealed headspace phase and the liquid stream rises up the flow cell into the sampling interface. A small diameter inlet was placed at the top of the flow cell to stop a vacuum being created and to allow the sampling interface to be inserted into the headspace.

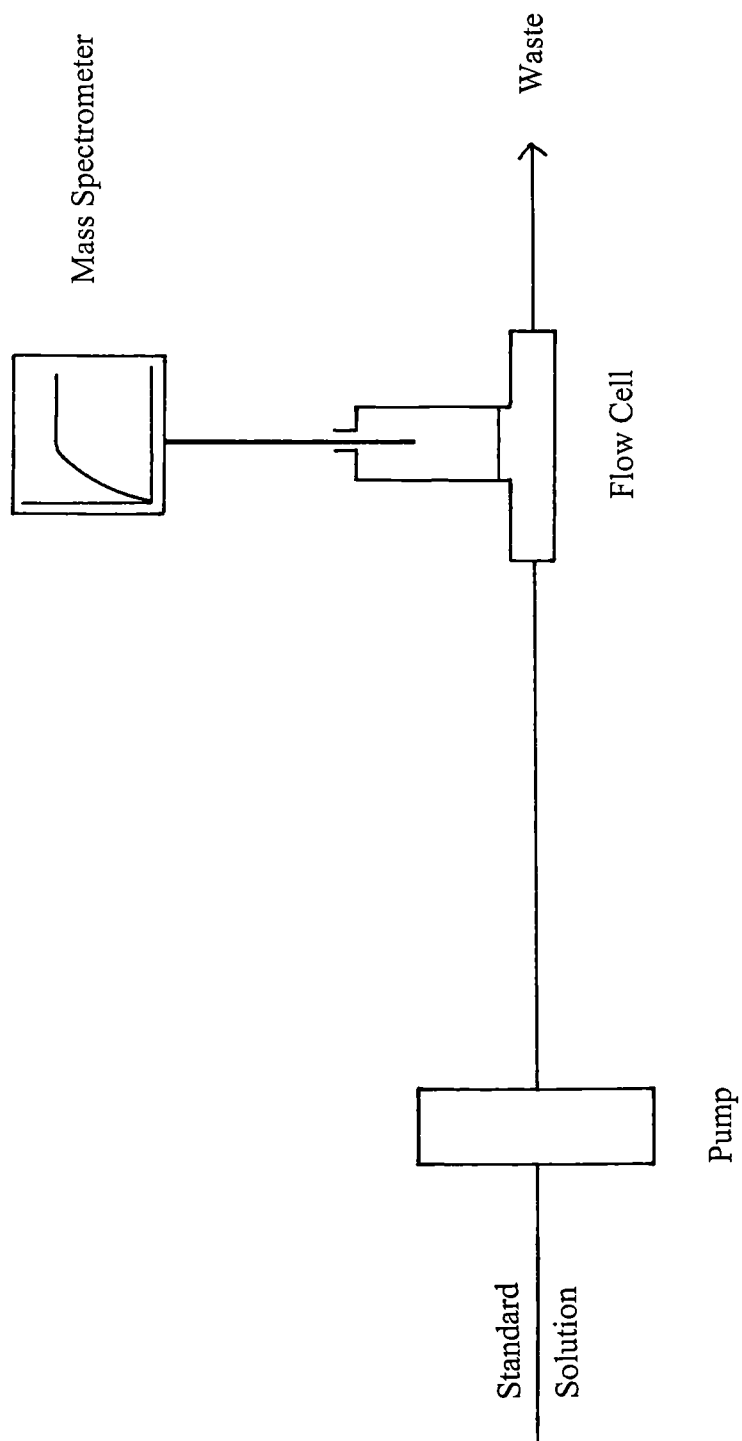


**Figure 5.3** The flow manifold

Three different flow cells were used during the work described in this chapter. The flow cells shown in Figures 5.4 and 5.5 were employed to analyse liquid streams at temperatures in the range 20 - 81°C. The single difference between the two flow cells is the volume of the headspace, 8.8 and 14.5 ml, respectively. To heat the flowing stream a glass coil (length = 720 mm, i.d. = 4 mm, o.d. = 10 mm) attached directly to a flow cell was used. The glass coil and flow cell were immersed in a water bath to heat the liquid stream and to eliminate condensation of compounds present in the headspace of the flow cell. The water bath comprised a hollow metal block containing the glass coil and flow cell, filled with water and heated by a LabLine Multi - blok heater (Melrose Park, Illinois, USA). The water bath temperature correlated accurately with the stream temperature as it passed through the flow cell (stream temperature = water bath temperature).

The third flow cell (gas purging flow cell, Figure 5.6) enabled a gas flow of instrument air to pass through the liquid stream in the form of small bubbles. A glass frit (porosity 2) was incorporated into the flow cell floor to enable the passage of gas through the liquid as it passed through the flow cell.

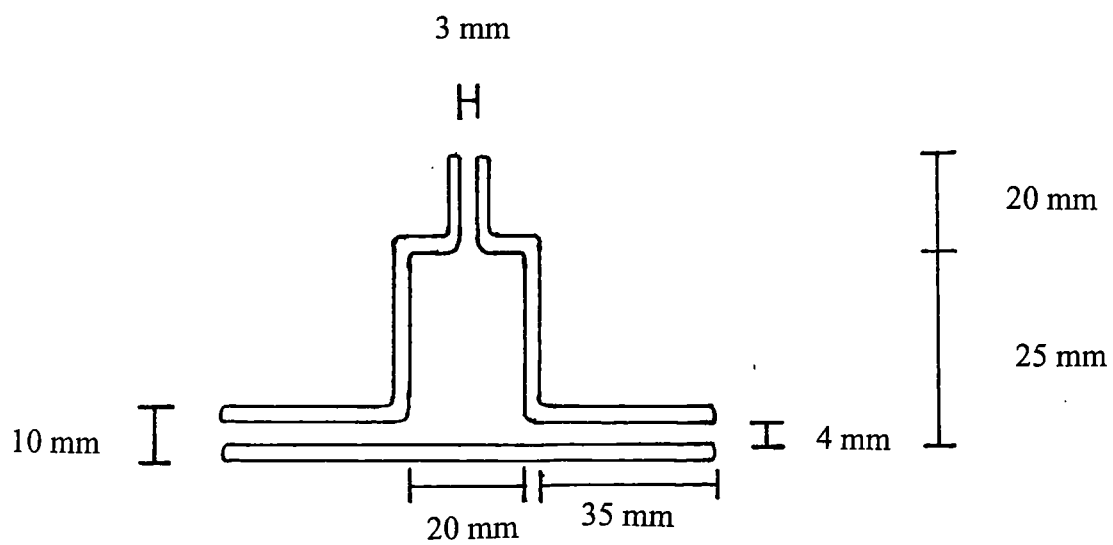


**Figure 5.4** Flow cell employed with a headspace volume of 8.8 ml

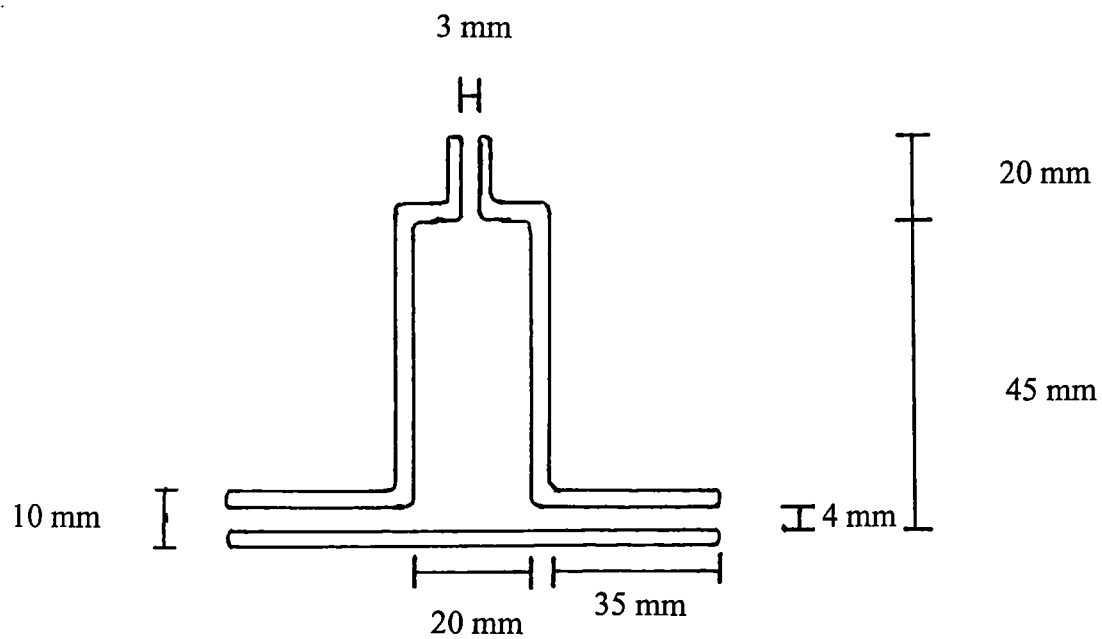


**Figure 5.5** Flow cell employed with a headspace volume of 14.5 ml

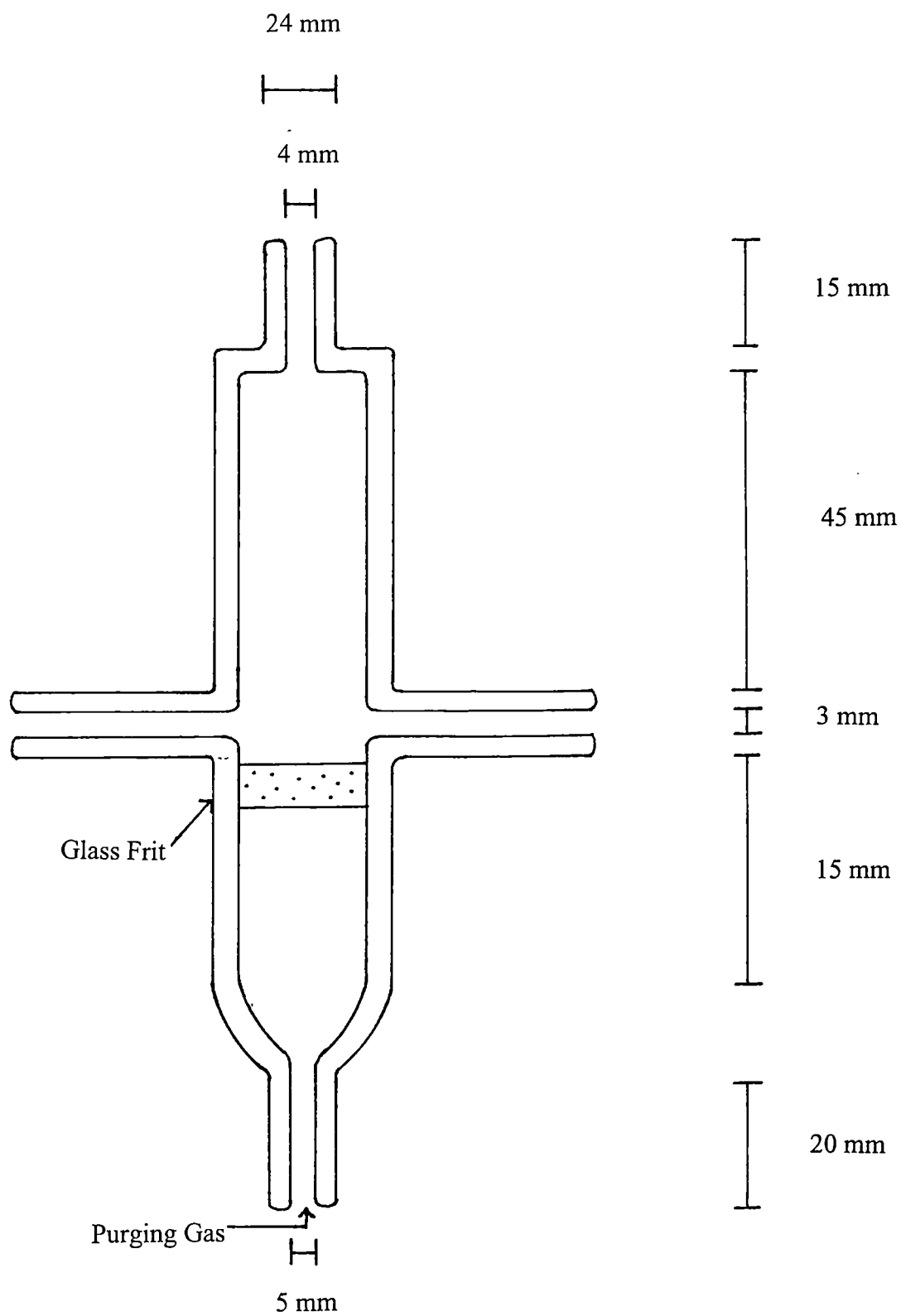


**Figure 5.6** The gas purged flow cell

The effects of stream temperature, liquid flow rate and purge gas flow rates were all studied and optimised to achieve high sensitivities and precision. The rise and fall times, described in section 5.3.3, were also determined at a variety of experimental conditions to investigate the response times achievable. Calibration data were collected using the optimised experimental variables at stream temperatures of 25 and 71°C and for the gas purging dynamic headspace technique. The change in the peak height of the ion used to monitor the analyte during a measurement time of six minutes was employed as the response. The measurement time is defined as the period in which standard solutions were pumped through the employed headspace flow cell. Six replicate analyses were performed for all optimisation experiments and collection of calibration data, with the exception of the optimisation experiments performed for methyl iodide at 71°C when three replicate analyses were performed.

### 5.3 Results and Discussion

#### 5.3.1 The Effect of the Liquid Stream Flow Rate

The effect of the flow rate of liquid passing through the flow cells employed was investigated at a stream temperature of 22°C with a 1.0 % acetone standard and a Faraday cup detector. The acetone - water stream was pumped through the flow cell for six minutes and the change in the partial pressure of the analyte measured by the mass spectrometer between 0 and 6 minutes for six replicate analyses was employed as the response. The results (Table 5.1) exhibit a small increase in the response as the flow rate is increased from 5 to 20 ml min<sup>-1</sup>. The rate of transfer of analyte from the liquid phase to the headspace is therefore independent of the liquid flow rate and analyte mass flow rate through the flow cell with a measurement time of six minutes. A flow rate of 5 ml min<sup>-1</sup> was employed in further work performed.

Liquid stream flow rate (ml min <sup>-1</sup> )	Response (10 <sup>-13</sup> bar)	RSD (n=6) (%)
5	1472	4.0
10	1425	2.7
15	1511	3.4
20	1524	2.9

**Table 5.1** The effect of the liquid stream flow rate

The residence time of the liquid stream in the flow cell is approximately 4 and 1 seconds at the flow rates of 5 and 20 ml min<sup>-1</sup> respectively. The transfer of analyte from

the liquid phase to the headspace must therefore be rapid to provide the headspace concentration of analyte required to produce the responses measured. The application of a shallow stream allows the more rapid diffusion of analyte from the bottom of the stream to the top and therefore the analyte molecules present near the bottom of the liquid stream have a high probability of approaching the liquid - headspace interface and subsequently passing into the headspace.

### 5.3.2 The Effect of the Stream Temperature

The use of elevated sample temperatures enabled more sensitive responses to be achieved with static headspace techniques. The effect of the stream temperature on the dynamic headspace response and therefore on the concentration of analyte in the headspace was investigated in the range 21 - 81°C. 1000  $\mu\text{g ml}^{-1}$  acetone and methyl iodide standards were used. A liquid flow rate of 5  $\text{ml min}^{-1}$  was employed. The results are shown in Figure 5.7.

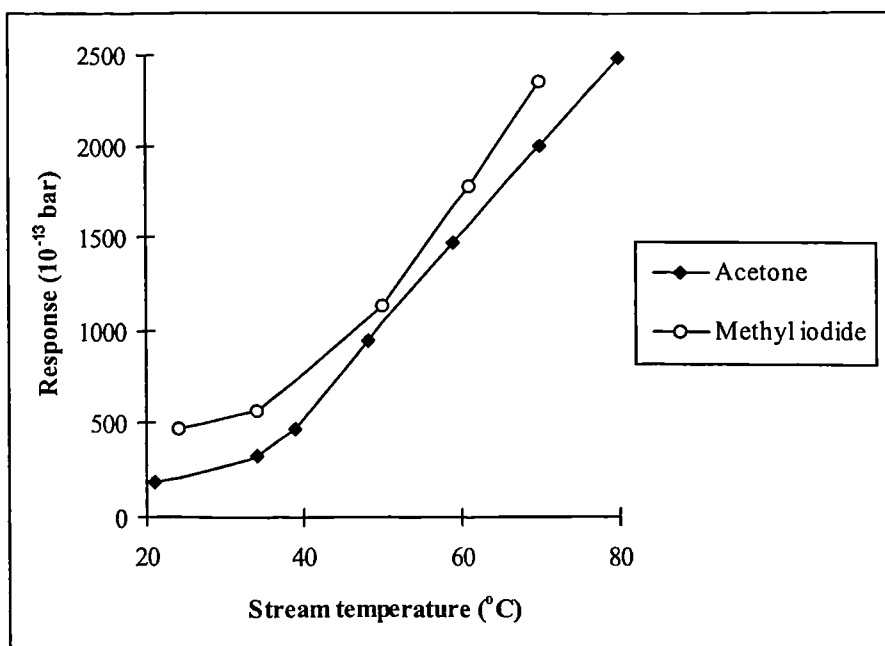


**Figure 5.7** The effect of stream temperature

As was observed with the static headspace technique elevation of the stream temperature increases the headspace response. The relationship between the temperature and response is linear for acetone in the range 30 - 80°C ( $r = 0.9991$ ;  $n = 7$ ) and appears to be linear for methyl iodide in the range 50 - 70°C ( $r = 0.9999$ ;  $n = 3$ ). The analyte concentration in the headspace therefore increases when the temperature is increased and this is caused by a greater rate of analyte transfer (volume of analyte per unit of time) from the liquid phase to the headspace at the elevated temperature. The greater rate of transfer is caused by the larger vibrational and rotational energies of the analyte molecules at the elevated temperatures which enables the molecules to transfer to the headspace.

### 5.3.3 Determination of the Rise and Fall Times

Figure 5.8 shows the change in response observed for a 0.5 % acetone standard when the time the standard is pumped through a flow cell at a flow rate of  $5 \text{ ml min}^{-1}$  increases. The temperature of the stream was  $24^\circ\text{C}$ . At time 0 the acetone standard entered the flow cell and at 30 minutes the acetone standard was replaced with a stream of water. The measurement time of the analysis was 30 minutes. As can be seen the response increases over a period of time before its value becomes constant.

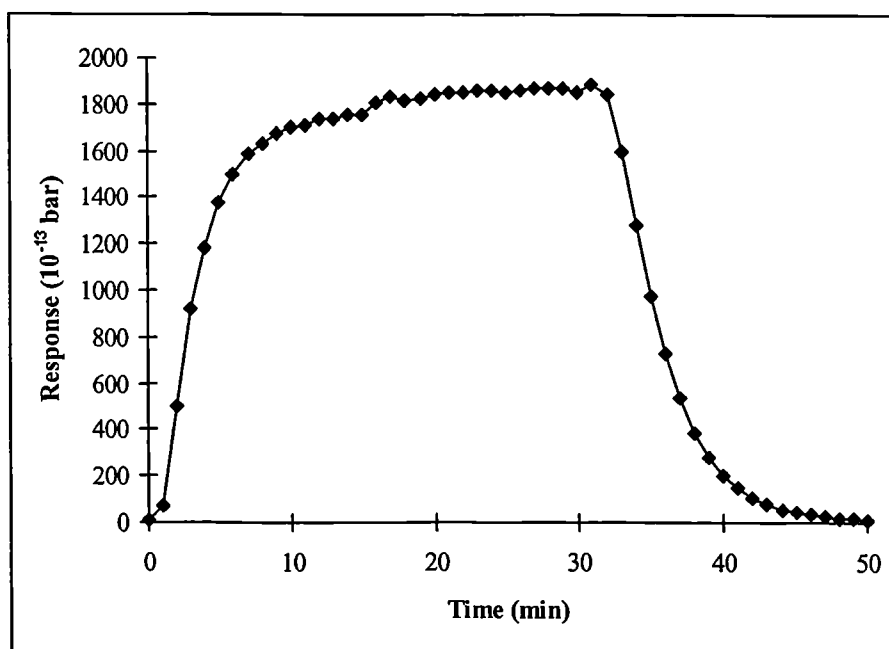


**Figure 5.8** Response curve for acetone using the flow cell with a headspace volume of 14 ml

The constant response indicates a uniform concentration of acetone in the headspace which does not change with time. A dynamic equilibrium is present in the flow cell and is represented as shown below:

$$\begin{array}{l} \text{Rate of analyte transfer from the} \\ \text{liquid to headspace phase} \end{array} = \begin{array}{l} \text{Rate of analyte pumped from the} \\ \text{headspace in to the mass spectrometer} \end{array}$$

The volume of analyte in the headspace which dissolves in the liquid stream is negligible because of the positive entropy change required for the analyte to pass from the gas to liquid phase.

Two parameters can be used to represent the time required for the analyte concentration in the headspace to change to a new constant value when the analyte concentration in the liquid phase changes. The rise time represents the time required for the headspace response to change from 10 to 90 % of the full change in response measured when the analyte concentration in the liquid stream increases to a new constant value. The fall time represents the time required for the headspace response to change from 90 to 10 % of the full change in response measured when the analyte concentration in the liquid stream decreases to a new constant value. The rise time is influenced by the rate of analyte transfer from the liquid stream to the headspace. The fall time is dependent on the time required to remove analyte from the headspace to create the new headspace concentration of analyte which represents the new concentration of the analyte in the liquid phase. The time required for the response to completely change from the two constant peak heights observed before and after the analyte concentration in the liquid phase changes is also quoted in all the results presented in this chapter.

Table 5.2 shows the effect of the headspace phase volume and needle tip position on the rise and fall times, and on the time required for the full response change to be observed. 0.5 % acetone streams pumped at a flow rate of 5 ml min<sup>-1</sup> and a temperature of 23°C was used. The flow cell with a small headspace volume achieves faster rise and fall times. The needle position does not significantly influence the rise and fall times for the small volume headspace flow cell. However the needle position does effect the response measured. Therefore the small headspace volume flow cell will be employed for the further investigation of the dynamic headspace technique because of the more rapid rise and fall times that are achievable.

Volume of headspace (ml)	Needle position	Rise time (min)	Fall time (min)	Time for dynamic equilibrium to be achieved (min)	Response at dynamic equilibrium (10 <sup>-13</sup> bar)
14.5	top	16.5	8.0	24	1282
	middle	8.8	8.0	22	1854
8.8	top	3.5	5.0	18	1574
	middle	3.5	5.5	16	1714

**Table 5.2** The equilibration time parameters for acetone at 23°C

Flow cells with small headspace volumes are more applicable to the on-line analysis of liquid streams because changes in the liquid stream concentration of the analyte need to be represented quickly by changes in the headspace concentration of the analyte and therefore the response measured by the mass spectrometer. The similar headspace concentration of analyte at dynamic equilibrium and therefore the similar headspace responses measured for both headspace volumes studied using the needle placed in the

middle of the headspace volume shows that the faster achievement of the new dynamic equilibrium with a small headspace volume reflects the smaller volume of analyte requiring transport into the headspace to achieve the equilibrium concentration in the headspace. Therefore small headspace volumes provide quicker observable changes in the concentration of analytes in the liquid phase. Alternatively a smaller gaseous volume needs to be pumped into the mass spectrometer to deplete the headspace concentration of analyte to zero and complete the fall time measurement. The observations discussed above are all dependent on a constant temperature, sample matrix and flow rate of headspace in to the mass spectrometer.

Figures 5.9 and 5.10 and Table 5.3 display the effect of the stream temperature on the time required to achieve a new dynamic equilibrium headspace concentration of analyte when the analyte concentration in the liquid stream changes. 5000  $\mu\text{g ml}^{-1}$  and 500  $\mu\text{g ml}^{-1}$  acetone standards were employed at temperatures of 25 and 71°C, respectively. 500  $\mu\text{g ml}^{-1}$  methyl iodide standards were used at both temperatures studied. A stream flow rate of 5  $\text{ml min}^{-1}$  was used. The measurement times used were 15 minutes except for the calculations performed with aqueous acetone standards where a measurement time of 30 minutes was employed. The rise and fall times represent the response change measured between the standard solutions and a stream composed of water or acetic acid only.

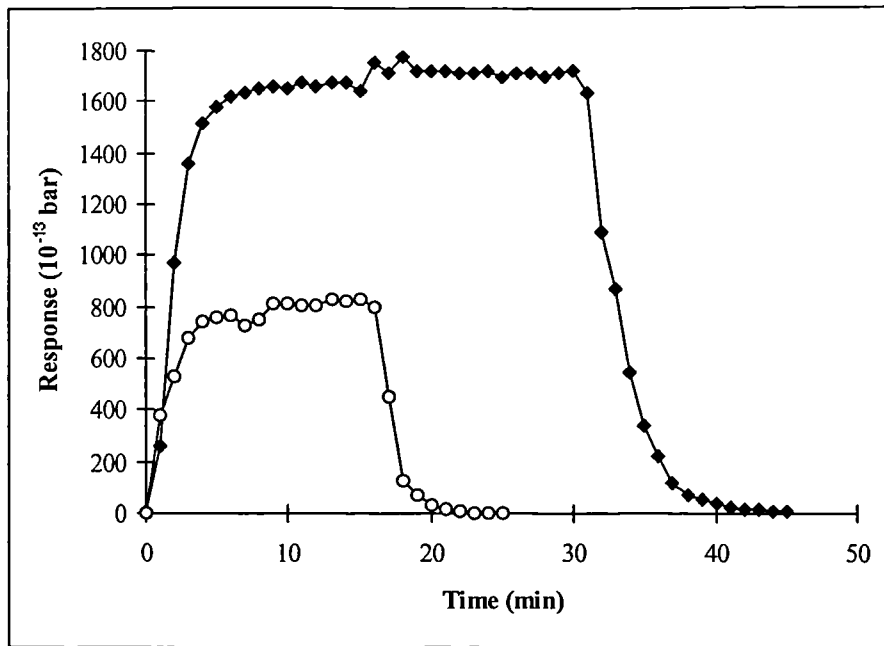


Figure 5.9 Response curves for acetone at 27 (◆) and 70 (○) °C

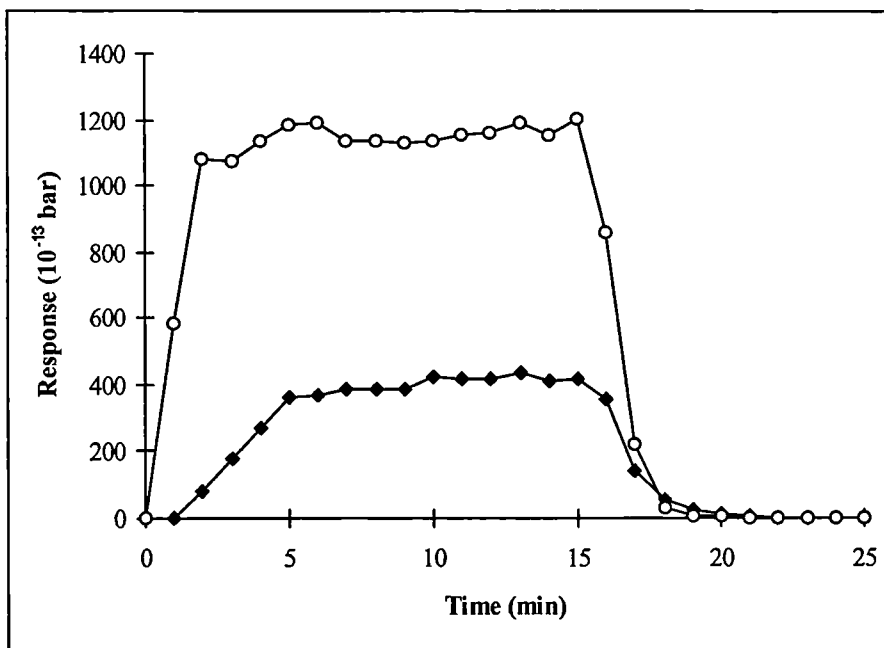


Figure 5.10 Response curves for methyl iodide at 21 (◆) and 70 (○) °C

Analyte	Temperature (°C)	Rise time (min)	Fall time (min)	Time for dynamic equilibrium to be achieved (min)
Acetone	27	3.5	5.5	18
	70	2.5	2.5	10
Methyl iodide	21	4.0	2.8	11
	70	1.5	2.3	6

**Table 5.3** Equilibration time parameters for acetone and methyl iodide

Elevated temperatures reduce the rise times observed and this is caused by the faster rate of analyte transfer from the liquid phase to achieve the headspace analyte concentration required for dynamic equilibrium to be present in the flow cell. The fall times observed are also smaller at elevated temperatures. Higher temperatures assist in the faster transport of the analyte to the mass spectrometer most probably caused by the faster gas phase velocities of the analyte at the higher temperatures. As can be observed from the results the rise and fall times are dependent on the analyte and sample matrix.

#### 5.3.4 Calibration

Calibration data were collected for acetone and methyl iodide at stream temperatures of 22 and 23°C, respectively, and 71°C. An electron multiplier detector was employed throughout the collection of data.. The experimental conditions used are shown in Table 5.4.

Liquid stream flow rate (ml min <sup>-1</sup> )	5
Measurement time (min)	6

**Table 5.4** Experimental conditions employed for the collection of calibration data.

The data was used to plot calibration graphs of response ( $10^{-13}$  bar) vs. analyte concentration ( $\mu\text{g ml}^{-1}$ ). The linear calibration ranges, equation of the calibration lines and correlation coefficients were all determined using the method of least squares<sup>27</sup>, as previously discussed in Chapter three (section 3.3.2.6). The limits of detection were calculated using the method described in Chapter three (section 3.3.2.6).

Table 5.5 and 5.6 show the calibration data collected for acetone at stream temperatures of 22 and 71°C, respectively.

[Acetone] ( $\mu\text{g ml}^{-1}$ )	Response ( $10^{-13}$ bar)	RSD (n=6) (%)
0	0.0	6.7
1	0.09	27.2
10	0.46	8.8
100	3.28	3.0
1000	68.5	5.3
10000	1147	5.8
50000	6115	1.4

$$y = 0.12x - 21.6$$

$$r = 0.9999 \text{ (n = 7)}$$

$$\text{Limit of detection} = 0.8 \mu\text{g ml}^{-1} \text{ (n = 4)}$$

Temperature = 21°C

**Table 5.5** Calibration data for acetone at 23°C using the electron multiplier detector

[Acetone] ( $\mu\text{g ml}^{-1}$ )	Response ( $10^{-13}$ bar)	RSD (n=6) (%)
0	0	7.1
1	0.93	16.5
10	5.05	12.4
50	31.9	7.3

$$y = 0.64x - 0.29$$

$$r = 0.9989 \text{ (n = 4)}$$

Limit of detection =  $0.1 \mu\text{g ml}^{-1}$

Temperature = 71°C

**Table 5.6** Calibration data for acetone at 71°C using the electron multiplier detector

The limits of detection decrease when the stream temperature is increased from 21 to 71°C. The higher transfer of analyte from the liquid phase to headspace at 71 with respect to 21°C result in the lower limit of detection achievable. No detectable response was observed when the blank standard was analysed. In this thesis relative standard deviation values less than 10 % exhibit adequate precision. The precision for replicate analyses described above is adequate.

The calibration data for methyl iodide collected at stream temperatures of 22 and 71°C are shown in Tables 5.7 and 5.8, respectively. The limit of detection is lower by a factor of ten when the temperature is elevated from 22 to 71°C. Lower limits of detection are achievable with the dynamic headspace technique with respect to the static headspace technique described in chapter three, showing that a greater transfer of the analyte is achieved by the dynamic headspace technique.

[Methyl iodide] ( $\mu\text{g ml}^{-1}$ )	Response ( $10^{-13}$ bar)	RSD (n=6) (%)
0	2.15	2.2
10	2.59	20.3
100	13.5	5.3
1000	86.7	5.4
5000	409	5.7
10000	853	3.2
50000	4200	4.3

$$y = 0.08x + 2.22$$

$$r = 0.9999 \text{ (n = 7)}$$

$$\text{Limit of detection} = 10.7 \mu\text{g ml}^{-1}$$

$$\text{Temperature} = 22^\circ\text{C}$$

**Table 5.7** Calibration data for methyl iodide at 22°C

[Methyl iodide] ( $\mu\text{g ml}^{-1}$ )	Response ( $10^{-13}$ bar)	RSD (n=6) (%)
0	0.05	173
0.5	0.82	8.4
1	1.96	6.7
10	20.9	4.9
100	258	10.8
500	1207	6.7

$$y = 2.42x + 1.89$$

$$r = 0.9999 \text{ (n = 6)}$$

$$\text{Limit of detection} = 0.1 \mu\text{g ml}^{-1} \text{ (n = 4)}$$

$$\text{Temperature} = 71^\circ\text{C}$$

**Table 5.8** Calibration data for methyl iodide at  $71^\circ\text{C}$

As was observed with the static headspace technique investigated, the increase in the temperature results in the reduction of the linear calibration range for acetone and methyl iodide standards. This is most likely caused by the presence of higher concentrations of the matrix in the electron impact ion source used at elevated temperatures which may affect the rate of analyte ionisation at analyte concentrations greater than those observed in the calibration range.

### 5.3.5 Gas Purging of the Liquid Stream

#### 5.3.5.1 The Effect of the Purging Gas Flow Rate

The effect of the flow rate of instrument air purged through the gas purged flow cell was investigated. 1000  $\mu\text{g ml}^{-1}$  acetone and methyl iodide standards were analysed at a stream flow rate of 5  $\text{ml min}^{-1}$  with a measurement time of six minutes.

The response increases as the purge gas flow rate is increased over the range of flow rates studied (Figure 5.11). The rate of increase in the response is similar for both analytes and a higher concentration of analyte in the headspace phase is obtained with gas purging of the liquid stream when compared to no gas purging at a stream temperature of 24°C.

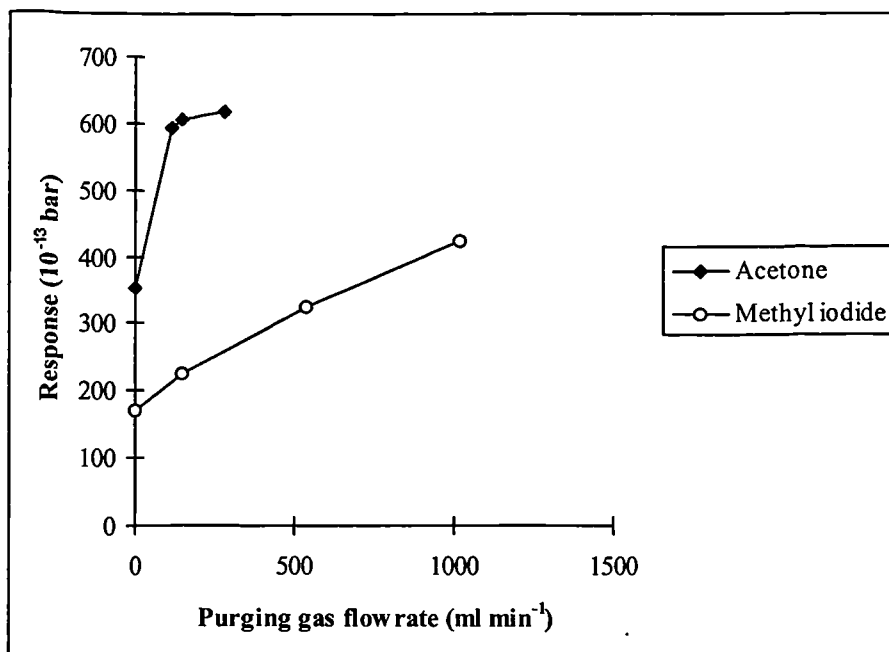


**Figure 5.11** The effect of the purging gas flow rate

Severe foaming of the liquid phase occurred at purge gas flow rates greater than 300 ml min<sup>-1</sup> (acetone in water) and 600 ml min<sup>-1</sup> (methyl iodide in acetic acid), which resulted in periodic blockages of the sampling interface needle with liquid. To eliminate this problem purge gas flow rates of approximately 300 and 600 ml min<sup>-1</sup> were used in further work for acetone and methyl iodide standards respectively. The variation in the maximum allowed purge gas flow rate is caused by the larger surface tension<sup>28</sup> at 20°C of water (73.1 x 10<sup>-3</sup> N m<sup>-1</sup>) with respect to acetic acid (27.8 x 10<sup>-3</sup> N m<sup>-1</sup>) and its effect on liquid foaming.

#### 5.3.5.2 The Effect of the Liquid Stream Flow Rate

The investigation of the effect of the liquid stream flow rate (1 - 15 ml min<sup>-1</sup>) was performed with 1000 µg ml<sup>-1</sup> acetone standards and a measurement time of six minutes. Table 5.9 shows the increase in the response as the flow rate is increased. The increase in response is significantly higher than was observed with the non-purged flow cell. The transfer rate of analyte from the liquid phase to the headspace is therefore dependent on the mass flow rate of analyte through the flow cell when gas purging of the liquid stream is used. Higher mass flow rates provide a greater flux of analyte to the flow cell which enables a greater rate of analyte transfer to the headspace to be achieved.

Liquid stream flow rate (ml min <sup>-1</sup> )	Response (10 <sup>-13</sup> bar)	RSD (n=6) (%)
1	491	5.0
5	632	3.3
10	714	5.2
15	853	6.6

**Table 5.9** The effect of the stream flow rate for acetone

In subsequent work a flow rate of 5 ml min<sup>-1</sup> was employed to reduce the volume of reagent used and waste produced. A relative decrease in the response of 35 % is observed for the response at the flow rate of 5 ml min<sup>-1</sup> with respect to 15 ml min<sup>-1</sup>.

#### 5.3.5.3 Determination of the Rise and Fall Times

The response curves (Figure 5.12) were determined for acetone and methyl iodide standards using 1000 µg ml<sup>-1</sup> standards pumped through the flow cell at 5 ml min<sup>-1</sup>. The rise and fall times for changes in the liquid phase concentrations (0 to 1000 and 1000 to 0 µg ml<sup>-1</sup>, respectively) for acetone and methyl iodide are displayed in Table 5.10. Measurement times of 10 and 15 minutes were used for methyl iodide and acetone standards, respectively.

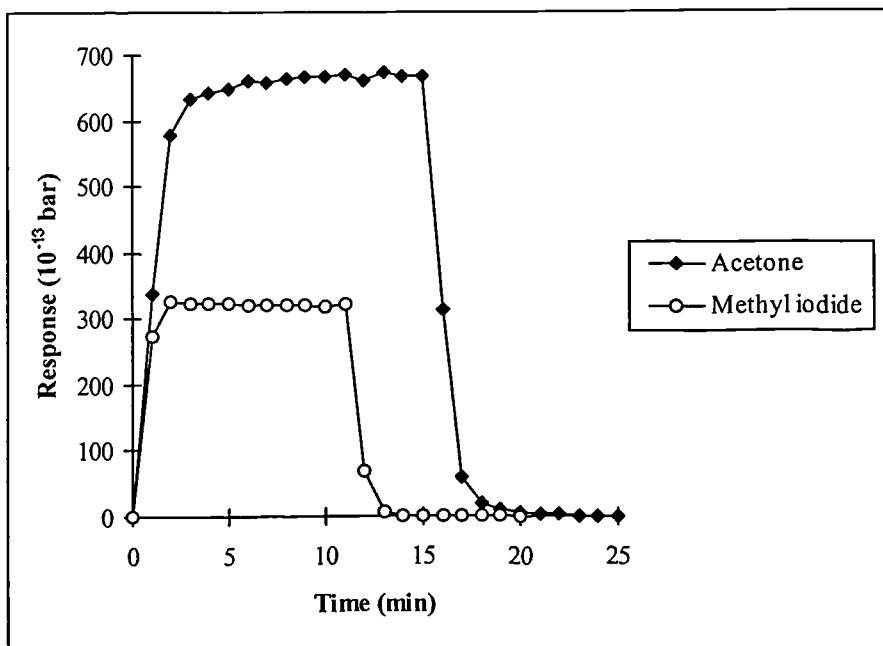


**Figure 5.12** Response curves for acetone and methyl iodide

Analyte	Rise time (min)	Fall time (min)	Time for dynamic equilibrium to be achieved (min)
Acetone	2.4	1.6	15
Methyl iodide	1.2	1.4	2

**Table 5.11** Equilibration time parameters for acetone and methyl iodide

The rise and fall times for both analytes are shorter when gas purging is employed compared to elevating the sample temperature from 25 to 71°C. Therefore the application of gas purging provides the faster rate of analyte transfer from the liquid phase to the headspace and subsequently the dynamic equilibrium concentration of analyte in the headspace is achieved more quickly. To provide the fast rise and fall times required for

on-line monitoring, gas purging of the liquid stream is the best technique to employ. The rise time for methyl iodide is shorter than the corresponding time for acetone. Therefore methyl iodide can be rapidly purged from acetic acid liquid phases. The higher polarity and greater solubility of acetone in water, with respect to methyl iodide in acetic acid, provide these differences in the observed rise times.

#### 5.3.5.4 Calibration

Calibration data was collected for acetone (Table 5.13) and methyl iodide (Table 5.14) using the gas purged headspace flow cell technique and the optimised experimental conditions shown in Table 5.12.

Analyte	Acetone	Methyl iodide
Liquid flow rate (ml min <sup>-1</sup> )	5	5
Purging gas flow rate (ml min <sup>-1</sup> )	300	600
Measurement time (min)	6	6

**Table 5.12** Experimental conditions for collection of calibration data

The calibration data was used as described in section 5.3.4.  $\mu\text{g l}^{-1}$  limits of detection are achievable and the technique provides similar limits of detection as was obtained using the dynamic headspace technique at a temperature of 71°C without gas purging. The precision obtained for replicate analyses was adequate (RSD < 10%). Linear calibration ranges covering a wider concentration range than was observed when the stream temperature was elevated to 71°C were achieved.

[Acetone] ( $\mu\text{g ml}^{-1}$ )	Response ( $10^{-13}$ bar)	RSD (n=6) (%)
0	0.02	245
1	1.16	13.6
10	3.16	9.5
50	14.4	6.3
100	32.3	9.7
500	169	7.5

$$y = 0.34x - 0.60$$

$$r = 0.9997 \text{ (n = 6)}$$

$$\text{Limit of detection} = 0.4 \mu\text{g ml}^{-1} \text{ (n = 4)}$$

$$\text{Temperature} = 24^\circ\text{C}$$

**Table 5.13** Calibration data for acetone

[Methyl iodide] ( $\mu\text{g ml}^{-1}$ )	Response ( $10^{-13}$ bar)	RSD (n=6) (%)
0	0.0	224
1	0.20	20.7
10	3.48	13.3
100	40.5	8.2
1000	295	8.3
5000	1420	7.6

$$y = 0.28x + 4.50$$

$$r = 0.9999 \text{ (n = 6)}$$

$$\text{Limit of detection} = 0.2 \mu\text{g ml}^{-1} \text{ (n = 4)}$$

Temperature = 24°C

**Table 5.14** Calibration data for methyl iodide

5.3.6 Relative Headspace Concentration of Matrix

The relative concentration of water and acetic acid present in the headspace was determined at the same experimental conditions as was employed for the collection of calibration data. Mass 18 Da was monitored for the determination of water and mass 60 Da was monitored for the determination of acetic acid. The results (Table 5.15) can be used for the comparison of conditions applied for acetone and methyl iodide, but not for the comparison of the two separate compounds. This is because of the different mass spectrometer sensitivities for water and acetic acid.

Matrix	Experimental conditions	Response ( $10^{-13}$ bar)
Water	24°C	193
	71°C	901
	gas purging	499
Acetic acid	24°C	76.5
	71°C	165
	gas purging	202

**Table 5.15** The relative concentrations of the matrix in the headspace

The concentration of water and acetic acid in the headspace increases when the stream temperature is elevated and when gas purging is employed with respect to analyses

performed at 24°C. The highest headspace concentration of water was observed when the stream temperature was elevated to 71°C and this correlates with the small linear calibration range observed for the calibration data set collected employing a stream temperature of 71°C. The relatively high headspace concentration of water therefore affects the rate of ion formation in the electron impact ion source. This was discussed in section 4.3.5.

The gas purging technique provides the highest concentration of acetic acid in the headspace and therefore the matrix influences its transfer to the headspace measured for the three different sets of experimental conditions. Water has a higher surface tension<sup>28</sup> ( $73.1 \times 10^{-3} \text{ N m}^{-1}$ ) than acetic acid ( $27.8 \times 10^{-3} \text{ N m}^{-1}$ ) at a temperature of 20°C and therefore a high temperature is required to disrupt the matrix and create a greater transfer of water to the headspace. Gas purging does not create this disruption of the water matrix to as high a degree and therefore the relative headspace response is smaller. The lower surface tension of acetic acid does not require as much heat to disrupt the matrix interactions at the surface as is required for water matrices, and gas purging is sufficiently efficient to transfer a relatively higher concentration of acetic acid to the headspace with respect to the elevation of the stream temperature.

### 5.3.7 The Determination of Acetone in a Process Sample

The composition of the sample matrix can influence the distribution of analyte between the liquid phase and the headspace<sup>4</sup>. To investigate the analytical accuracy that can be achieved using the gas purged headspace flow cell a process sample obtained from BP Chemicals in Hull was analysed to determine the concentration of acetone present in the process sample. The composition of process sample one is described in Chapter three (section 3.3.4).

The gas purged headspace flow cell, described in section 5.2.2 was used throughout the investigation. Liquid stream and purging gas flow rates of 5 and 255 ml min<sup>-1</sup> were employed with a measurement time of four minutes. Mass 58 Da was monitored to detect acetone because acetic acid present in process sample one contributes significantly to the response measured at mass 43 Da. The response was determined as the mean change in peak height during the measurement time for six replicate analyses.

#### 5.3.7.1 The Effect of the Calibration Matrix

Process sample one is composed of a range of organic compounds and water and the compound present at the highest concentration is acetic acid (30 %). To investigate the effect of the process sample matrix the relationship between the concentration of acetic acid present in an aqueous solution and response was determined using the gas purged headspace flow cell and the experimental conditions described in section 5.3.7. 10 % acetone solutions containing 0, 1, 10, 30 or 50 % acetic acid were used. The results are shown in Table 5.16.

[Acetic acid] (%)	Response (10 <sup>-13</sup> bar)	RSD (n=6) (%)
0	227	1.9
1	215	3.2
10	223	4.2
30	133	2.2
50	93.6	2.5

**Table 5.16** The effect of the acetic acid concentration present in an aqueous solution on the response

The response is constant in the acetic acid concentration range of 0 - 10 %. However, as the concentration of acetic acid increases above 10 % the response decreases. The presence of acetic acid at concentrations higher than 10 % in aqueous acetone solutions therefore influences the response measured. The interactions of acetone and acetic acid present at concentrations higher than 10 % in the liquid phase therefore affect the transfer of acetone from the liquid phase to the headspace. The interactions become more influential and the transfer of acetone becomes lower as the acetic acid concentration increases.

#### 5.3.7.2 Calibration

The response measured during the analysis of aqueous acetone solutions has been shown in section 5.3.7.1 to be affected by the presence of acetic acid in the solution. The process sample analysed in section 5.3.7.3 contains 30 % acetic acid and therefore

accurate standards containing acetone, water and acetic acid need to be prepared to collect calibration data used to determine the concentration of acetone in process sample one. It would not be easy to prepare accurate standard solutions containing all eleven compounds present in the process sample. Therefore calibration data were collected using aqueous acetone standards containing 30 % acetic acid. The other nine organic compounds are present in the process sample at concentrations less than 10 %, except pentane, and therefore it is hoped that these compounds will not affect the partitioning of acetone between the liquid phase and headspace.

Calibration data were collected using the experimental conditions described in section 5.3.7 and the gas purged headspace flow cell. Calibration graphs of response ( $10^{-13}$  bar) vs. acetone concentration (%) were plotted. The method of least squares, described in Chapter three (section 3.3.2.6), was used to calculate the linear calibration range, equation of the calibration line and correlation coefficient. The limit of detection ( $3\sigma$ ) was also calculated as described in Chapter three (section 3.3.2.6).

The calibration data for acetone can be seen in Table 5.17.

[Acetone] ( $\mu\text{g ml}^{-1}$ )	Response ( $10^{-13}$ bar)	RSD (n=6) (%)
0	0	28.1
0.1	1.51	16.0
1	18.2	1.9
5	79.2	1.4
10	166	2.8

$$y = 16.5x - 0.03$$

$$r = 0.9997$$

$$\text{Limit of detection} = 0.01 \%$$

**Table 5.17** Calibration data for acetone

A calibration range covering three decades of concentration was achieved with good precision [RSD (n=6) < 3 % for 1 % or higher acetone standards]. The limit of detection (0.02 %) is lower than can be achieved with the Faraday cup when employed with the total vaporisation (Chapter three) and membrane introduction mass spectrometry (Chapter six) techniques.

### 5.3.7.3 Analysis of the Process Sample

Three compounds (acetone, 2-pentanone and 3-hexanone) present in process sample one contribute to the response at mass 58 Da. The method to calculate the peak height at mass 58 Da for acetone only was described in Chapter three (section 3.3.4.3) and will be employed to determine the concentration of acetone in process sample one. Using equation 5.6 and monitoring the response at masses 58, 86 and 100 Da the value for  $\text{PH}^{58}_{(\text{acetone})}$  can be determined. Using this value the concentration of acetone present in process sample one can be determined using the calibration data collected in section 5.3.7.2. The values of  $0.67\text{PH}^{86}$  and  $6.17\text{PH}^{100}$  were experimentally determined to be accurate using the manifold employed.

$$R^{58} = PH^{58}_{(\text{acetone})} + 0.67PH^{86} + 6.17PH^{100} \quad (5.6)$$

Process sample one was analysed using the gas purged headspace flow cell and the conditions described in section 5.3.7. The responses measured at masses 58, 86 and 100 Da are shown in Table 5.18 and were used to calculate  $PH^{58}_{(\text{acetone})}$ . The calculated value for  $PH^{58}_{(\text{acetone})}$  was used to determine the concentration of acetone in process sample one using the calibration data collected in section 5.3.7.

Response measured at mass 58 Da ( $10^{-13}$ bar)	Response measured at mass 86 Da ( $10^{-13}$ bar)	Response measured at mass 100 Da ( $10^{-13}$ bar)
85.7	7.54	7.10

**Table 5.18** The responses measured for process sample one using the gas purged headspace flow cell

The calculated concentration of acetone present in process sample one is  $7.1 \pm 0.5$  %. The actual concentration of acetone in the process sample is  $9.4 \pm 0.2$  % as determined using gas chromatography at BP Chemicals in Hull. The gas purged headspace flow cell technique therefore does not provide accurate determination of the acetone concentration in process samples using the technique and calibration matrix employed. The inaccuracy observed is most probably caused by the nine compounds present in the process sample, but not in the calibration standards, affecting the distribution of acetone between the liquid sample and headspace. The composition of process samples analysed continuously

change and therefore it is not possible to accurately prepare standards for validation of the technique. To successfully quantify the concentration of acetone in the process sample the influence of each compound in process sample one would need to be determined over a range of concentrations for each compound. Multi-variate calibration techniques would be the most applicable techniques to use.

#### **5.4 Conclusions**

Dynamic headspace techniques employing elevated temperatures or gas purging to increase the transfer of analyte from the liquid phase to the headspace for analysis has shown that  $\mu\text{g l}^{-1}$  limits of detection can be achieved with adequate precision represented by RSD values less than 10 % for replicate analyses. The liquid stream flow rate, liquid stream temperature, purging gas flow rate and the analyte and sample matrix affect the transfer rate of analyte to the headspace from the liquid phase.

The application of elevated temperatures or gas purging allow a change in the liquid stream concentration of an analyte to be observed in less than three minutes. The measured rise and fall times are similar for methods of increasing the rate of transfer of analyte to the headspace. The techniques could therefore be applied to the on-line monitoring of liquid streams. However, streams containing many compounds can effect the rate of transfer of the analyte from the liquid phase to the headspace. Therefore for the determination of analyte concentrations in the liquid stream the influence of each compound in the stream would need to be studied and quantified.

## 5.5 References

- 1) Ioffe, B.V., and Vitenburg, A.G., *Head-Space Analysis and Related Methods in Gas Chromatography*, Wiley, Chichester, 1984.
- 2) Poole, C.F., and Poole, S.K., *Chromatography Today*, Elsevier, Oxford, 1991, p 818.
- 3) Namiesnik, J., Gõrecki, T., Biziuk, M., and Torres, L., *Anal. Chim. Acta*, 1990, **237**, 1.
- 4) Drozd, J., and Novák, J., *J. Chromatogr.*, 1979, **165**, 142.
- 5) Grob, K., *J. Chromatogr.*, 1973, **84**, 255.
- 6) Swinnerton, J.W., and Linnenbom, V.J., *J. Gas Chromatogr.*, 1967, **5**, 570.
- 7) Bellar, T.A., and Lichtenberg, J.J., *J. Am. Water Works Assoc.*, 1974, **66**, 739.
- 8) Hu, H.C., and Weiner, P.H., *J. Chromatographic. Sci.*, 1980, **18**, 333.
- 9) Michael, L.C., Erichson, M.D., Parks, S.P., and Pellizzari, E.D., *Anal. Chem.*, 1980, **52**, 1836.
- 10) Ramstad, T., and Nicholson, L.W., *Anal. Chem.*, 1982, **54**, 1191.
- 10) Hu, H.C., and Weiner, P.H., *J. Chromatographic. Sci.*, 1980, **18**, 333.
- 11) Erickson M.D., Alsup, M.K., and Hyldburg, P.A., *Anal. Chem.*, 1981, **53**, 1265.
- 12) Rose, M.E., and Colby, B.N., *Anal. Chem.*, 1979, **51**, 2176.
- 13) Technical data, Chrompack, purge and trap system, 1992.
- 14) Grob, K., and Grob, G., *J. Chromatogr.*, 1974, **90**, 303.
- 15) Grob, K., Grob, G., and Habich, A., *J. High Res. Chromatogr. & Chromatogr. Comm.*, 1984, **7**, 340.

- 16) Liska, I., Krupcik, J., and Leclercq, P.A., *J. High Res. Chromatogr.*, 1989, **12**, 577.
- 17) Badings, H.T., Jong, C.D., and Dooper, R.P.M., *J. High Res. Chromatogr. & Chromatogr. Comm*, 1985, **8**, 755.
- 18) Noij, Th., Es, A.V., Cramers, C., Rijks, J., and Dooper, R., *J. High Res. Chromatogr. & Chromatogr. Comm*, 1987, **10**, 60.
- 19) Pankow, J.F., and Rosen, M.E., *J. High Res. Chromatogr. & Chromatogr. Comm*, 1984, **7**, 504.
- 20) Soleta, D.D., *Am. Lab.*, 1989, **21**, 21.
- 21) Schieck, D., and Brown, F., *Proc. Cont. Qual.*, 1994, **5**, 251.
- 22) Lesage, S., and Brown, S., *Anal. Chem.*, 1994, **66**, 572.
- 23) Kozlowski, E., Sienkowska, E.S., and Górecki, T., *Fresenius J. Anal. Chem.*, 1991, **339**, 19.
- 24) Matz, G., and Kesners, P., *Anal. Chem.*, 1993, **65**, 2366.
- 25) Baykut, G., and Voigt, A., *Anal. Chem.*, 1992, **64**, 677.
- 26) St-Germain, F., Mamer, O., Brunet, J., Vachon, B., Tardif, R., Abribat, T., Rosiers, C.D., and Montgomery, J., *Anal. Chem.*, 1995, **67**, 4536.
- 27) Miller, J.C., and Miller, J.N., *Statistics for Analytical Chemistry*, Ellis Horwood, Chichester, 2nd Edition, 1992, p 109.
- 28) Lide, D.R. (Editor-in-chief), *Handbook of Chemistry and Physics*, CRC Press, Boston, 72nd Edition, 1991, p 6-118.

## **Chapter Six**

### **Membrane Introduction Mass**

### **Spectrometry**

## **6.1 Introduction**

The inclusion of sample pre-treatment stages in analytical protocols is frequently required for the analysis of compounds present in a complex sample matrix. Techniques that remove or separate analytes from sample matrix components which are detrimental to the analytical result or instrument can improve the sensitivity and selectivity of a subsequent analysis stage.

Headspace techniques are used to separate volatile and semi-volatile analytes from a sample matrix and the variety of methods currently employed are discussed in Chapters four and five. An alternative range of techniques employ membranes as a physical barrier (interphase) located between two stagnant or flowing fluid phases<sup>1,2,3,4</sup>. Compounds present in a sample matrix (donor phase) may be able to transfer through the membrane to a second fluid (acceptor phase). The mass transfer of compounds across the membrane can be employed for a range of different applications<sup>1,5</sup>, however, the most frequently used application is to selectively separate analytes from their sample matrix by providing their transfer to a clean and normally inert acceptor phase. The analytes can then be analysed with or without further sample pre-treatment stages.

In this chapter membrane introduction mass spectrometry (MIMS)<sup>6</sup> is applied to selectively separate compounds through a permselective membrane from a liquid donor phase (sample) to a gaseous acceptor phase. Mass spectrometric detection is continuously performed to analyse the compounds present in the acceptor gas phase. The technique of MIMS allows an electron impact mass spectrometer to indirectly obtain qualitative and quantitative information regarding the composition of a liquid phase by analysis of a gas phase into which compounds from the sample phase have been transported.

Although permselective membranes are employed, most or all of the compounds present in the sample will transfer through the membrane to the acceptor phase. Analytes and matrix compounds can normally be detected in the gas acceptor phase. Therefore the complete separation of the analyte from the sample matrix is never achieved and 100 % selectivity of one compound with respect to another compound is never observed. The flux<sup>7</sup> of compound i ( $J_i$ ) diffusing through a membrane is proportional to the number of molecules (n) that is transported through a membrane with a surface area (A) in time t.

$$J_i \propto n A t \quad (6.1)$$

The flux through a membrane of different compounds present in a sample can be controlled by the correct choice of the membrane material as well as other experimental parameters. A higher flux of the analytes with respect to other compounds present in the sample matrix can be, and is normally, observed<sup>4</sup>. Partial separation of compounds and a degree of selectivity can therefore be achieved. The greater flux of analyte, with respect to other compounds, also provides analyte enrichment in the acceptor phase and this enables a higher sensitivity to be achieved.

### 6.1.1 Membrane Types<sup>1,2,3,4</sup>

The majority of materials employed in analytical scale membrane separations are constructed with organic polymers which include polydimethylsiloxane (silicone rubber), polytetrafluoroethylene and polypropylene<sup>4</sup>. The range of polymers currently available provide a range of membranes with different physical characteristics which include

polarity. This allows a suitably chosen membrane to selectively allow a larger analyte flux to travel through the membrane when compared to matrix components<sup>4</sup>. Partial separation and selectivity is therefore achieved. In their physical form thin membranes (thickness < 1 mm) provide fast transfer times of compounds across a membrane barrier<sup>4</sup>. The ratio of the active membrane surface area to the volume of the donor phase is also important. The large ratios available with hollow fibres allow a high flux of compounds through the membrane available when compared with sheet or tubular membranes<sup>4</sup>. Hollow fibre membranes are manufactured with inner diameters less than 1 mm. Other forms of membranes used include flat sheets and tubes with inner diameters larger than observed with hollow fibres.

Two types of membranes (nonporous and microporous) with different physical structures and mechanisms of transmembrane transport are currently employed for the majority of MIMS applications.

#### 6.1.1.1 Nonporous Membranes<sup>2,3,4</sup>

Nonporous membranes are described as dense homogeneous films prepared from organic polymers which contain no microscopic pores and of which all of the unoccupied volume present in the membrane is composed of the free space between polymer chains<sup>2,4</sup>. The membranes exhibit high physical stability and resistance to membrane fouling, though the flux of compounds of interest through the polymer is smaller by 1-2 orders of magnitude than is observed with microporous membranes<sup>4</sup>. Silicone rubber polymers are the most frequently applied membrane in MIMS applications because they

provide a high degree of selectivity for small low molecular weight (MW) volatile organic compounds (VOCs) with respect to the most frequently used matrix i.e. water.

The transmembrane transport mechanism of compounds through a nonporous membrane is described as pervaporation, so called because of the evaporation of liquid phase compounds during transfer through a permselective membrane. Described by Binning et al.<sup>8</sup>, pervaporation<sup>1,6</sup> for a single compound is a three stage process and is shown in Figure 6.1:

- (1) adsorption of a compound on to the membrane at the donor-membrane interface,
- (2) diffusion of the compound through the membrane under the force of a concentration gradient,
- (3) desorption of the compound into the gas phase at the acceptor-membrane interface.

Stages (1) and (2) are considered as the rate determining stages and are described by the solution diffusion model<sup>2</sup>. The model states that compounds dissolve in the dense nonporous membrane materials by the interaction with polymer chains [stage (1)] and subsequently diffuse through the membrane material [stage (2)].

Stage (1) is partly controlled by the presence of a depletion layer at the membrane - donor phase interface, whose width is dependant on the stirring rate or flow rate of the liquid phase<sup>9</sup>. The depletion layer controls the diffusion rate of compounds to the membrane surface and therefore thinner layers, created by a large degree of stirring or high flow rates, allow the faster diffusion of compounds to the membrane surface<sup>9</sup>.

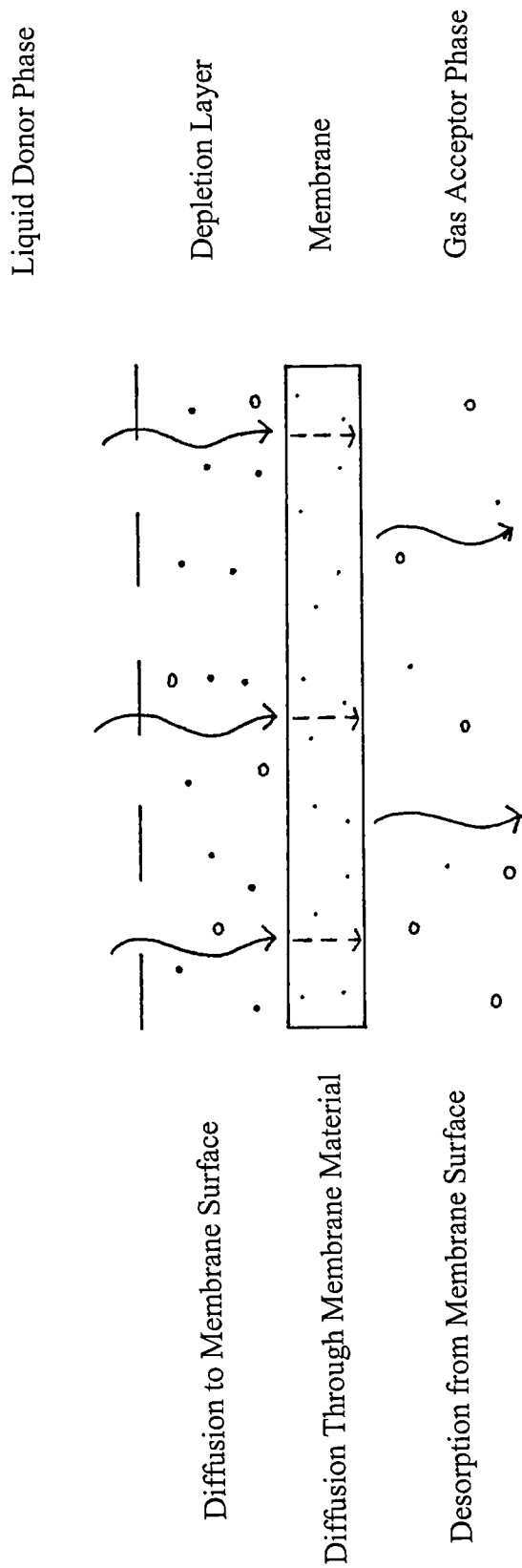


**Figure 6.1** The mechanism of pervaporation

Transmembrane transfer of compounds through the membrane is observed in stage (2) and is controlled by a chemical, or in some cases electrical, potential gradient present between the liquid sample phase and acceptor gas phase<sup>1,2</sup>. The potential gradient is created by differences between the concentration, pressure or a combination of both of these parameters between the two phases. The flux of compounds down the chemical potential gradient to the gas acceptor phase is controlled by two parameters<sup>1</sup>; the physico-chemical interactions of a compound with the membrane material and the compound's diffusion through the membrane. The flux of compounds is therefore dependant on the solubility of the compound in the membrane material and also by the molecular diffusivity of the compound in the membrane matrix. Derivations of Fick's first law of diffusion describe these dependencies<sup>7</sup>:

$$J_i = -D_i (dN / dz) \quad (6.2)$$

$J_i$  = flux of compound i through the membrane (mole of compound per unit of membrane area per unit of time)

$D_i$  = diffusion coefficient of compound i in the membrane (unit of membrane area per unit of time)

$dN / dz$  = concentration gradient of species i parallel to the z axis

The flux is greater for compounds highly soluble in the membrane and for compounds with high diffusion rates across the membrane (large values of  $D_i$ ).

Membranes are chosen to have high solubilities and/or large diffusion rates for analytes with respect to the matrix compounds to provide selective separation and enrichment of the analytes in the gas acceptor phase.

The enrichment of compounds with silicone rubber membranes is achieved by a greater solubility in the membrane material and the higher diffusivity through the membrane of low MW volatile organic compounds with respect to the commonly employed water matrix or other polar compounds<sup>6</sup>. Significant differences in the fluxes of compounds can be achieved and therefore selectivity and analyte enrichment can be obtained.

#### 6.1.1.2 Microporous Membranes<sup>2,3,4</sup>

Homogeneous nonporous polymers described above can be chemically or physically modified to produce a highly voided physical structure composed of randomly distributed interconnected pores<sup>2,4</sup>. Microporous membranes prepared in this way have pore diameters of 0.01 - 1  $\mu\text{m}$  and act similarly to filters by allowing or rejecting the passage of molecules through the pores. Passage through the membrane is dependant on molecular sizes<sup>2</sup>. Membrane materials used include porous polypropylene, polytetrafluoroethylene (PTFE) and poly(vinylidene difluoride) (PVDF).

Figure 6.2 shows the transmembrane transport of compounds through microporous membranes. Molecules with diameters smaller than the pore diameter approaching the membrane surface can enter the gas filled pores and diffuse to the acceptor phase whereas molecules with larger diameters will be prevented from entering the pores. Selectivity is therefore achieved by differences in molecular size<sup>2</sup>. However microporous

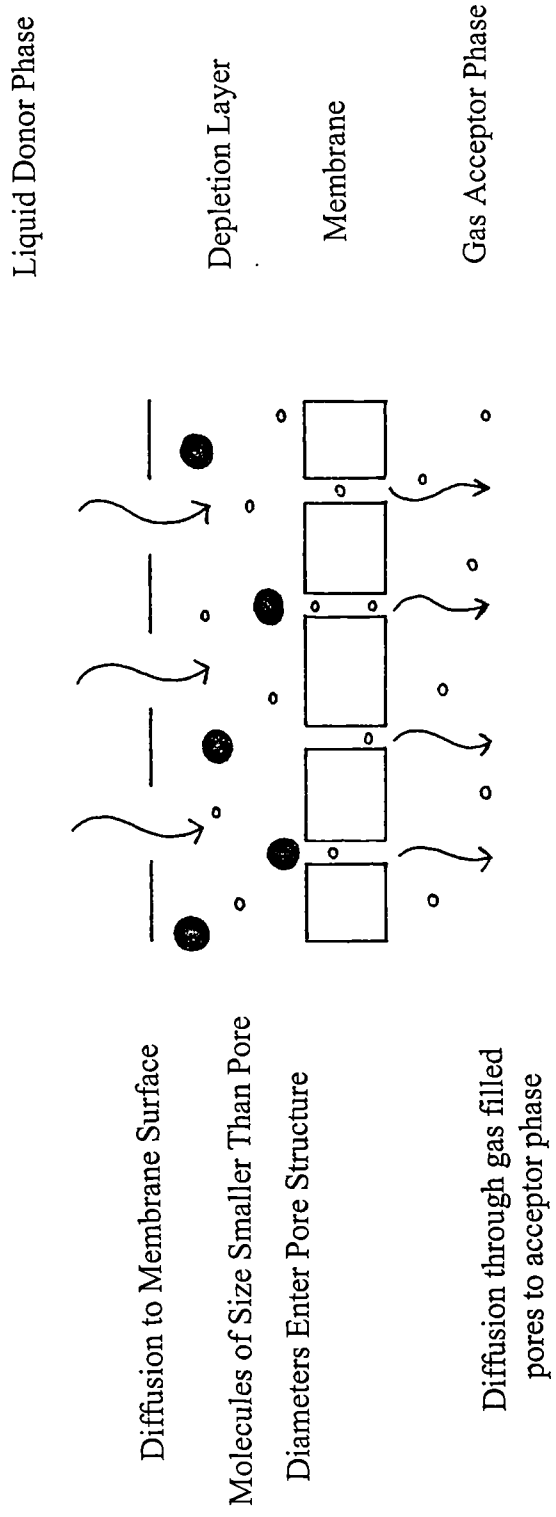


**Figure 6.2** Transmembrane transport through a microporous membrane

membranes will allow molecules of up to and over 1000 Da to be transported through the pores and therefore these membranes act as a barrier between two different phases in MIMS applications. The majority of compounds present in the liquid streams analysed in this thesis have molecular diameters smaller than 5 nm and therefore all of these compounds will pass through the membrane into the acceptor gas phase.

The pressure on either side of the microporous membrane and the pore diameter aids the resistance to leakage of the liquid phase into the gas filled pores and out of the opposite side into the gas phase, for most of the membranes and liquid matrices currently used<sup>4</sup>. The pore diameter is larger than the mean free path of molecules in the gas phase and therefore the compounds present in the gas filled pores will permeate by convective flow through the membrane to the acceptor phase<sup>3</sup>. Transport is dependant on the pore size and structure and on the molecular size. Diffusion through the membrane pores is controlled in the same manner as was described for nonporous membranes, by the presence of a chemical potential gradient created by differences in the concentration and/or pressures between the liquid donor and gaseous acceptor phase.

As transport occurs through the gas medium the flux of compounds is dependant on the partition coefficient of a compound between the liquid and gas phases and is also dependant on the diffusion coefficient of the compound in the gas filled pores<sup>4</sup>. As the membrane solubility is not influential a wider range of gases and volatile / semivolatile compounds can be transported through the membrane into the gas phase<sup>4</sup>. The diffusivity of molecules in the gas phase with respect to the membrane phase is also higher and therefore faster response times and higher fluxes can be obtained with respect to nonporous membranes. However selectivity and compound enrichment is dependant on the partition coefficients and diffusion coefficients of the compounds present in the

liquid donor phase. Only small differences in the fluxes between different compounds can be observed and therefore poor selectivity is achieved<sup>4</sup>. Secondary techniques can be used to enrich the analytes and provide a degree of selectivity.

### 6.1.2 Applications of MIMS

Membrane introduction mass spectrometry offers a range of advantages<sup>6,10</sup> which are shown in Table 6.1.

Simple and rugged
Fast response times (normally less than one minute)
Sensitive (detection limits in the range $\text{ng l}^{-1}$ to $\mu\text{g ml}^{-1}$ achievable)
Quantification is convenient with the use of flow injection manifolds
Multi-component analysis capability
High specificity achievable
Automation and on-line monitoring of liquid streams possible
Matrix effects are not normally observed
Compatible with a range of mass spectrometer designs

**Table 6.1** The advantages of membrane introduction mass spectrometry

These advantages enable MIMS to be used for a range of different applications including environmental and manufacturing process monitoring and the monitoring of reactions occurring in biological or nonbiological matrices in the laboratory. Several review articles<sup>6,9,10,11,12,13</sup> have been published detailing the variety of applications and the effect of several physical characteristics on the performance (sensitivity and

selectivity) of MIMS techniques. Membrane thickness<sup>9,14,15,16</sup> and material<sup>17,18</sup>, liquid flow rate<sup>9,15,16</sup> and temperature<sup>9,16</sup> pressure<sup>19</sup> and pneumatic transport of the acceptor phase<sup>16</sup> have all been shown to effect the performance. In the short review shown here silicone membranes were used unless otherwise stated.

The first application of MIMS was reported in 1963 by Hoch and Kok<sup>20</sup> who used polyethylene and PTFE membranes separately to transport O<sub>2</sub> and CO<sub>2</sub> into the acceptor phase for analysis by a mass spectrometer. The results were used to study the kinetics of photosynthesis in plants. The technique exhibited the ability to analyse small MW compounds in real-time without the need for extensive sample pre-treatment of the complex biological matrix and also without the need to sample large volumes of the liquid sample phase which may disrupt the progression of the reaction and subsequently the reaction kinetics measured. Other early applications employed silicone covered stainless steel cannulae placed in rat and dog arteries for in-vivo measurement of oxygen and carbon dioxide<sup>21</sup> and halothane<sup>22</sup>, respectively. More recently a silicone hollow fibre probe has been placed intravenously in a rat to detect dichloromethane, methoxyflurane and styrene at concentrations of 1 µg ml<sup>-1</sup> or lower<sup>23</sup>. A microdialysis probe has been employed with continuous flow fast atom bombardment tandem mass spectrometry for in-vivo monitoring of tris (2-chloroethyl) phosphate in rats and to determine the elimination rates of the compound<sup>24</sup>.

MIMS can also be used to deduce reaction mechanisms and determine physical constants in matrices less complex than those of a biological origin. Tou, Westover and Sonnabend<sup>25</sup> have inferred the hydrolysis mechanisms of bis(chloromethyl) ether in basic and acidic conditions. Research groups at Ohio State University<sup>26,27</sup> have studied the reaction mechanisms of α - chymotrypsin catalysed transesterification of p-nitrophenyl-

5-n-alkyl furoates to propose rate limiting steps of the reaction and determine reaction step rate constants. Kotiaho et al. have used on-line MIMS in the laboratory for detecting chloroamines produced in water treatment at sub  $\mu\text{g ml}^{-1}$  concentrations to assist in the characterisation of the formation of several of these compounds<sup>28</sup>. Reactions occurring in the gas phase have also been studied to measure stability rates<sup>29</sup>, exchange rates<sup>30</sup> and the permeation of gases through polymer films<sup>31</sup>.

Several research groups have monitored electrochemical reactions in the liquid phase on-line by allowing the permeation of membrane permeable volatile reactants or products into a mass spectrometer. Bruckenstein and Gadde<sup>32</sup> first introduced electrochemical mass spectrometry using a porous frit to act as a membrane. It has the advantage of separating electroactive materials from electrolytes and solvents which may increase the signal-to-noise ratio of the measurement. Controlled potential experiments have been used to study the reduction of dibromocyclohexane to cyclohexene<sup>33</sup>. Modulated currents applied to an electrode can also be used to provide modulated mass spectrometry ion currents which enable users to distinguish between the signal for the analyte and the signal for the background and solvent/electrolyte compounds<sup>34</sup>. The accuracy and selectivity of electrochemical mass spectrometry is improved by this method.

The transfer of MIMS from the laboratory onto larger scale process plants has been fulfilled by Tou et al. for on-line monitoring of nitrogen trichloride during wastewater treatment<sup>35</sup>. Nitrogen trichloride is explosively unstable at concentrations greater than  $2000 \mu\text{g ml}^{-1}$  and therefore real-time monitoring of the process is required to ensure this concentration is never reached. Similarly LaPack et al. at Dow Chemicals (America) have monitored aerobic biological wastewater treatment processes using MIMS<sup>36</sup>. The analysis of organic compounds in influent and effluent water and air streams allowed

mass balances to be calculated and the processes controlled and optimised. Recently a valved sampling cell for MIMS has been designed and tested for process monitoring applications<sup>37</sup>. The pressure surge resulting from a membrane rupture closes the valve and eliminates the passage of liquids into the mass spectrometer. This operation is important in process monitoring where membranes may not be chemically stable in liquid process streams when operated for long periods.

MIMS has been widely employed in the process monitoring of volatiles and dissolved gases formed in the production of a range of organic compounds by fermentation processes. The technique requires a range of sensitivities, fast response times and high accuracy to be obtained. The groups led by Heinzle<sup>38,39,40</sup> and Bohatka<sup>41,42</sup> have both used silicone rubber membrane probes placed in the fermentation broth and the subsequent transfer of permeated compounds along long transfer lines to the mass spectrometer. Problems of the adsorption of compounds on the transfer lines, long response times, membrane clogging and the inability to produce quantitative data led to a second generation of interfaces. Flow injection (FI) manifolds<sup>43</sup> were used to deliver plugs of fermentation broth to a membrane probe placed in or near to the ion source to eliminate the problems described above. Standard solution plugs could be introduced to the manifold for quantification and sample filtering could also be performed on-line. Bier and Cooks<sup>44</sup> first injected off-line prepared plugs and described the use of direct insertion probes (DIPs) and chemical ionisation for monitoring aldehydes and ketones produced in *Klebsiella oxytoca* fermentations at concentrations of  $10^{-2}$  to  $10^{-6}$  M. Hayward et al. used MIMS for monitoring two fermentations with on-line sample filtering and transport to the probe<sup>45,46</sup>. These authors have used quadrupole<sup>45</sup> and ion trap mass spectrometers<sup>46</sup>

(ITMS) for fermentation monitoring and modelling<sup>47</sup>. Tandem mass spectrometry can be employed for structure determination, which is unavailable with chemical ionisation<sup>45,48</sup>. Finally Srinivasan et al.<sup>49</sup> fully automated FI-MIMS-ITMS for monitoring ethanol at g / l concentrations and employed the results for feedback control of a glucose fermentation using yeast strain 1400.

The measurement of other non-permeable species present in fermentation broths can also be performed. Pungor et al. have used chemical esterification of 2-oxoglutaric acid with methanol to monitor this otherwise non-volatile compound in penicillin fermentation broths<sup>50</sup>. As an alternative Weaver and Abrams used a variable pH MIMS interface<sup>51</sup> to provide undissociated volatile acids and bases (eg acetic acid and ammonia) to the membrane which can be partially dissociated at other frequently employed fermentation broth conditions.

The major improvements in the MIMS technique have occurred over the last ten years during research concerned with fermentation and environmental monitoring. Improvements observed during research performed to provide fermentation monitoring with MIMS was discussed in the previous two paragraphs. However these methods measured low percent or higher concentrations of compounds. For MIMS to compete with the routinely used gas chromatography - mass spectrometry (GC-MS) technique for environmental analyses improvement in the detection limits to sub  $\mu\text{g l}^{-1}$  concentrations was required.

In early research<sup>52,53</sup> silicone rubber hollow fibres probes were placed in the aqueous solution, to provide a limit of detection of  $10 \mu\text{g l}^{-1}$  for chloroform<sup>52</sup>. The problem of adsorption on long transfer lines and long response times was solved in 1985 by Brodbelt

and Cooks who positioned a DIP close to the ion source and flowed an aqueous stream through it<sup>54</sup>. This arrangement of the membrane and donor phase was called a flow-through hollow fibre configuration. The probe has been combined with quadrupole mass spectrometers for monitoring chloroamines<sup>55</sup>, acrolein and acrylonitrile<sup>56</sup> and low MW aldehydes<sup>57</sup> in water at low  $\mu\text{g l}^{-1}$  ( $1\text{-}20 \mu\text{g l}^{-1}$ ) levels and for detecting chloro-ethylenes at concentrations of  $\text{ng l}^{-1}$  in biological reactions<sup>58</sup>.

Flow-over hollow fibres inlets have also been designed and allow the sample to flow over the outer surface of the hollow fibre while the inner surface is exposed to a flow of helium to aid the transport of permeants to the mass spectrometer and help improve the sensitivity and decrease the response times<sup>59,60</sup>.

The coupling of ion trap mass spectrometers (ITMS) with DIPs<sup>61</sup> and flow-over membrane configurations allowed an improvement in the sensitivity to be achieved;  $\text{ng l}^{-1}$  (ppt) and  $\text{pg l}^{-1}$  (ppq) detection limits of VOCs in water were observed<sup>61,63,64</sup> with a technique quicker than GC-MS. ITMS are generally more sensitive than quadrupole mass spectrometers, especially when broad band wave forms are used to eject all unwanted ions and collect ions over longer ionisation times to provide  $\text{pg l}^{-1}$  limits of detection<sup>64</sup>. Also the application of jet separators as a method of secondary enrichment for removal of sample matrix compounds and helium from the acceptor phase provides limits of detection<sup>65,66</sup> in the range  $30 \text{ ng l}^{-1}$  to  $\mu\text{g l}^{-1}$ . Bauer has published a report<sup>63</sup> on the application of DIP-MIMS-ITMS for the analysis of 59 VOCs present at  $\text{ng ml}^{-1}$  concentrations and listed in the Environmental Protection Agency (USA) method 524.2. Untreated river and seawater containing strong acids and bases had no effect on response. The paper shows a higher speed and similar if not better sensitivity than can be achieved with GC-MS.

Compounds can also be analysed with a DIP and a less selective microporous membrane. These membranes allow the transport of sufficient concentrations of water<sup>67</sup> or organic matrix solvents<sup>68</sup> to the acceptor phase to use as a reagent gas for chemical ionisation. The technique can be used for monitoring polar organic compounds with detection limits one order of magnitude (sub  $\mu\text{g ml}^{-1}$ ) lower than is achievable with a DIP composed of a silicone membrane<sup>67</sup>.

Improvements in the selectivity of the separation have been sought in recent studies. Affinity MIMS<sup>69</sup> uses chemically modified cellulose membranes to very selectively absorb analytes with particular functional groups and subsequently desorb these analytes for analysis after enrichment with a jet separator. Xu et al.<sup>68</sup> have exhibited detection at low  $\mu\text{g l}^{-1}$  concentrations for benzaldehydes absorbed by the formation imine complexes<sup>69</sup>. Alternatively electric fields have been used to stimulate ion emission through highly perforated membranes from a liquid phase into a time of flight mass analyser<sup>70</sup>. Higher mass compounds, such as nicotinic acid, can be transported through membranes for analysis than was previously achievable.

In this chapter a comparison of the applicability to on-line process monitoring of nonporous silicone rubber and porous propylene membranes is to be performed

## **6.2 Experimental**

### **6.2.1 Reagents**

Standard solutions were prepared in 100 ml volumetric flasks on a volume to volume (v/v) basis. AR Grade acetone (Fisons Scientific Equipment, Loughborough, Leicestershire, UK) and methyl iodide (Aldrich, Gillingham, Dorset, UK) were dissolved, respectively, in doubly deionised water (Elgastat,  $18 \text{ M}\Omega \text{ cm}^{-1}$ ) and acetic acid (99.9 % purity, BP Chemicals, Hull, East Yorkshire, UK). Standard solutions of concentration  $10 \text{ mg ml}^{-1}$  or greater were prepared by dissolving the analyte directly in the solvent. Serial dilution was employed for the preparation of standards of concentration less than  $10 \text{ mg ml}^{-1}$ .

### **6.2.2 Instrumentation and Procedures**

A VG Gas Analysis Systems SX200 mass spectrometer (Middlewich, Cheshire, UK) was employed while performing the work described in this chapter. The instrument and its optimised operating parameters were described in Chapter 2.

#### **6.2.2.1 The Membrane Flow Cell**

The membrane flow cell used (Figure 6.3) consisted of three inlet pipes A, B and C (length = 50 mm, i.d. = 3 mm, o.d. = 5 mm) perpendicularly connected to a hollow glass

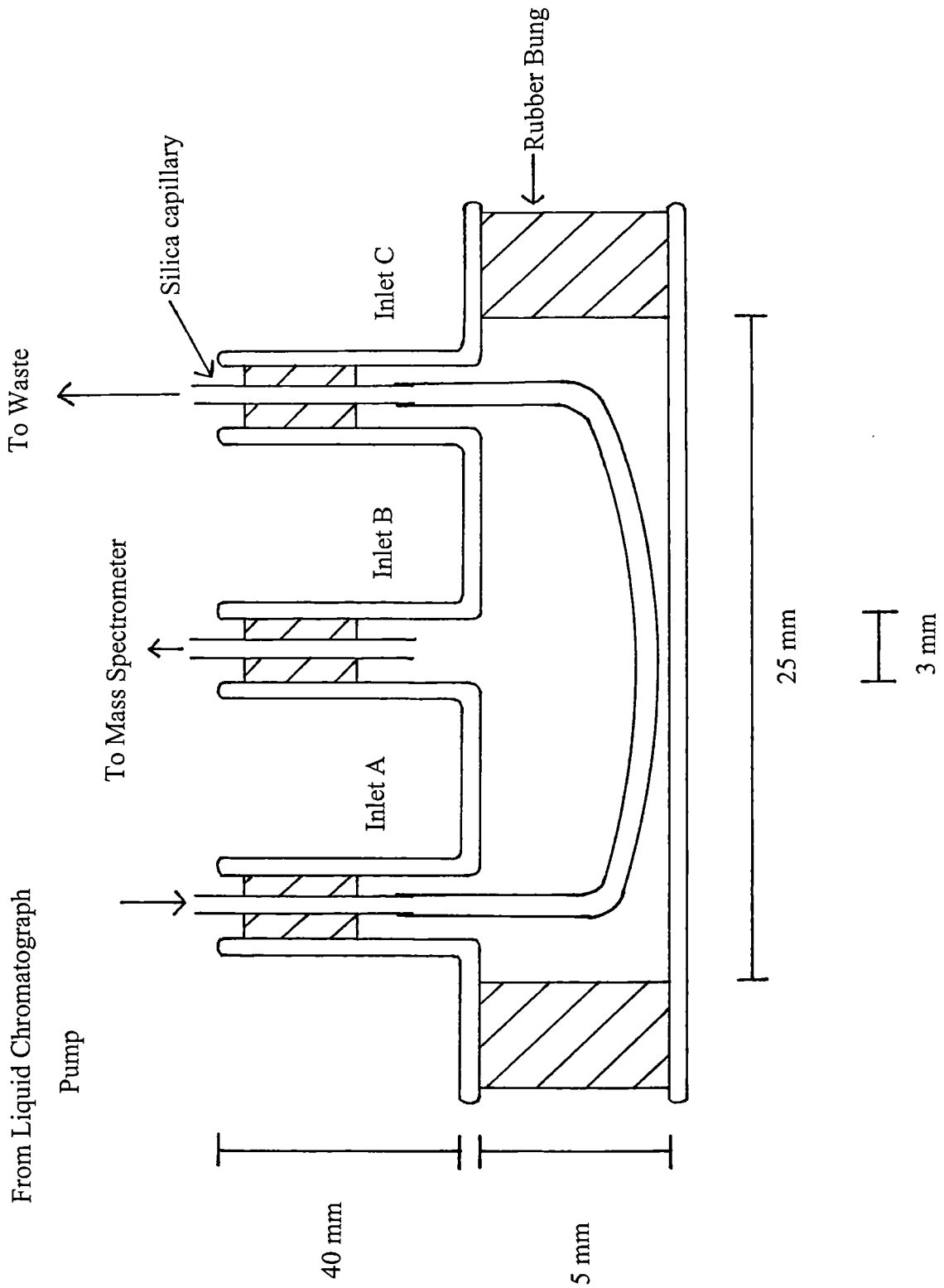


**Figure 6.3** The flow-through hollow fibre membrane flow cell

tube (length = 30 mm, i.d. = 5 mm, o.d. = 8 mm) which to allow easy access for membrane installation was not sealed with glass at each end. All three inlet pipes and the two ends of the glass tube were sealed after membrane installation with rubber bungs (length = 10 mm, o.d. = 6 or 4 mm) to provide a water tight seal and to enclose a volume of 0.81 ml.

The hollow fibre membranes (length = 80 mm) used were connected tightly onto two fused silica capillaries (length = 20 mm, i.d. = 0.3 mm, o.d. = 0.6 mm) inserted through the rubber bungs present in glass inlets A and C. The membranes were soaked in pentane for five minutes before they were inserted into the flow cell. Standard solutions were pumped through the hollow fibre membranes with a liquid chromatography pump (Kontron Instruments, Watford, Hertfordshire, UK) to waste. Compounds present in the standard solutions diffuse through the membrane into the enclosed gas phase. A fused silica capillary (length = 20 mm, i.d. = 0.3 mm, o.d. = 0.6 mm) placed in the bung present in glass inlet B was connected to the mass spectrometer's heated capillary inlet and allowed the gas phase to be continuously sampled into the mass spectrometer.

The temperature of the standard solutions was increased by passing the solutions through a glass coil (length = 90 mm, i.d. = 3 mm, o.d. = 5 mm) heated in a water bath. The water bath was constructed of a hollow metal block filled with water and heated by a Lab-line Multi-blok heater (Melrose Park, Illinois, USA). The measured water bath temperatures were equal to the temperature of the liquid stream. The membrane flow cell was also immersed in the water bath when elevated temperatures were used to ensure the permeate present in the gas acceptor phase did not condense in the membrane flow cell.

Two membranes were employed during the work; nonporous silicone rubber (Silastic, Dow Corning, MI, USA; o.d. = 0.64 mm, i.d. = 0.31 mm) and microporous polypropylene (Microdyn, Wuppertal, Germany; 0.2  $\mu\text{m}$  pore size, o.d. = 0.8 mm, i.d. = 0.4 mm).

In this chapter the application of silicone rubber and polypropylene membranes for MIMS applications concerned with monitoring liquid process streams is investigated. Silicone rubber membranes were chosen because of their selectivity for nonpolar volatile organic compounds with respect to polar compounds. Microporous polypropylene membranes were chosen to act as a barrier between the liquid and gas phases but allow the majority of compounds present in the liquid phase to permeate with a sufficient flux to allow detection by the mass spectrometer.

Two process streams are simulated to aid the investigation; acetone (analyte) in water and methyl iodide (analyte) in acetic acid. The effect of the liquid flow rate and liquid temperature were investigated, the rise and fall times were determined and calibration data were also collected with both membranes for the analytes acetone and methyl iodide. All of the responses are calculated as the mean peak height change measured for six replicate analyses. The peak height change was measured in the period of standard solution infusion through the membrane (measurement time) and represented the change between the baseline and steady state responses. The steady state is represented by a constant response over a period of time.

## 6.3 Results and Discussion

### 6.3.1 The Determination of Acetone Present in Water Streams

#### 6.3.1.1 The Effect of the Liquid Flow Rate

The relationship between the response and flow rate of liquid passing through the silicone and polypropylene hollow fibre membranes was investigated using  $1000 \mu\text{g ml}^{-1}$  acetone standards flowed through the membrane for five minutes. The response was measured as the mean peak height change over the five minute infusion period for six replicate analyses. The temperature of the stream was  $23^{\circ}\text{C}$ .

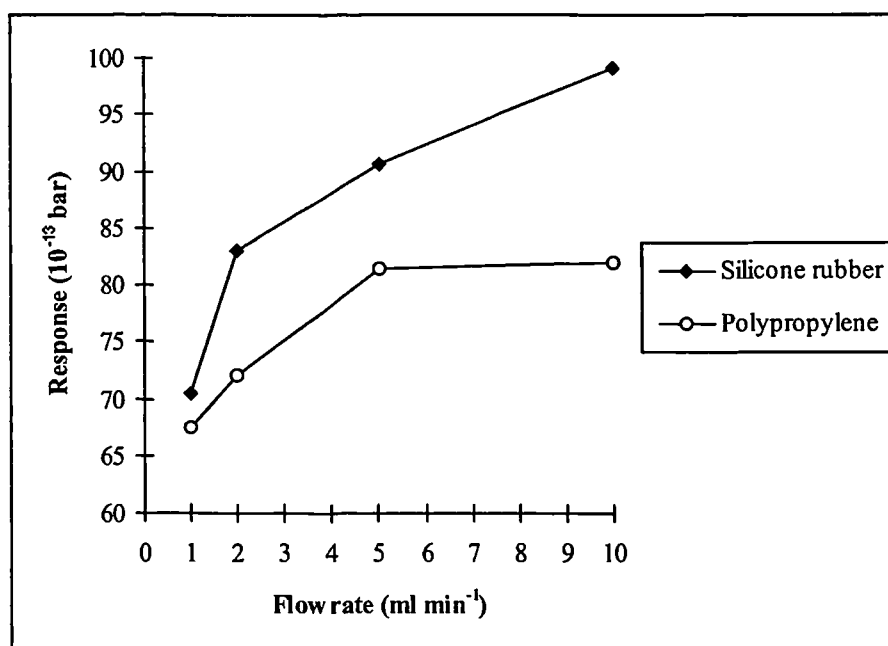


**Figure 6.4** The effect of the liquid flow rate on the response for acetone

The response increases as the stream flow rate increases (Figure 6.4). The increase, however, is small for the range of flow rates investigated, 39 % and 19 % for the silicone rubber and polypropylene membranes, respectively.

As previously reported<sup>16</sup> for different samples the results show that the rate limiting stage affecting the pervaporation process is the diffusion of acetone in the water matrix to the membrane surface, which proceeds more slowly than the diffusion of acetone through the two membranes. If the rate of acetone diffusion through the water matrix was higher than the rate of diffusion through the membrane the flow rate would have no influence on the response measured. A depletion layer forms at the liquid phase - membrane interface because of the inadequate replenishment of acetone in the region close to the membrane surface in contact with the liquid phase. This is caused by the slower diffusion of acetone to the membrane surface with respect to the rate of acetone diffusion through the membrane. As the flow rate is increased turbulence in the hollow fibre membranes also increases and the width of the depletion layer is reduced<sup>15</sup>. This allows faster replenishment of acetone in the region close to the membrane surface and therefore a faster acetone diffusion (and a higher acetone flux) through the membrane, which is represented by the larger responses measured at higher flow rates.

No significant depletion layer is formed for analytes which have high rates of diffusion in the liquid stream<sup>16</sup>. For example, the flow rate affects the response for aqueous benzene solutions where diffusion of benzene through water is slow, but the flow rate does not affect the response for aqueous ethanol solutions where diffusion is rapid. Therefore the diffusion rate of acetone through a liquid aqueous matrix is small enough to affect the response for different liquid flow rates.

A flow rate of  $5 \text{ ml min}^{-1}$  was used in future experiments to provide a relatively high sensitivity without using a large volume of reagents.

### 6.3.1.2 The Effect of the Stream Temperature

The response was measured over a range of stream temperatures with  $1000 \mu\text{g ml}^{-1}$  acetone standards flowing at a rate of  $5 \text{ ml min}^{-1}$ . The standard solutions were passed through the membrane for five minutes and the response was measured as the mean peak height change in the five minute infusion period for six replicate analyses. Microdyn report a maximum operating temperature of  $60^\circ\text{C}$  for polypropylene<sup>71</sup> and therefore the highest temperature employed was  $60^\circ\text{C}$ . Figure 6.5 shows the increase in response as the temperature is increased.

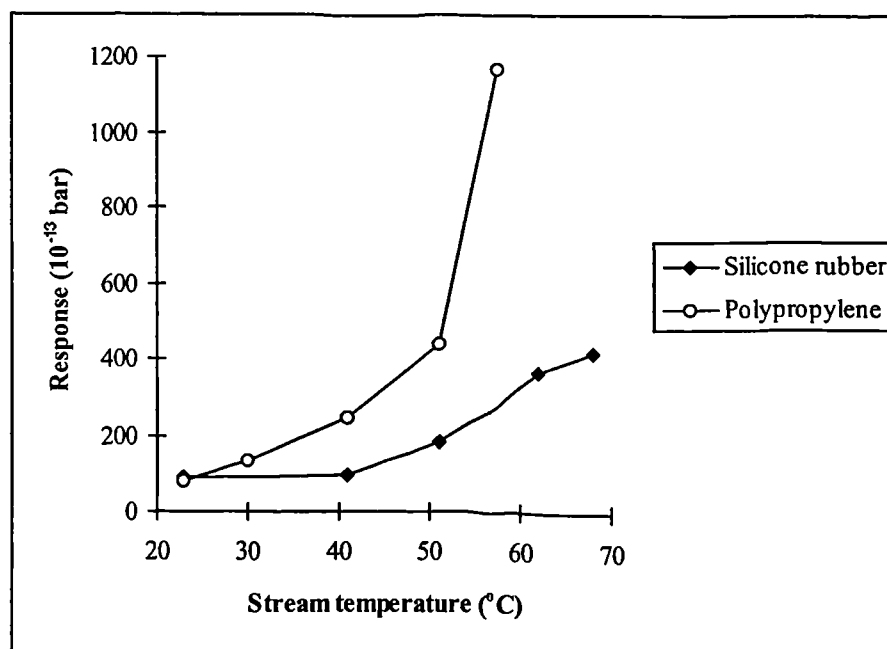


**Figure 6.5** The effect of the stream temperature on the response for acetone

The flux of acetone through the silicone rubber and polypropylene membranes is dependant on the temperature of the liquid stream. At higher temperatures the partition coefficients of acetone between the liquid phase and the interphase transport medium (membrane material for silicone rubber membranes and air for polypropylene membranes) and the diffusion coefficient of acetone through the interphase transport medium are larger<sup>9</sup>. The flux of acetone through the membrane is directly proportional to the partition coefficient and diffusion coefficient and therefore it can be expected that an increase in the stream temperature would provide an increase in the response. Elevated temperatures may also reduce the dimensions of the depletion layer by increasing the turbulence in the hollow fibre membranes. This would result in the greater transport of acetone to the membrane surface and a higher analyte flux to the acceptor phase.

The increase in the response for the range of temperatures investigated is greater for polypropylene membranes and is most likely caused by the exponential increase in the partition coefficient of acetone between water and air matrices as the temperature is increased. The partition coefficient for acetone between the aqueous and silicone rubber matrices is expected to be much smaller. The higher responses observed with the polypropylene membrane demonstrate a larger flux of acetone passing through the membrane.

Stream temperatures of 70 and 60°C were employed in future work using the silicone rubber and polypropylene membranes, respectively. At temperatures greater than 70°C gas bubbles form in the liquid stream and this can affect the measured response<sup>19</sup>.

### 6.3.1.3 Determination of the Rise and Fall Times

The rise and fall times were discussed in Chapter five and represent the time required for the peak height (or response) to change from 10 to 90 % and 90 to 10 %, respectively, of the steady state peak height (or response). The steady state is represented by a peak height which remains constant over a period of time. The rise and fall times represent the time required for changes in the liquid stream concentration to be measured by the mass spectrometer.

The response curves for acetone were plotted by pumping  $1000 \mu\text{g ml}^{-1}$  standards through silicone rubber and polypropylene hollow fibre membranes six times at  $5 \text{ ml min}^{-1}$  from time 1 to 11 minutes. At all other times a solution of water was pumped through the membranes. The response curves for silicone rubber (Figure 6.6) and polypropylene (Figure 6.7) membranes were plotted at stream temperatures of 67 and 59°C, respectively.

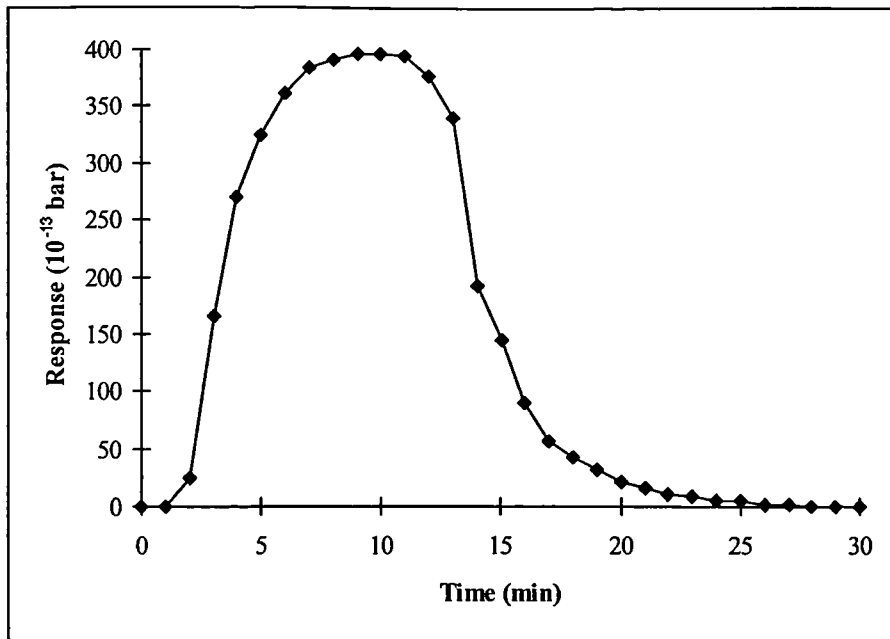


**Figure 6.6** The response curve for acetone using a silicone rubber membrane

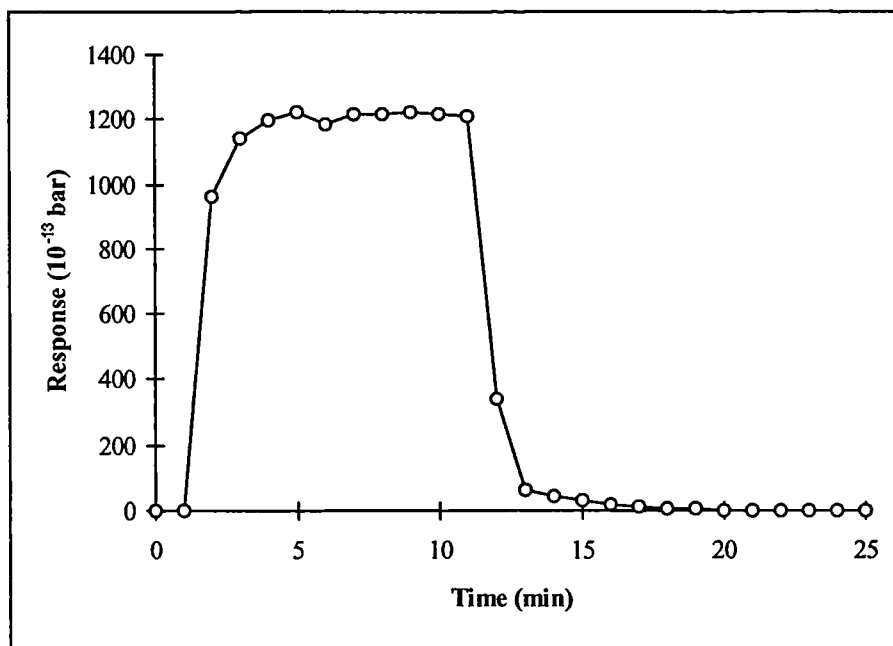


**Figure 6.7** The response curve for acetone using a polypropylene membrane

The constant response observed with both response curves displays a steady state condition at which the acetone concentration in the gas acceptor phase remains constant over time. At steady state conditions the rate of transfer of acetone through the membrane to the acceptor phase is equivalent to the rate of transfer of acetone to the mass spectrometer.

Membrane	Rise time (min)	Fall time (min)	Time for steady state response to be achieved (min)
Silicone rubber	4	6	9
Polypropylene	2	2	4

**Table 6.2** The rise and fall times for acetone using silicone rubber and polypropylene membranes

The rise and fall times (Table 6.2) are shorter for the polypropylene membrane than for the silicone rubber membrane. A very rapid change in the response is observed during the first minute of the standard solution infusion through the polypropylene hollow fibre membrane. The dissimilar transport mechanisms of each membrane accounts for these differences. Diffusion of molecules through gas filled pores (polypropylene membrane) has a lower resistance than diffusion through a membrane material with a greater molecular density (silicone rubber membrane). Therefore faster rates of acetone diffusion can be obtained through a microporous polypropylene membrane and the steady state concentration of acetone in the acceptor phase can be achieved more quickly. Also the release of residual acetone from the membrane when the stream composition is changed to water will be more rapid when it occurs by gas diffusion rather than by diffusion

through a membrane material. Therefore the fall time for the polypropylene membrane is also smaller.

#### 6.3.1.4 Calibration

Calibration data was collected for acetone using the electron multiplier detector. Stream temperatures of 70 and 59°C were used for the silicone rubber and polypropylene membranes, respectively, and a flow rate of 5 ml min<sup>-1</sup> was employed. Standard solutions were pumped through the silicone rubber and polypropylene membranes for 4 and 2 minutes, respectively, and the response was measured as the mean change in the peak height over this time period for six replicate analyses.

Calibration graphs of response (10<sup>-13</sup> bar) vs. acetone concentration in the liquid phase (µg ml<sup>-1</sup>) were plotted using the calibration data collected for both membrane materials. The linear ranges of calibration, equations of the calibration lines, correlation coefficients and limits of detection (3σ) were all determined using the method of least squares<sup>72</sup>. The method of least squares was described in Chapter three (section 3.4.6). The parameters y and x quoted in the equation of the calibration lines represent the response measured and analyte concentration, respectively. Tables 6.3 and 6.4 show the calibration data collected for silicone rubber and polypropylene membranes, respectively.

[Acetone] ( $\mu\text{g ml}^{-1}$ )	Response ( $10^{-13}$ bar)	RSD (n=6) (%)
0	0.0	10.8
10	2.07	13.2
50	13.0	3.1
100	28.4	4.2

Equation of calibration line  $y = 0.29x - 0.56$

Correlation coefficient = 0.9990 (n=4)

Limit of detection =  $3 \mu\text{g ml}^{-1}$

**Table 6.3** Calibration data for acetone using the silicone rubber membrane

[Acetone] ( $\mu\text{g ml}^{-1}$ )	Response (10-13 bar)	RSD (n=6) (%)
0	0.0	8.3
5	0.93	35.0
10	2.85	9.0
50	15.9	13.2
100	32.2	9.6

Equation of calibration line  $y = 0.33x - 0.36$

Correlation coefficient = 0.9998 (n=5)

Limit of detection =  $2 \mu\text{g ml}^{-1}$

**Table 6.4** Calibration data for acetone using a polypropylene membrane

Calibration ranges extending over two decades of concentration were observed for both membranes. Larger calibration ranges have been observed with a mass spectrometer in Chapters three, four and five. It is most probable that the flux of water through both membranes provides a sufficient concentration of water in the ion source to affect the rate of ionisation of acetone at concentrations of acetone greater than  $100 \mu\text{g ml}^{-1}$  with respect to smaller concentrations. The rate of ionisation increases at concentrations greater than  $100 \mu\text{g ml}^{-1}$  and provides a non-linear calibration range at these concentrations. Linearity over the calibration ranges, however, was good ( $r \geq 0.9990$ ,  $n = 4$  [silicone rubber] and  $n = 5$  [polypropylene]).

Limits of detection (LODs) of  $3$  and  $2 \mu\text{g ml}^{-1}$  were achieved and show that a similar concentration of acetone in the gas phase was measured with both of the membranes investigated. Polypropylene membranes provide a larger flux of acetone than silicone rubber membranes, but the latter provide a greater degree of enrichment of acetone in the gas acceptor phase with respect to water. Even though the separate transmembrane transport mechanisms are different and provide different acetone fluxes they provide a similar relative concentration of acetone in the gas acceptor phase. The LODs are higher than those achieved with the dynamic headspace techniques ( $\text{LOD} < 1 \mu\text{g ml}^{-1}$ ). If adequate precision in this thesis is defined as a relative standard deviation (RSD) for replicate results of less than 10 %, inadequate precision was observed over part or all of the calibration ranges. This was caused by the relatively small responses being measured.

### 6.3.2 The Determination of Methyl Iodide Present in Acetic Acid Streams

Initial experiments using a microporous polypropylene membrane and a flowing stream of acetic acid were unsuccessful. The liquid matrix rapidly leaked through the microporous membrane when infused through the flow cell. This shows the inability of microporous polypropylene membranes to stop acetic acid streams flowing into the gas filled pores. Therefore the pressure of the gas phase required to maintain no leakage of acetic acid is too low. No leakage was observed with a water stream and the ability of the acetic acid to leak through the membrane is most likely caused by the differences in the surface tensions<sup>73</sup> at 20°C of acetic acid ( $27.8 \times 10^{-3} \text{ N m}^{-1}$ ) with respect to water ( $73.1 \times 10^{-3} \text{ N m}^{-1}$ ).

In further experiments only a silicone rubber membrane was used to investigate the determination of methyl iodide in acetic acid using the MIMS technique. These membranes showed physical and chemical stability when acetic acid streams were infused through them for long periods of time (4 weeks).

#### 6.3.2.1 The Effect of the Stream Flow Rate

The influence of the stream flow rate on the response was measured for  $1000 \mu\text{g ml}^{-1}$  methyl iodide standards flowed through the membrane for five minutes. The temperature of the liquid stream was 23°C. The response was measured as the mean peak height change observed during the five minute infusion period for six replicate analyses. Figure 6.8 shows the decrease in the response as the flow rate is increased.

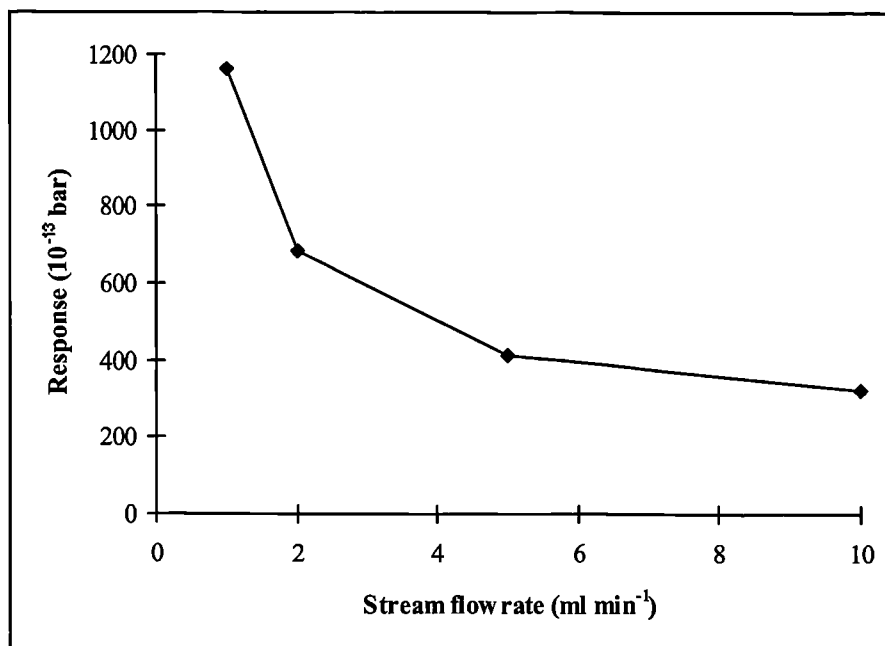


**Figure 6.8** The effect of the stream flow rate on the methyl iodide response

Low flow rates provide the largest responses and therefore the highest rates of methyl iodide diffusion through the membrane to the acceptor gas phase. The change in response as the flow rate is increased shows, as previously discussed<sup>16</sup>, that the diffusion of methyl iodide to the membrane surface in the acetic acid stream is the rate limiting step in the pervaporation process, and the rate of diffusion of methyl iodide in the acetic acid matrix is slower than the rate of diffusion in the silicone rubber membrane. This explanation is surprising because it would be expected that diffusion would be greater through a liquid matrix compared to a solid matrix. However, if the rate of diffusion to the membrane surface in the acetic acid stream was higher than the rate of diffusion in the silicone rubber membrane no change in the response would be observed for the range of flow rates investigated<sup>16</sup>.

The application of low flow rates provides the greatest responses, therefore the residence time of the sample in the hollow fibre membrane is important. Wider depletion layers form at the lower flow rates<sup>9</sup> and the effect of the wider depletion layer means that molecules require more time to diffuse to the membrane surface. Therefore low flow rates provide a greater response because of longer residence times and the higher probability of methyl iodide diffusing through the acetic acid matrix to the membrane surface.

A different relationship between response and flow rate through the silicone rubber hollow fibre membrane is measured for acetone and methyl iodide standards. The diffusion coefficients of small organic molecules do not vary considerably in water and acetic acid matrices and therefore the diffusion of analyte molecules through the liquid phase can not explain the different relationships measured. The difference in the relationship is currently not accounted for.

A flow rate of  $1 \text{ ml min}^{-1}$  was employed in future calibration data collection to provide a relatively high sensitivity.

#### 6.3.2.2 The Effect of the Stream Temperature

The response was measured over a range of stream temperatures with a  $1000 \text{ } \mu\text{g ml}^{-1}$  methyl iodide standard and a flow rate of  $5 \text{ ml min}^{-1}$ . The standard solution was pumped through the membrane for five minutes and the response was measured as the mean peak height change over the five minute period for six replicate analyses.

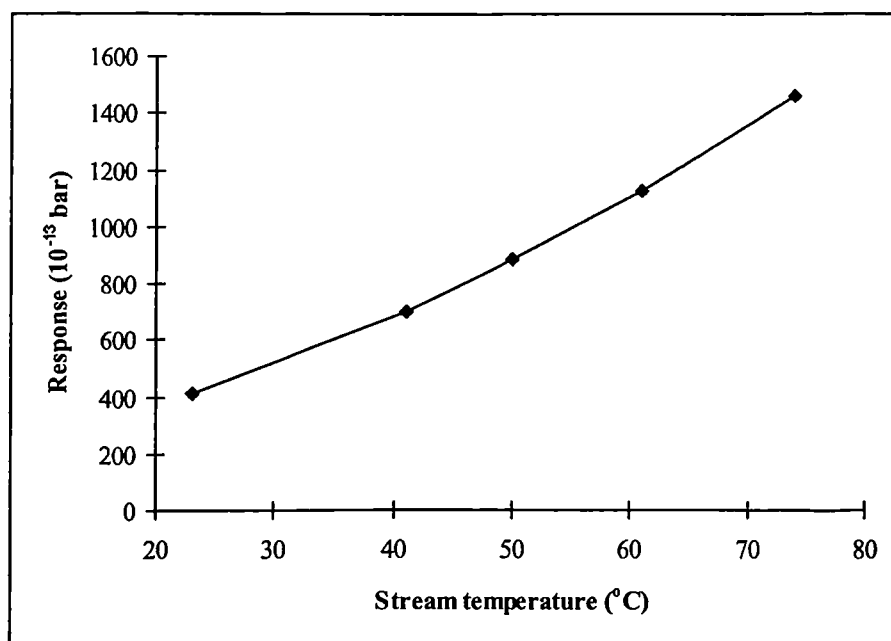


**Figure 6.9** The effect of the stream temperature on the response for methyl iodide

The response increases as the stream temperature increases (Figure 6.9) and shows a similar relationship to that observed for the analysis of acetone standards (section 6.3.1.2). The flux of methyl iodide through the membrane increases as the temperature increases because the partition coefficient of methyl iodide between the acetic acid stream and membrane material and / or the diffusion coefficient of methyl iodide through the silicone rubber membrane increases. This was explained in section 6.3.1.2. A stream temperature of 70°C was employed during future experiments. At higher temperatures gas bubbles form in the acetic acid stream.

### 6.3.2.3 Determination of the Rise and Fall Time

A response curve (Figure 6.10) was plotted using the response measured for a  $1000 \mu\text{g ml}^{-1}$  methyl iodide standard flowing at  $69^\circ\text{C}$ . The standard was pumped through the flow cell at  $1 \text{ ml min}^{-1}$  from time 1 to 16 minutes. A stream of pure acetic acid was pumped through the flow cell at all other times.

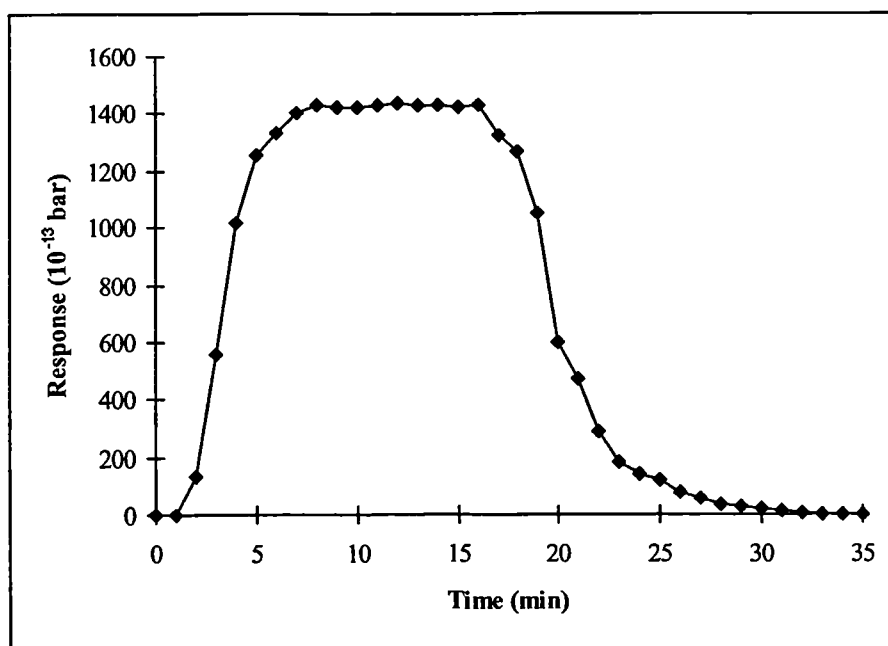


**Figure 6.10** The response curve for methyl iodide using a silicone rubber membrane

The rise and fall times for the measurement of methyl iodide with a silicone rubber membrane were determined as 4 and 6 minutes, respectively. These are the same as was determined for the permeation of acetone through the same membrane material from an aqueous matrix. Therefore the time required for the steady state concentration to be achieved in the gas acceptor phase is the same for both samples with the silicone rubber

membrane. It must be remembered that flow rates of 5 and 1 ml min<sup>-1</sup> were employed for the acetone and methyl iodide samples, respectively, and therefore the analyte was transported to the flow cell and to the membrane surfaces at different rates. It can not be deduced that the fluxes of acetone and methyl iodide through the membrane are equal because the steady state responses are different for the two analytes and therefore the steady state concentrations are different. The steady state response can be expected to be greater for methyl iodide than for acetone because of the greater flux of the more volatile and less polar methyl iodide through the silicone rubber membrane with respect to the acetone.

#### 6.3.2.4 Calibration

Calibration data were collected for methyl iodide using the electron multiplier detector. A stream temperature of 70°C was used for the silicone rubber membrane and a flow rate of 1 ml min<sup>-1</sup> was employed. Standard solutions were pumped through the silicone rubber membrane for 4 minutes and the response was measured as the mean change in the peak height over this time period for six replicate analyses.

Calibration graphs of response (10<sup>-13</sup> bar) vs. methyl iodide concentration in the liquid phase (μg ml<sup>-1</sup>) were plotted using the calibration data collected for the silicone rubber membrane. The linear calibration range, equation of the calibration line, correlation coefficient and limit of detection (3σ) were all determined using the method of least squares<sup>72</sup>. The method of least squares was described in Chapter three (section 3.4.6). Table 6.5 shows the calibration data collected for silicone rubber membranes.

[Methyl iodide] ( $\mu\text{g ml}^{-1}$ )	Response ( $10^{-13}$ bar)	RSD (n=6) (%)
0	0.0	5.4
1	2.05	7.4
5	31.0	6.3
10	54.9	4.4
50	275	5.1
100	555	0.8

Equation of calibration line  $y = 5.55x - 0.48$

Correlation coefficient = 0.9999 (n=6)

Limit of detection =  $0.4 \mu\text{g ml}^{-1}$

**Table 6.5** Calibration data for methyl iodide using the silicone rubber membrane

A lower limit of detection ( $0.4 \mu\text{g ml}^{-1}$ ) was calculated when using methyl iodide standards than was achieved for acetone standards ( $2.0 \mu\text{g ml}^{-1}$ ) with a silicone rubber membrane. The flux of methyl iodide through the membrane under the conditions employed provides a higher concentration of methyl iodide in the gas acceptor phase at steady state conditions when compared with acetone. This was expected because methyl iodide is less polar and more volatile than acetone, and silicone rubber exhibits greater selectivity for nonpolar volatile organic compounds.

The presence of a high enough concentration of acetic acid in the ion source, caused by a relatively high flux through the membrane, affects the ionisation efficiency for methyl iodide at concentrations greater than  $100 \mu\text{g ml}^{-1}$ , as was described for water matrices in section 6.3.1.4. Excellent linearity ( $r = 0.9999$ ,  $n = 6$ ) is shown for the linear

calibration range 0 - 100  $\mu\text{g ml}^{-1}$ . An adequate precision is defined as a RSD value of less than 10 % for replicate analyses. The precision for six replicate analyses is adequate [RSD (n=6) < 8 %] over the calibration range even though small responses are being measured at concentrations of 10  $\mu\text{g ml}^{-1}$  and less.

### 6.3.3 The Relative Concentration of Water and Acetic Acid in the Acceptor Gas

#### Phase

The relative concentrations of water and acetic acid present in the acceptor phase at steady state conditions was determined using the same experimental conditions employed for the collection of acetone (section 6.3.1.4) and methyl iodide (section 6.3.2.4) calibration data. Relative concentrations are determined because the mass spectrometer sensitivities for each compound are different. The results are shown in Table 6.6.

Membrane material	Matrix component	Temperature ( $^{\circ}\text{C}$ )	Response ( $10^{-13}$ bar)
Silicone rubber	water	22	114
		70	138
Silicone rubber	acetic acid	22	100
		70	208
Polypropylene	water	20	179
		59	259

**Table 6.6** The relative concentrations of water and acetic acid in the acceptor phase for silicone rubber and polypropylene membranes at different operating conditions

The relative concentration of water in the gas acceptor phase increases as the temperature increases with the silicone rubber and polypropylene membranes. The polypropylene membrane allows a greater flux of water to be transported to the gas phase when compared with the silicone rubber membrane. The relative concentration of acetic acid in the gas phase also increases as the temperature is elevated when silicone rubber membranes are used. The same explanation as was given in section 6.3.1.2 can be applied here. The partition coefficient of a compound between the liquid phase and transport medium and the diffusion coefficient in the transport medium increase as the temperature is increased. Therefore larger fluxes should be observed at elevated temperatures resulting in the higher concentrations of water and acetic acid in the gas acceptor phase. However the relative concentrations are smaller than was observed with the dynamic headspace technique, with one exception. When acetic acid streams are analysed with the dynamic headspace technique at a temperature of 24°C the relative concentration (76.5) is smaller than was observed with the use of polypropylene membranes at a temperature of 59°C. Generally, though, membranes do limit the transfer of matrix species to the gas phase more than do the dynamic headspace techniques.

#### 6.3.4 The Quantification of Acetone in a Process Sample

The applicability of the membrane introduction mass spectrometry (MIMS) technique for the analysis of complex process samples composed of several different compounds was investigated using a process sample obtained from BP Chemicals in Hull. The composition of the analysed process sample one is described in Chapter three (section

3.3.4). The presence of acetic acid in the process sample did not allow the use of a polypropylene membrane in the investigation.

#### 6.3.4.1 The Effect of the Concentration of Acetic Acid in the Sample Matrix

It has been shown for the total vaporisation (Chapter three) and dynamic headspace (Chapter five) techniques that the response for acetone can be affected by the presence of acetic acid in the liquid sample matrix. The relationship between the concentration of acetic acid in the aqueous standard solution and response was investigated using 10.0 % aqueous acetone standards containing 0, 10, 30 or 50 % (v/v) acetic acid. The silicone rubber membrane flow cell was used with a liquid flow rate of 5 ml min<sup>-1</sup> and a stream temperature of 24°C. A Faraday cup detector was employed to detect the ion current representative of acetone at mass 58 Da. The standard solutions were pumped through the flow cell for four minutes. The response was measured as the mean change in the peak height over this time period for six replicate analyses.

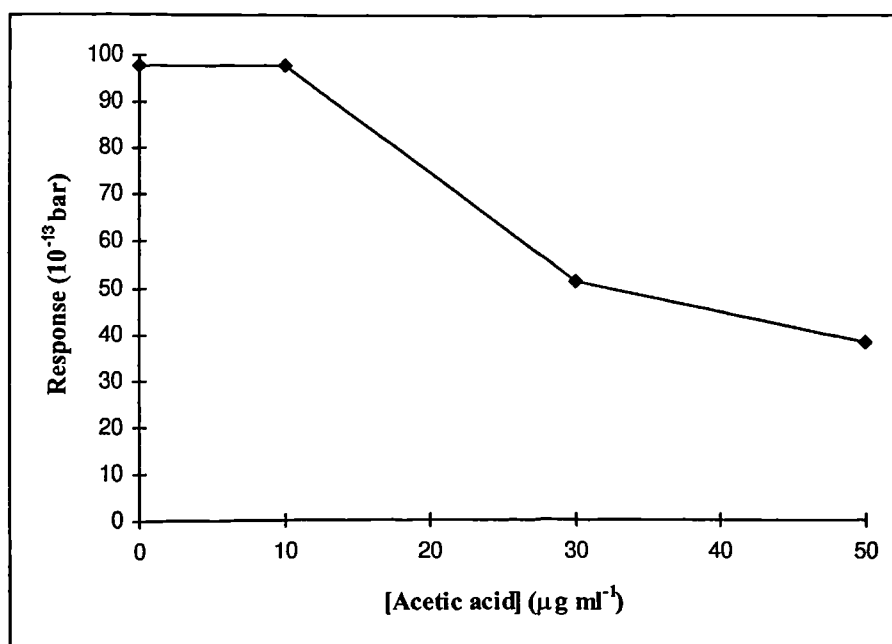


**Figure 6.11** The effect of the concentration of acetic acid on the response using the MIMS technique

The results (Figure 6.11) show that the response is significantly affected at acetic acid concentrations greater than 10 % (v/v). The decrease in the response is most likely caused by the reduction in the flux of acetone through the membrane. A reduction in the flux of acetone through the membrane will result in a lower concentration of acetone in the gas acceptor phase being measured by the mass spectrometer. It has been shown that the acetone flux is dependant on the rate of diffusion of the analyte through the liquid sample matrix to the membrane surface (section 6.3.1.1). The presence of acetic acid at concentrations greater than 10 % therefore reduces the rate of diffusion of acetone through the liquid matrix. The most probable cause of this reduction in response is the partial dissociation of the acetic acid affecting the diffusion of acetone through the liquid

matrix. Stronger interactions or repulsions between acetone molecules and proton and acetate ions present in the stream may reduce the rate of diffusion of acetone molecules.

For the quantification of acetone in process samples which are composed of acetic acid at concentrations greater than 10 %, accurately prepared standards composed of acetic acid and water at the same compositions as in the process sample are required and are used in future investigations.

#### 6.3.4.2 Calibration

Calibration data were collected for acetone using a standard matrix composed of 30 % acetic acid and 70 % water. A stream flow rate of 5 ml min<sup>-1</sup> was employed at a temperature of 24°C. The Faraday cup detector was used to monitor acetone at mass 58 Da and the standard solutions were pumped through the membrane flow cell for four minutes. The response was measured as the mean change in the peak height during the four minute period for six replicate analyses. At all other times water was pumped through the membrane flow cell.

Calibration graphs of response (10<sup>-13</sup> bar) vs. acetone concentration in the liquid phase (µg ml<sup>-1</sup>) were plotted using the calibration data collected with the silicone rubber membrane. The linear ranges of calibration, equation of the calibration line, correlation coefficients and limits of detection (3σ) were all determined using the method of least squares<sup>72</sup> discussed in Chapter three (section 3.4.6) The calibration data collected can be seen in Table 6.7.

[Acetone] ( $\mu\text{g ml}^{-1}$ )	Response ( $10^{-13}$ bar)	RSD (n=6) (%)
0	0.0	10.4
1	7.09	3.5
5	34.3	3.0
10	66.7	2.4
15	104	3.6

Equation of calibration line  $y = 6.87x - 0.16$

Correlation coefficient = 0.9997 (n=5)

Limit of detection = 0.04 %

**Table 6.7** Calibration data for acetone using the silicone rubber membrane and Faraday cup detector

A calibration range of 0 - 15 % was observed with excellent linearity ( $r = 0.9997$ ,  $n = 5$ ), though the calibration range is smaller than is observed with the total vapourisation and dynamic headspace techniques. It is expected that the transport of water through the membrane is sufficient to change the ionisation efficiency observed at concentrations greater than 15 %, with respect to, concentrations of 15 % or less. The limit of detection of 0.04 % is not as low as can be achieved with the more sensitive electron multiplier detector. An adequate precision [RSD (n=6) < 4 %] is achieved over the calibration range.

### 6.3.4.3 Analysis of the Process Sample

As was explained in Chapter three (section 3.6), mass 58 Da is monitored for the quantification of acetone in the process samples analysed because of the contribution of several sample components to the response at mass 43 Da. The response at mass 58 Da is composed of the contribution from acetone, 2-pentanone and 3-hexanone present in the sample. Employing the method described in Chapter three the response for acetone at mass 58 Da can be calculated by monitoring the peak heights at masses 58, 86 and 100 Da and using equation (6.3) :

$$PH^{58} = R^{58}_{(acetone)} + 0.67PH^{86} + 6.17PH^{100} \quad (6.3)$$

where

$PH^a$  = the peak height measured at mass a Da

$R^{58}_{(acetone)}$  = the response at mass 58 Da composed of the peak height for acetone only

The  $R^{58}_{(acetone)}$  value can then be used to calculate the concentration of acetone in process sample one with the calibration graph plotted in section 6.4.3.3. The values of  $0.67PH^{86}$  and  $6.17PH^{100}$  employed in Chapter three are accurate with the membrane flow cell and experimental conditions employed.

Process sample one was analysed with the experimental conditions described in section 6.3.4.2. A Faraday cup detector was used to continuously monitor the peak heights at masses 58, 86 and 100 Da. The process sample was pumped through the

membrane flow cell for 4 minutes and at all other times a water stream was pumped through the flow cell. The peak heights shown in Table 6.8 were measured as the mean peak height for three analyses of process sample one.

Peak height at mass 58 Da ( $10^{-13}$ bar)	Peak height at mass 86 Da ( $10^{-13}$ bar)	Peak height at mass 100 Da ( $10^{-13}$ bar)
66.2	12.5	0.39

**Table 6.8** The peak heights measured for process sample one at masses 58, 86 and 100 Da

The concentration of acetone in the process sample was calculated to be  $8.1 \pm 0.3$  % using equation 6.3 and the calibration data collected in section 6.3.4.2. The actual concentration of acetone calculated using gas chromatography at BP Chemicals in Hull was  $9.4 \pm 0.2$  %. Therefore the MIMS technique employed in this chapter does not provide an accurate determination of process samples composed of many different compounds. The inaccuracy is most likely caused by the variety of compounds in the liquid matrix effecting the rate limiting stage of the pervaporation process, which is the rate of diffusion of acetone to the membrane surface. Alternatively the relatively high concentrations (%) of each compound present may inhibit the diffusion of acetone through the membrane because of compounds other than acetone saturating the membrane and affecting the chemical potential gradient which controls the flux of acetone through the membrane. This is a less probable cause, however. The sample composition changes from one sample to another and therefore the preparation of an

accurate calibration matrix is not possible to obtain a higher accuracy for the acetone concentration.

#### **6.4 Conclusions**

Membrane introduction mass spectrometry shows promise for the monitoring of process streams, even though the current number of reported applications is small. Using silicone rubber and propylene membranes detection limits of  $\mu\text{g ml}^{-1}$  or high  $\mu\text{g l}^{-1}$  are achievable with a simple membrane flow cell which unlike other recently employed flow cells does not require a flow of gas to transport the permeate to the mass spectrometer. Compounds present in chemical process liquid streams at lower concentrations will rarely need to be quantified.

Of the two membranes investigated (silicone rubber and polypropylene) silicone rubber was more applicable. Although polypropylene showed high acetone fluxes it did not provide a better sensitivity than the silicone membrane and could not be used with acetic acid streams. Polypropylene membranes, however, are more sensitive for analysis of highly polar compounds<sup>67</sup> and provide a faster response to changes in the concentration of the analyte in the liquid phase, which may be beneficial in small volume processes where changes can be rapid. The investigations described in this chapter have demonstrated why silicone rubber membranes are currently widely used for the determination of low MW organic compounds.

The application of MIMS to the accurate analysis of process samples containing many compounds present at percent concentrations is not easily achievable. The process

sample analysed in these investigations did not provide an accurate result when compared with a gas chromatographic analysis. The multi-component sample affects either the diffusion rate of acetone to the membrane surface or the chemical potential gradient which controls the flux of acetone through the membrane. Accurately prepared calibration matrices would need to be prepared, however, in many cases the sample matrix composition can change continuously over a considerable range of concentrations for several components. Therefore the accurate preparation of calibration standards is not possible.

## 6.5 References

- 1) Fleming, H.L., and Slater, C.S. in *Membrane Handbook*, Ho, W.S.W, and Sirkar, K.K. (Editors), Van Nostrand Reinhold, New York, 1992, Chapters 7 -10.
- 2) Paul, D.R., and Morel, G., in *Kirk-Othmer Encyclopedia of Chemical Technology*, Wiley, Chichester, 1993, 3rd Edition, Volume 15, p 92.
- 3) Baker, R.W., in *Kirk-Othmer Encyclopedia of Chemical Technology*, Wiley, Chichester, 1995, 4th Edition, Volume 16, p 135.
- 4) Kubà, V., *Critical Reviews in Anal. Chem.*, 1992, **23**, 323.
- 5) Majors, R.E., *LC-GC Int.*, 1995, **8**, 375.
- 6) Bauer, S., *Trends in Anal. Chem.*, 1995, **14**, 202.
- 7) Atkins, P.W., *Physical Chemistry*, Oxford University Press, 1990, 4th Edition, p 768.
- 8) Binning, R.C., and James, F.E., *Petroleum Refiner.*, 1958, **37**, 214.
- 9) LaPack, M.A., Tou, J.C., and Enke, C.G., *Anal. Chem.*, 1990, **62**, 1265.
- 10) Bauer, S.J., and Cooks, R.G., *Spectroscopy*, 1993, **10**, 35.
- 11) Kotiaho, T., Lauritsen, F.R., Choudhury, T.K., Cooks, R.G., and Tsao, G.T., *Anal. Chem.*, 1991, **63**, 875A.
- 12) Patrick, J.S., Wong, P., Xu, C., Soni, M., Kasthurikrishnan, N., Srinivasan, N., and Cooks, R.G., *Proc. Cont. Qual.*, 1995, **7**, 117.
- 13) Bohatka, S., in *Proceedings of the 13th International Mass Spectrometry Conference*, Cornides, I., Horvath, G., and Vekey, K. (Editors), Wiley, Chichester, 1995, p 199.

- 14) Nijhuis, H.H., Mulder, M.H.V., and Smolders, C.A., *J. Membrane Sci.*, 1991, **61**, 99.
- 15) Tsai, G-J, Austin, G.D., Syu, M.J., Tsao, G.T., Hayward, M.J., Kotiaho, T., and Cooks, R.G., *Anal. Chem.*, 1991, **63**, 2460.
- 16) Dongrè, A.R., and Hayward, M.J., *Anal. Chim. Acta*, 1996, **327**, 1.
- 17) Maden, A.J., and Hayward, M.J., *Anal. Chem.*, 1996, **68**, 1805.
- 18) Kasthurikrishnan, N., Cooks, R.G., and Bauer, S., *Rapid Commun. Mass Spectrom.*, 1996, **10**, 751
- 19) Futò, I., and Degn, H., *Anal. Chim. Acta*, 1994, **294**, 177.
- 20) Hoch, G., and Kok, B., *Arch. Biochem. Biophys.*, 1963, **101**, 160.
- 21) Woldring, S., Owens, G., and Woolford, D.C., *Science*, 1966, **153**, 885.
- 22) Roberts, M., Colton, E.T., Owens, G., Thomas, D.D., and Watkins, G.M., *Med. Biol. Eng.*, 1975, **13**, 535.
- 23) Brodbelt, J.S., Cooks, R.G., Tou, J.C., Kallos, G.J., and Dryzga, M.D., *Anal. Chem.*, 1987, **59**, 454.
- 24) Deterding, L.J., Dix, K., Burka, L.T., and Tomer, K.B., *Anal. Chem.*, 1992, **64**, 2636.
- 25) Tou, J.C., Westover, L.B., and Sonnabend, L.F., *J. Phys. Chem.*, 1974, **78**, 1096.
- 26) Calvo, K.C., Weisenberger, C.R., Anderson, L.B., and Klapper, M.H., *Anal. Chem.*, 1981, **53**, 981.
- 27) Mishra, A.K., and Klapper, M.H., *Biochemistry*, 1986, **25**, 7328.
- 28) Kotiaho, T., Lister, A.K., Hayward, M.J., and Cooks, R.G., *Talanta*, 1991, **38**, 195.
- 29) Tou, J.C., and Kallos, G.J., *Anal. Chem.*, 1974, **46**, 1866.

- 30) Degn, H., and Lauritsen, F.R., *J. Phys. Chem.*, 1989, **93**, 2781.
- 31) Tou, J.C., Rulf, D.C., and DeLassus, P.T., *Anal. Chem.*, 1990, **62**, 592.
- 32) Bruckenstein, S., and Gadde, R.R., *J. Am. Chem. Soc.*, 1971, **93**, 793.
- 33) Pinnick, W.J., Lavine, B.K., Weisenberger, C.R., and Anderson, L.B., *Anal. Chem.*, 1980, **52**, 1102.
- 34) Ren, H., Szpylka, J., and Anderson, L.B., *Anal. Chem.*, 1996, **68**, 243.
- 35) Savickas, P.J., LaPack, M.A., and Tou, J.C., *Anal. Chem.*, 1989, **61**, 2332.
- 36) LaPack, M.A., Tou, J.C., and Enke, C.G., *Anal. Chem.*, 1991, **63**, 1631.
- 37) LaPack, M.A., Tou, J.C., Cole, M.J., and Enke, C.G., *Anal. Chem.*, 1996, **68**, 3072.
- 38) Heinzle, E., Furukawa, K., and Dunn, I.J., *International J. Mass Spectrom. Ion Physics*, 1983, **48**, 273.
- 39) Heinzle, E., Kramer, H., and Dunn, I.J., *Biotechnol. Bioeng.*, 1985, **27**, 238.
- 40) Heinzle, E., Moes, J., Griot, M., Kramer, H., Dunn, I.J., and Bourne, J.R., *Anal. Chim. Acta*, 1984, **163**, 219.
- 41) Berecz, I., Bohátka, S., Diós, Z., Gàl, I., Gàl, J., Kiss, L., Kovacs, R.M., Langer, G., Molnàr, J., Paàl, A., Sepsy, K., Szabó, I., and Székely, G., *Vacuum*, 1987, **37**, 85.
- 42) Bohátka, S., Futó, I., Gàl, I., Gàl, J., Langer, G., Molnàr, J., Paàl, A., Pintèr, G., Simon, M., Szàdai, J., Székely, G., and Szilàgyi, J., *Vacuum*, 1993, **44**, 669.
- 43) Ruzicka, J., and Hansen, E.H., *Flow Injection Analysis*, Wiley, Chichester, 1988, 2nd Edition.
- 44) Bier, M.E., and Cooks, R.G., *Anal. Chem.*, 1987, **59**, 597.
- 45) Hayward, M.J., Kotiaho, T., Lister, A.K., Cooks, R.G., Austin, G.D., Narayan, R., and Tsao, G.T., *Anal. Chem.*, 1990, **62**, 1798.

- 46) Hayward, M.J., Riederer, D.E., Kotiaho, T., Cooks, R.G., Austin, G.D., Syu, M-J., and Tsao, G.T., *Proc. Cont. Qual.*, 1991, **1**, 105.
- 47) Austin, G.D., Tsao, G.T., Hayward, M.J., Kotiaho, T., Lister, A.K., and Cooks, R.G., *Proc. Cont. Qual.*, 1991, **1**, 117.
- 48) Hayward, M.J., Lister, A.K., Kotiaho, T., Cooks, R.G., Austin, G.D., Narayan, R., and Tsao, G.T., *Biotech. Techniques.*, 1991, **3**, 361.
- 49) Srinivasan, N., Kasthurikrishnan, N., Cooks, R.G., Krishnan, M.S., and Tsao, G.T., *Anal. Chim. Acta*, 1995, **316**, 269.
- 50) Pungor Jr, E., Pecs, M., Szigeti, L., Nyeste, L., and Szilagyi, J., *Anal. Chim. Acta*, 1984, **163**, 185.
- 51) Weaver, J.C., and Abrams, J.H., *Rev. Sci. Instrum.*, 1979, **50**, 478.
- 52) Westover, L.B., Tou, J.C., and Mark, J.H., *Anal. Chem.*, 1974, **46**, 568.
- 53) Kallos, G.J., and Mahle, N.H., *Anal. Chem.*, 1983, **55**, 813.
- 54) Brodbelt, J.S., and Cooks, R.G., *Anal. Chem.*, 1985, **57**, 1153.
- 55) Kotiaho, T., Hayward, M.J., and Cooks, R.G., *Anal. Chem.*, 1991, **63**, 1794.
- 56) Choudhury, T.K., Kotiaho, T., and Cooks, R.G., *Talanta*, 1992, **39**, 1113.
- 57) Choudhury, T.K., Kotiaho, T., and Cooks, R.G., *Talanta*, 1992, **39**, 573.
- 58) Lauritsen, F.R., and Gylling, S., *Anal. Chem.*, 1995, **67**, 1418.
- 59) Slivon, L.E., Bauer, M.R., Ho, J.S., and Budde, W.L., *Anal. Chem.*, 1991, **63**, 1335.
- 60) Virkki, V.T., Ketola, R.A., Ojala, M., Kotiaho, T., Komppa, V., Grove, A., and Facchetti, S., *Anal. Chem.*, 1995, **67**, 1421.
- 61) Bauer, S.J., and Cooks, R.G., *Talanta*, 1993, **40**, 1031.
- 62) Creaser, C.S., and Stygall, J.W., *Anal. Proc. incl. Anal. Comm.*, 1995, **32**, 7.

- 63) Bauer, S., and Solyom, D., *Anal. Chem.*, 1994, **66**, 4422.
- 64) Soni, M., Bauer, S., Amy, J.W., Wong, P., and Cooks, R.G., *Anal. Chem.*, 1995, **67**,1409.
- 65) Dejarne, L.E., Bauer, S.J., Cooks, R.G., Lauritsen, F.R., Kotiaho, T., and Graf, T., *Rapid Comm. Mass Spectrom.*, 1993, **7**, 935.
- 66) Wong, P.S.H., and Cooks, R.G., *Anal. Chim. Acta*, 1995, **310**, 387.
- 67) Lauritsen, F.R., Choudhury, T.K., Dejarne, L.E., and Cooks, R.G., *Anal. Chim. Acta*, 1992, **266**, 1.
- 68) Lauritsen, F.R., Kotiaho, T., Choudhury, T.K., and Cooks, R.G., *Anal. Chem.*, 1992, **64**, 1205.
- 69) Xu, C., Patrick, J.S., and Cooks, R.G., *Anal. Chem.*, 1995, **67**, 724.
- 70) Yakovlev, B.S., Talrose, V.L., and Fenselau, C., *Anal. Chem.*, 1994, **66**, 1704.
- 71) Polypropylene membrane applications brochure, Microdyn (Germany), 1994.
- 72) Miller, J.C., and Miller, J.N., *Statistics For Analytical Chemistry*, Ellis Horwood London, 1992, 2nd Edition, p 109.
- 73) Lide, D.R. (Editor-in-chief), *Handbook of Chemistry and Physics*, CRC Press, Boston, 72nd Edition, 1991, p 6-118.

## **Preliminary Results**

### **Atmospheric Pressure Ionisation**

## **7.1 Introduction**

Arpino<sup>1</sup> first described the coupling of a liquid chromatograph and a mass spectrometer as an impossible marriage between a fish and a bird. These symbolic creatures represented, respectively, the liquid chromatograph operating at relatively high pressures and the mass spectrometer operating with a gaseous phase at low pressures. To successfully couple the two instruments several problems need to be solved concerned with maintaining the required mass spectrometer vacuum pressures and not introducing non-volatile compounds into the mass spectrometer<sup>2</sup>, which could contaminate the instrument. These problems have been solved by employing a variety of interfaces<sup>2,3,4,5</sup> to either introduce a gas to an electron impact ion source for ionisation (moving belt, particle beam and direct liquid introduction interfaces) or to provide ionisation at higher pressures (atmospheric pressure chemical ionisation, electrospray ionisation, ionspray ionisation and thermospray ionisation).

The direct analysis of liquid process streams with an electron impact ion source mass spectrometer have the same demanding objectives as for the analysis of liquid chromatograph effluents and require the vaporisation of the liquid flow with sufficient energy. This strategy for liquid analysis has been performed in Chapters three to six. However the greatest problem is the requirement of vapour production which produces a volume of vapour that is normally too large to be introduced to the electron impact ion source without increasing the pressure above required levels<sup>2</sup>. Introduction of large volumes of vapour is required, however, to achieve a high sensitivity.

Atmospheric pressure ionisation<sup>2,5,6</sup> (API) alleviates the problem of introducing large volumes of vapour into the mass spectrometer vacuum system, by decoupling the inlet

and ionisation stages from the vacuum stages of the mass spectrometer<sup>6</sup>. Atmospheric pressure chemical ionisation (APCI) and electrospray ionisation (ESI) are performed at atmospheric pressure after a liquid stream has been sprayed into the appropriate ion source. Gas phase ions are formed and transferred to the mass analyser operating at a vacuum pressure for mass separation and detection without the transfer of a large volume of vapour.

In this chapter the direct introduction and ionisation of liquids in an ion source operating at atmospheric pressure will be employed as an alternative to the analysis of liquids with a mass spectrometer constructed with an electron impact ion source.

### 7.1.1 Atmospheric Pressure Ion Sources<sup>2,5,6,7,8,9</sup>

Atmospheric pressure ion sources operate by nebulising a liquid stream into a spray chamber where gas phase ions can be created by different mechanisms and subsequently sampled from the atmospheric pressure region to the mass analyser operating at vacuum pressures. The spraying of liquids from a capillary to form droplets (nebulisation) will be discussed in the sections describing the mechanisms of gas phase ion creation. Ion sampling will be described in this section.

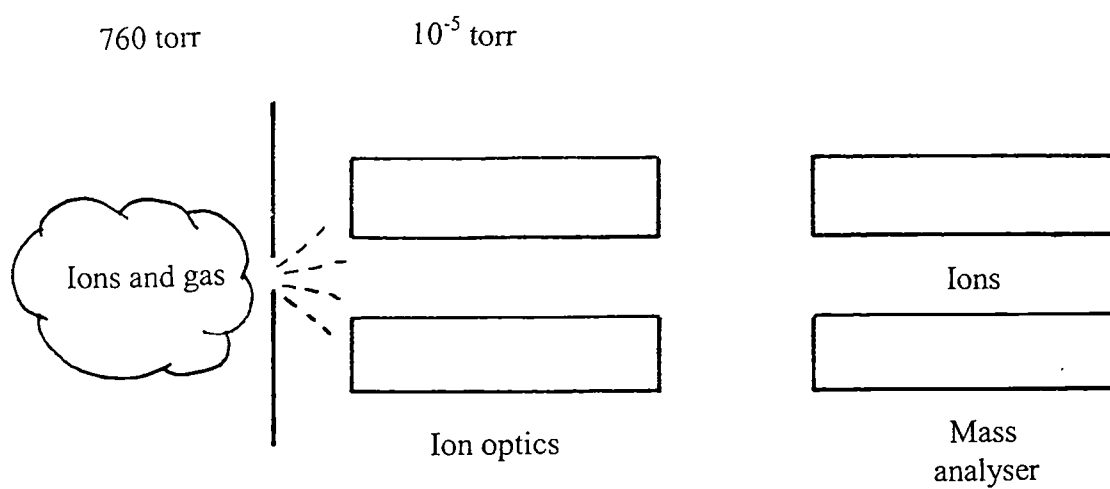
Before Dole<sup>10</sup> and Horning<sup>11</sup> first used ESI and APCI, ions had been sampled from atmospheric pressure flames<sup>12</sup> and corona discharges<sup>13</sup> into a mass spectrometer for mass analysis. More recently the inductively coupled plasma - mass spectrometer (ICP-MS) has been introduced<sup>14</sup> which samples ions from an atmospheric pressure plasma operating at temperatures greater than 6000 K. The efficiency of ion transfer from these atmospheric pressure regions through an ion passageway with a  $10^7$  -  $10^8$  fold pressure

reduction to the mass analyser determines the sensitivity achievable<sup>7</sup>. Two strategies are currently used for the transfer of ions from the atmospheric pressure source; single stage and three stage vacuum systems. Two stage differentially pumped vacuum systems have also been used<sup>8</sup>.

After formation, ions are transferred from the atmospheric pressure ion source to a region of lower pressure through a small diameter orifice positioned in the ion source wall opposite the spraying capillary. The orifice may be a small hole present in a cone tip<sup>14</sup> or in a flat disk<sup>11</sup>. Alternatively a short heated glass tube<sup>15</sup> or metal capillary<sup>16</sup> may be used. In mass spectrometers constructed with a single stage system<sup>11</sup> (Figure 7.1, a) ions are transferred directly into the mass analyser vacuum envelope and the pumping speed used determines the orifice diameter that can be employed<sup>8</sup>. Low pumping speed pumps (oil diffusion pumps,  $1000 \text{ l s}^{-1}$ ) require small diameter orifices to ensure that all of the gas entering the mass analyser region is pumped away to maintain the vacuum. Cryo-pumps have a much higher pumping speed ( $100\ 000 \text{ l s}^{-1}$ ) and therefore a larger orifice can be used and a larger volume of gas can be introduced while the vacuum pressures are maintained. This will normally provide a higher sensitivity because of the larger number of ions that can be transferred through the larger orifice. In the vacuum envelope ion focusing is performed with electric fields (lenses) or a rf-only quadrupole before they are introduced into the mass analyser. Gas molecules are pumped away.

Alternative instruments use a three stage vacuum system<sup>7,8</sup> (Figure 7.1, b) to reduce the pressure in three stages in series. The aim of each stage is to increase the ratio of ions to gas molecules by pumping away gas while sampling ions into the next stage. In stage one the pressure is reduced to approximately 1 torr and the central portion of the

(a)



(b)

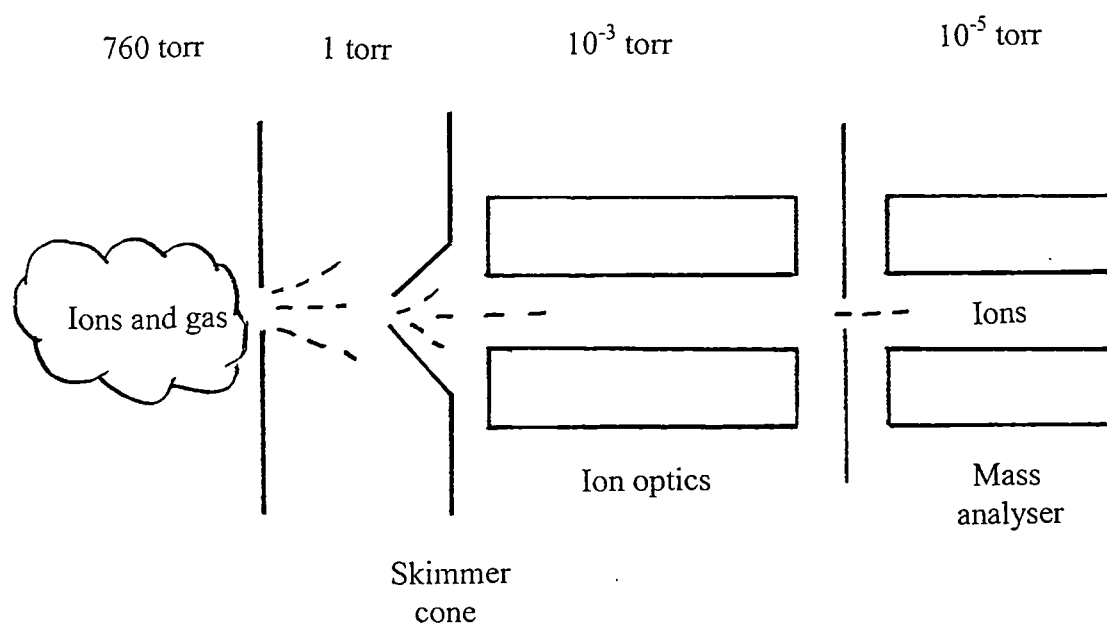


**Figure 7.1** One stage (a) and three stage (b) pumped vacuum systems

expanding jet of gas and ions formed after the passage of gas and ions through a small orifice is efficiently sampled by a cone<sup>17</sup> into a second region of pressure  $10^{-3}$  torr. In this stage ions are focused with lenses or an rf-only quadrupole and introduced through an orifice to the mass analyser operating at  $10^{-5}$  torr in stage three. Gas present in each stage is pumped away.

The transfer of gas and ions through a small orifice from a high to low pressure region produces an expanding supersonic jet which has directional motion along its central axis<sup>17</sup>. Strong adiabatic cooling of gas molecules and ions results in the production of ion-solvent clusters<sup>6,7,8,18</sup>. The clusters are created by the production of weak bonds between ions and polar molecules. The mass spectrum of the analyte molecule is disguised and therefore clustering needs to be prevented or if formed, clusters need to be dissociated. Cluster formation can be prevented by heating the ion source to ensure the temperature of the gas molecules and ions does not reach a level where clustering can proceed<sup>8</sup>. An alternative approach<sup>7,8</sup> uses a perpendicular flow of dry nitrogen gas (curtain gas) across the sampling orifice which will transport neutral molecules and dust away from the orifice back into the ion source while the application of electrical potentials will drive ions into the lower pressure regions of the mass spectrometer.

In some cases ion-solvent clusters are allowed to form in the expanding supersonic jet due to adiabatic cooling. In these cases a potential difference applied between the entrance plates of the first and second stage regions of the mass spectrometer will accelerate ion-solvent clusters. Collisions involving gas molecules and accelerated clusters can result in solvent molecules being stripped from the ion<sup>19</sup>. The process of collision induced dissociation (CID) will strip weakly associated solvent molecules from

ions but will not break stronger covalent bonds unless large potential differences are used. The potential difference employed is called the cone voltage.

#### 7.1.1.1 Atmospheric Pressure Chemical Ionisation

First described<sup>11,20</sup> by Horning et al., APCI sources<sup>2,7,8,9</sup> (Figure 7.2) employ pneumatic nebulisation, of a 0.5 - 2.0 ml min<sup>-1</sup> flow of liquid with a countercurrent flow of nitrogen, and the subsequent vaporisation of the droplets formed in a heated quartz tube. A gaseous mixture of solvent and analyte molecules exit the quartz tube. Chemical ionisation at atmospheric pressure can then proceed using the large excess of solvent molecules present as the reagent gas. A percentage of ions formed in the chemical ionisation (CI) plasma are extracted from the ion source field for mass analysis and detection by an applied electric field.

Chemical ionisation at atmospheric pressure proceeds in two stages:

- 1) ionisation of the reagent gas to create reagent ions, normally associated with solvent molecules,
- 2) analyte ionisation via analyte - reagent ion interaction.

The high pressures used provide short mean free paths of reagent ions and analyte molecules and longer lifetimes of the reagent ions created. Analyte-reagent ion interactions are therefore highly probable and a 10<sup>3</sup> -10<sup>4</sup> fold greater ionisation efficiency is obtained compared with the electron impact ion source<sup>9</sup>. However the extraction of ions to the mass analyser has a low efficiency with respect to the electron impact ion

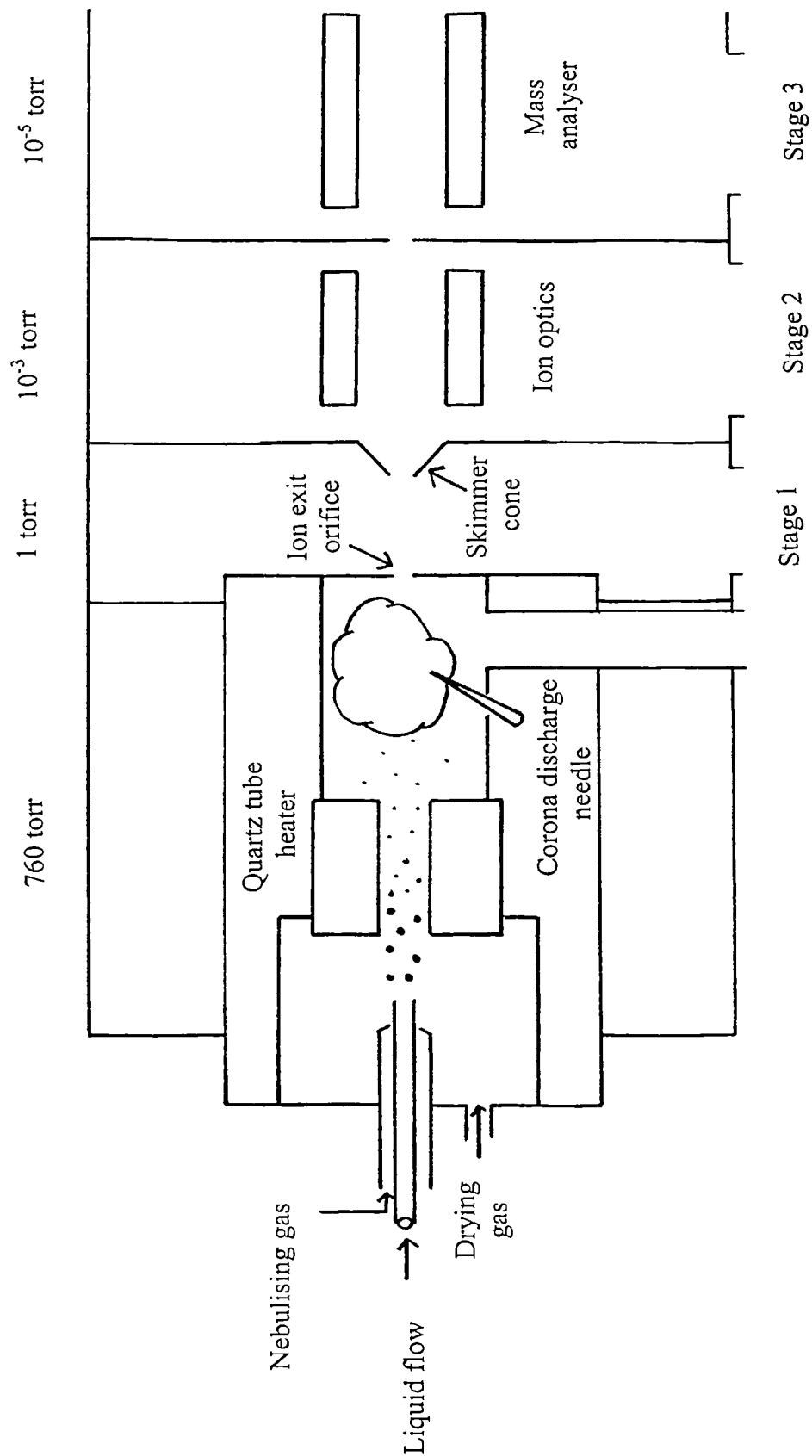
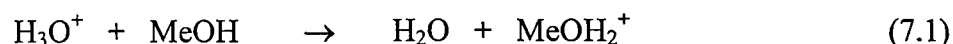


**Figure 7.2** The atmospheric pressure chemical ionisation source

source and therefore the mass spectrometer does not normally provide a  $10^3$  - $10^4$  fold higher degree of sensitivity<sup>6</sup>. Detection limits of  $\text{ng l}^{-1}$  have been achieved with gas phase samples, however<sup>21</sup>.

Reagent gas ionisation proceeds by the introduction of high energy ionising electrons from either a  $^{63}\text{Ni}$  radioactive foil<sup>11</sup> or more commonly from a corona discharge needle<sup>19</sup> operating at a 5-10 kV voltage. The reagent ions are formed because they are in great excess and therefore have a higher probability of interaction with an electron than an analyte molecule.

Ion-molecule reactions provide the most abundant source of ion formation at atmospheric pressure via gas phase acid-base chemistry<sup>2,7,8</sup>. Positive ion APCI uses acidic reagent ions including  $\text{H}_3\text{O}^+$  (from water) and  $\text{CH}_3\text{CNH}^+$  (from acetonitrile). When analyte molecules of weaker acidity are present proton transfer will occur to the basic site of the analyte molecule<sup>7</sup>:

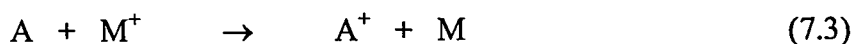


This reaction will only occur when the proton affinity of the analyte is greater than the proton affinity of the reagent ion. Negative ion formation<sup>9</sup> proceeds between a strongly acidic analyte molecule (M) and a weakly acidic reagent ion ( $[\text{A-H}]^-$ ) by proton abstraction to form a deprotonated reagent ion ( $[\text{A-H}]^-$ ):



Bruins has listed<sup>8</sup> the acidity and basicity of many ions and neutral molecules to aid in the determination of the ions formed in a chemical ionisation plasma.

Other processes less probable than protonation or proton abstraction reactions can lead to ionisation of analyte molecules. When protons are not available ions have to be created by different mechanisms. Charge exchange<sup>2,8,9</sup> from a reagent cation will occur when the ionisation potential of the reagent ion molecule (M) is higher than the analyte molecule (A):

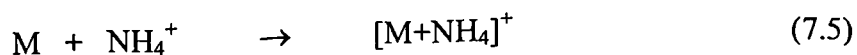


Alternatively the presence of thermalised electrons ( $e_{th}^-$ ) in the chemical ionisation plasma can provide a source of electrons for molecules of high electron affinity which are capable of electron capture<sup>2,9</sup>:



Electron auto-detachment is energetically feasible because of the high energies imparted to the analyte molecule (A) on electron attachment. However the high pressures present provide collisional stabilisation of the anion by removal of the excess internal energy<sup>2</sup>.

Finally the electrophilic addition of cations to molecules<sup>5</sup> can occur when the proton affinities of the analyte and reagent gas are approximately equal. For example ammonium ions present to act as a buffer in LC-MS can react with other high proton affinity molecules:



### 7.1.1.2 Electrospray Ionisation <sup>2,5,8,22,23,24</sup>

Electrospray ionisation transfers preformed ions present in a liquid phase solution to the gas phase by the endoergic process<sup>22</sup> of field induced ion evaporation<sup>25</sup>. Ion transfer is performed from small highly charged droplets produced by the application of an electric field to a spraying capillary. Ions need to be preformed in solution or the mechanisms described below can not occur. The analyte never passes through significantly hot regions that are experienced in APCI and therefore thermally labile compounds can be determined.

Zeleny<sup>26</sup> first described the electrospray phenomenon of producing fine sprays from a capillary operating at potential differences with respect to the surrounding container. In 1968 Dole<sup>10</sup> discussed the use of electrospray for producing ions for mass analysis and the technique was later improved in the 1980s by the two groups of Iribarne and Thomson<sup>25,27</sup> and Yamashita and Fenn<sup>15,28</sup>. The mechanism of transferring ions to the gas phase from solution is not fully understood, though it is composed of four different stages which in series require less than one millisecond to be performed<sup>22</sup>. These are<sup>22</sup>:

- 1) charged droplet formation from the liquid flow;
- 2) shrinkage of the droplet by solvent evaporation;
- 3) droplet fission;
- 4) ion evaporation from the droplet surface.

In this section positive ion electrospray ionisation will be described only. Negative ion production<sup>29</sup> is also possible by operating with a needle functioning with a negative potential difference in the ion source. This change in polarity provides different charge separation and electrochemical reactions present during operation with respect to positive ion electrospray ionisation.

The positive ion electrospray ionisation source<sup>5</sup> (Figure 7.3) is composed of a stainless steel capillary which transports a 1 - 40  $\mu\text{l min}^{-1}$  flow of liquid to the spray chamber. A potential difference voltage of + 3-5 kV is applied between the capillary and the opposite source wall up to 2 cm away containing an ion transfer orifice. The ion source wall acts as a counter electrode with respect to the spraying capillary. The electric field at the capillary tip is very high<sup>22</sup> (approximately  $10^6 \text{ V m}^{-1}$ ) and penetrates the liquid phase to provide electrophoretic charge separation of positive and negative ions which acts to nullify the electric field present<sup>23</sup>. Positive ions migrate in the liquid towards the counter electrode operating at a relative negative potential and this results in the liquid surface at the capillary tip being extended to create a so called Taylor cone<sup>5,22</sup>. This equilibrium conical shape is composed of an excess of positive ions at the liquid-gas interface. The negative ions present in solution migrate against the liquid flow along the capillary. At a certain ion concentration the coulombic repulsion forces operating at the Taylor cone tip are sufficiently larger than the surface tension forces of the liquid and allow a droplet carrying excess positive charge at its surface to detach from the liquid cone and migrate towards the counter electrode<sup>22,30,31</sup>. In the flowing stream used this process is continuous and produces a stream of small charged droplets with a narrow size distribution<sup>22</sup> centred around a droplet diameter of 1.5  $\mu\text{m}$ . The small flow rates used in ESI are

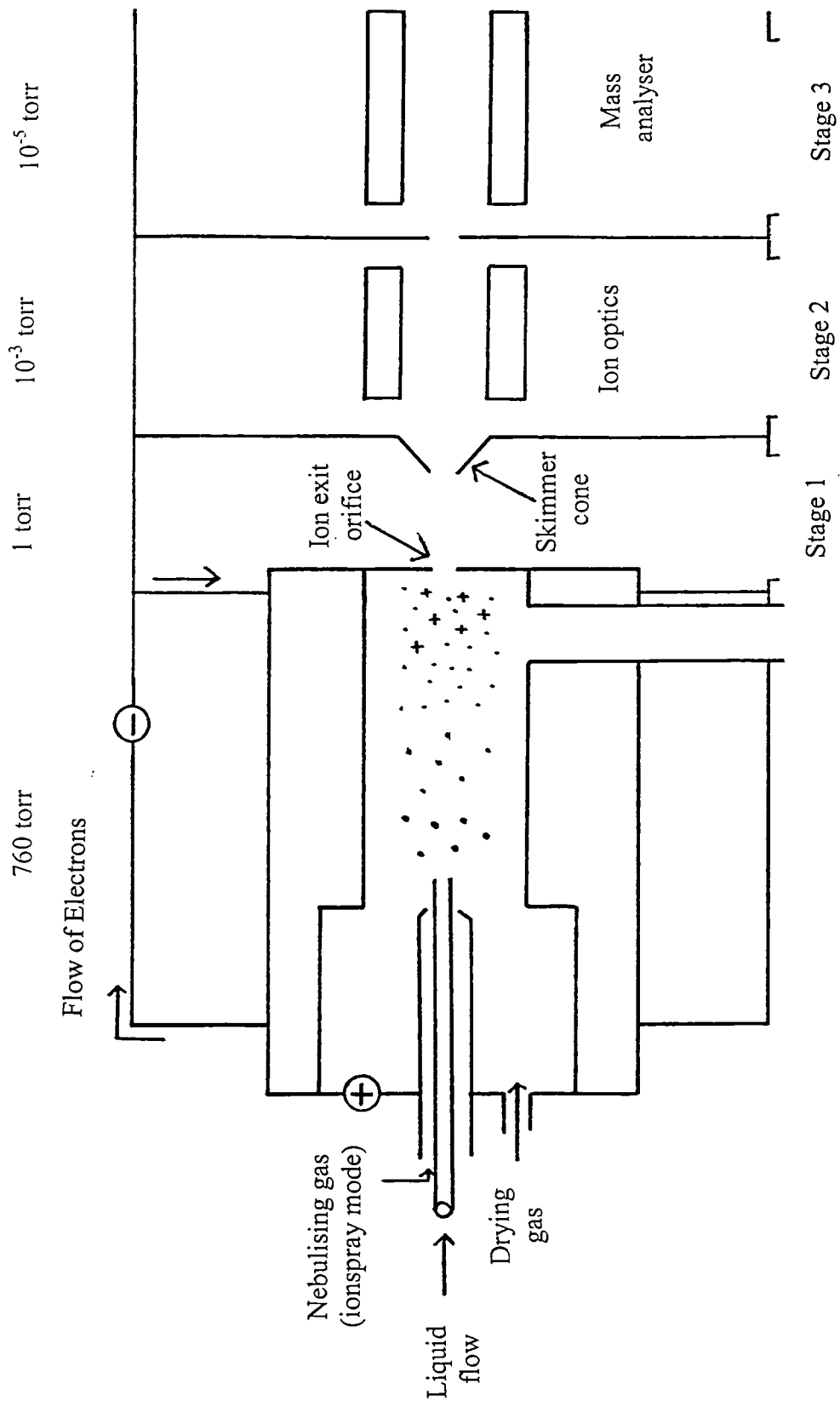
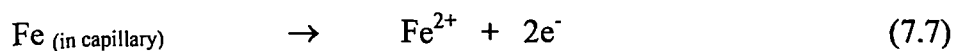


Figure 7.3 The electro spray ionisation source

required because only a limited volume of liquid can be removed from the Taylor cone by electrical shear force.

For the electrophoretic separation process described above to be continuous charge balancing is required<sup>22</sup>, which if absent would result in the removal of an electric field in the liquid and the cessation of charge separation. Charge balancing therefore drives the electrospray mechanism and occurs at the metal capillary-liquid phase interface by electrochemical oxidation<sup>32</sup>. Electrons produced by oxidation reactions can then flow to the counter electrode to neutralise the ions striking the electrode. Oxidation of anions to neutral molecules (7.6) or oxidation of the metal capillary (7.7) can proceed to produce electrons:



Oxidation at the capillary surface has been shown to occur. The detection of oxidised iron and zinc present in the capillary material<sup>32</sup> and the detection of oxidised neutral molecules in the liquid phase<sup>33,34,35</sup> have shown that electrochemical oxidation does take place in the capillary.

The electrochemical reactions and processes in the ion source are similar to those observed in a liquid phase electrolytic cell. Therefore the ion source can be described as a special kind of electrolytic cell<sup>32,36</sup>. Normally ion transport occurs completely in the liquid phase, however in the electrospray ionisation source some ion transport occurs in the gas phase.

Droplet shrinkage (stage two) occurs by convective heat transfer from the heated ion source walls or from a countercurrent gas flow employed to aid evaporation and transfer droplets closer to the counter electrode. The removal of solvent molecules increases the number of ions at the liquid surface and therefore the electric field strength on the surface also increases<sup>5</sup>. When the droplets reach a certain diameter the Rayleigh instability limit is being approached and the coulombic repulsion forces of the cations are large enough to overcome the surface tension of the liquid droplet. The resulting coulombic explosions<sup>22,37</sup> provide fission of the droplet which proceeds to produce a large number of smaller droplets which contain on average 2% of the mass but 15% of the charge of the parent droplet<sup>22</sup>. Therefore the mass to charge ratio decreases during fission and this enables multiple charged large molecules to be detected<sup>38</sup>.

The process of solvent evaporation and droplet fission can proceed many times until the coulombic repulsion forces between cations are equivalent to the cohesive forces of the droplets. At this stage in the droplet development it is kinetically and energetically possible for the electric field in the droplet to provide field induced ion evaporation<sup>22,25</sup> from the droplet surface, with or without associated solvent molecules. This theory of gas phase ion production was first described by Iribarne and Thomson<sup>25,27</sup> and the process has been calculated to occur only when droplets have diameters less than 8 nm and carry more than 70 elementary charges<sup>22</sup>. Ions transferred to the gas phase are either transported to the mass analyser or are neutralised by electrons during ion-counter electrode collisions. A second theory concludes that droplet desolvation and fission proceeds until single ions associated with solvent molecules are created, however, this theory is thought very unlikely<sup>22</sup>.

The constraints of the low liquid flow rates employed with electrospray ion sources have been lessened by the introduction of pneumatically assisted electrospray (ionspray) by Bruins<sup>39</sup>. This technique uses a flow of coaxial gas at the capillary tip to provide mechanical disruption and nebulisation of the Taylor cone, while the potential difference still employed provides electrophoretic charge separation. Higher liquid flow rates up to 200  $\mu\text{l min}^{-1}$  can be used and aqueous samples can be analysed<sup>5</sup>. The high surface tension of water creates an unstable spray of droplets with larger diameters during electrospray nebulisation and therefore require more time to provide droplets of small enough diameter to allow the evaporation of ions from the droplet surface. Ionspray sources can provide water droplets of small diameters in a stable spray, which is often not achievable with electrospray sources.

#### 7.1.1.3 Applications of Atmospheric Pressure Ionisation - Mass Spectrometry

Commercial API-MS instruments have only been manufactured in the last 10 -15 years even though the first applications of the technique were reported in 1968<sup>10</sup>. Therefore the largest range of developments for the APCI and ESI instruments on a world wide scale have been limited and have taken place in the last ten years.

The major application of APCI-MS for liquid analyses is for the detection of compounds present in liquid chromatograph effluents<sup>40</sup>, which was the reason for its primary development<sup>11</sup>. Only one reported use of the technique has been discovered for reaction monitoring. Henion et al. used LC-APCI-MS for pharmacokinetic studies of phenylbutazone in a horse<sup>41</sup>. The majority of reported applications of APCI are for the

process monitoring of ultrapure gases<sup>19,42</sup> for contaminants present at  $\mu\text{g l}^{-1}$  and  $\text{ng l}^{-1}$  concentrations, and for the detection of compounds present in air<sup>43</sup>.

The development of electrospray ionisation has been much more rapid and has been assisted by the discovery that large molecular weight (MW) multiply charged compounds can be desorbed intact from the liquid phase<sup>38</sup>. The relatively small mass-to-charge ratios can then be detected using a quadrupole mass analyser of limited mass range which is less expensive than other mass analysers. These discoveries have now centred on the use of ESI for the MW determination<sup>44,45</sup> of proteins or large biomolecules over 100 kDa. Detection can be performed with or without prior chromatographic separation. A recent review discusses the use of ESI-MS for biochemical analysis<sup>46</sup>. Quadrupole<sup>35</sup>, magnetic sector<sup>47</sup>, ion trap<sup>48,49</sup> and Fourier-transform ion cyclotron resonance<sup>50</sup> mass analysers have been coupled with the electrospray ion source.

The investigation of reactions using electrospray or ionspray ionisation has an advantage over APCI that it uses a lower rate of liquid consumption and therefore will not disrupt the reaction kinetics being studied by sampling large volumes of the reaction mixture. Lee et al. first showed the potential of its use for studying a range of reactions<sup>51</sup>. Since this time several authors have applied ESI-MS for studying ligand exchange reactions<sup>52,53</sup> and photosubstitution reactions of transition metal complexes<sup>54</sup>, phosphine mediated reactions which proceed via ionic intermediates<sup>55</sup>, iron(III) complex reactions which proceed via radical cations<sup>56</sup> and porcine pancreatic elastase inhibition reactions<sup>57</sup>. However a more recent area of interest is the coupling of electrochemistry and electrospray ionisation mass spectrometers to enable electrochemical reagents or products to be monitored and reaction mechanisms to be determined<sup>58,59</sup>. Also electrochemical oxidation of neutral analytes is being performed in the spraying

capillary<sup>60</sup> to enlarge the number of compounds that can be analysed by ESI-MS. Finally Gatlin et al. have applied ESI-MS with liquid chromatography or off-line solvent extraction for the analysis of Cu(I) and Cu(II) species present in jet fuel<sup>61</sup>. This has demonstrated the potential of the technique for process analysis and monitoring at  $\mu\text{g l}^{-1}$  levels.

In this chapter the determination of a range of compounds using APCI-MS and ESI-MS is to be investigated. The compounds to be determined are formic, acetic and propionic acids and toluene in separate acetic acid and water matrices.

## 7.2 Experimental

### 7.2.1 Reagents

Six standard solutions (Table 7.1) were prepared on a volume to volume (v/v) basis with doubly deionised water (Elgastat, 18 MΩ cm<sup>-1</sup>), AR grade toluene (Aldrich, Gillingham, Dorset, UK) and formic, acetic and propionic acids (99.9 % purity, BP Chemicals, Hull, East Yorkshire, UK).

Sample	Matrix	Other compounds present
one	acetic acid	formic acid (500 µg ml <sup>-1</sup> ) toluene (10 µg ml <sup>-1</sup> )
two	acetic acid	propionic acid (500 µg ml <sup>-1</sup> )
three	water	acetic acid (200 µg ml <sup>-1</sup> )
four	water	formic acid (200 µg ml <sup>-1</sup> )
five	water	propionic acid (200 µg ml <sup>-1</sup> )
six	water	formic acid (200 µg ml <sup>-1</sup> ) acetic acid (200 µg ml <sup>-1</sup> ) propionic acid (200 µg ml <sup>-1</sup> )

**Table 7.1** The compositions of the six standard solutions analysed

### 7.2.2 Instrumentation and Procedures

A three stage differentially pumped VG Platform mass spectrometer (VG Biotech, Altrincham, Cheshire, UK)<sup>62</sup> was employed. The instrument enabled positive and

negative ions to be produced and detected in the same ion source using APCI and ESI. The ion source was maintained at 120°C for both ionisation modes and the source probe was maintained at 400°C in the APCI mode to provide rapid droplet vaporisation. A nitrogen gas flow rate of 10 l h<sup>-1</sup> was employed for aiding droplet desolvation and a 500 l h<sup>-1</sup> flow of nebulising gas was used in the APCI mode. The voltage employed for extraction of ions from the source in both ionisation modes was 20 V and a positive or negative 3.5 kV potential was applied between the stainless steel capillary and source walls in the positive and negative electrospray mode, respectively. A cone voltage of 20 V was applied between the entrance walls of stages one and two to provide cluster breakdown. The second stage of the pumping system contained a rf-only quadrupole filter for ion focusing and the third stage contained a quadrupole mass filter.

During mass scanning to collect mass spectra the mass range of 2 - 100 Da was used except during the detection of positive ions when the mass range 1 - 200 Da was scanned. In single ion monitoring of more than one mass a dwell time at each mass of 0.1 s was employed. Ions were separated with a quadrupole mass analyser and detected with a Dynolite<sup>TM</sup> detector operating at a detection voltage of 600 V. The detector operates by the collision of accelerated ions with a light emitting phosphor plate to produce photons whose intensity represents the intensity of the ion beam. The photons produced are amplified with a photomultiplier tube and detected to provide a measured current representative of the ion beam intensity. A Fisons Windows based MassLynx II datasystem was employed for instrument control, data acquisition and data presentation.

50 % Aqueous acetonitrile solutions were continuously pumped into the ESI and APCI ion sources at flow rates of 0.2 and 1.0 ml min<sup>-1</sup>, respectively. Standard solutions

were introduced into the aqueous acetonitrile flow as 10  $\mu\text{l}$  sample plugs with a loop injector after they had been diluted 1 : 1 with the carrier flow off-line to ensure a degree of mixing occurred between the standard solutions and carrier flow. The actual concentrations of analytes in the injected solution is therefore half of that quoted in the reagents section (Table 7.1).

## 7.3 Results and Discussion

### 7.3.1 The Analysis of Samples Composed of a Water Matrix

The correct choice of the ionisation mode (APCI or ESI, positive or negative ion) used to detect compounds is essential to provide adequate sensitivity when minor components present in a liquid matrix are to be detected. The acidity in aqueous solution of the carboxylic acids studied should be exhibited by their partial dissociation to provide a proton and formate ( $\text{HCO}_2^-$ ), acetate ( $\text{CH}_3\text{CO}_2^-$ ) and propionate ( $\text{C}_2\text{H}_5\text{CO}_2^-$ ) anions. Figures 7.4 and 7.5 show the mass spectra of a  $200 \mu\text{g ml}^{-1}$  aqueous acetic acid standard using the positive ion and negative ion electrospray ionisation modes, respectively. It can clearly be seen that in the negative ion mode the acetate anion is present as the base peak at mass 59 Da, and the formate anion at mass 45 Da is also present. The presence of formic acid as an impurity in the acetic acid used provides the formate ion. The absence of cations at masses 59-61 Da in the positive ion mass spectrum exhibits the energetically non-feasibility of carboxylic acids to form cations in solution. The base peak observed at mass 41 Da in the positive ion mass spectrum corresponds to the acetonitrile present in the flowing stream used to transport samples to the ion source. Negative ion detection will be used in all the work described below .

The ESI and APCI negative ion mass spectra for a  $200 \mu\text{g ml}^{-1}$  aqueous formic acid standard is shown in Figures 7.6 and 7.7, respectively. The base peak for both spectra is the formate anion at mass 45 Da, and the spectrum is thereafter composed of only a few low intensity ions, which at mass 91 Da in the ESI mass spectrum represents the  $\text{C}_6\text{H}_5\text{CH}_2^-$  anion created from toluene.

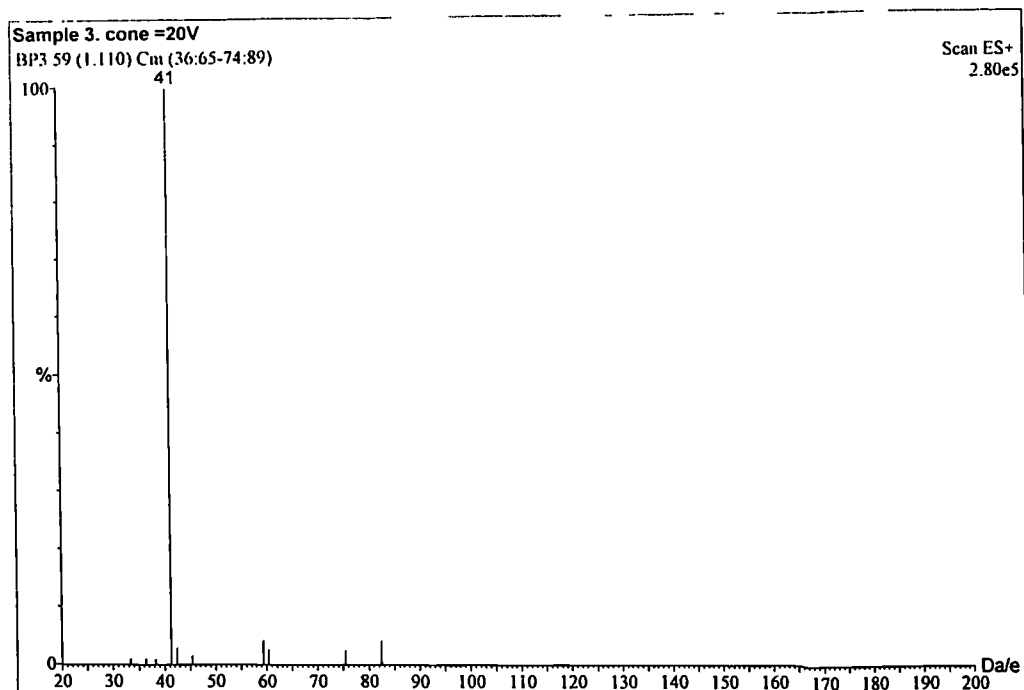


**Figure 7.4** Positive ion electrospray ionisation mass spectrum of a  $200 \mu\text{g ml}^{-1}$  aqueous acetic acid standard (sample three)

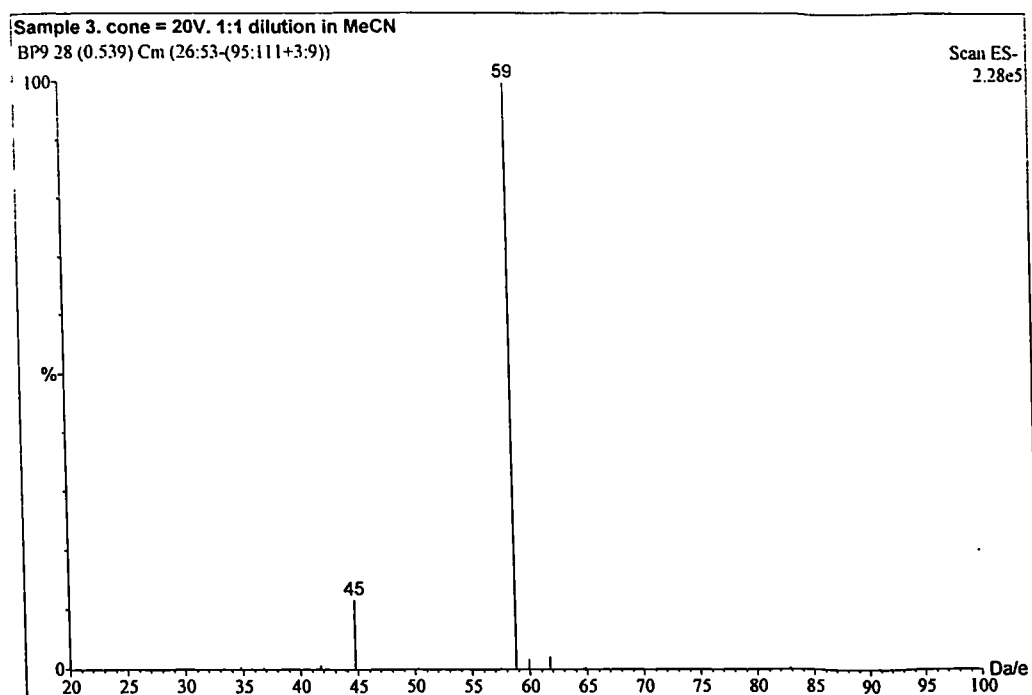


**Figure 7.5** Negative ion electrospray ionisation mass spectrum of a  $200 \mu\text{g ml}^{-1}$  aqueous acetic acid standard (sample 3)

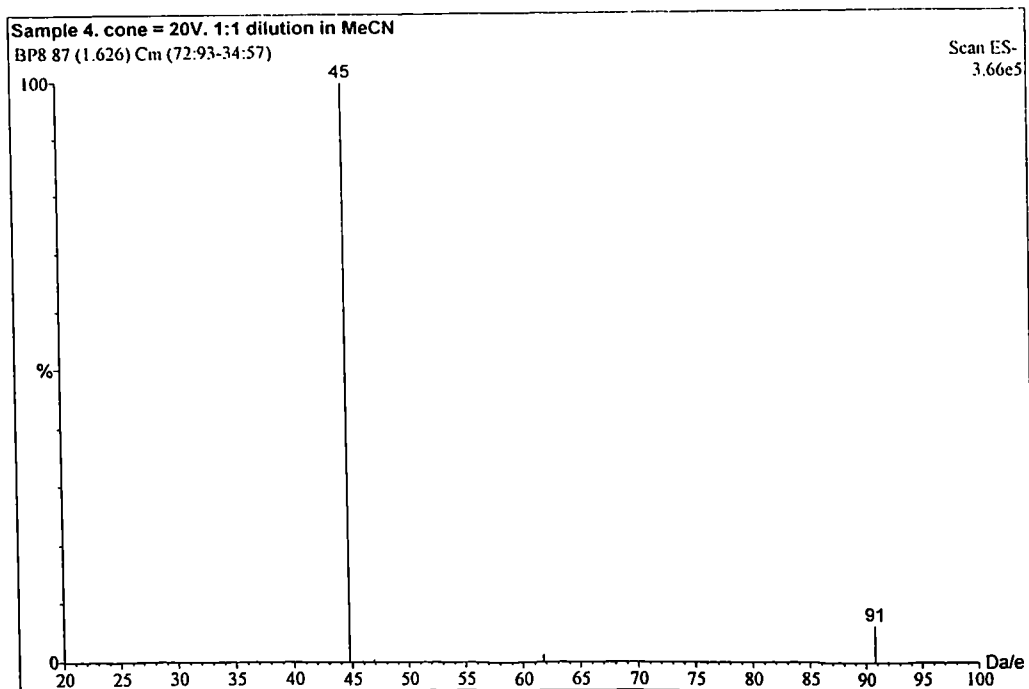


**Figure 7.6** Negative ion electrospray ionisation mass spectrum of a  $200 \mu\text{g ml}^{-1}$  aqueous formic acid standard (sample 4)

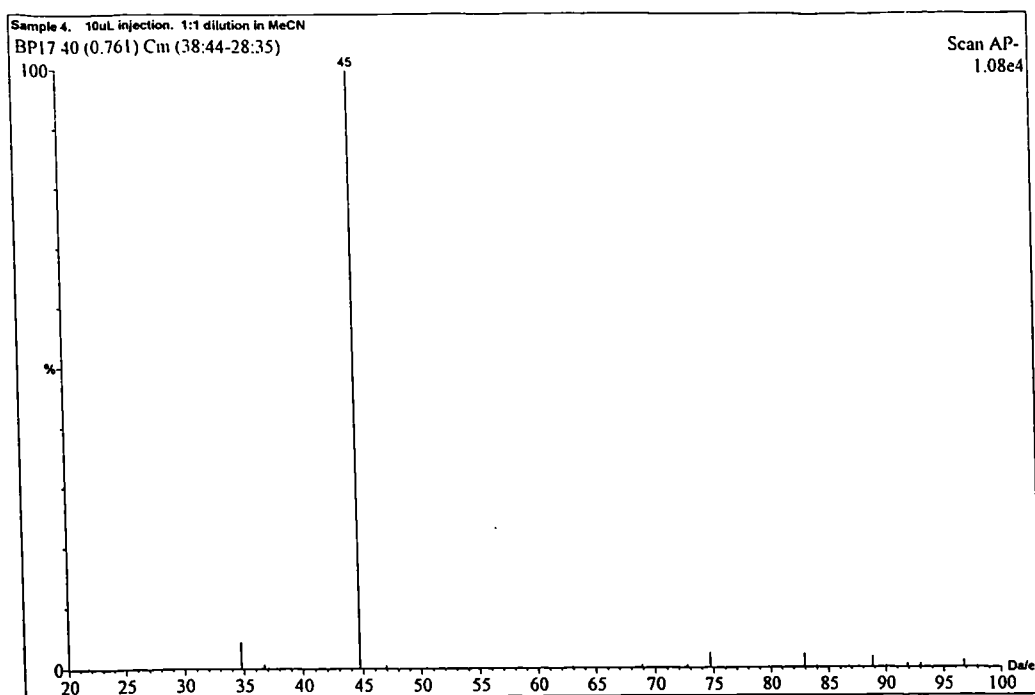


**Figure 7.7** Negative ion atmospheric pressure chemical ionisation mass spectrum of a  $200 \mu\text{g ml}^{-1}$  aqueous formic acid standard (sample 4)

The formation of formate anions in the CI plasma proceeds by the abstraction of a proton from formic acid by the  $\text{CH}_2\text{CN}^-$  ion, produced from acetonitrile present in the liquid carrier stream:



The ESI and APCI negative ion mass spectra are shown in Figures 7.8 and 7.9, respectively, for an aqueous  $200 \mu\text{g ml}^{-1}$  propionic acid standard. The ESI mass spectrum is composed of a base peak at mass 73 Da for the propionate anion, but the formate and acetate ions present as impurities in the propionic acid can also be observed at masses 45 and 59 Da. However these two impurities cannot be observed in the APCI mass spectrum where the propionate anion is the only ion detected. In summary ESI or APCI in the negative ion detection mode can be used for monitoring  $\text{C}_1 - \text{C}_3$  carboxylic acids in water. However the lower sensitivity shown later in this section for the APCI technique provides a degree of selectivity because of its inability to observe ions that were detected using the ESI mode.

The application of atmospheric pressure ionisation would most likely be used for off-line or on-line monitoring of aqueous effluent streams and therefore  $\mu\text{g l}^{-1}$  or lower detection limits would be required. It has been shown in Figures 7.4 - 7.9 that all three carboxylic acids can be detected at concentrations of  $100 \mu\text{g ml}^{-1}$ . Single ion monitoring (SIM) was employed to monitor the ion currents for the formate, acetate and propionate anions of each carboxylic acid to plot total ion chromatograms and to allow a comparison of the limits of detection.

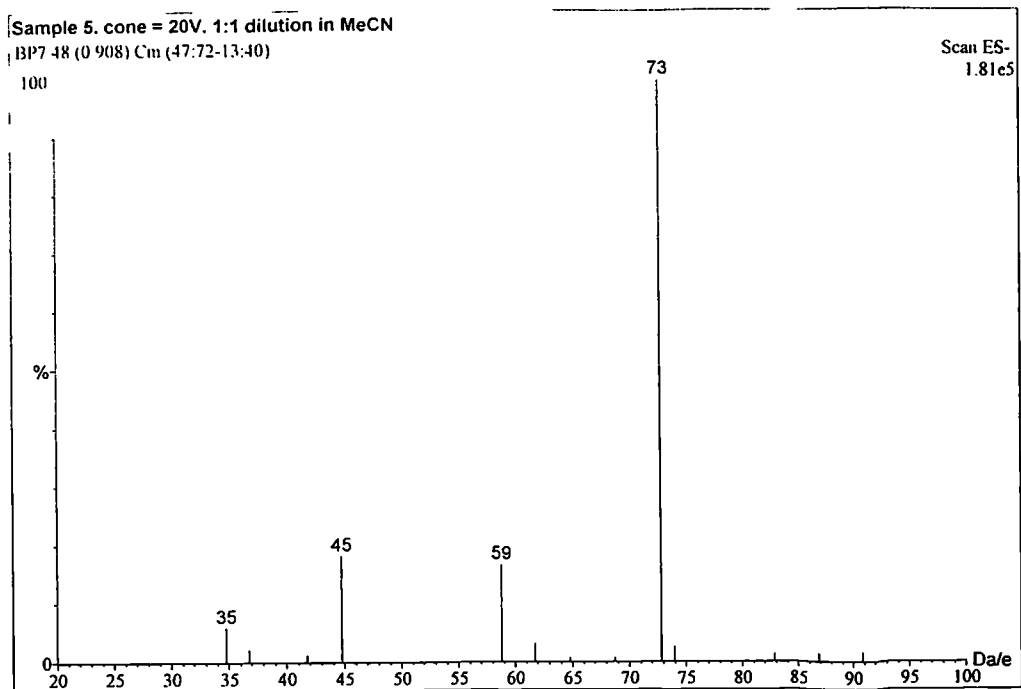


**Figure 7.8** Negative ion electrospray ionisation mass spectrum of a  $200 \mu\text{g ml}^{-1}$  aqueous propionic acid standard

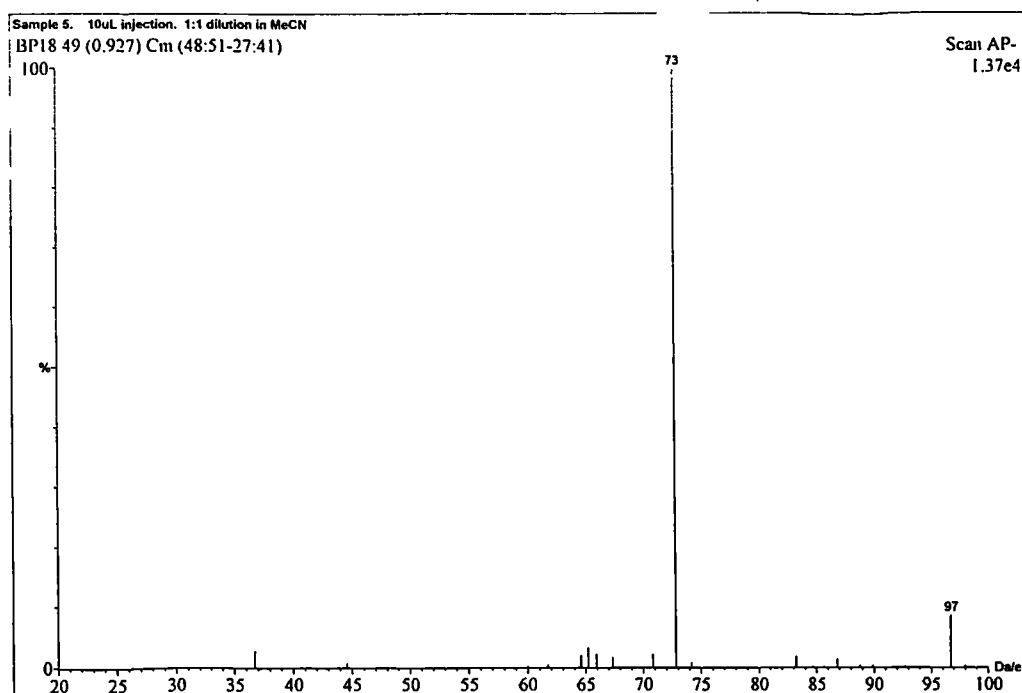


**Figure 7.9** Negative ion atmospheric pressure chemical ionisation mass spectrum of a  $200 \mu\text{g ml}^{-1}$  aqueous propionic acid standard

The total ion chromatograms (TICs) using APCI negative ion mode for formic, acetic and propionic acid were measured for three replicate injections and are shown in Figures 7.10, 7.11, and 7.12, respectively. The acids were monitored at masses 44.8, 58.9 and 73.0 Da. Concentrations lower than  $100 \mu\text{g ml}^{-1}$  can be detected for formic and propionic acids but a limit of detection ( $3\sigma$ ) of approximately  $100 \mu\text{g ml}^{-1}$  can be achieved for acetic acid because of the lower signal to noise ratio (S/N) observed. The same standards were monitored at the same masses using the ESI negative ion mode. The TICs are shown in Figures 7.13, 7.14 and 7.15, respectively. The S/N values are higher for the ESI technique and therefore lower limits of detection are achievable at  $\mu\text{g ml}^{-1}$  or  $\mu\text{g l}^{-1}$  concentrations. The order of sensitivity can be determined by visual inspection of the baselines and show the following order (lowest limit of detection first):

$$\text{Propionic acid} < \text{Formic acid} < \text{Acetic acid} \quad (7.9)$$

Collection of calibration data would be required to enable more accurate limits of detection to be calculated than the limits of detection shown above which were determined only approximately using TICs. However the higher limits of detection observed for the APCI mode are most likely caused by the lower number of anions created in the CI plasma with respect to the number of preformed ions in solution transferring to the gas phase.

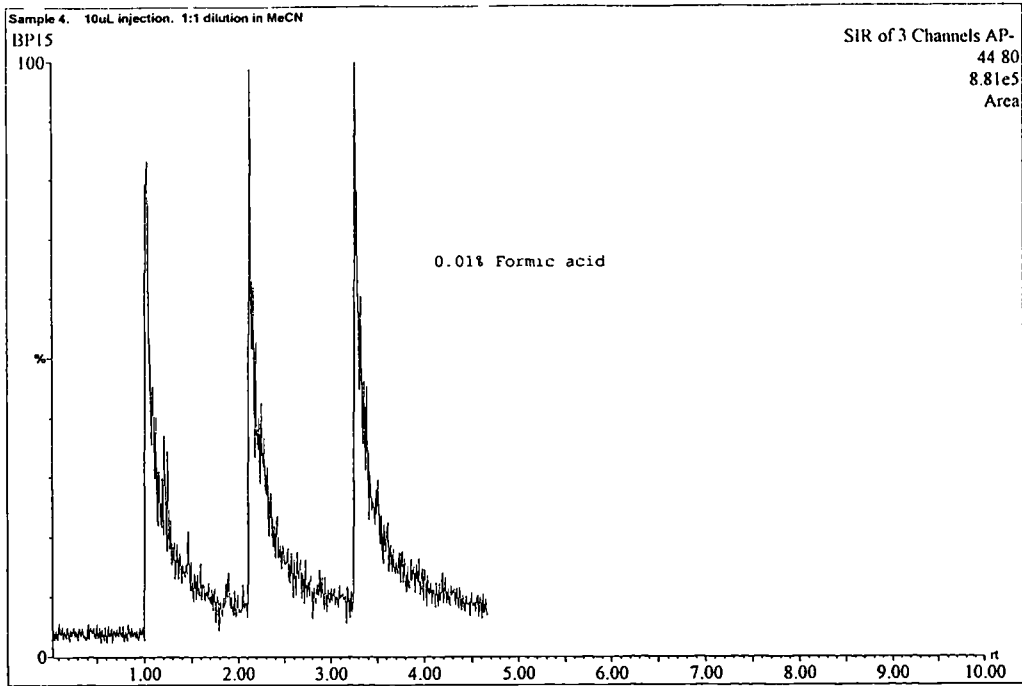


**Figure 7.10** Total ion chromatogram for formic acid at mass 44.8 Da using the negative ion atmospheric pressure chemical ionisation mode

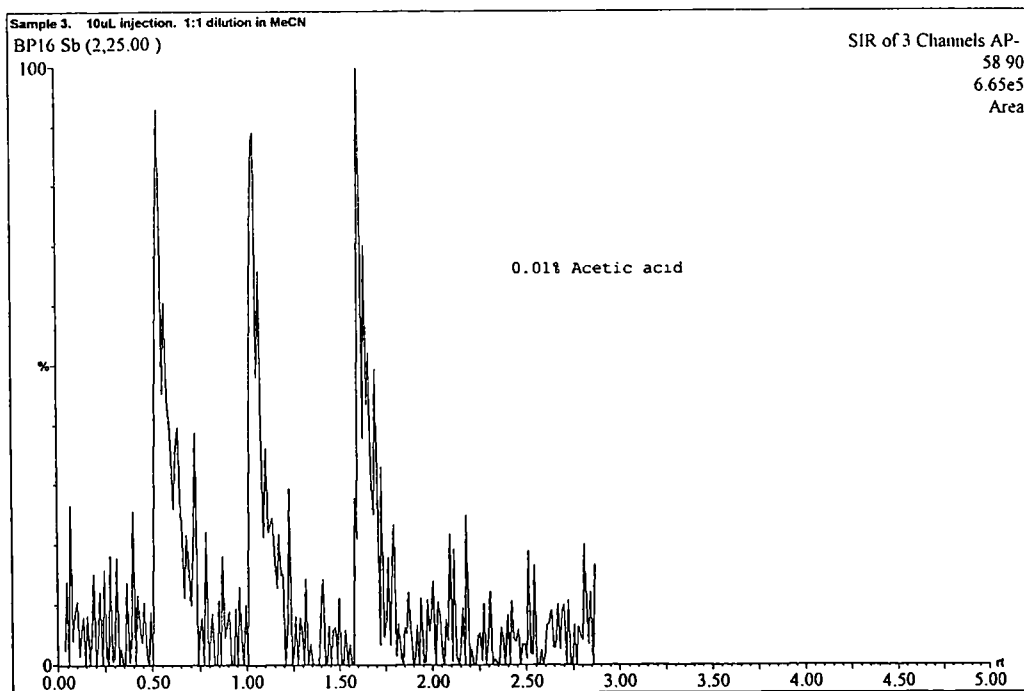


**Figure 7.11** Total ion chromatogram for acetic acid at mass 58.9 Da using the negative ion atmospheric pressure chemical ionisation mode

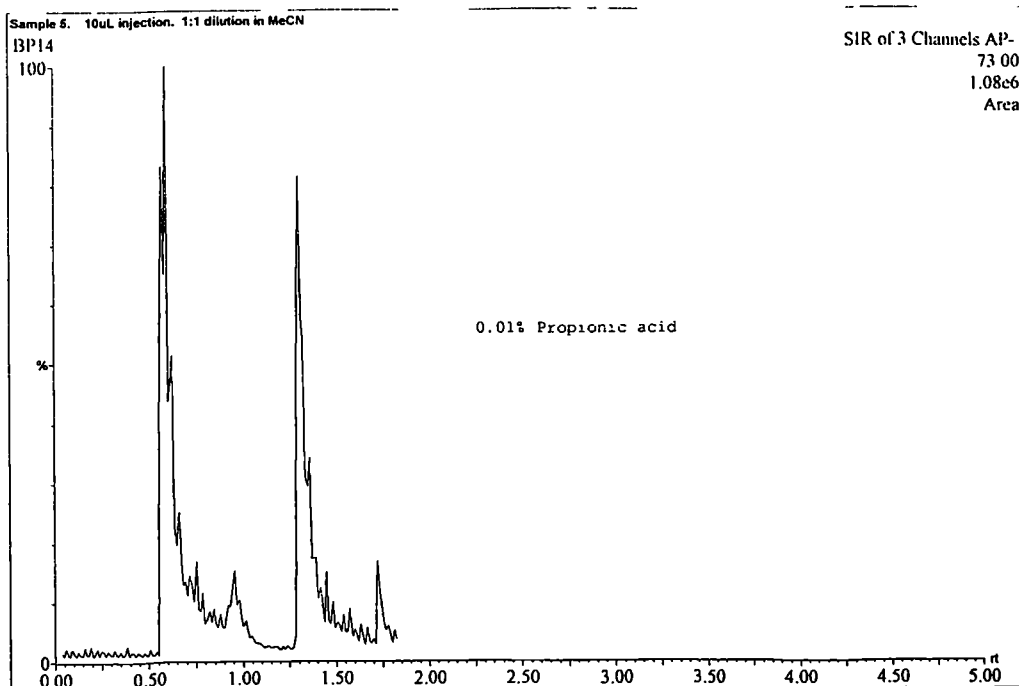


**Figure 7.12** Total ion chromatogram for propionic acid at mass 73.0 Da using the negative ion atmospheric pressure chemical ionisation mode

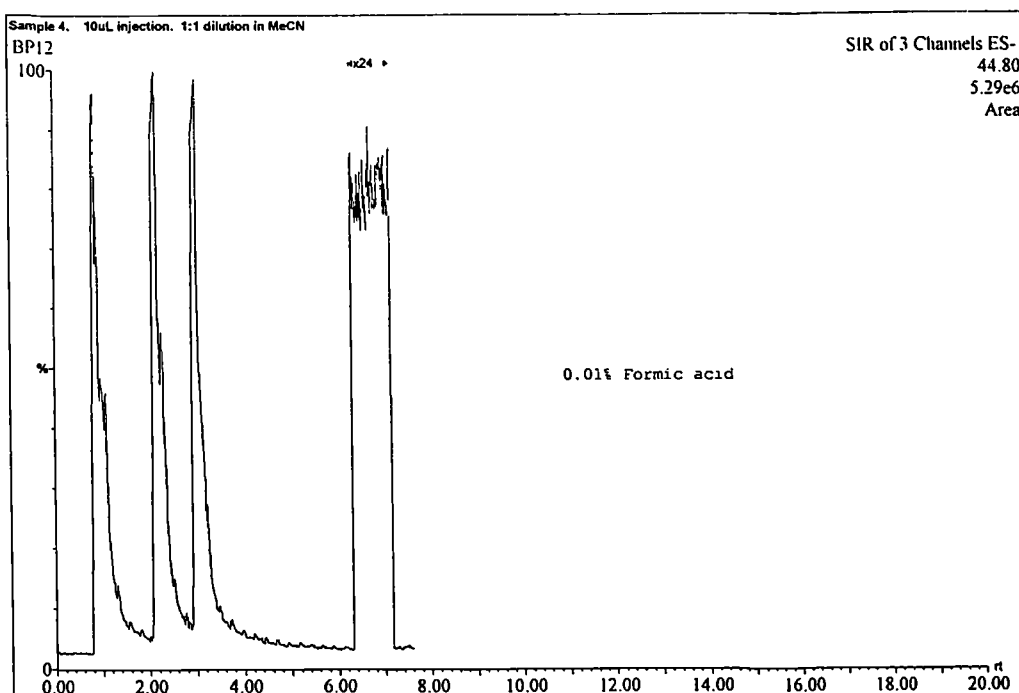


**Figure 7.13** Total ion chromatogram for formic acid at mass 44.8 Da using the negative ion electrospray ionisation mode

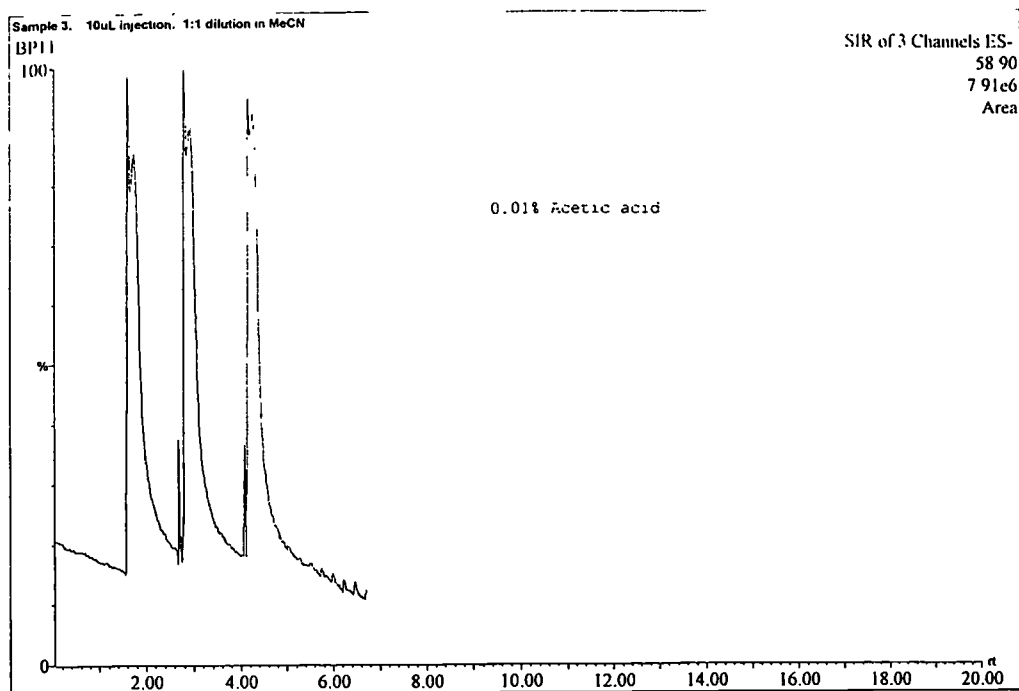


**Figure 7.14** Total ion chromatogram for acetic acid at mass 58.9 Da using the negative ion electrospray ionisation mode

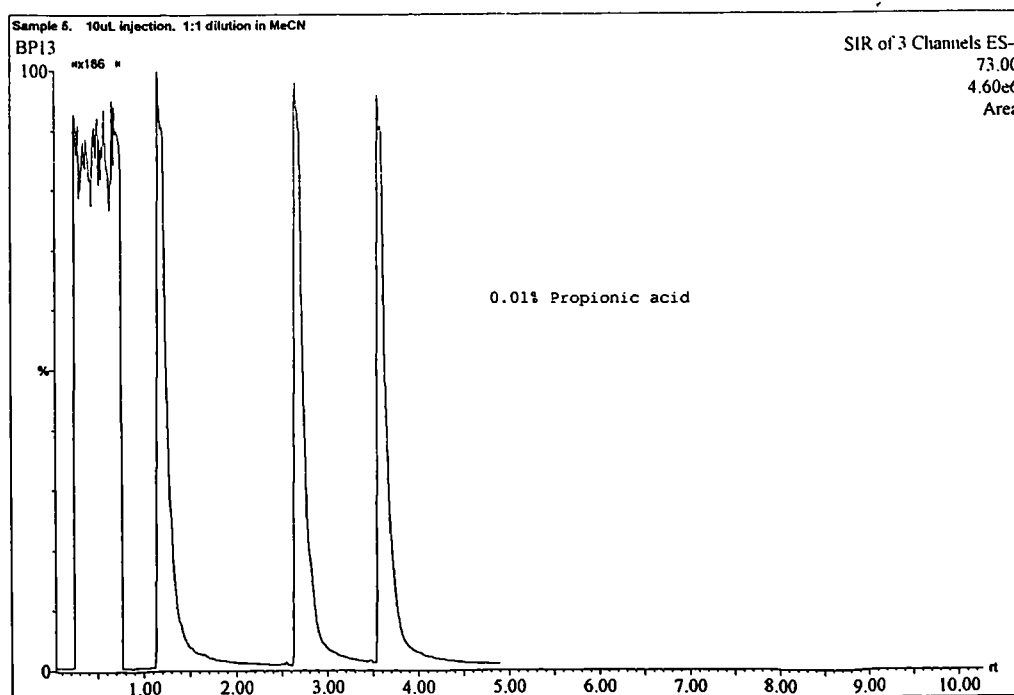


**Figure 7.15** Total ion chromatogram for propionic acid at mass 73.0 Da using the negative ion electrospray ionisation mode

It would be desirable for all three carboxylic acids to be detected simultaneously in aqueous effluent streams and therefore the ESI and APCI mass spectra data for an aqueous standard containing  $200 \mu\text{g ml}^{-1}$  each of formic, acetic and propionic acids was collected. The mass spectra (Figures 7.16 and 7.17) show that formic and propionic acids could be detected in the presence of each other with differing sensitivities. Acetic acid is not detected in these samples but is present as shown in the ESI-TIC for each acid (Figure 7.18). The high baseline at mass 58.9 Da may cause the inability to observe acetic acid. All mass spectra are background subtracted and the response for acetic acid may not be significantly larger than the background response.

The difference in ion intensities measured for formic and propionic acid is most probably caused by their differing acidities<sup>62</sup>. Formic acid is the most acidic ( $K_a = 1.8 \times 10^{-4} \text{ mol l}^{-1}$ ) with respect to propionic acid ( $K_a = 1.8 \times 10^{-5} \text{ mol l}^{-1}$ ). There will be a higher concentration of formate ions, with respect to propionate ions, in solution resulting in the higher ion currents measured for the formate ions. The acid-base chemistry present in the CI plasma means that compounds with a higher acidity are more likely to provide a proton to a weaker acid in the plasma.  $\text{CH}_2\text{CN}^-$  formed from acetonitrile is present in the plasma and is a weaker acid than formic acid. Therefore proton abstraction is performed by the  $\text{CH}_2\text{CN}^-$  ion from gaseous formic acid molecules. The lower acidity of propionic acid results in the lesser degree of proton abstraction with respect to formic acid. It would be expected to observe acetic acid at a response lying between formic and propionic acid because its  $K_a$  value ( $1.4 \times 10^{-5} \text{ mol l}^{-1}$ ) also lies between those of these two acids. Some of the ion intensity measured at mass 45 may be caused by formic acid present as an impurity in acetic or propionic acid.

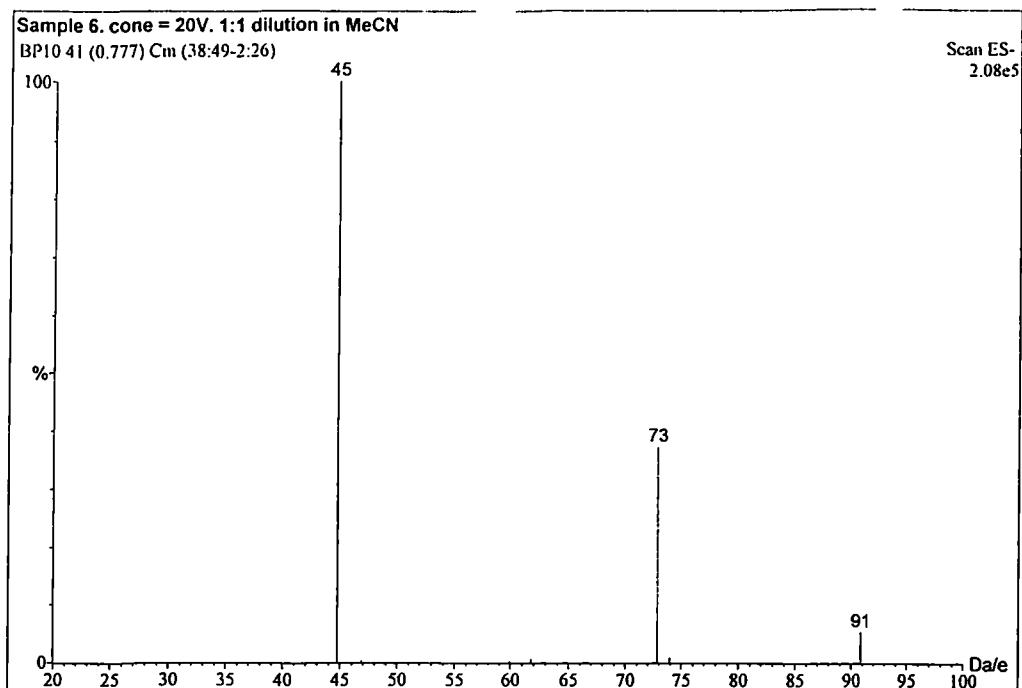


**Figure 7.16** Negative ion electrospray ionisation mass spectrum of an aqueous solution containing  $200 \mu\text{g ml}^{-1}$  formic, acetic and propionic acid

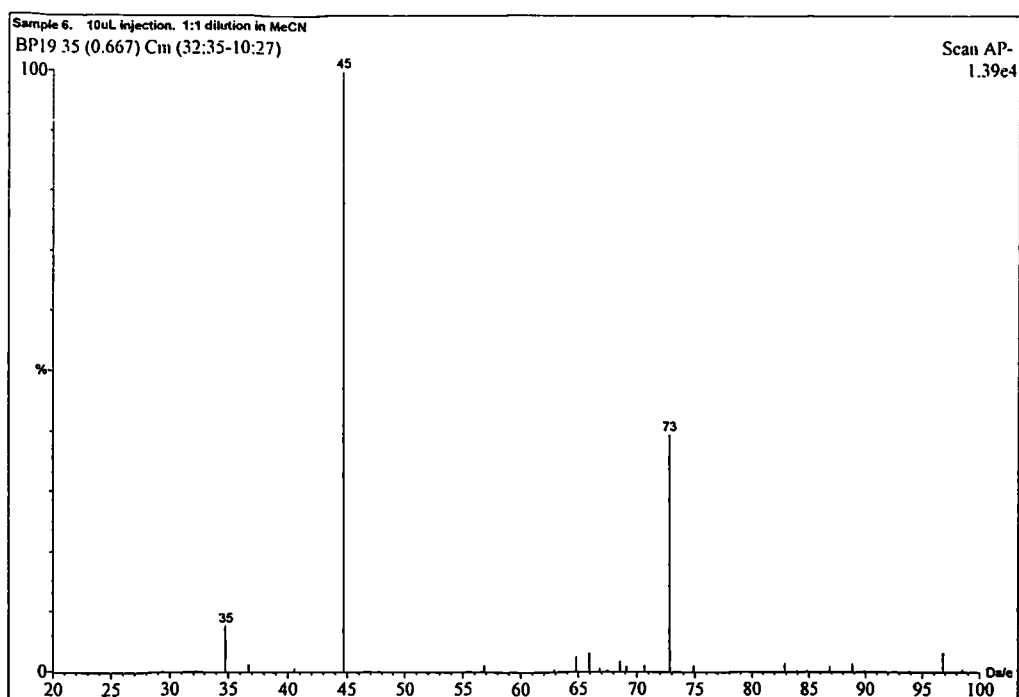


**Figure 7.17** Negative ion atmospheric pressure chemical ionisation mass spectrum of an aqueous solution containing  $200 \mu\text{g ml}^{-1}$  formic, acetic and propionic acid

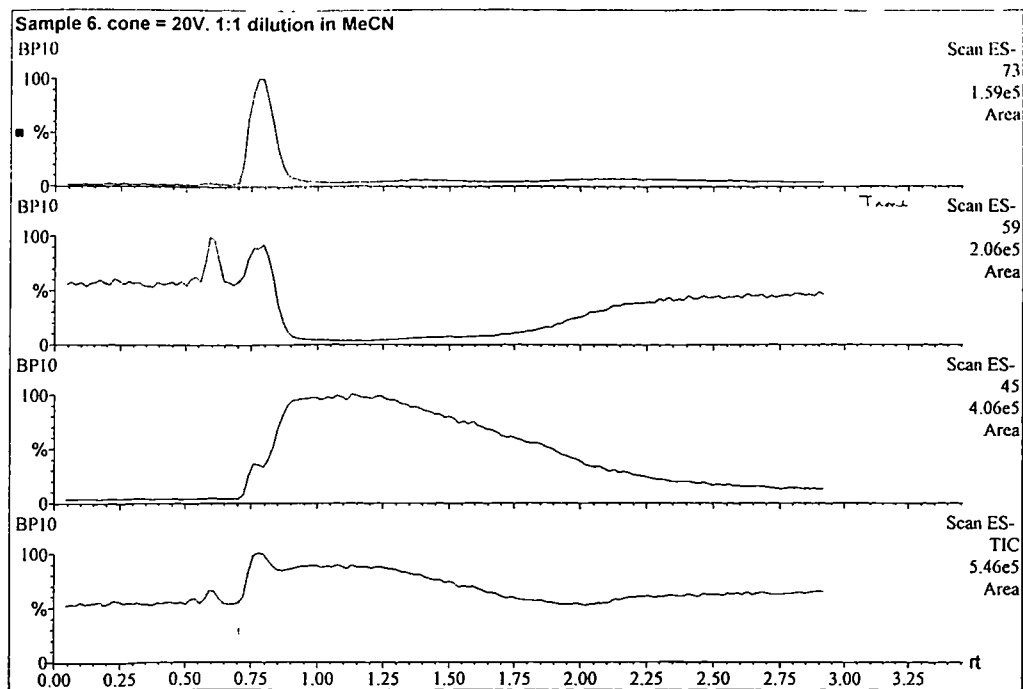


**Figure 7.18** Negative ion electrospray ionisation total ion chromatograms for masses 43, 59 and 73 Da

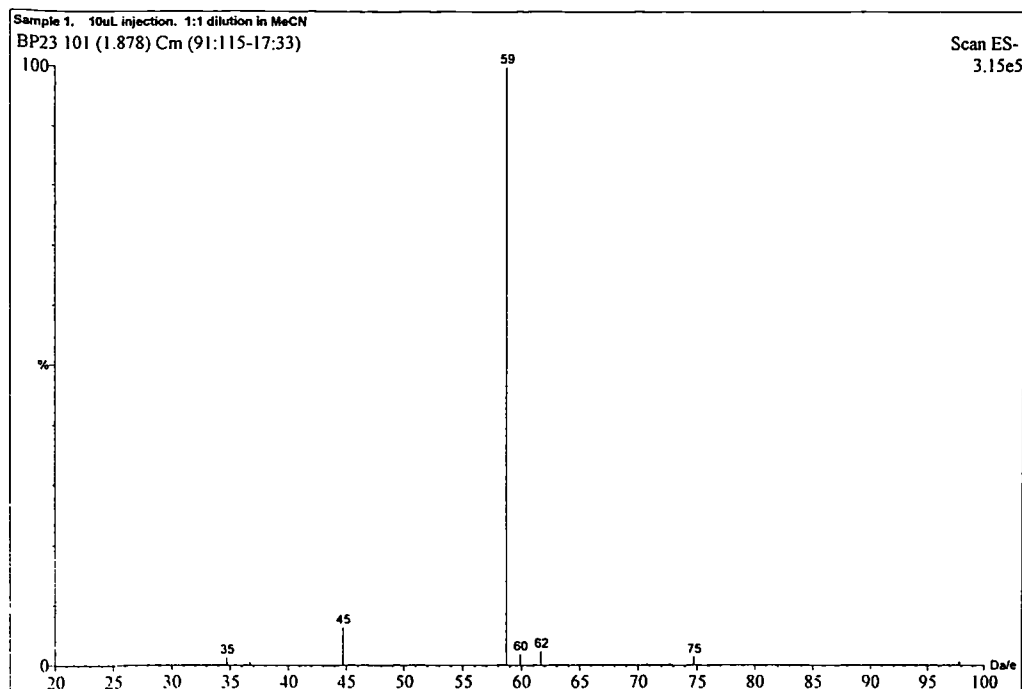


**Figure 7.19** Negative ion electrospray ionisation mass spectrum of an acetic acid solution containing 500  $\mu\text{g ml}^{-1}$  formic acid and 10  $\mu\text{g ml}^{-1}$  toluene

The ESI-TIC for each acid at masses 45, 59 and 73 Da show the different peak shapes measured (Figure 7.18). The peak width for propionic acid is small with respect to the wide peak shape observed for formic acid. An increase in the response is observed for acetic acid before the response falls to the baseline and then slowly increases to a higher value. It was expected that the ion source was contaminated with acetic acid from experiments performed with samples containing 50 % acetic acid, described in section 7.3.2.

With the removal of the baseline at mass 59 Da, possibly by increasing the ion source temperature to desorb acetic acid adsorbed onto the ion source walls, the quantification of all three acids is possible with calibration for each compound being performed separately. There is no competition for ionisation when the acids are present at  $\mu\text{g ml}^{-1}$  concentrations, which would otherwise complicate the calibration procedures.

### 7.3.2 The Analysis of Samples Composed of an Acetic Acid Matrix

The analysis of compounds present at low concentrations in a matrix of higher conductivity and therefore containing a higher concentration of ions, with respect to water, was investigated using acetic acid as the matrix compound.

Figures 7.19 and 7.20, respectively, show the ESI and APCI negative ion mass spectra for an acetic acid standard containing  $500 \mu\text{g ml}^{-1}$  formic acid and  $10 \mu\text{g ml}^{-1}$  toluene. The APCI mass spectrum showed only acetic acid and therefore acetic acid dominates the acid - base chemistry present in the CI plasma. The ESI mass spectrum did provide a measurable ion current at mass 45 Da corresponding to formic acid and therefore this technique could be used to detect formic acid at a concentration of  $250 \mu\text{g ml}^{-1}$  or lower.

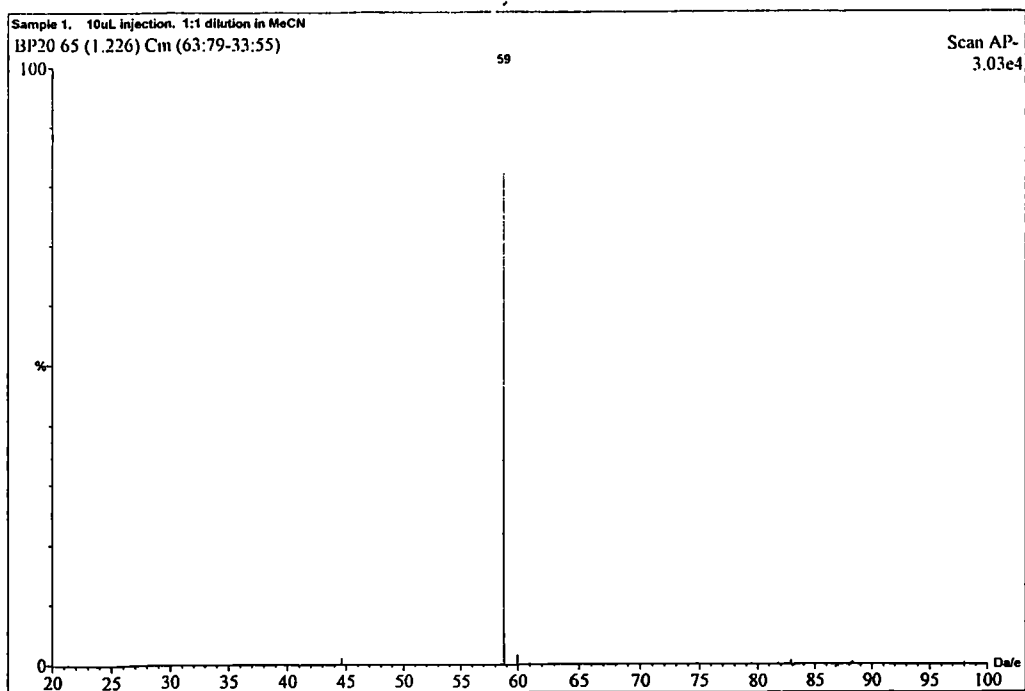


**Figure 7.20** Negative ion atmospheric pressure chemical ionisation mass spectrum of an acetic acid solution containing  $500 \mu\text{g ml}^{-1}$  formic acid and  $10 \mu\text{g ml}^{-1}$  toluene

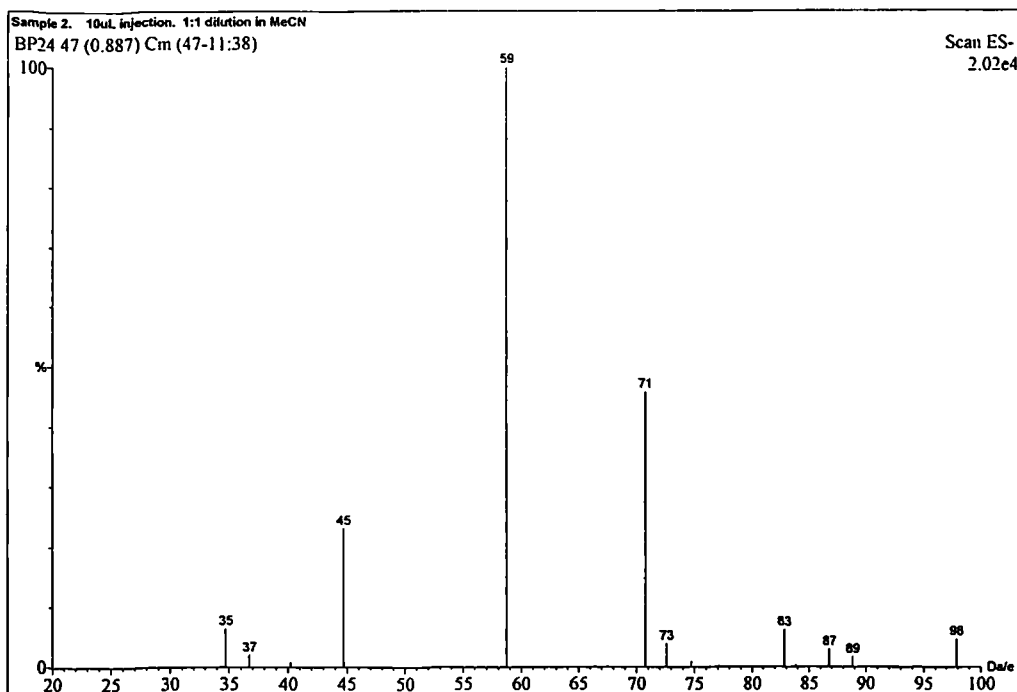


**Figure 7.21** Negative ion electrospray ionisation mass spectrum of an acetic acid solution containing  $500 \mu\text{g ml}^{-1}$  propionic acid

The analysis of a standard composed of  $500 \mu\text{g ml}^{-1}$  propionic acid present in acetic acid was also performed. The ESI and APCI mass spectra are shown in Figures 7.21 and 7.22, respectively. Only acetic acid was detected in the APCI mass spectrum. Formic acid present as an impurity in the acetic acid could be detected relatively easily using the ESI mode. An ion current was also measured at mass 73 Da in the ESI mass spectrum. This could represent propionate anions or  $\text{HCl}_2$  ( $\text{HCl}^{35}\text{Cl}^{37}$ ). The presence of chlorine in the sample can be shown by the peaks at masses 35 and 37 and their relative abundance of 3 : 1, which represents the isotope pattern for chlorine.

In summary, the detection of ionic species present in a more highly electrical conducting matrix than water is possible only when using ESI, which provides preformed ions in solution for mass analysis and is therefore dependant on the degree of ionisation of ionic compounds in the liquid matrix. Ionic and neutral compounds present in solution could not be detected using APCI because of the control of the acid - base chemistry in the CI plasma by acetic acid which is present in a minimum 1000-fold excess.

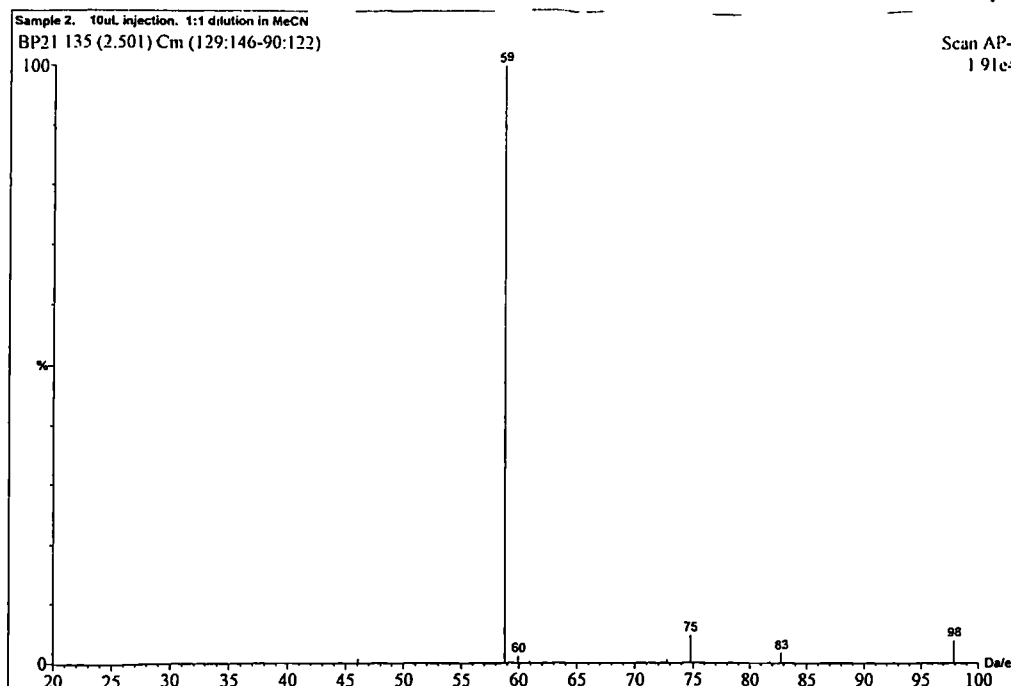


**Figure 7.22** Negative ion atmospheric pressure chemical ionisation mass spectrum of an acetic acid solution containing  $500 \mu\text{g ml}^{-1}$  propionic acid

#### 7.4 Conclusions

The work presented in this chapter shows the ability of atmospheric pressure ionisation - mass spectrometry (negative ion APCI and ESI) to detect the presence of  $\text{C}_1$  -  $\text{C}_3$  carboxylic acids in water at concentrations of  $100 \text{ g ml}^{-1}$  or lower and also to detect formic, and possibly propionic, acids present at concentrations of  $250 \mu\text{g ml}^{-1}$  in acetic acid. Therefore the techniques discussed could be employed for off-line and on-line monitoring of liquid process or effluent streams.

Low  $\mu\text{g ml}^{-1}$  or  $\mu\text{g l}^{-1}$  detection limits are expected to be achieved for acids present in aqueous solutions using the negative ion electrospray ionisation mode, however lower limits of detection are only possible when the negative ion APCI mode is employed. The

simultaneous detection of all three carboxylic acids present at  $\mu\text{g ml}^{-1}$  concentrations in aqueous media can be performed without interferences from other carboxylic acids. The dissimilar acidity of the three acids provides different concentrations of the detected formate, acetate and propionate anions in the gas phase.

The detection of ionic species present in a matrix composed of acetic acid is not possible when the APCI mode is employed. The acetic acid present at a concentration of 50 % and therefore in a very large excess does not allow the provision of sufficient numbers of other ions to either be created via the acid-base chemistry in the CI plasma or to be extracted from the atmospheric pressure ion source to the mass analyser. Formic and possibly propionic acid can be detected when present at concentrations of  $250 \mu\text{g ml}^{-1}$  in a solution containing 50 % acetic acid using the electrospray ionisation technique. The dependence of the gas phase concentration of ions is dependant on the capability of the ionic species to dissociate in aqueous solution.

The continuous infusion of aqueous or acetic acid matrices into the ion source is possible with the APCI mode but consumes  $0.5 - 2.0 \text{ ml min}^{-1}$  of liquid. This is acceptable when effluent streams are to be analysed. However the application of the electrospray source with pneumatically assisted nebulisation, which will only consume  $0.01 - 1.0 \text{ ml min}^{-1}$ , is a more acceptable technique to use because of the lower rate of consumption of process products. Alternatively aliquots of the liquid stream can be injected into a continuously infused carrier stream for periodic analyses. This is more acceptable with matrices composed of acetic acid, which are not recommended to be continuously sprayed into the ion source because of the effect of corrosion on the stainless steel constructed ion sources at atmospheric pressures.

## 7.5 References

- 1) Arpino, P.J., *Trends in Anal. Chem.*, 1982, **1**, 154.
- 2) Chapman, J.R., *Practical Organic Mass Spectrometry*, Wiley, Chichester, 1993, 2nd Edition, Chapters 2 and 6.
- 3) Garcia, J.F., and Barcelo, D., *J. High Res. Chromatogr.*, 1993, **16**, 633.
- 4) Covey, T.R., Lee, E.D., Bruins, A.P., and Henion, J.D., *Anal. Chem.*, 1986, **58**, 1451A.
- 5) Niessen, W.M.A., and Greef, J.V.D., *Liquid Chromatography - Mass Spectrometry*, Marcel Dekker, New York, 1992.
- 6) Huang, E.C., Wachs, T., Conboy, J.J., and Henion, J.D., *Anal. Chem.*, 1990, **62**, 713A.
- 7) Bruins, A.P., *Trends in Anal. Chem.*, 1994, **13**, 37.
- 8) Bruins, A.P., *Mass Spectrometry Rev.*, 1991, **10**, 53.
- 9) Proctor, C.J., and Todd, J.F.J., *Organic Mass Spectrom.*, 1983, **18**, 509.
- 10) Dole, M., Mack, L.L., Hines, R.L., Mobley, R.C., Ferguson, L.D., and Alice, M.B., *J. Chem. Phys.*, 1968, **49**, 2240.
- 11) Horning, E.C., Horning, M.G., Carroll, D.I., Dzidic, I., and Stillwell, R.N., *Anal. Chem.*, 1973, **45**, 936.
- 12) Knewstubb, P.F., and Sugden, T.M., *Proc. Roy. Soc. A*, 1966, **255**, 520.
- 13) Shahin, M.M., *J. Chem. Phys.*, 1966, **45**, 2600.
- 14) Gray, A.L., *Analyst*, 1975, **100**, 289.
- 15) Whitehouse, C.M., Dreyer, R.N., Yamashita, M., and Fenn, J.B., *Anal. Chem.*, 1985, **57**, 675.

- 16) Chowdhury, S.K., Katta, V., and Chait, B., *Rapid Commun. Mass Spectrom.*, 1990, **4**, 81.
- 17) Campargue, R., *J. Phys. Chem.*, 1984, **88**, 4466.
- 18) Searcy, J.Q., and Fenn, J.B., *J. Chem. Phys.*, 1974, **61**, 5282.
- 19) Kambara, H., and Kanomata, I., *Anal. Chem.*, 1977, **49**, 270.
- 20) Horning, E.C., Carroll, D.I., Dzidic, I., Haegele, K.D., Horning, M.G., and Stillwell, R.N., *J. Chromatogr. Sci.*, 1974, **12**, 725.
- 21) Sieferting, K., Berger, H., and Whitlock, W., *J. Vac. Sci. Technol. A*, 1993, **11**, 1593.
- 22) Kebarle, P., and Tang, L., *Anal. Chem.*, 1993, **65**, 972A.
- 23) Ikononou, M.G., Blades, A.T., and Kebarle, P., *Anal. Chem.*, 1991, **63**, 1989.
- 24) Tang, L., and Kebarle, P., *Anal. Chem.*, 1993, **65**, 3654.
- 25) Iribarne, J.V., and Thomson, B.A., *J. Chem. Phys.*, 1976, **64**, 2287.
- 26) Zeleny, J., *Phys. Rev.*, 1917, **10**, 1.
- 27) Thomson, B.A., and Iribarne, J.V., *J. Chem. Phys.*, 1979, **71**, 4451.
- 28) Yamashita, M., and Fenn, J.B., *J. Phys. Chem.*, 1984, **88**, 4451.
- 29) Yamashita, M., and Fenn, J.B., *J. Phys. Chem.*, 1984, **88**, 4671.
- 30) Hayati, I., Bailey, A.I., and Tadros, Th.F., *J. Colloid Interface Sci.*, 1987, **117**, 205.
- 31) Hayati, I., Bailey, A.I., and Tadros, Th.F., *J. Colloid Interface Sci.*, 1987, **117**, 222.
- 32) Blades, A.T., Ikononou, M.G., and Kebarle, P., *Anal. Chem.*, 1991, **63**, 2109.
- 33) Berkel, G.J.V., McLuckey, S.A., and Glish, G.L., *Anal. Chem.*, 1991, **63**, 2064.
- 34) Berkel, G.J.V., McLuckey, S.A., and Glish, G.L., *Anal. Chem.*, 1992, **64**, 1586.

- 35) Xu, X., Nolan, S.P., and Cole, R.B., *Anal. Chem.*, 1994, **66**, 119.
- 36) Berkel, G.J.V., and Zhou, F., *Anal. Chem.*, 1995, **67**, 2916.
- 37) Taflin, D.C., Ward, T.L., and Davis, E.J., *Langmuir*, 1989, **5**, 376.
- 38) Wong, S.F., Meng, C.K., and Fenn, J.B., *J. Phys. Chem.*, 1988, **92**, 546.
- 39) Bruins, A.P., Covey, T.R., and Henion, J.D., *Anal. Chem.*, 1987, **59**, 2642.
- 40) Carroll, D.I., Dzidic, I., Stillwell, R.N., Haegele, K.D., and Horning, E.C., *Anal. Chem.*, 1975, **47**, 2369.
- 41) Covey, T.R., Lee, E.D., and Henion, J.D., *Anal. Chem.*, 1986, **58**, 2453.
- 42) Briesacher, J.L., Nakamura, M., and Ohmi, T., *J. Electrochem. Soc.*, 1991, **138**, 3717.
- 43) Ketkar, S.N., Dulak, J.G., Fite, W.L., Buchner, J.D., and Dheandhanoo, S., *Anal. Chem.*, 1989, **61**, 260.
- 44) Fenn, J.B., Mann, M., Meng, C.K., Wong, S.F., and Whitehouse, C.M., *Science*, 1989, **246**, 64.
- 45) Smith, R.D., Loo, J.A., Edmonds, C.G., Barinaga, C.J., and Udseth, H.R., *Anal. Chem.*, 1990, **62**, 882.
- 46) Burlingame, A.L., Boyd, R.K., and Gaskell, S.J., *Anal. Chem.*, 1996, **68**, 599R.
- 47) Larsen, B.S., and McEwen, C.N., *J. Am. Soc. Mass Spectrom.*, 1991, **2**, 205.
- 48) Berkel, G.J.V., Glish, G.L., and McLuckey, S.A., *Anal. Chem.*, 1990, **62**, 1284.
- 49) Mordehai, A.V., and Henion, J.D., *Rapid Comm. Mass Spectrom.*, 1993, **7**, 205.
- 50) Henry, K.D., and McLafferty, F.W., *Org. Mass Spectrom.*, 1990, **25**, 490.
- 51) Lee, E.D., Muck, W., Henion, J.D., and Covey, T.R., *J. Am. Chem. Soc.*, 1989, **111**, 4600.

- 52) Bergen, A.V.D., Colton, R., Percy, M., and West, B.O., *Inorg. Chem.*, 1993, **32**, 3408.
- 53) Bond, A.M., Colton, R., Mah, Y.A., and Traeger, J.C., *Inorg. Chem.*, 1994, **33**, 2548.
- 54) Arakawa, R., Tachiyashiki, S., and Matsuo, T., *Anal. Chem.*, 1995, **67**, 4133.
- 55) Wilson, S.R., Perez, J., and Pasternak, A., *J. Am. Chem. Soc.*, 1993, **115**, 1994.
- 56) Schäfer, A., Paul, H., Fischer, B., Hesse, M., and Viscontini, M., *Helv. Chim. Acta*, 1995, **78**, 1763.
- 57) Aplin, R.T., Robinson, C.V., Schofield, C.J., and Westwood, N.J., *J. Chem. Soc. Chem. Commun.*, 1992, **22**, 1650
- 58) Zhou, F., and Berkel, G.J.V., *Anal. Chem.*, 1995, **67**, 3643.
- 59) Bond, A.M., Colton, R., D'Agostino, A., Downard, A.J., and Traeger, J.C., *Anal. Chem.*, 1995, **67**, 1691.
- 60) Dupont, A., Gisselbrecht, J-P., Leize, E., Wagner, L., and Dorsselaer, A.V., *Tetrahedron Letters*, 1994, **35**, 6083.
- 61) Gatlin, C.L., Turecek, F., and Vaisar, T., *Anal. Chem.*, 1994, **66**, 3950.
- 62) Fisons Instruments sales literature, VG Platform II, 1994.
- 63) Stark, J.G., and Wallace, H.G., *Chemistry Data Book*, John Murray, London, 1982, 2nd Edition, p 96.

# **Chapter Eight**

## **General Conclusions**

The work presented in this thesis has shown the potential of applying four different techniques with mass spectrometry detection for the off-line and on-line analysis of low molecular weight liquid process streams in the chemical industry. Two liquid streams were used to investigate the potential of three of the techniques; acetone (analyte) in water and methyl iodide (analyte) in acetic acid.

The total vaporisation manifold employed a gas chromatograph heated inlet to completely vaporise liquid samples followed by the analysis of the vapour created with an electron impact quadrupole mass spectrometer. Liquid samples were introduced for vaporisation with a syringe or four-port sampling valve for off-line and on-line analyses, respectively. The increase in the volume of the sample during vaporisation resulted in the requirement of a buffer volume, to separate the vaporisation region and the mass spectrometer, to protect the mass spectrometer from periodic pressure increases. The dilution with helium gas in the buffer volume does, however, reduce the measured response by a factor of four. Limits of detection of 1-20  $\mu\text{g ml}^{-1}$  were achieved when optimised operating parameters were employed. The response measured was influenced by the buffer volume, injection temperature, injection volume, helium flow rate and the sample and matrix. Water matrices required longer vaporisation times when compared with acetic acid matrices. Analysis frequencies of 30-60  $\text{h}^{-1}$  were obtained and therefore the technique can provide real-time monitoring of liquid streams when employed for on-line analyses. The use of total vaporisation analysis has displayed the greatest potential because it can detect low  $\mu\text{g ml}^{-1}$  concentrations with good precision [RSD (n=10) < 5 %] when compared to other techniques and the effect of the matrix on quantification of

analytes can be overcome. Only in a minority of applications would concentrations lower than  $1 \mu\text{g ml}^{-1}$  need to be detected in process analysis applications.

Headspace analysis techniques enabled compounds to transfer from a liquid sample to a gas phase (headspace). The analysis of the headspace with an electron impact quadrupole mass spectrometer provided information regarding the composition of the liquid phase. Static headspace analysis used partitioning of the two phases in a sealed vial for off-line analyses. The sampling time of the headspace, temperature, phase ratio and matrix all effected the partitioning of compounds between the two phases. Limits of detection of  $0.1 - 5.0 \mu\text{g ml}^{-1}$  were achieved at  $70^\circ\text{C}$ , however, the higher concentration of matrix compounds present in the headspace at this temperature affected the ionisation of analyte in the ion source and reduced the linear calibration range.

Dynamic headspace analysis continuously passes a liquid stream through a glass headspace flow cell. Compounds partially transfer to the headspace present in the flow cell during their short residence time (1-5 s) and an electron impact quadrupole mass spectrometer continuously sampled and analysed the headspace. Elevated temperatures above  $20^\circ\text{C}$  and gas purging of the liquid stream both provided efficient transfer of analyte from the liquid stream into the headspace. The times (rise and fall times) required to quantitatively determine changes in the concentration of compounds in the liquid stream were generally less than three minutes when the optimised experimental conditions were used and therefore the technique can be employed for continuous real-time monitoring of liquid streams. The technique also provided the lowest limits of detection achieved ( $< 1 \mu\text{g ml}^{-1}$ ).

Membrane introduction mass spectrometry is similar to the headspace techniques except the liquid stream and gas phase are separated by a membrane which is employed to provide a greater degree of selectivity of the transport of compounds to the gas phase. Employing a flow-through membrane flow cell two different membrane materials (nonporous silicone rubber and microporous polypropylene) were investigated for their application to the on-line analysis and monitoring of liquid streams. The membrane material, stream temperature and liquid flow rate all influenced the transport of analytes from the liquid stream to the gas phase. The polypropylene membrane material could not be employed for the analysis of compounds present in acetic acid streams because of the leakage of acetic acid through the membrane, however, aqueous streams could be analysed with a limit of detection of  $2 \mu\text{g ml}^{-1}$ . Silicone rubber membranes provided limits of detection of 3 and  $0.4 \mu\text{g ml}^{-1}$  for acetone in aqueous streams and methyl iodide in acetic acid streams, respectively. The times required to quantitatively determine concentration changes in the liquid stream were less than six minutes at elevated temperatures and therefore near real-time stream monitoring can be performed with the technique.

Of the three techniques described above only off-line and on-line total vaporisation analysis and static headspace analysis provided accurate determination of acetone in a process sample composed of thirteen different compounds present at percent concentrations. Standard additions calibration was employed with the static headspace technique. The techniques of on-line dynamic headspace analysis and membrane introduction mass spectrometry did not provide accurate determination of acetone in process samples. The transfer of analyte to the headspace phase is influenced by the

matrix and the matrix can not be accurately reproduced because of its complexity and periodic changes in compound concentrations. The application of each technique to the analysis of samples different to those analysed in this thesis would need to be investigated. The choice of interface for off-line and on-line analysis depends on the application it will be employed for. The requirement of vaporisation in the techniques limits their use to relatively low boiling point compounds.

As an alternative to the selective or complete transfer of compounds to the gas phase before ionisation in an electron impact ion source, atmospheric pressure ionisation (electrospray and atmospheric pressure chemical ionisation) can be performed. These two techniques nebulise samples into an ion source operating at atmospheric pressure. Ions are created depending on the experimental conditions employed and the ions are transferred to the mass analyser operated at vacuum pressure. Electrospray and atmospheric pressure chemical ionisation was investigated for the detection of formic, acetic and propionic acid present in either aqueous or carboxylic acid streams. The detection of the three acids was achieved at concentrations of  $100 \mu\text{g ml}^{-1}$  in aqueous and acidic streams using electrospray ionisation and in aqueous streams using atmospheric pressure chemical ionisation. The detection of concentrations lower than  $100 \mu\text{g ml}^{-1}$  is possible with electrospray ionisation. Electrospray is a more appropriate technique to use for off-line or on-line process analysis of carboxylic acids because of the low flow rates consumed ( $< 1 \text{ ml min}^{-1}$ ) and the ability of the technique to detect ionic species present in ionic matrices which was not achieved with the atmospheric pressure chemical ionisation technique. The on-line techniques discussed above recirculate the analysed stream to the process stream and therefore sample consumption is negligible.

## **Chapter Nine**

### **Suggestions for Further Work**

Although the work presented in this thesis has shown the potential of the techniques investigated, further work could be performed to enlarge the range of applications or improve the sensitivity and accuracy of the techniques.

Further validation can be performed by employing the techniques regularly for the off-line and on-line analysis of liquid process streams. The continued and regular use of techniques will provide an outlook of their true applicability and limitations. For regular use industrial companies need to decide whether the techniques described can provide a significant advantage when compared with other techniques currently employed.

The complexity of the process samples analysed in this thesis are frequently observed in the chemical industry. The accurate determination of acetone in process samples can not always be achieved because of the effect of the sample matrix on the transfer of compounds to the gas phase. The study of the effect of different matrix compounds on the transfer of acetone from the liquid to gas phases is required before dynamic headspace analysis and membrane introduction mass spectrometry can be employed. The use of multivariate calibration techniques would be most appropriate for these studies.

Dilution of the gaseous phase with matrix compounds or helium can affect the achievable limits of detection and linear calibration ranges. Helium or the matrix and its effect can be partially removed using a jet separator and this application should be studied. Alternatively helium or water can be used as reagent gases in a chemical ionisation ion source.

Finally the use of ion trap, instead of quadrupole, mass spectrometers may provide lower achievable limits of detection if required. The lower limits of detection with ion trap mass spectrometers have been shown with the technique of membrane introduction mass spectrometry discussed in Chapter six.